

**EXPERIMENTAL AND NUMERICAL INVESTIGATIONS OF
CABLE BOLT SUPPORT SYSTEMS**

by

HOSSEIN RAJAIE

A thesis submitted to the Faculty of Graduate Studies and
Research in partial fulfillment of the
requirement for the degree of
Doctor of Philosophy

Department of Mining and Metallurgical Engineering,
McGill University,
Montreal, Canada
June 1990

Copyright © 1990 by Hossein Rajaie

ABSTRACT

In this thesis the behavior of fully grouted, untensioned cable bolts and their application to the stabilization of underground openings are investigated. The study program undertaken involves field, laboratory and numerical studies which aim to improve understanding of the role of passive cable bolting in rock mass support. The higher residual load carrying capacity of the cable and the grout-aggregate mix is compared with that of the conventional grout (cement+water).

Based on the variational approach, an analytical model has been developed to calculate the distribution of shear bond stress along the embedded length of a cable bolt. A parametric study is then undertaken to illustrate the support behavior of cable bolts with different grout compositions.

A special finite element for the cable bolt was formulated and integrated into existing finite element code called MSAP2D, in order to allow the simulation of cable bolts in underground excavations.

A practical example is presented to demonstrate the effect of cable bolts on the stability of the opening. The simulation is carried out using the newly developed numerical model with cable bolt simulation capability.

RESUME

Ce présente mémoire présente les résultats de recherches effectuées sur le comportement de système d'ancrages injectés (câble, coulis de scellement et roche) non tendus ainsi que leur application à la stabilisation des fouilles souterraines. Le programme d'étude comprend des essais en chantier et en laboratoire ainsi qu'une analyse numérique afin de mieux comprendre le rôle des ancrages passifs dans le support d'un massif rocheux. L'augmentation de la charge résiduelle supportée par le système d'ancrage (câble, coulis-granulats et roche) a été comparée avec un coulis conventionnel (ciment+eau).

En se basant sur l'approche variationnelle, un modèle analytique a été développé afin de calculer la distribution des contraintes d'adhérence le long d'un ancrage scellé. Ensuite, une étude paramétrique a été effectuée pour illustrer le comportement des ancrages utilisés comme support, en tenant compte de différents mélanges de coulis.

Aussi, un type d'élément fini a été développé et intégré dans le système MSAP2D déjà en place, afin de permettre la simulation des ancrages dans les excavations souterraines.

Un exemple pratique est présenté pour démontrer l'effet des ancrages sur la stabilité des fouilles. La simulation est réalisée en utilisant le nouveau modèle numérique ayant la possibilité de simuler les ancrages.

ACKNOWLEDGEMENT

I would like to express my sincere appreciation and gratitude to my thesis supervisor, Professor F.P. Hassani and co-supervisor, Professor H.S. Mitri, for their invaluable guidance, encouragement and useful comments throughout the course of this research.

My deep gratitude also goes to the mining staff of the Department of Mining and Metallurgical Engineering, in particular to Professor M.J. Scobel, who has been helpful through his constructive comments and thorough review of my work in the Ph.D. preliminary and comprehensive examinations.

Special thanks are extended to Mr. K. Shakaiani for his technical assistance during the laboratory and field testing program. Thanks are also given to my colleague Moh Momayezadeh for his help on the computer aspects and translating the abstract of the thesis. I wish to acknowledge the help of all of my colleagues, who either directly or indirectly were involved in this research for helped me in collecting necessary materials.

Finally, this dissertation is dedicated to my parents, who had supported, nurtured and prepared me to undertake this project during my early education, and to my wife and children, who have been patient and supportive throughout the period it has taken me to carry out the task.

CONTENTS

	page	
ABSTRACT	i	
RESUME	ii	
ACKNOWLEDGEMENT	iii	
TABLE OF CONTENTS	iv	
LIST OF FIGURES	viii	
LIST OF TABLES	xiii	
CHAPTER 1	INTRODUCTION	
1.1	General	1
1.2	Thesis outline	4
1.3	Objectives	7
CHAPTER 2	BACKGROUND	
2.1	Introduction	9
2.2	Rock-support interaction	11
2.3	Type of support	13
2.3.1	External support	14
2.3.2	Internal support	15
2.4	Cable bolting	17
2.5	History of cable bolting	22
2.6	The mechanism of cable bolting	27
2.7	Design of cable bolt support system	28
2.7.1	Empirical design rules developed in practice	28

	2.7.2	Laboratory-based empirical formulae	30
	2.7.3	Empirical guidelines based on rock classification	30
	2.8	The nature of shear bond stress	38
	2.9	The bond-slip mechanism	39
	2.10	Elements of cable bolt support systems	41
	2.10.1	Cable bolt	43
	2.10.2	Bonding element or grout	48
	2.11	Distribution of shear bond stress	56
	2.12	Conclusion	62
CHAPTER 3		SCOPE AND OBJECTIVES	
	3.1	Introduction	64
	3.2	Problem definition	65
	3.3	Objectives and methodology	69
CHAPTER 4		IN SITU INVESTIGATION	
	4.1	Introduction	71
	4.2	Material specifications	71
	4.3	Testing equipment	73
	4.4	Testing site	75
	4.5	Field performance of the grout pump	77
	4.6	Installation technique	80
	4.7	Efficiency of the grout	82
	4.8	Strength evaluation of the grout	88
	4.9	In situ results	88
	4.10	Conclusion	92
CHAPTER 5		EXPERIMENTAL PROGRAM	
	5.1	Introduction	93
	5.2	Testing arrangement	94

5.3	Sample preparation	97
5.4	Materials properties	99
	5.4.1 Ordinary portland cement	99
	5.4.2 Cable bolt	100
	5.4.3 Aggregate	100
	5.4.4 Water	103
5.5	Testing system	103
	5.5.1 Testing technique	104
5.6	Preparation of grout-aggregate mix	106
5.7	Test results	111
	5.7.1 Effect of sample diameter	111
	5.7.2 Diameter of borehole	117
	5.7.3 Effect of water-cement and aggregate-cement ratio	117
	5.7.4 Effect of embedded length of cable	126
5.8	Experimental conclusions	134
CHAPTER 6	DISTRIBUTION OF SHEAR BOND STRESS	
6.1	Introduction	136
6.2	Analytical model	137
6.3	Variational approach	141
6.4	Total potential energy	144
	6.4.1 Strain energy in the cable bolt	145
	6.4.2 Strain energy stored in the grout or Winkler springs (U_p)	146
	6.4.3 Strain energy in the host	149
	6.4.4 Potential of load (V_p)	153
6.5	Minimization of total potential energy	156
6.6	Parametric studies	165
6.7	Conclusion	176

CHAPTER 7	FINITE ELEMENT MODEL	
7.1	Introduction	177
7.2	Basic modeling technique	178
7.3	Formulation of cable element	182
7.4	Equation of equilibrium	185
7.5	Equation solver	185
7.6	Cable bolt analysis system	186
7.7	Solution procedure	194
CHAPTER 8	MODEL VERIFICATION	
8.1	Introduction	195
8.2	Model verification	195
8.3	Practical example	202
	8.3.1 Results	205
8.4	Conclusion	217
CHAPTER 9	CONCLUSIONS	
9.1	Conclusions	218
9.2	Suggestions for further research	220
REFERENCES		222

LIST OF FIGURES

Figure		Page
1-1	Possible failure modes of cable bolts	3
2-1a	Diagram of ground stability	12
2-1b	Rock-support interaction diagram	12
2-2	Interior rock reinforcement	16
2-3	Method I: Installation of cable with breather hose	19
2-4	Method II: Installation of cable bolt without breather hose	20
2-5	Method III: Mechanized installation	21
2-6	Different patterns of cable bolting in open stoping	25
2-7	Flow chart for design of cable bolt	32
2-8	Step D - Cable design flow chart	33
2-9	Modified stability graph	34
2-10	Bolt density versus hydraulic radius	35
2-11	Cable length versus hydraulic radius	37
2-12	Deformation of matrix around a bar	41
2-13	Effect of surface conditions	45
2-14	Bond stress of cable bolt versus the compressive strength of the grout	50
2-15	Steel stress versus shear bond stress	58
2-16	Stress distribution along the embedded length	58

2-17	Distribution of load along the embedded length	59
3-1	Force in the cable is transmitted to the surrounding matrix through the bond element (grout)	66
3-2	Modification of exposed surface of a cable	67
4-1	View of the jack and potentiometer	74
4-2	Layout of the in situ test area, Dome Mine	76
4-3	Cable bolt together with rock surface	78
4-4	View of the in situ grouting operation	79
4-5	Installation technique	81
4-6	View of 9m plexi-glass tube	83
4-7	Weight versus length for 180 cm length	85
4-8	Weight versus length for 90 cm length	86
4-9	Weight versus length for 30 cm length	87
4-10	Effect of curing time on the behavior of cable bolt	90
4-11	Effect of embedded length on the behavior of cable bolt	91
5-1	Different testing arrangements	95
5-2	Preparation of a test specimen for a pull-out test	98
5-3	Size distribution of aggregates	102
5-4	Testing arrangement	105
5-5	Workability in terms of water-cement ratio for different grout-aggregate mixes.	109
5-6	Development of radial cracks in the sample	114
5-7	Load carrying capacity for different external diameter of sample	115

5-8	Load-displacement behavior of cable with conventional grout for different diameter of borehole	118
5-9	Load versus displacement (mix GAC0)	119
5-10	Load versus displacement (mix GAC2)	119
5-11	Load versus displacement (mix GAC3)	120
5-12	Load versus displacement (mix GAC4)	120
5-13	Propagation of cracks observed in the grout-aggregate	123
5-14	Load versus displacement for different mixes	124
5-15	Configuration of cable in the sample after pull-out test	127
5-16	Configuration of cable at the unloaded face of sample after pull-out test	128
5-17	Load-displacement behavior for different embedded length of cable with grout-aggregate mix type I	129
5-18	Load carrying capacity versus embedded length for conventional grout	130
5-19	Load carrying capacity versus embedded length for grout-aggregate mix (type I)	131
6-1	Simulation of grout and interfaces	138
6-2	Definition of stress and deformation components	140
6-3	True and varied curves in a variational problem	142
6-4	Simulation of actual and idealized system.	147
6-5	Slip characteristics of the Winkler spring	148
6-6	Definition of displacement components at loaded end of cable	154

6-7	Boundary and compatibility conditions for CASE I	158
6-8	Boundary and compatibility conditions for CASE II	160
6-9	Boundary and compatibility conditions of the Winkler springs in elastic-softening-plastic range	162
6-10	Flow chart of program distribution of shear bond stress	164
6-11	Load carrying capacity versus embedded length of cable	167
6-12	Distribution of shear bond stress along the cable for different embedded lengths	168
6-13	Comparison of distribution of shear bond stress along the length of cable	169
6-14	Comparison of distribution of load for different slips	170
6-15	Effect of perimeter of cable on the load distribution	171
6-16	Effect of cross sectional area of cable on the load distribution	172
6-17	Effect of peak bond stress on the load distribution	173
6-18	Effect of slip at peak bond stress on the load distribution	174
6-19	Effect of residual strength on the load distribution	175
7-1	Quadrilateral isoparametric element	178
7-2	Simulation of grout and slip for cable bolt	179
7-3	Geometry and degrees of freedom of a cable element	180
7-4	Flow chart of CAB analysis system	188
7-5	Description of model zone	190

8-1	Geometry of pull-out test	196
8-2	Finite element meshes	198
8-3	Comparison of load distributions	199
8-4	Comparison of shear bond stress distributions	200
8-5	Geometry and material properties	203
8-6	Finite element mesh when stope is not supported	207
8-7	Finite element mesh for localized cable bolt support	208
8-8	Finite element mesh when cables are installed from top access drift	209
8-9	Variation of ratio of average horizontal stress to vertical stress with depth below surface	210
8-10	Plot of vertical stress against depth below surface	211
8-11	Typical distribution of displacement around the opening	212
8-12	Typical distribution of principal stresses around the opening	213
8-13	Safety level when stope is not supported	214
8-14	Safety level when stope is supported by localized cable bolting	215
8-15	Safety level when stope is supported by the cable bolting from top access drift	216

LIST OF TABLES

Table		Page
2-1	Major components of cable bolts	42
4-1	Cable bolt specifications	72
4-2	Mix proportion of grout-aggregate	72
4-3	Grading limits for combined aggregates	73
4-4	Dimensions of the cable and borehole parameters	75
4-5	Durations of the grout-aggregate filling of 9 m tubes	84
5-1	Specifications of cable bolt	100
5-2	Sieve analysis and CSA specification grading requirement	103
5-3	Workability simulation of conventional grout with grout-aggregate mix	107
5-4	Experimental test-program	110
5-5	Compressive strength, cohesion and friction angle of grout and grout-aggregate.	113
5-6	Load carrying capacity of cable for different external diameters of thick wall concrete cylinder and 200 mm embedded length with conventional grout	116
5-7	Load carrying capacity of cable for different borehole diameters of thick wall concrete cylinder and 200 mm embedded length with conventional grout	116

5-8	Shear bond strength of cable for different grout and grout-aggregate material with 200 mm embedded length	125
5-9	Load carrying capacity with normal grout for different embedded length of cable by means of pull-out test	132
5-10	Load carrying capacity with the grout-aggregate material and workability type I for different embedded length of the cable by means of pull-out test	133
7-1	Failure criteria and required parameters	193
7-2	Means of assessing material safety level	193
8-1	Comparison of end displacements for different models and the experimental results	201
8-2	Types and properties of material	202

CHAPTER 1

INTRODUCTION

1.1 GENERAL

Fully grouted cable bolts have evolved as a support system for reinforcement of surface and underground rock excavations during the past decade. It is possible to apply this type of support either in tension prior to grouting (active) or without any tensioning (passive). The cables can be installed in underground excavations with very low headroom, irrespective of the length of the support element. It is recognized that the elimination of the pre-tensioning makes the performance of this type of support system much faster and more efficient.

Untensioned fully grouted cable bolts are installed in the rock mass well before stress relaxation and rock deformation take place. After stoping, relative displacement between the rock and the steel strands generates tension in the cable, especially where rock is primarily under high horizontal compressive stresses. In certain mining applications, such as the reinforcement of cut and fill stopes and ore or waste passes, cable bolts have shown their unique support capability [1]. The load carrying capacity of the cable bolt depends on characteristics of the three major elements in the support system:

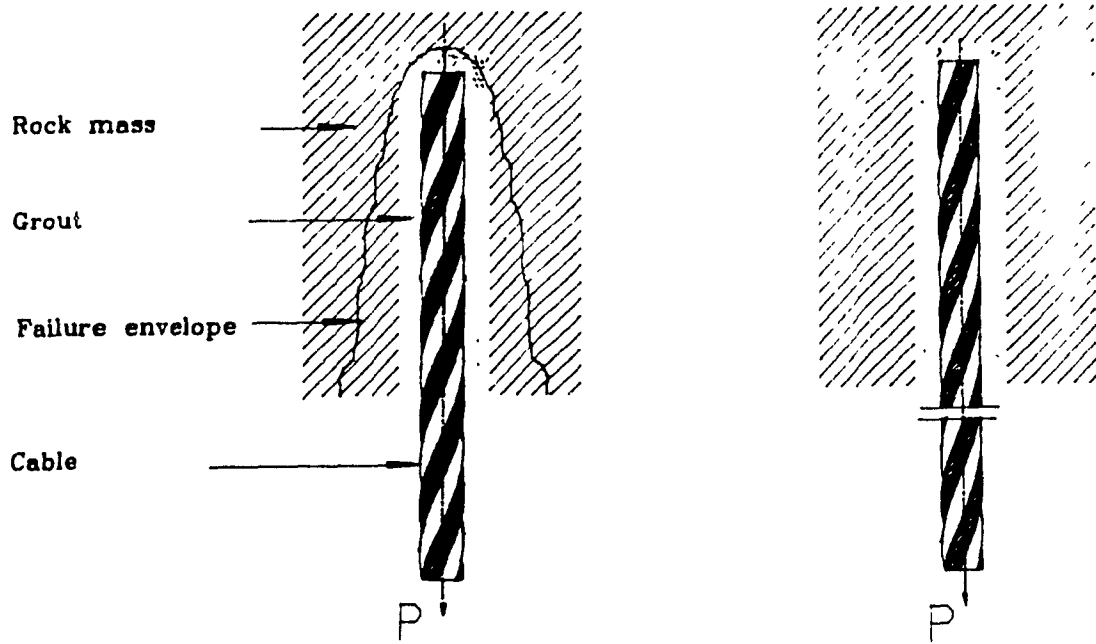
- Shape, type and preparation of steel strands in the cable bolt.
- Bonding element which in conventional grout consists of water and cement and additives if required.
- Host medium which consists of geological material with inherent discontinuities at different stress regimes.

The possible failure modes of a cable bolt are shown in Fig. 1-1 and generally these can be classified as follows [2]:

- Failure within rock mass;
- Failure of the cable bolt;
- Failure of the rock-grout interface;
- Failure of the grout-cable interface.

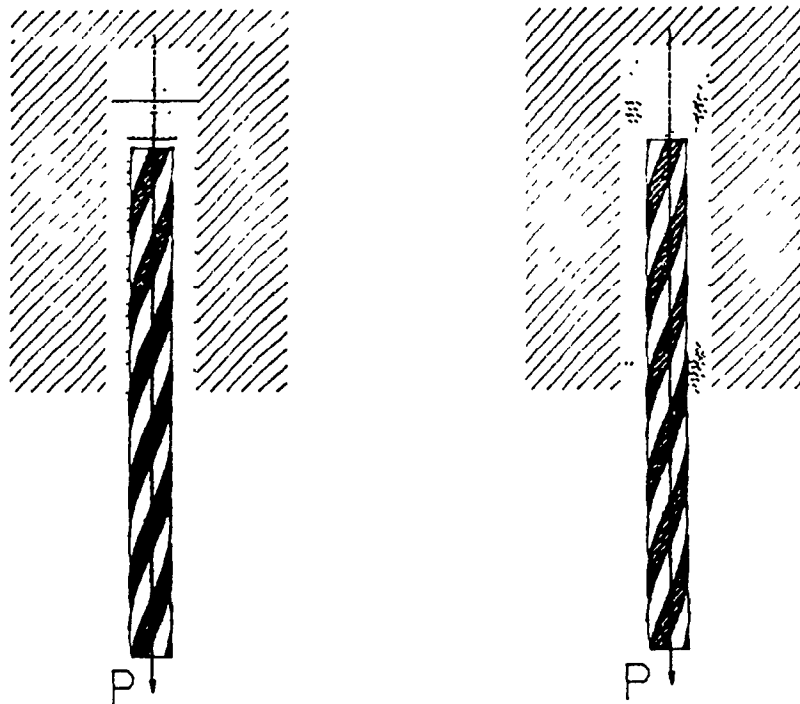
Only a few failures of cable bolting due to breaking of steel strands have been reported. Most reported failures have been due to large blocks slipping off the cables; the strands tend to be left with a curled and twisted shape and totally stripped off the grout.

One of the principal problems in cable bolting is the transfer of the load from the rock mass to the cable elements through the shear bond interface. Therefore, the behavior of the bonding element between the two materials is one of the most important parameters in cable bolting design. Further, the efficiency of grouted untensioned cable bolt reinforcement lies in the bonding preparations to transfer the load from the rock mass to the reinforcing elements [3].



a) Rock failure

b) Cable failure



c) Failure along rock-grout interface

d) Failure along cable-grout interface

Fig. 1-1 Possible failure modes of cable bolts

1.2 THESIS OUTLINE

Since the bond strength in most cases is the weakest link between the cable and the surrounding matrix, the intuitive approach was to maximize the bond strength in order to increase the load carrying capacity of the cable bolt. Past attempts to improve the load carrying capacity of the cable bolt have considered either

- increasing the number of standard cables in the borehole (generally 2 in a borehole),
- attaching friction cylinder, ("button"), to the cable, or
- changing the configuration of the standard cable to form Birdcage cable bolts.

An investigation of the properties of grout material used in cable bolting has been conducted [4]. The modification of the grout material to contribute to the resistance of the cable bolt to failure or debonding has tended to be overlooked both by researchers as well as the mining industry. The understanding of this phenomenon is the key that will contribute to the development of a modified cable bolting support element. The author believes and will demonstrate that the mixture of conventional grout with aggregate has the potential to increase the friction and the mechanical interlocking between the cable and the surrounding rock mass. Therefore, by variation of the constituents of the grout, a different cable bolting support element with different support capability can be engineered to meet the site support requirement [5,6].

Hence, a comprehensive study to evaluate the behavior of cable bolt with conventional grout and grout-aggregate was initiated.

The main body of the thesis is divided into 2 parts; first part experimental investigation, the second part analytical and numerical modelling for better understanding the influence of parameters and design procedure. In more detail, it is divided into 9 chapters including general introduction and conclusions. A brief summary of each chapter follows.

Chapter 1 presents a general introduction on cable bolting, application and possible failure modes of cable bolt. The proposed program to study the behavior of cable bolt with grout and grout-aggregate material experimentally and analytically is also outlined.

Chapter 2 gives a comprehensive literature search of all relevant information on cable bolting. The study extensively reviews laboratory, in situ testing technique. The available empirical and theoretical design methods of cable bolting are reconsidered.

Chapter 3 describes the principal advantages and disadvantages of cable bolting. The grout-aggregate mix is introduced and the scope of the research is presented in this Chapter.

Installation technique of cable bolt with grout-aggregate material is explained in Chapter 4. The results of the in situ pull-out test for different lengths and different curing times is also presented.

A comprehensive laboratory investigation is considered to identify the physical characteristics and behavior of the cable

bolt with grout-aggregate and conventional grout mix. Chapter 5 contains the testing procedure and the results of this experimental study.

To predict load carrying capacity of cable bolt, an analytical approach based on the variational method is detailed in Chapter 6. A parametric study to improve the understanding of the behavior of cable bolt is also presented in this chapter

Chapter 7 describes the formulation of the cable element based on the assumption that the grout material and slip occurring between the cable surface and the surrounding matrix can be simulated by a continuous tangential spring. When this is invoked into MSAP2D, a new numerical model called CAB (CABLE stress analysis) evolves. Then the CAB system with all including its modules the mesh generator and all pre and post processors are described.

Chapter 8 compares the load and shear bond distribution of a pull-out test with variational method and numerical model. To illustrate the use of the program a practical example is given in this chapter and all relative results are included.

General comments and remarks are made in Chapter 9, relating to the factors which are not considered or ignored, and on the assumptions made for typical elastic analysis.

1.3 OBJECTIVES

The following are the objectives of this study.

1- To evaluate by appropriate field trials and testing

a- The concept and feasibility of using grout-aggregate mix (aggregate+cement+water) instead of the normal grout (water+cement) as an alternative bonding material in cable bolting

b- The pumpability of this mixture.

c- The practicability of the installation technique as well as installed cable bolt support capability.

2- To develop an appropriate grout-aggregate mix which would give the optimum bonding resistance between the cable bolt surface and the surrounding matrix. This objective is to be met by a laboratory based testing program of pull-out tests on cylindrical segments of concrete with a central hole that hosts the cable and the grout-aggregate mix. The laboratory investigation is to cover a number of important design parameters such as the specimen size, its length and the mix properties, e.g. water/cement ratio and aggregate/cement ratio.

3- To develop an analytical model that is capable of calculating the shear bond stress distribution along the cable bolt surface. The variational method is to be employed in the formulation of the analytical model. The model is to be verified using the test results from the laboratory. A parametric study

will then be undertaken for a better understanding of the support strength characteristic of cable bolts in the different mix properties.

4- To develop a numerical model based on the finite element method which would have the capability of simulating cable bolts in underground excavations in rock. The finite element computer model called MSAP2D (Microcomputer Static Analysis Program for two Dimensional problems) which has been developed at McGill for the design/analysis of underground openings in rock mass(es) is to be further developed to include the simulation of cable bolts. A special cable bolt "element" is to be formulated and incorporated into the MSAP2D software.

5- To demonstrate the simulation capability of the program. It is planned to undertake a study on a practical example to examine the effect of cable bolts on the stability of the mine stope. The simulations will be carried out using the above mentioned numerical model with the cable bolt simulation capability.

CHAPTER 2 BACKGROUND

2.1 INTRODUCTION

Over the past two decades in the mining industry, due to safety requirements during operation and construction as well as the requirement for long term stability of excavations, a wide choice of support systems has been developed. Poor rock mass conditions, structural discontinuities and high stresses associated with underground excavation, as well as the demands for increased productivity and reduced costs have all played an important role in support system selection [7].

There is a tendency for an opening in a rock mass to close once it has been excavated. The mechanism of this deformation involves movement of individual blocks and the dilation of joints. If no support is present then the opening will continue to close until a state of stable equilibrium or instability is reached. Variation of the mechanical properties of the rock mass with time, the initial stresses and the type of support are some of the factors which affect the magnitude and the rate of the closure of the opening. However, of paramount importance is the knowledge of the stress state of the rock surrounding the excavation, which might be above or below rock strength [8].

In general, after development of an excavation, one of the following types of stability/instability can develop (see Fig. 2-1a) [7].

- a) Stable ground exhibits rock deformability below the yield point, without development of rock fissuring and cracking. Under these conditions, if support is installed, the rock and support are stable during the service life of the excavation.
- b) Semi-stable ground exhibits rock deformability close to yielding fracture. Support which has a degree of stability greater than rock stability is required. The maintenance of installed support is required and local rock falls are expected. The excavation has a potential for losing stability during its service life.
- c) Unstable ground exhibits rock deformability, which progress to rock fissuring and failure. Maintaining the excavation opening will require heavy support.

An important factor for the strength of a rock mass is the degree of geometrical interlocking of joint blocks and the roughness properties of the joint fractures. The degree of interlock will decrease with the relaxation of the rock mass and relative displacement of individual blocks around the opening [9]. This will reduce the rock strength and increase the opportunity for rotational and toppling modes of failure. The induced rock movement due to the excavation of the opening acts in two ways: firstly, to support the load, and secondly to generate internal bending moments and shear stress in an attempt to be self supporting. Support systems are traditionally designed to resist stress-induced deformation and hence they may be overdesigned. In reality, the engineer must make a judgement on the support requirements. The principal objective of any support design is to contribute to the self supporting capability of the rock mass.

2.2 ROCK-SUPPORT INTERACTION

The concept of rock-support interaction described in detail by Deer et al. [10] and has since been used and discussed by Rabcewicz [11], Daemen and Fairhurst [12], Ladanyi [13], Jukes [14], and Hoek and Brown [15] in connection with underground openings. The rock-support interaction diagram Fig. 2-1b shows two characteristic curves: the first (curve KLMN) represents the rock mass and the second (curve AB) represents the excavation support system. The ordinate of the rock characteristic curve represents the radial force required to maintain stability, in other words to arrest closure, after a given magnitude of radial displacement, as given by the abscissa. The radial component of the stress field prior to mining (the virgin stress field) is given by point K on the curve. Upon excavation of the tunnel this component is reduced to zero, thus indicating the removal of radial restraint and the freedom for the tunnel walls to strain inwards.

Initially, the close proximity of the excavation face will prevent the displacement of the walls from developing fully. However, as the face is advanced, and its supporting effect is reduced, then the walls will deform further into the opening (i.e. Δr increases).

As this deformation proceeds then a greater proportion of the inherent rock strength is mobilized and more stress is redistributed around the opening. The process of stress redistribution is completed, if time-dependency effects are neglected, when the closure of the excavation walls is halted and equilibrium is restored to the system.

In the case of strong and competent rock masses the stress redistribution may be accomplished with sufficient self-supporting strength being generated by the rock itself, in which case no additional support is required (curve KLP).

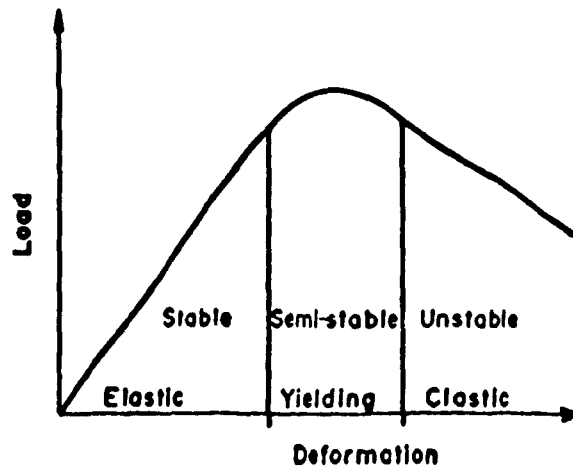


Fig. 2-1a Diagram of ground stability [7]

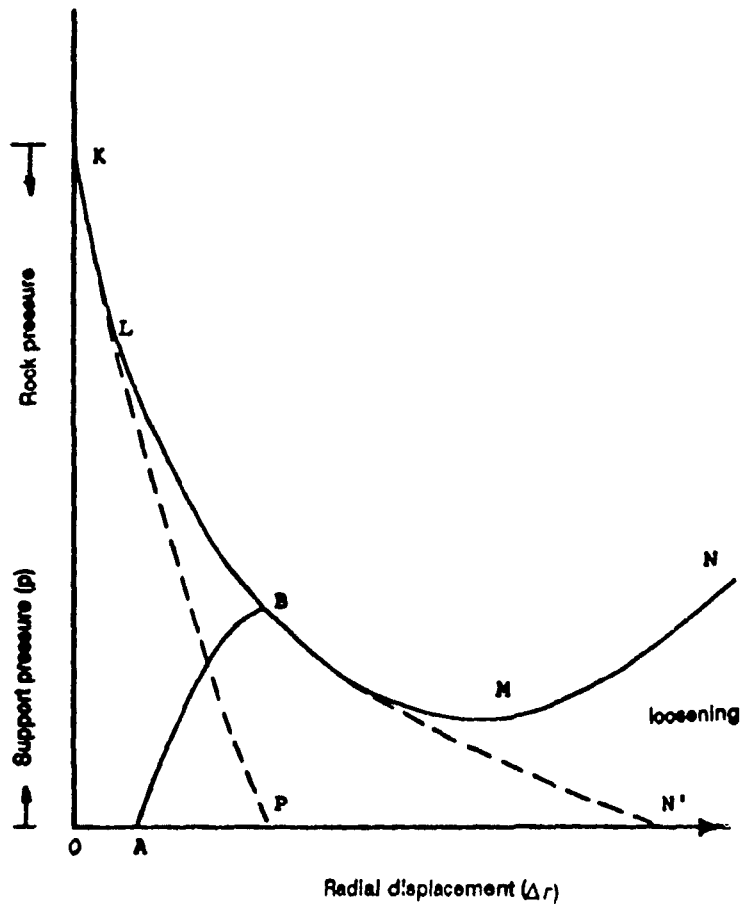


Fig. 2-1b Rock support interaction diagram [14]

However, when either considering weaker incompetent rocks or larger opening spans, then stress redistribution will almost certainly cause excessive deformation and failure of the opening walls. Equilibrium can only be achieved at the expense of large and usually unacceptable levels of radial displacement (curve KLN). The effect of gravity loading of the excavating walls by detached roof blocks is to give the rock a rising characteristic curve (as shown by curve KLMN). The result of this "loosening pressure" is to ensure that equilibrium is only attainable through the use of additional support because the maximum rock strength (given by point M) is insufficient to halt closure.

There is no time lag for cable bolt support, because it is installed in the rock mass before blasting. However, the installation of pre-support (cable bolts) or installation of the support with time lag for example Δt which corresponds to radial yield displacement Δr will have an effective influence on the stability of a rock excavation. Successful support installation will depend on the time lag. Installation time, particularly for external support, is an important factor because it will permit ground strength to develop fully.

2.3 TYPE OF SUPPORT

The most basic method of support in hard rock mining consists of leaving ore behind to support the backs and walls of excavations. As the mining industry has been forced to become more competitive, support methods in underground openings have become more economical and cost effective. In general, support methods can be divided into two broad categories: Internal and external support.

2.3.1 EXTERNAL SUPPORT

External support in most cases is passive, providing a restraining load on the rock face to prevent movement and failure of the rock mass. This takes the form of wood or steel sets and wood cribs which take load as the rock mass deforms onto the support. Shotcrete is an effective form of external support which has gained some application in mining environments. A cement, often mixed with various chemical additives or with steel or synthetic fibres, is sprayed onto the rock surface [16]. The shotcrete forms a lining on the rock face which can provide appreciable support, especially if the opening dimensions are favorable. Backfilling of an excavation is also a common effective method of providing support.

Grouting treatments can be used which are injected into the rock mass, ahead of the excavation, to improve its strength characteristics. These treatments act to fill open joints and help bond the joint surface together to increase overall strength. Freezing of very weak ground before excavation is also used to provide short term strength to the rock mass until more permanent support can be installed.

An extruded tunnel lining system is a support method which is similar to shotcrete in that it consists of a cement bonded directly to the rock surface. Some degree of rock displacement almost invariably occurs prior to the installation of the tunnel linings. Most tunnel linings offer support of a passive nature, in other words a build-up in support strength occurs with increasing distortion of the lining due to strata loading. The build-up in support strength continues until the supporting pressure exerted by the lining is equal to that value required to prevent further rock displacement. This value is indicated by point B in Fig. 2-1b and its attainment represents the restoration of equilibrium.

2.3.2 INTERNAL SUPPORT

Internal support consists primarily of rock reinforcement which acts to support the underground excavation, as well as knit the rock together to increase its overall strength. In general, two different concepts, passive and active support, are employed for rock reinforcement [17]. The reinforcement elements which are pre-tensioned at the time of installation apply an active load to the surrounding matrix. The passive ones are not in tension at the time of installation and therefore do not play a role as a ground support system unless the mass moves and subsequently loads the reinforcement elements. Lang [17] compared the behavior of pre-stressed and reinforced concrete respectively, and developed the classical treatment of active reinforcement with particular reference to underground excavations. A number of available rock support systems are discussed by Scott [18], shown schematically in Fig. 2-2. Internal rock reinforcement uses three main anchoring systems as follows [19, 20]:

- a) Frictional support, providing the primary anchoring force in both swellex and split set bolts. The friction between the steel bolt and the rock mass provides the force resisting rock movement.
- b) Bonded or grouted reinforcement, which relies on the strength of the bond between the rock/grout/bolt system, as well as the frictional force between the components of the system after the bond has been broken. Either chemical or cement grouts are used with rebar or steel cable anchors.
- c) Mechanical anchors, which rely on a gripping mechanism whereby the bolt cuts into the rock providing a restraining or anchoring force. This provides point support at the anchor point and the bolt plate.

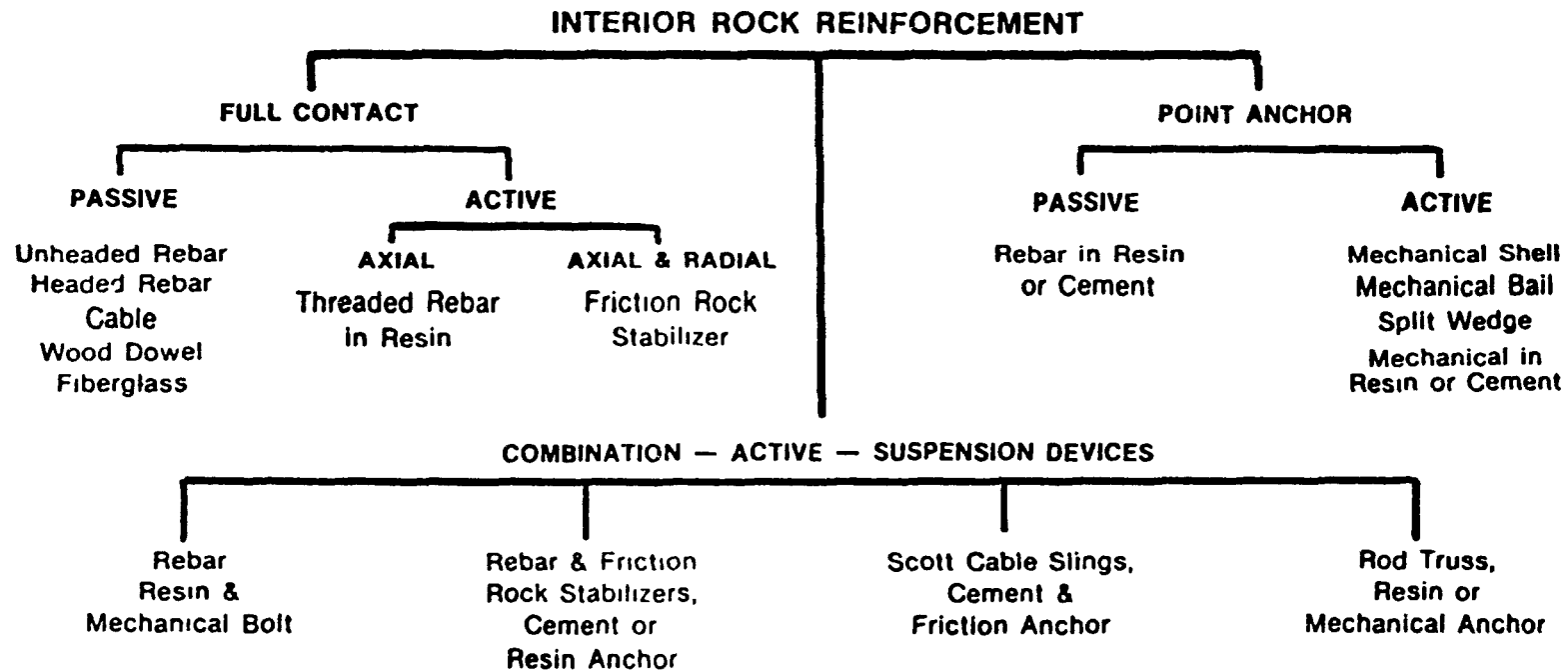


Fig. 2-2 Interior rock reinforcement [18]

Internal rock support systems are in a state of evolution. Mechanical point anchors have been the most widely used method of ground support. Recently, full column anchors with resin and cement have been replacing mechanical rock bolts in all types of ground conditions where they had not been suitable. The use of long, untensioned, grouted cables in underground mining has been a particularly important innovation, which has resulted in significant improvements in safety and mining costs in massive orebodies [21].

2.4 CABLE BOLTING

Cable bolts consist of several steel strands which are fixed into a borehole by grout. When the grout hardens, then the resultant cohesion and interlocking between cable and surrounding matrix will transfer the load of the rock mass to the steel strands. After the borehole is drilled then installation of the cable bolt and grouting can be undertaken. Cable bolts are used in applications and lengths ranging from relatively short 5 m lengths, to 20 - 35 m lengths to support large ground masses around various types of underground openings. Experience has proved that the cable must be clean and especially with no grease, which may compromise the bond between cable and surrounding matrix [6]. Currently, there are three common methods employed for installing cable bolts as follows [22]:

METHOD I: The clean cable is pre-cut, and a spring steel star is fitted to the end button with a nut and used as the end holding device. The breather tube is fastened to the end of the cable, which is then manually or with a simple roller assembly pushed into the end of the hole. Once the cable bolt is inserted, cotton waste or a plug is packed firmly around

the collar to create a grout seal. On long holes (20 ~ 35 m) the cotton waste may need to be soaked in a thick grout mix before placement. The grout tube provides a conduit through which grout is pumped into the hole. The grout tube usually has a 1.25 cm internal diameter and should be taped to the cable about 40 cm from the collar end as is shown in Fig. 2-3. Grout is pumped into the hole until air stops coming out of the breather tube. In this method the water-cement ratio is between 0.40 and 0.50.

METHOD II: The cable is fastened with the grout tube and the complete set is pushed into the bottom of the hole. In this method there is no need for the plug or cotton. The grout is pumped and the hole is filled from the toe to the collar. It can be seen clearly in Fig. 2-4, there is no need for a breather tube in this method. This method is practised underground in up-holes where the grout is sufficiently viscous (i.e. water to cement ratio is 0.3).

METHOD III: A third method is used in mechanized cable bolting, such as applied by the Tamrock Cabolt machine [22]. In this method the hole is drilled, a grout hose is fed to the bottom of the hole and grout is pumped from the toe of the hole to the collar as the grout hose is withdrawn. The synchronization of pumping and pulling of the grout hose can be adjusted to control the amount of grout in the hole (see Fig. 2-5).

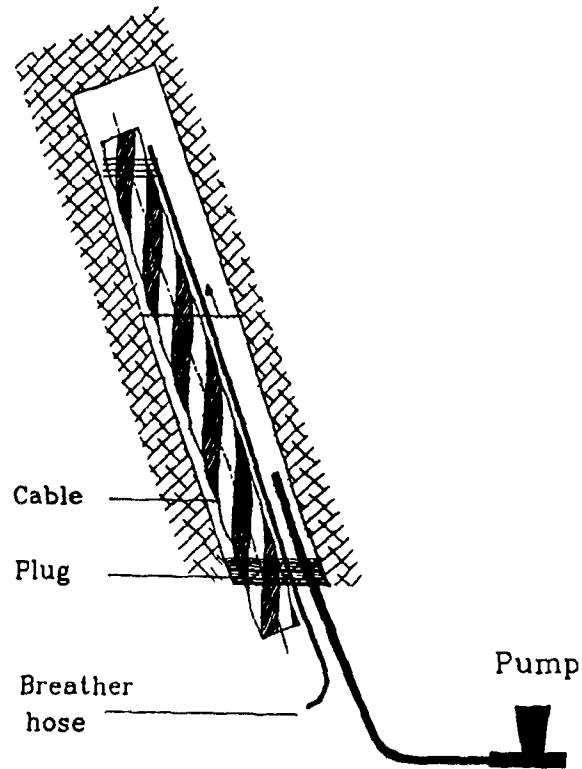


Fig. 2-3 Method I, Installation of cable with breather hose

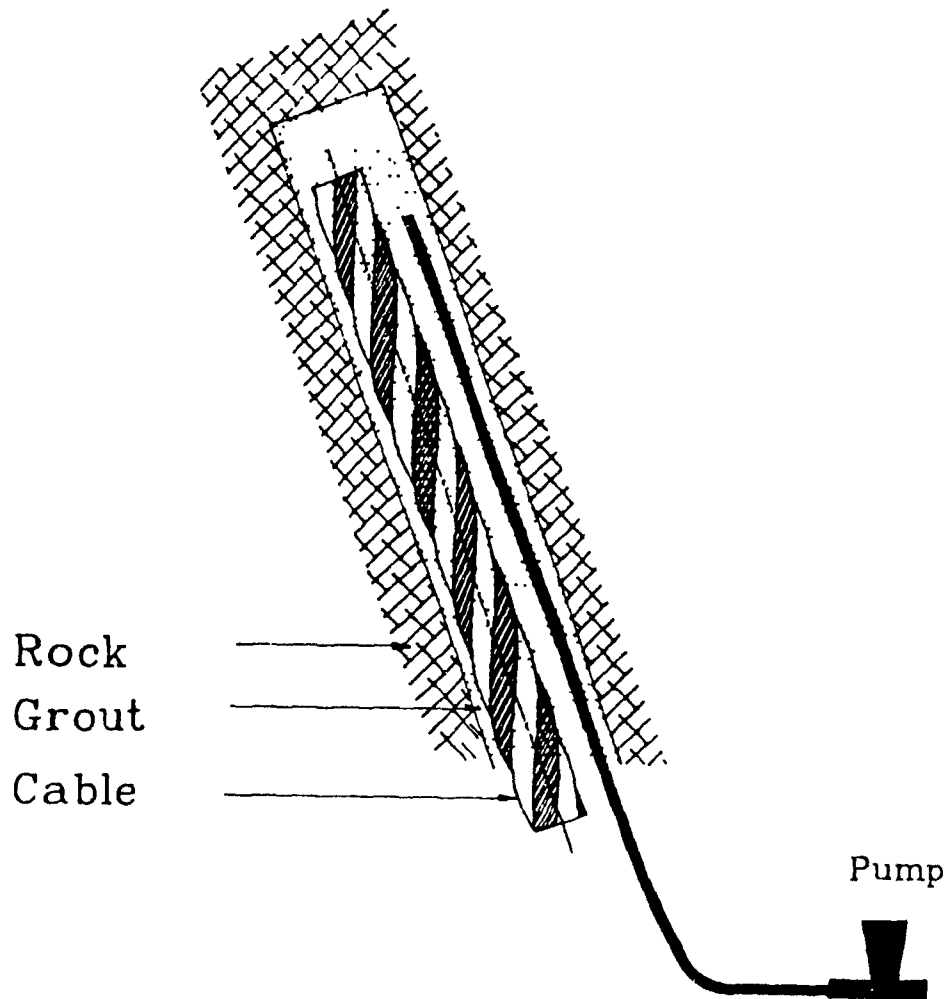


Fig. 2-4 Method II, Installation of cable without breather hose

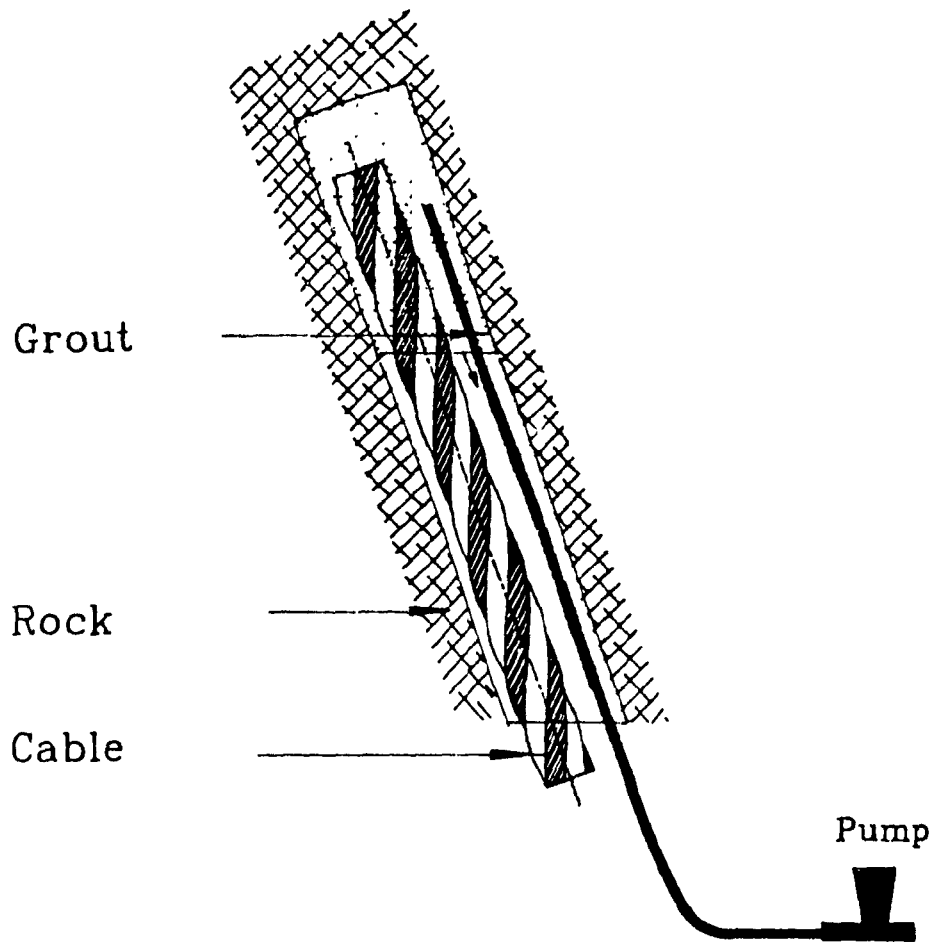


Fig. 2-5 Method III, Mechanized installation

2.5 HISTORY OF CABLE BOLTING

It is not known exactly when internal reinforcement was first used. According to Litteljohn [23], bars were employed in rocks to secure the roof in the Mir Mine, located in Upper Silesia, Poland, in 1918. In 1926, grouted bars in a fan pattern were used to secure a rock mass against caving in Chustenice shale in Czechoslovakia. The earliest example in the field of Civil engineering is the use of reinforcing cables in the Cheufes Dam in 1943.

This type of support has improved to such a degree in the last three decades that it has become one of the most popular support techniques against ground movement, and prevention of rock falls in underground and surface excavations.

Historically, cable bolt support was introduced to the mining industry about 20 years ago in Australia and several years later it was applied in Canada. Gramoli [24] reported that the first Canadian cable bolting experiment was conducted at the Noranda Geco Division in Manitowadge, Ontario, to reinforce the backs and walls of large open stopes. Hoist and slusher rope and high tensile strength wires were installed to act as pretension cables and were termed "cable bolts". The technique involved two stages of grouting. Firstly, a short length of grout extending approximately 900 mm at the top of the borehole was installed. The cable was then inserted into the borehole and grouted section before it had set, in order to form an anchor. The cable was tensioned up to approximately 350 kN force. The second stage involved grouting the rest of the cable length seven days later. Thus the pretension cable system developed an active reaction. The method was successful and economical in controlling both the overloading and the dilation in the stope. This approach was applied in several

mines and it was reported that back conditions were significantly improved, even when the cables were not pretensioned [25, 26].

Long tensioned anchors reaching far above the natural arch zone above an underground excavation develop very large loads. Since these loads are point support from excavation surface, they prevented the ability for arching action to develop and provide an irregular strain pattern contrary to the ideal natural arch conditions. On the other hand in surface mining the natural arch does not exist and consequently, the utilization of active reinforcement is not only fairly harmless but also beneficial enough by creating an artificial arch or structural member.

The direct measurement of cable performance conducted by Fuller [1] in Australian mines showed that pretensioning is not required in the majority of cut and fill stoping situations. In regions where the lateral pressure on the cable bolt is low, e.g. in shallow stopes, pretensioning may be necessary to provide additional confinement in the rock mass. However, elimination of pretensioning in steel strands improves the efficiency of cable bolting in cut and fill mining.

In recent years the use of long untensioned, grouted cables (20 to 35 m) in underground mining has gained considerable popularity due to significant improvements, offered in safety and mining costs in massive ore bodies. Since 1977, the Australian and recently the Canadian and Swedish mining industries have tried to use this type of support system in open stopes [3]. One of the difficulties in employing cable bolting in open stopes is poor access for installation. The other problem relates to the larger spans experienced in open stopes compared to cut and fill stope. The stress distribution due to frequent blasting is also accumulated to a greater extent.

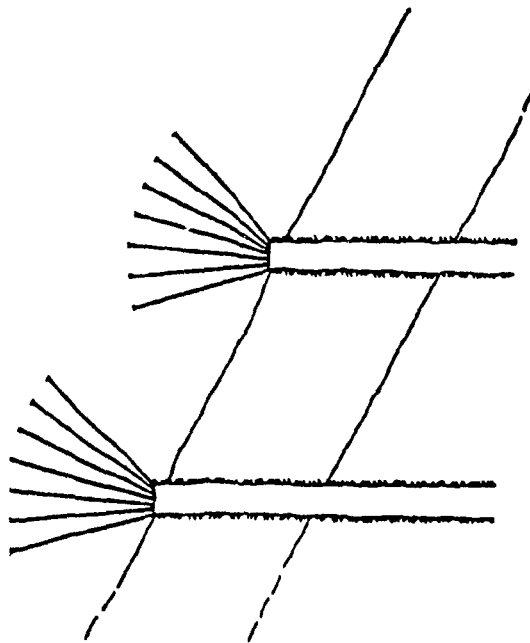
Productivity can be improved with cable bolting in a number of ways. Such support can allow an increase in the width of the stope by pre-reinforcing the opening. The stope height and hence the height of the exposed hanging wall can also be increased with pre-reinforcing. Also, by taking advantage of the high shear bond strength between cable and surrounding matrix the length of the bolts in the stope can be increased. This can give additional cuts before the next bolting cycle is required.

In open stoping or sublevel stoping, the stresses in the surrounding rock generally concentrate on the hanging wall side, stope floor, stope back and ends of the orebody. All of these critical areas can be pre-reinforced with cable bolting. Depending on the application, the cable bolting can be done from within the orebody itself or from outside the orebody.

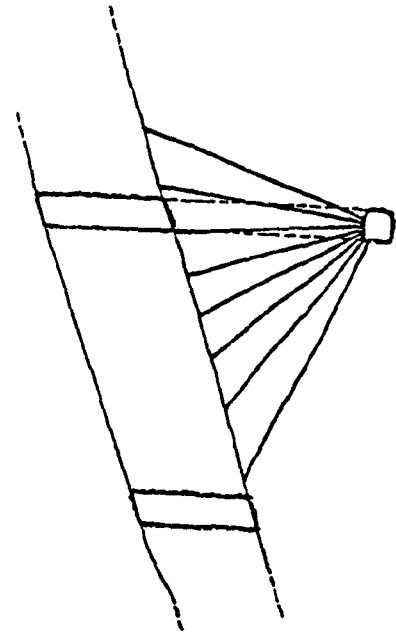
The Geco Mine employed the installation technique used for cut and fill stopes because the top sill was opened to the total planned stope area and access for the installation of cables was available. In wider stopes, where different multiple strike drifts were driven from a crosscut, then cable arrays in vertical fanned upholes provided a reasonably even density of cables above the back. Close to the back, relatively large spans remain unsupported. Often this difficulty can be overcome if a crown pillar is formed above the stope and access is available above the crown from previous workings [27].

Different patterns of cable bolting have been devised in order to overcome the difficulty of installation and requirement to increase stability, as shown in Fig. 2-6.

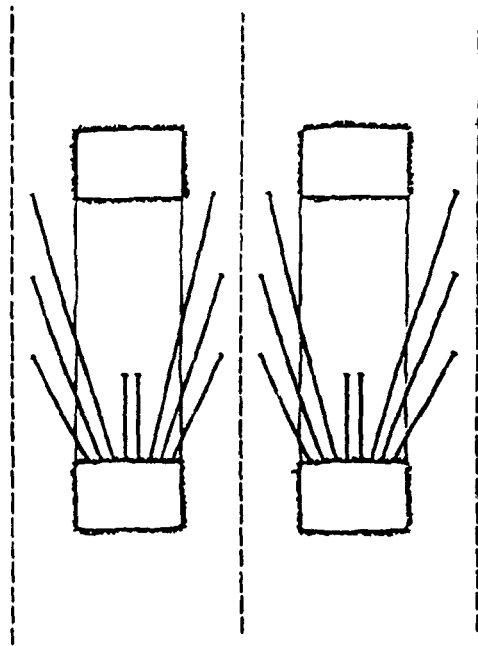
Cable bolts can be used to improve two key areas in typical room and pillar mining: roofs and pillars. Cable bolts that are both longer and better quality than conventional bolts will allow the distance between pillars to be increased. If required, cables can also be used for trussing.



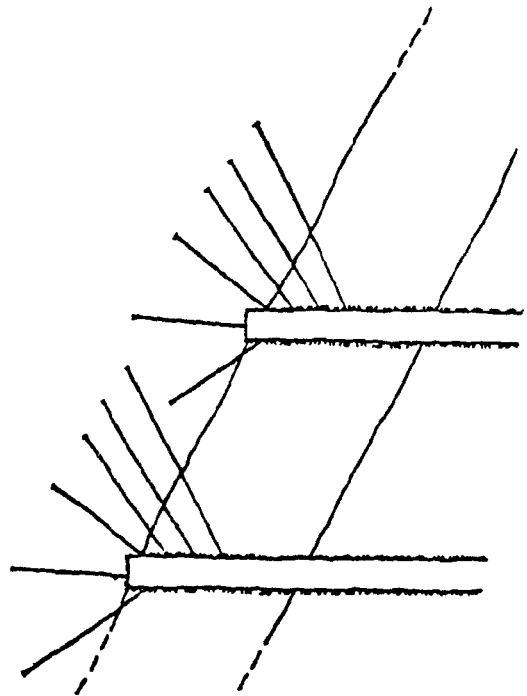
a) Localized cable bolt



b) Hanging wall is supported by cable bolt from tope access



c) Fan shape cable bolting



d) A pattern of cable bolting for hanging wall

Fig. 2-6 Different patterns of cable bolting in open stoping [3]

In many areas, cable bolting is combined with other types of support such as resin rebars, strapping, and swellex bolts. Successful operation with cable bolting support systems have been reported in open pit mines (tensioned multicable bolts) and in underground mines (tensioned and untensioned bolts) and some histories are given below.

A one inch diameter, degreased hoisting cable was used in the cable bolting program in Falconbridge mines to obtain regional support in blast hole stopes and to prevent wall sloughing and minimize dilution [25]. Based on experience, the cable bolt pattern of 1.8 m x 1.8 m was employed above the cave profile. The design was based on three factors:

- rock mass structure with Rock Quality Designation (RQD) values of ranging from 40 to 50 percent;
- modeling using a finite element program to predict stresses generated by different mining sequences;
- cable bolts were designed to be compatible with the block size; typical joint spacing varied from 1 to 3 m.

The support system in cut and fill stopes has contributed to safe and productive mining in deteriorating ground conditions without significant alteration to the basic mining method [28].

At the Cone Mine in the North West Territories the cable bolting method has proven to be an efficient and cost-effective way to resist ground movement and also to carry large rock blocks. In this case, 22 m long cable bolts were installed into 57 mm diameter holes, through the stope back and extending at least 4.6 m into the projected hanging wall. The holes were drilled to a 2.4 m square spacing and were inclined at an angle of 75 degrees. One additional row of cable bolts was inserted after each lift from the footwall, to cover any newly exposed ground. The cables were constructed from 16 mm diameter stranded

steel cable with an ultimate tensile load of about 270 kN [8].

Similarly at the Number 12 Mine of Brunswick Mining and Smelting Ltd., cable bolting has been shown to be a practical means of ground support and has been increasingly used in the production cycle [29].

2-6 THE MECHANISM OF CABLE BOLTING

The most successful support systems are those that are installed immediately after excavation has occurred [15]. Untensioned fully grouted cable bolts are deployed in the rock mass before stress relaxation and rock deformation. After stoping, relative displacement between the rock and the steel strands generates tension in the cable, especially where rock is primarily under high horizontal compressive stresses. Thus, cable bolts act as a means of passive resistance to rock mass movement.

Fuller [1] carried out extensive monitoring of cable bolts, examining the effect of length, studding, grid pattern and blasting. It was shown that the cables were in tension up to 5 m above the back at the time of blasting and sudden re-adjustments of strain could occur up to 2 hours after the blasting. In a few cases re-adjustments due to initial blasting represented dynamic loading which have led to failure of the bond between the cable and surrounding matrix. The investigation confirmed that a fully grouted untensioned cable support system with a grid pattern of 2 m stabilized the rock mass even immediately after the blasts.

According to Potvin [3] only a small proportion of cable bolting failures take place due to the breakage of the steel strands; most failures are due to large blocks slipping off cables, the strands tending to be left with a curled and twisted

shape and totally stripped of grout. The critical feature of a cable bolt support system is the bond strength between the steel strands and grout.

Fundamental investigations of the behavior of passive reinforcing in a discontinuous rock mass were made by Dight [30]. The results indicated that the maximum resistance to joint shear appeared when the cable (diameter 30 mm) made an angle between 15 to 30 degrees with the intersection of a joint, when strands were placed in tension by the shear movement.

2.7 DESIGN OF CABLE BOLT SUPPORT SYSTEM

The design of rock bolt and the cable bolt support systems has traditionally been restricted to the following:

- a) Empirical design rules developed from field practice and experience [8].
- b) Empirical formulae developed from laboratory physical modeling and analysis [32, 33, 34].
- c) Empirical support design guidelines related to rock mass classification studies [3].

2.7.1 EMPIRICAL DESIGN RULES DEVELOPED IN PRACTICE

The evaluation of the rock mass to be supported is the most important and also the most difficult parameter to be calculated for the design of cable bolt support systems. Owing to the number of unknown parameters, both geological and physical, many assumptions have to be made. These usually only pertain to local conditions and therefore will vary from mine to mine. The empirical method of design relates practical experience gained on previous experience to the conditions anticipated at a proposed site. However, based on the obser-

vation and assumption of uniform patterns in geological structures, the formation of an equilibrium arch above the stope back has been considered by some engineers [31]. The arch is often approximated using parabolic or elliptical geometry, where the horizontal axis depends on the length of the stope span and the vertical axis depends upon the stiffness of the rock mass and initial stresses.

The adequate embedded length of cable bolt depends upon the mechanical properties of the bonding element between the cable and borehole's wall, the mechanical properties and geological structure of the rock mass, the angle of the cable bolts to the horizontal and density of the cable bolts per unit area. Based on experience at Con Mine, Cassidy [8] reported a simple equation for calculating cable bolt spacing as follows.

$$S = \sqrt{\frac{N \times U \times V}{T \times SF \times (\sin \alpha)^3}} \quad (2-1)$$

where

- S = spacing between cable bolts (ft)
- N = number of cables per hole
- U = ultimate tensile strength of the cable (ton)
- V = specific volume of rock mass (cubic ft / ton)
- T = Max. thickness of rock mass to be supported
- α = angle that the cable makes with horizontal
- SF = safety factor

2.7.2 LABORATORY-BASED EMPIRICAL FORMULAE

Ballivy [32] proposed a design procedure to determine the embedded length of passive anchors in the rock mass. The procedure is based on the equation first developed by Hawks and Evans [33] and then modified by Philips [68]. The method was established for hard rock environments in which rupture of the anchor occurs at the grout-steel interface. However, application of this method in design of cable bolts is not verified in the mine.

Brian [34] reported on a method devised by Fuller for different design procedures accounting for the geometry and rock mass conditions, as well as the support specification for each cable bolt failure mode. The behavior of the cable for different properties of rock mass and grout is evaluated based on the laboratory pull-out test and analytical approach. The implementation of this design technique has met some problems regarding the identifications and definition of field data required. The design chart is shown in Fig. 2-7 and Fig. 2-8.

2.7.3 EMPIRICAL GUIDELINES BASED ON ROCK MASS CLASSIFICATION

Rock mass classification forms the backbone of most empirical design approaches [9]. In order to establish a relationship between RMR (Geomechanics Classification of Rock Mass Rating System) value and reinforcing density, trials were completed by Choquet [35]. It was shown that there was no correlation between bolt design pattern and rock mass quality.

The Golder Method was proposed by Matthews et al. [36] in which selected geotechnical factors have been combined as a stability number (N) and plotted against a shape factor (F) to assess empirically the stability of the surface boundary of an open stope. The stability number accounts for rock mass

quality, state of stress and orientation of exposed surfaces. The shape factor takes into consideration the shape and size of opening. Thus a high stability number and low shape factor should reflect stable exposures while the opposite should reflect instability. The stability number is briefly outlined below.

$$(N) = Q' \times A \times B \times C \quad (2-2)$$

Where

- Q' = Modified NGI Rock mass rating
- A = stress factor
- B = rock orientation factor
- C = design surface orientation factor

The stability graph method was modified by Potvin [3] to develop design guidelines, based on a study of 66 case histories collected in Canadian open stopes. The key parameters characterizing the rock mass and stress conditions are quantified in order to determine optimum stope dimensions. The modified stability numbers and hydraulic radii calculated for all case studies are shown in Fig. 2-9. The conditions in which cable bolt systems are capable of stabilizing open stopes are defined on the graph. It is reasonable to assume that the intensity of bolting should increase as a case plots closer to the dashed line.

The modified Barton Classification Q' is adjusted for the relative intensity of support as shown in Fig. 2-10. It is necessary to mention that the technique is applicable to areas with uniform bolting patterns and should be used in cases such as hanging walls, where support is only applied, for example at sublevel access points.

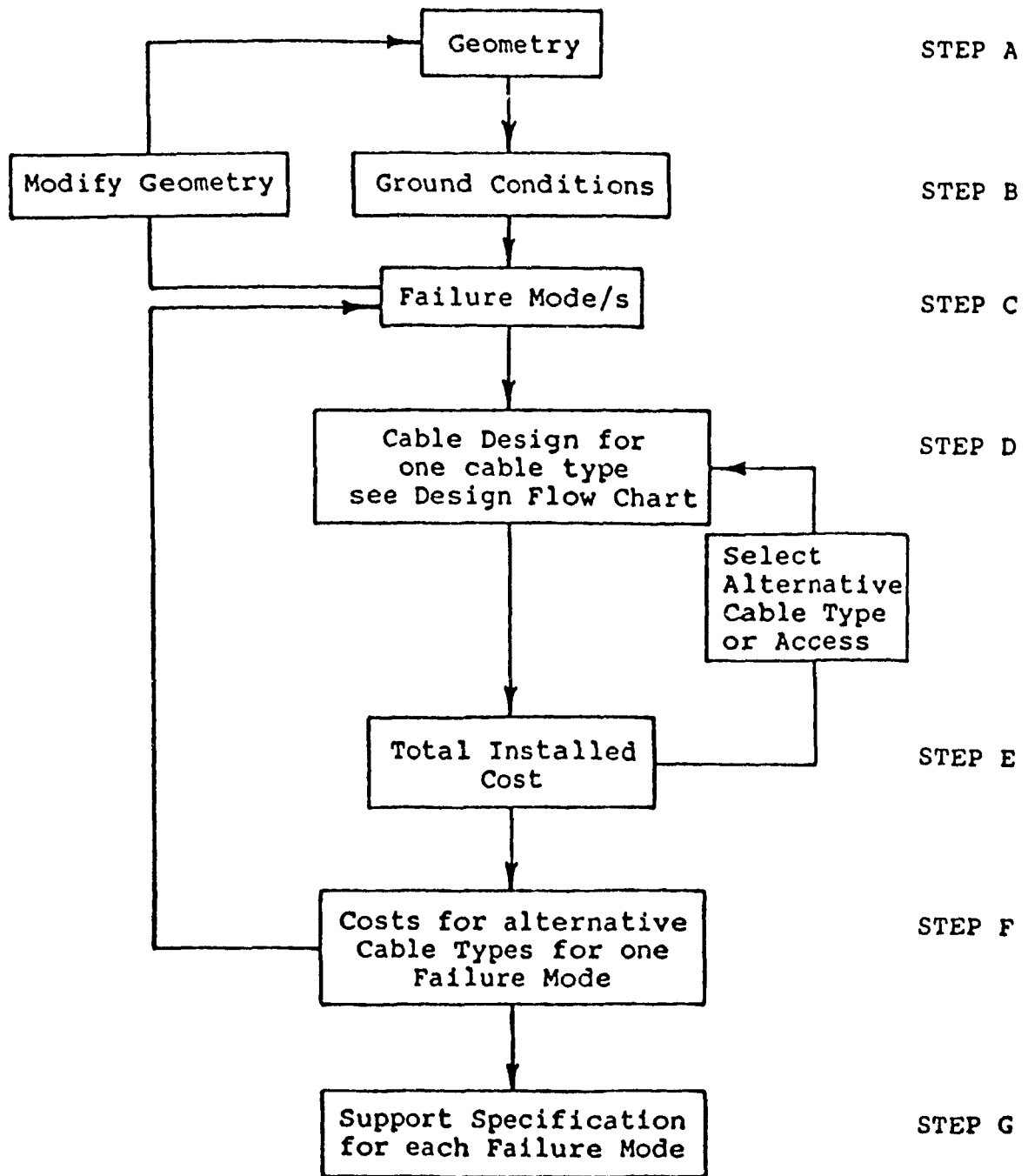


Fig. 2-7 Flow chart for design of cable bolt [34]

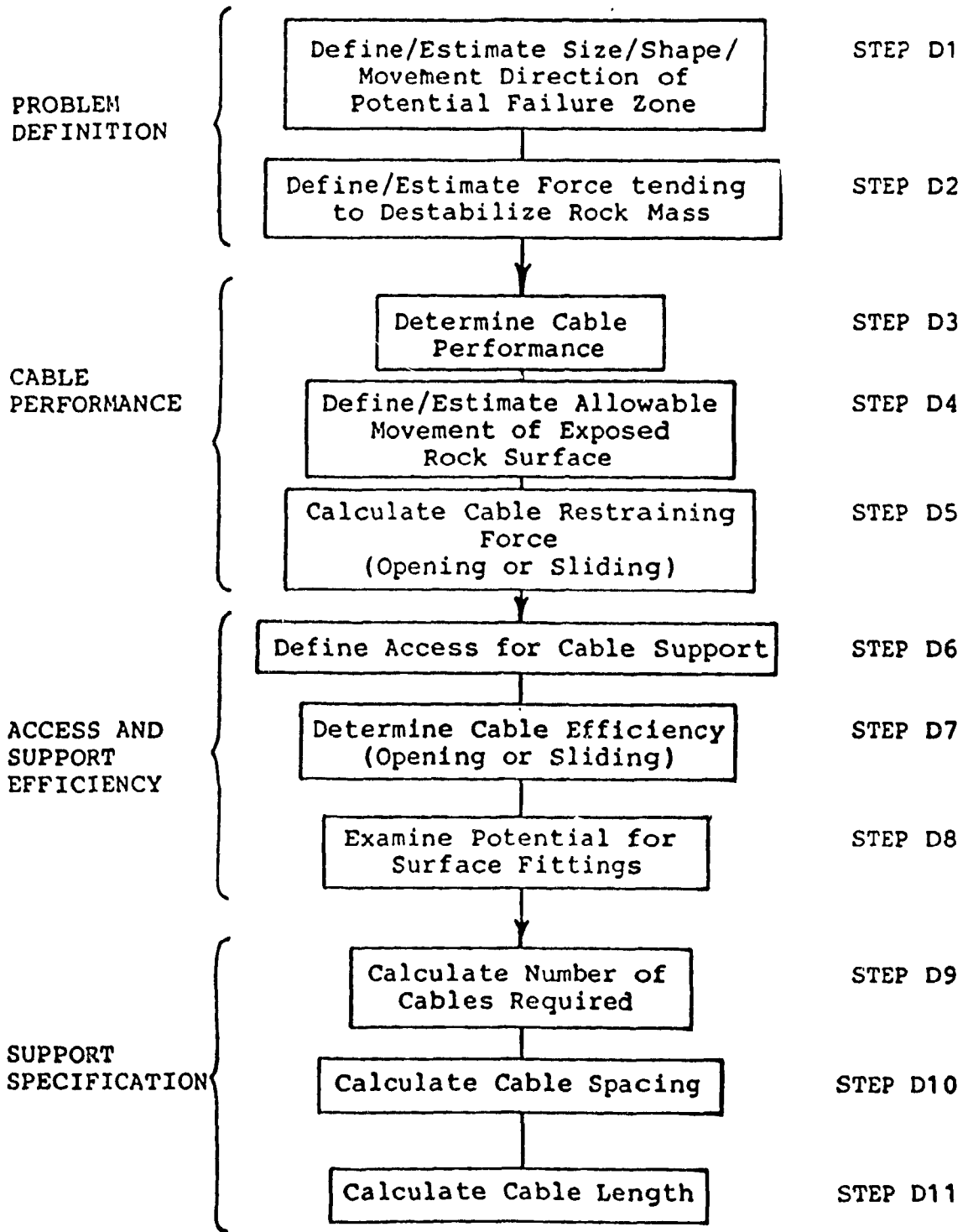
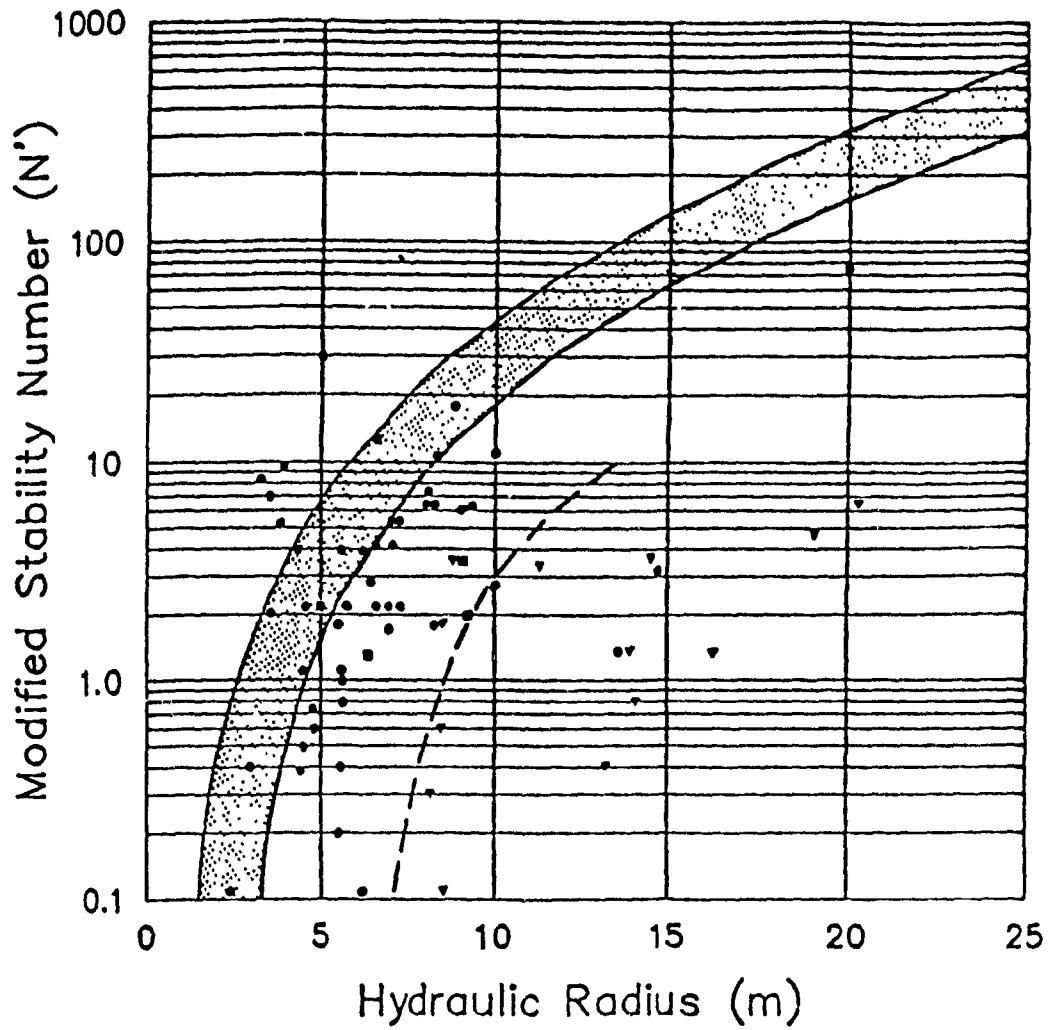


Fig. 2-8 Step D - Cable design flow chart [34]



- Stable Slope Surface
- Unstable Slope Surface
- ▼ Caved Slope Surface
- ▼ Caved Slope Where Cables Have Slid

Fig. 2-9 Modified stability graph [3]

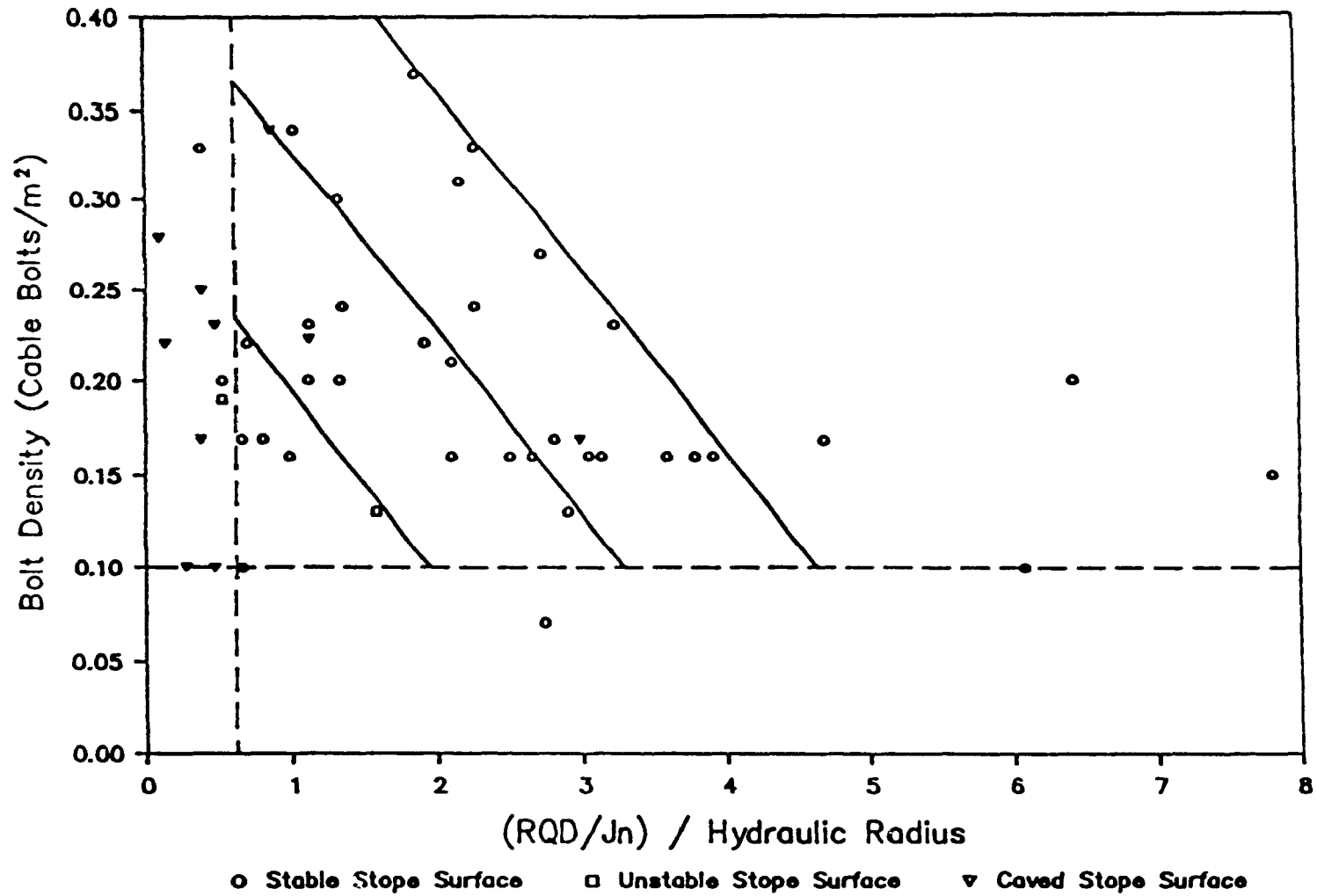


Fig. 2-10 Bolt density versus hydraulic radius [3]

I
The length of cable bolts must be designed in order to provide a proper anchor. Some form of relationship is expected to exist between the hydraulic radius of the stope surfaces and the length of cable bolt. These two parameters were plotted by Potvin [3] and are shown in Fig. 2-11 for the case of supported backs in the data base, and the following observations can be made.

- The data is scattered, indicating the lack of guidelines for support design and the trial and error process employed.
- The use of cable bolts in very large open stopes has had little success.
- The minimum stope plane dimension in which cable bolts have been installed has a hydraulic radius of approximately three meters.
- The minimum cable bolt length in the data base was three meters. This was decided arbitrarily prior to the data collection in order to differentiate cable bolt action and other kinds of shorter rock anchors.
- A conservative guideline is derived from the plot of cable bolt length and hydraulic radius.

Although the popularity of cable bolting has increased during this past decade, it seems that there is still no reliable design method.

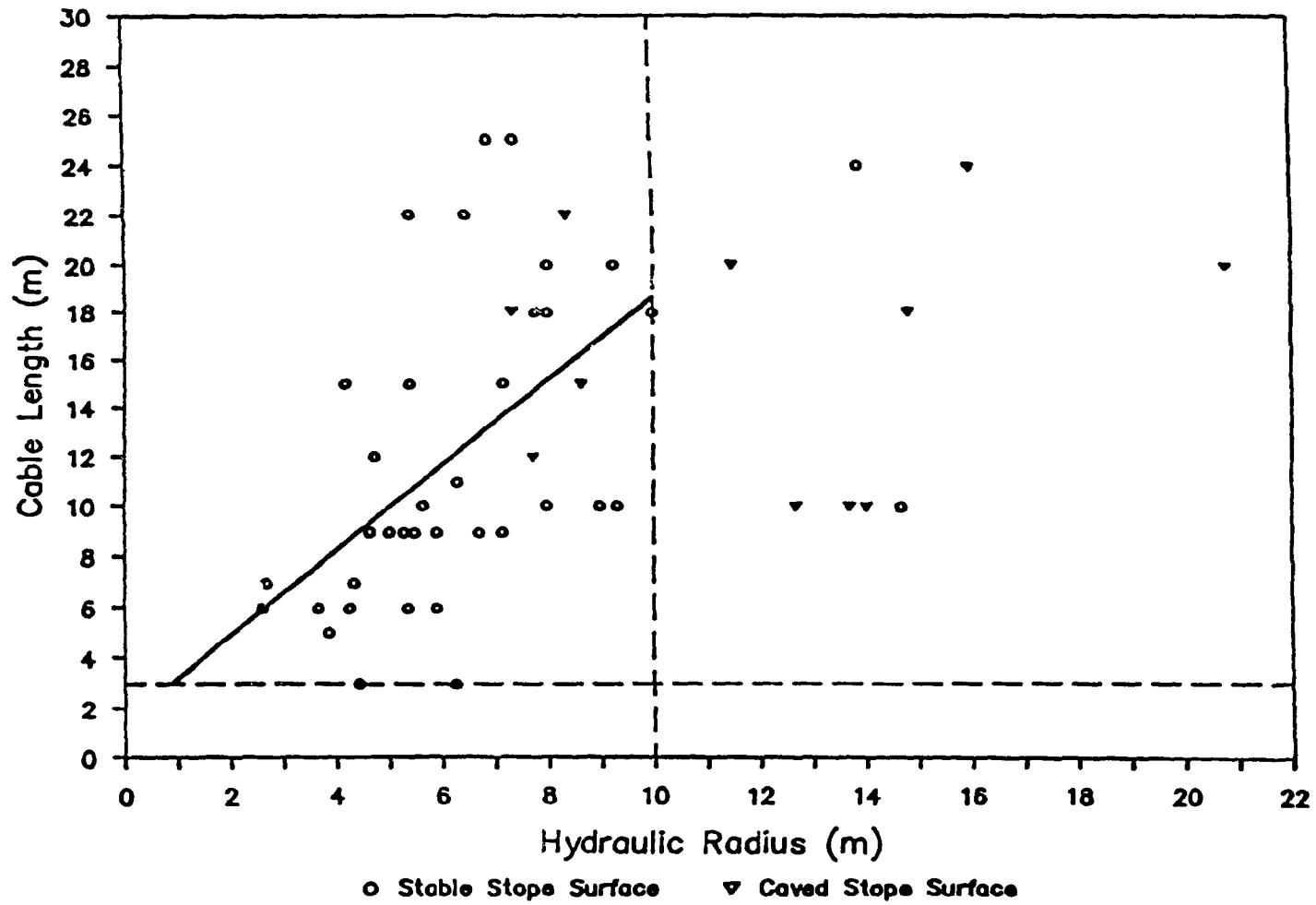


Fig. 2-11 Cable length versus hydraulic radius [3]

2.8 THE NATURE OF SHEAR BOND STRESS

Since cable bolting with grout is used in the vast majority of cases, the bond strength between the two materials is of considerable interest. Bond stress may be defined as the shear force per unit length, which acts parallel to the cable axis at the grout-steel interface. The force in the cable is transmitted to the grout by the bond, and vice versa, [37, 38]. Thus the bond stress can modify the cable stress. Another measure of the bond stress is the rate of change of stress in the cable bolt. There is no bond stress unless the cable stress changes, and there can be no change in the cable stress without change in the bond stress.

In the case of smooth bars, the bond between steel and grout is attributed to friction and chemical cohesion between the two materials. Bond failure in specimens reinforced with smooth bars can be characterized by the extraction of the bar from the grouted specimen. Cable bolts, however, depend primarily on mechanical interlocking. This does not mean that friction and chemical cohesion do not exist, but that they are of secondary importance.

In bond-type specimen testing, e.g. by pull-out testing, with deformed reinforcing bars, most bond failures are seen to be splitting failures of the surrounding matrix. Strictly speaking, splitting is not the same thing as bond failure. Splitting generally results from the wedging action of the lugs against the grout. Splitting failures are basically a tensional phenomenon, but the data available is too scarce, in respect to the strength and deformation properties of the grout in tension, to permit a separate analysis of the splitting phenomenon. Presently, splitting must be analyzed together with the shear stress phenomenon. Progressive splitting is

usually the primary evidence of bond distress in a pull-out specimen. It can progress to the outside, resulting in a final collapse of the bond.

2.9 THE BOND-SLIP MECHANISM

Since bond conditions at a rib differ significantly from those at locations between the ribs, it is impossible to obtain a bond-stress distribution which is applicable to all points on cable bolts. The average bond resistance increases as the slip progresses until the ribs begin to crush the surrounding matrix. Therefore, for strands with higher yield stresses, cracking becomes one of the most important factors in the pull-out test [39]. For this reason, extensive studies on crack formation within the grout adjacent to the deformed reinforcing bars have been carried out by researchers. Lutz [40] studied the fundamental mechanics of bond transfer between the bar and the grout. He established experimentally that slips result from deterioration of the grout, which crushed under high bearing pressures and shearing stresses from the bar ribs. Breoms [41] and later Goto [42] devised ingenious techniques to study the internal crack formations in the pull-out test. Breoms [41] injected colored resin near the bar ribs of pull-out specimens which were reinforced with a single steel bar to study the location, width and extent of internal cracks. Goto [42] replaced the resin by red ink, and his specimens were then sawed to examine the crack pattern. Numerous internal cracks were found to have formed around the deformed bar. These cracks formed cones with apexes near the bar lugs and with bases generally directed towards the nearest primary crack or towards the end of the specimen. According to Goto [42] the formation of internal cracks usually starts at low stresses

in steel and is influenced by the surface deformation of the reinforcing bars. He indicated that cohesion between steel and grout can be lost in some parts of the bar, and that therefore the bond between the deformed bar and the matrix depends on the mechanical resistance of the lugs and the frictional resistance between steel and matrix. The bearing pressure that develops at the lug interface can be resolved into two components (Fig. 2-12):

- 1) A component parallel to the bar concentric with its ribs, which is due to shearing stress in the cylinder of the matrix.
- 2) A radial component which tends to split the surrounding matrix; a phenomenon similar to bursting pressure in a pipe.

As mentioned earlier, internal cracks have a great influence on the bond mechanism. A pattern in Fig. 2-12 shows the teeth of the grout which are deformed by the compressive forces transmitted through the ribs of the bar as the tensile force in the steel is increased. Goto [42] noted that after internal cracks have been formed, the complete relaxation of the external tensile on the steel bar never reaches zero again. From this observation he concluded that if the pattern as in Fig. 2-12 is formed and undergoes plastic deformation, then it does not return to its former state as prior to loading, even where the tensile force in steel is relaxed; this is due to interlocking friction at the surfaces of the internal cracks.

To verify the analysis of the slip given by Lutz [40] and other investigators, Houde [43] tested sixty two concentric tensile specimens, each reinforced with only one central bar. Thirteen of the tests were conducted on specimens reinforced with special bars which were internally instrumented. After

testing, five of them were sawn parallel to the bar axis to expose the imprint of the bar. The examination of the sliced specimens revealed that the bar deformations were sharply stamped into concrete. Upon examination, Houde [43] did not detect any powdery areas, due to crushing under the rib pressure, nor polished surfaces due to sliding of the bar. Houde [43] concluded that the slip at the steel-concrete interface can be described as the internal cracking of the first layer of concrete that surrounds the reinforcing bar and as bending of the small concrete teeth, see Fig. 2-12.

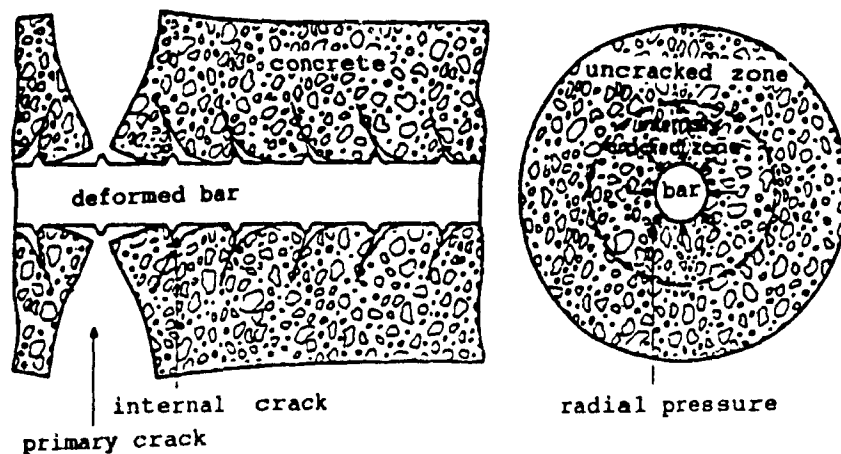


Fig. 2-12 Deformation of matrix around a bar [42]

2.10 ELEMENTS OF A CABLE BOLT SUPPORT SYSTEM

Due to the complex nature of the phenomena acting between the cable bolt and the grout, bond strength depends on a number of parameters. There is a general agreement among the majority of researchers as to the characteristics of grout which can influence bond strength, but it is difficult to estimate correctly their quantitative influence because of the diversity

of testing methods and the difficulty of interpreting the results. According to others, it is not easy to show separately the influence of the grout and rock characteristics on the bond, either because they act against the bond or directly against each other. Nevertheless, the load carrying capacity of the cable bolt depends upon several factors which may be categorized into three major elements, such as summarized in Table 2-1.

Support element	cable bolt	consists of different shapes and types of steel strand
Bonding element	grout	consists of cement + water and additives
host medium	rock mass	consists of geological material with inherent discontinuities at different stress regimes.

Table 2-1 Major components of cable bolts

These elements could have their own unique properties and behavior and most importantly, when integrated to comprise a support system, their interaction governs the total performance of the reinforcement and resultant stability. The support element and the bonding element are controllable, meaning that they can be engineered to meet the support requirement of the excavation. The host element or rock mass is a variable and site specific, and therefore is an uncontrollable element. It is important to bear in mind that the properties and behavior

of a rock mass together with its stress regime and excavation configuration plays an important part in the final design of excavation support.

2.10.1 CABLE BOLT

The strength of cable with respect to the axial load is determined by conducting appropriate laboratory tensile tests. The important physical properties are yield stress, axial and radial elongation, and modulus of elasticity. Based on the failure mode of cable, which in most cases is due to the weakness of the bond element between the cable and the borehole's wall, the surface properties of the cable are an important factor in design. In the following subsections the important parameters which affect the improvement of the bond element are reviewed:

a) The surface condition effect: The bond characteristics of cable bolts do not appear to be adversely affected by varying degrees of surface rust of the ordinary mild steel. On the contrary, it can actually be beneficial to the bond, and it is practical to assume that cable bolts with rust or scale are satisfactory [44]. Provided that a cleaned piece of bar meets the minimum requirements of the standard specifications. This conclusion was drawn by Kemp [45] after an extensive series of bond tests with deformed bars where varying amounts of rust and mill scale were the controlled variable. These have also found that it is not necessary to clean or wipe the bar surface before the bar is placed in the grout. It has been observed that in a given rust causing environment, the thickness of the rust will be about the same for all bar sizes. Therefore, the cable bolts of larger diameter, which and higher ribs, will be less affected by rust.

According to Stillborg [4] the surface properties of the cable have a significant effect on the bond strength. For a given grout under fixed curing conditions, a clean and rough surface of wires will improve the bond strength. The opposite is true if the wire surface is smooth and greasy. He also concluded that the increase in the bond strength, or in the load carrying capacity of the cable, is not proportional to the increase in the embedded length of the cable.

Fuller [44] examined the bond strength between cable and grout by pull-out tests. He explained that any protrusion in the surface of a cable significantly enhance the load transfer whereas indentations produce only minor improvement (see Fig. 2-13). Rust on an initially smooth surface is helpful in terms of load transfer but the achievement is much less marked with a rougher shape. They concluded that the steel-grout bond (cohesion) failed with small displacement between the wire and grout interface. Also, where the bond failure had occurred, friction between the failed surfaces contributed to the pull-out resistance.

b) The effect of profile of cable bolt: The cable profile effect is a more important parameter than the surface condition of the bar. Clark [45, 46] conducted some pull-out tests to determine the resistance to slip in concrete of seventeen different designs of deformed reinforcing bars (7/8 inch diameter) cast in the horizontal position. It can be deduced from his experiments that the height of deformation appears as an important factor when the concrete settlement is concerned. The pattern of deformation does not seem to be of any importance in determining the bond resistance, but the slope of the lugs appears to be a critical factor.

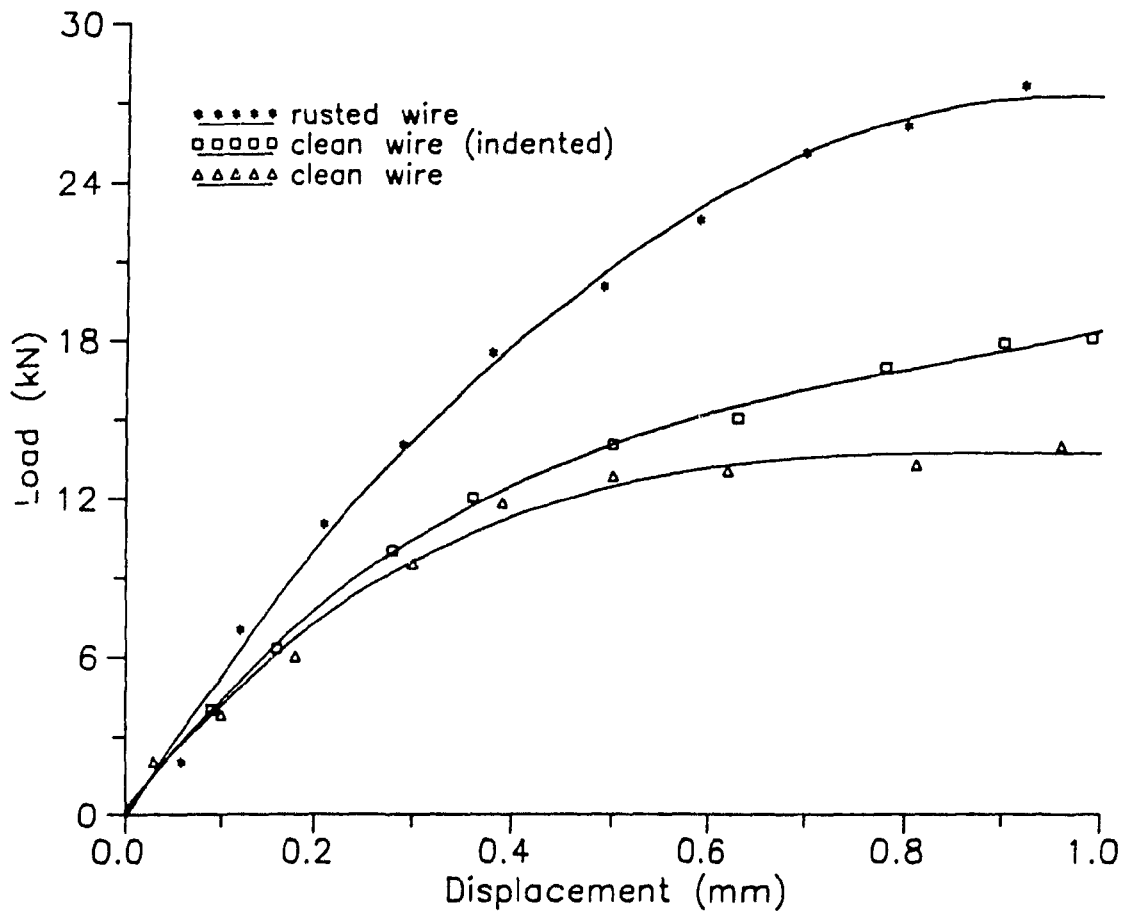


Fig. 2-13 Effect of surface conditions [6]

Wilhelm [47] proposed a study of the comparative bond efficiency of reinforcing bars with heights and spacings of ribs differing from the ASTM specifications. The purpose of the study was to determine if the height of the deformation could be lowered a relatively reduced spacing without adversely affecting the bond strength. It was found that changes in the deformation height do not affect the bond strength significantly, provided the total bearing area per unit length of the bar is the same.

The work of the past few years leads to the conclusion that the exposed surface area per unit length of the bar is probably the critical bond strength parameter for deformations of the reinforcing bar where the requirement is imposed that the face angle be not less than 45° . The height and spacing of deformations are important in the case of specimens with bottom case bars only, insofar as they affect the bearing area.

The behavior of several manufactured configurations of cables bolts have been experimentally demonstrated by Goris [48]. The objectives of the study conducted on grouted cable with conventional cable bolts, epoxy coated strands, birdcage strands and cables with buttons were to determine the basic qualities, influence and performance of the strands under various support conditions. The button is made of a heavy gauge annular piece of steel which is attached to the cable. It is shown that the different configurations of cable with embedded length 254 mm have a load capacity at least 77.8 KN. The behavior of birdcage strands and cables with buttons is influenced by many factors, the important one being the location of the nodes in birdcage cable and buttons in button cable bolts.

The manufacturing process of birdcage cable allows for a wide variety of configurations and capacity up to 500 kN.

Combination of a standard cable and a birdcage pattern allows for both improved load transfer and means for securing surface hardware [49].

Jeremic [50] also experimentally demonstrated the behavior of cable with buttons. It increases the bond stress by providing a greater shear stress resistance between two metal surfaces than would be obtained within the grout-cable interface, while transferring this additional resistance into the grout, so that the compressive strength to the grout may withstand it. If the button succeeds in increasing the strength of the system, then the manner in which it does so also creates a situation where cable stretch will be exaggerated between the button and the applied load. If the cable is forced to stretch more because the system can tolerate a greater load, then the lateral deformation or reduction in diameter of the cable will also be greater. This will bring more rapid destruction of the bond at the grout-cable interface forcing the button to carry a greater portion of the load.

c) The cable bolt diameter effect: In the area of reinforced concrete many authors have used either pull-out tests or beam tests to study the influence of the bar diameter on the bond strength. In some tests, the embedment length is held constant while the diameter of the bar varies; in others the ratio of the embedment length to the bar diameter is constant. The results differ greatly among the authors. Bernander [51] concluded from the pull-out tests performed on the deformed bars that, practically, the bar diameter does not have any influence on the bond strength. According to Jonsson [52], in the majority of cases the bond strength values decrease with the increase in the bar diameter for a given length to diameter ratio. This decrease is smaller for plain bars than for deformed bars. However, there is no unanimity as to the general validity

of the conclusion of Ferguson [53] who showed that the slips of large bars were somewhat greater than those of smaller bars. He also concluded that it appeared to be a reasonable approximation that the loaded-end slip of large bars increased roughly in proportion to the diameters of the bars.

Fuller and Cox [44] reported that friction between the cable bolt and the grout interface is very sensitive to even small variations in the diameter of the wires along its length.

2.10.2 BONDING ELEMENT OR GROUT

Since grout is the bonding agent between the cable and the surrounding rock mass its properties are important. Grout may be defined as the injection of suitable materials under pressure into the borehole in order to fix the cable bolt in place. One of the most popular types of grout is a mixture of water and Portland cement, because it is readily available with relatively low cost. For special purposes, additives or various chemical solutions as well as a number of other materials such as aggregate may be used in the mixture. In the following sections important parameters which affect the grout are reviewed:

a) The effect of water/cement ratio: It is one of the main factors in the grout mix. The chemical action in the formation of cement by hydration requires an optimum water-cement ratio of less than 0.3 [54]. From the practical point of view, the grout must have the properties that allow transportation and pumping into the borehole with a reasonable amount of work and cost. These depend upon the pumping facility performance and in the case of the presence of aggregate, then its shape, amount and size distribution will also affect to the amount of water-cement ratio.

Excess water results in bleeding of the mix and low strength, as well as greater shrinkage and lower durability of the hardened grout. The composition and type of Portland cement also affect the properties of the grout. Additives may be put in the grout mixture in order to increase its workability, so that the value of water-cement ratio may be decreased. It is necessary to ensure that the use of additives for one purpose do not affect the other properties of the grout.

In Fig. 2-14 the shear bond stress of cable versus the compressive stress of the grout are shown for various water to cement, cement to sand and additive ratios [50]. As can be seen the parameters which increase the compressive strength of the grout material can increase the shear bond stress of cable. It is shown that there is no straight relationship between compressive stress and shear bond stress.

b) The strength of the grout: This is assumed to be of primary importance in the development of the bond resistance and has received considerable attention from many researchers in the field of reinforcement concrete. It has been generally agreed that the slip resistance of steel reinforcement increases with the concrete strength for both plain and deformed bars, and for any type of bond test. Davis [55] attributed this increase in slip resistance to the compressive strength of concrete. Jonsson and Osterman [52] and others suggested different equations for this ultimate bond strength: they represent it as a function of the strength of concrete. In Europe the following linear variation has been most commonly proposed:

$$\tau_m = k_1 f'_c + k_2 \quad (2-3)$$

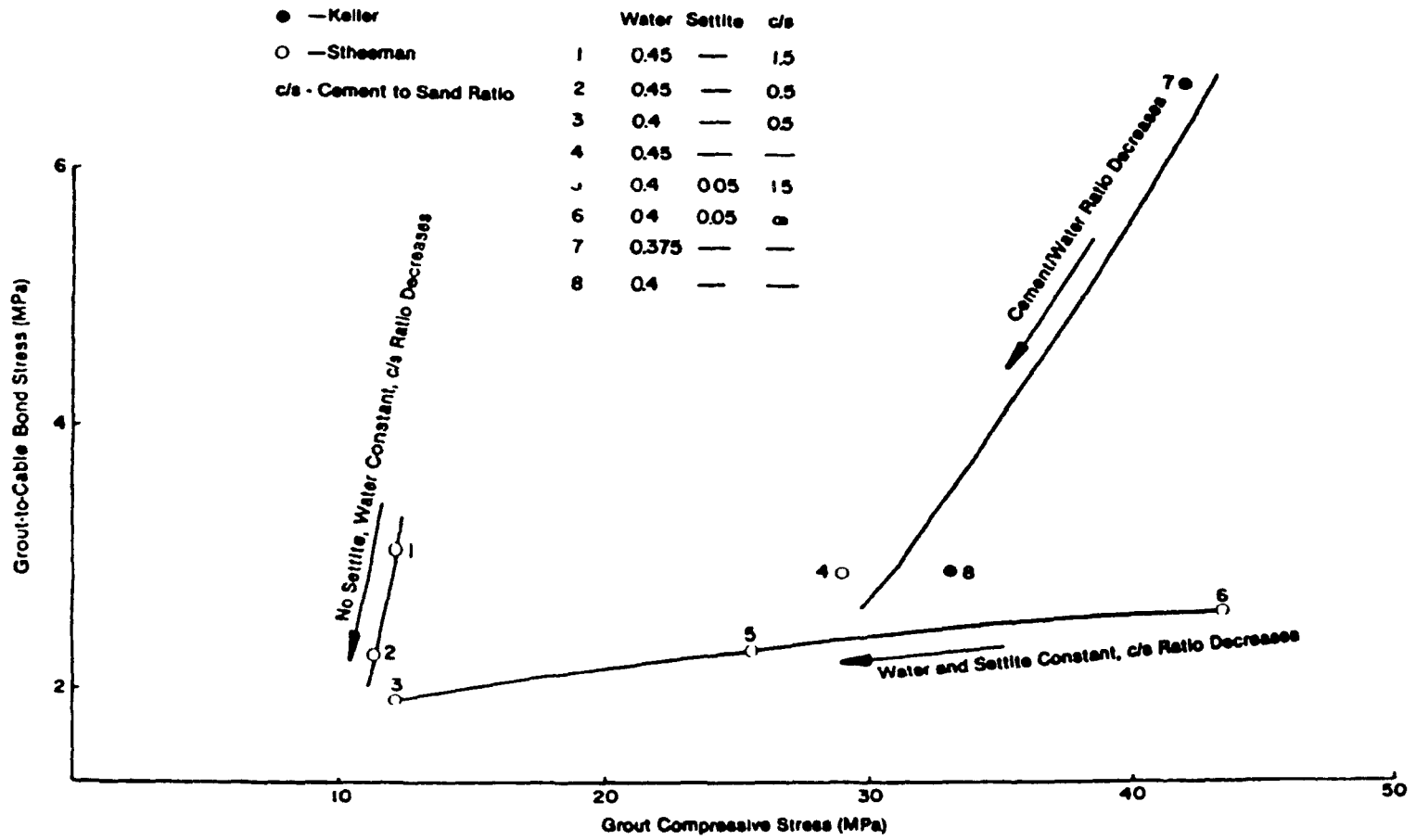


Fig. 2-14 Bond stress of cable bolt versus the compressive strength c' of the grout [50]

τ_m , f'_c represent the bond strength and the concrete compressive strength respectively, k_1 , k_2 are empirical coefficients which depend on the type of bar, the diameter, embedment length and the type of test.

Based on this data, Ferguson [53] established that the bond resistance varied approximately with the square root of the compressive strength and proposed the following equation:

$$\tau_m = k\sqrt{f'_c} \quad (2-4)$$

Pull-out tests with different types of cable bolts sealed by cement grout with or without additives were conducted by Stillborg [4]. In general it has been found that there is no correlation between the compressive or tensile strength of the grout in standard tests and the bond strength in pull-out tests.

c) The cement effect: The type of cement used in bond stress has received little attention from the researchers, but based on the work of Muline and Strova [56], the following conclusions can be drawn:

- i) For plain bars, Portland pozzolan cement and modified Portland cement reduces the bond from 25 to 75 percent, as compared to ordinary Portland cement. The type of aggregate is not important but by decreasing the water-cement ratio then the bond strength can be improved.
- ii) For deformed bars, the bond varies significantly with the quality of cement and the nature of aggregates. The bond increases with the amount of gravel, but there is no unanimous agreement on the influence of the cement content on the bond between steel and the grout.

d) The type of aggregates: The desirable and undesirable properties of aggregates, which can influence the mix design, have been surveyed in a number of text books on concrete technology [54, 57, 58, 59]. The most important factor is that the aggregates remain stable within the sand grout (shotcrete) through its design life and in the particular environment involved. A good aggregate specification depends on the resources available; in general, grading, cleanliness and mechanical properties are important (BS. 882, 1983). Where clay, silt and dust are present, they may occur as particle coatings and this can have an adverse effect on the aggregate matrix bond. Clay may also occur in the form of discrete particles or clay lumps, which due to normal dust coating, are often visually recognized in the field as different from the aggregate particles. This presence may become apparent if the aggregate is wetted or washed. Water absorption is an indirect measure of permeability of the aggregate, which in turn is related to the strength and durability of the grout.

The goal of combining different sizes of aggregate is to provide a material which will have the lowest possible surface area and void content per unit volume. However, lower unit surface area requires a lower water-cement ratio and also increases the desirable workability and shear strength.

In the case of presence of aggregate in the grout, the shape of the aggregate may affect in the properties of grout mix in both the fresh and hardened state. Flakiness of the aggregate can have an adverse influence on the workability of the grout; also the strength of the grout will tend to be reduced. According to Nevil [54], the surface texture can adversely affect the compressive and tension strength of the grout, when the bond with the cement matrix is not sufficiently strong to enable the maximum shear strength of the grout to be realized.

The presence of organic matter, mica, chalk, shell, sulfates, chlorides, metallic impurities, etc. has also to be considered in the design procedure.

The effect of sand in the grout has been considered to study the shear bond strength of the cable bolt. Stheeman [60] demonstrated the effect of fine aggregate in the grout mix by means of pull-out tests on the shear bond strength of the cable bolt. Since the tests were performed in the field, the environmental condition could not be controlled well. However, the results showed lower shear strength than for cement grout.

e) Thickness of the grout: The thickness between the cable and the borehole's wall may be calculated based on the equilibrium condition in the direction of the cable bolt for the load carrying capacity at the cable-grout and grout-rock interfaces. According to Littlejohn [61] the pull-out force can be:

$$P = 2\pi\tau_{\max} \cdot r_c \quad (2-5)$$

where τ_{\max} is the ultimate bond or skin friction at rock-grout contact.

Most countries, for example, Canada, France, Australia, Switzerland and USA, use this equation, whose validity is based on the following assumptions:

- i Uniformity of the bond stress distribution, over the entire perimeter of the fixed anchor.
- ii Diameter of the borehole and the fixed anchor are identical.
- iii No discontinuity or inherent weakness plane exists, along which the failure could be induced.
- iv No local debonding at the grout-rock contact exists.

The maximum average shear bond strength at the grout-rock contact should not exceed the minimum shear strength of the rock mass with a safety factor, which normally is more than two. Based on short-term failure tests, Littlejohn and Bruce [61] recommended, the maximum shear bond strength at grout-rock interface equivalent to 10 percent of the uniaxial compressive strength of rock mass for a deformed bar and should be less than 4.2 MPa.

The Australian Code SAS [62] states that a higher value of 1.05 N/mm^2 has been used in a wide range of igneous and sedimentary rocks. However, site testing has permitted bond values up to 2.1 N/mm^2 to be employed.

The Canadian Manual C.M.F.E [63] recommends 1.4 MPa, or the minimum of:

- 1/30 times the uniaxial compressive strength of the rock.
- 1/30 times the uniaxial compressive strength of the grout.

With regard to the failure of the grout-rock interface two considerations could be made. Coates [64] has suggested that the grout may shrink in the curing process. In this case the bond would already be broken and the only remaining support for the system would be the tensile stress created in the rock beyond the end of the anchor. If the failure of the anchor is due to tensile stresses in the rock with failure initiated at the bottom of the anchor, then this will create an inverted cone of rock bounded by planes on which diagonal tensile act. The other case is that the hole will shrink instead of the grout, causing an increased pressure at the grout-rock interface, and subsequently an intense frictional force which will resist movement of grout.

f) The environmental effect: This includes the storage condition of specimens and materials as well as temperature effects and weathering conditions (freezing and thawing, wetting and drying). These parameters have not been investigated for cable bolting but for rebars have been studied by numerous investigators [65, 66, 67]. The general conclusion is that the bond strength is more sensitive to environmental factors than the compressive strength.

It was shown in experimental work that in most cases, regardless of the duration of curing, the maximum bond strength for air stored specimens is greater by approximately 40 percent than that for specimens continuously maintained moist. Also the shear bond strength is substantially affected by either an increase or a decrease in temperature.

Koh [66] studied the effect of freezing and thawing on the bond strength of pull-out specimens at an early age. It was concluded from pull-out tests that the maximum bond strength is substantially reduced by repetition of freezing and thawing at an early age. The effect is more pronounced when the grout contains more water. The temperature during the first three days of hardening has a great impact. A thin layer of ice on the surface of the bar at the time of grouting reduces the bond strength considerably.

Stillborg [4] presented the compressive and tensile strength of the grout for different conditions of curing. In general the temperature effect is less important than the water-cement ratio and humidity effect. Temperature has an influence on the speed at which the grout strength grows. The difference in temperature is only significant if the grout is to be loaded in the first 40 days of the curing period. In pull-out tests it has been shown that the compressive strength

of the grout controls the failure process of the grout when the interlock between the wires of the cable and the grout is broken.

2.11 DISTRIBUTION OF SHEAR BOND STRESS

The behavior of fully grouted anchors subjected to axial load was examined by Hawkes and Evans [33]. The results are shown in Fig. 2-15, representing a linear relationship between normal stress and bond stress before slipping occurs. The mathematical distribution of the bond stress was formulated as follows:

$$\tau_0 = \tau_l \text{Exp} \left[\frac{-2Ax}{r_c} \right] \quad (2-6)$$

$$P = \frac{\pi r_c^2 \tau_l}{A} (1 - \text{Exp}(-2AL/r_c)) \quad (2-7)$$

Where

- x = distance from end load face of sample;
- A = slope of variation of normal stress of anchor with respect to the bond stress;
- τ = bond stress at section x ;
- τ_l = bond stress at end load face;
- P = load at section x ;
- r_c = radius of cable bolt;
- L = length of specimen.

Later, Philips [68] simplified the mathematical relationship of Hawkes and Evans [33]. By assuming that the pull-out load equals the shear force which acts on the exposed surface of the anchor, then the following equations were derived:

$$P = \frac{4\pi r_c^2 \tau_l}{A} (1 - \text{Exp}(-AL/2r_c)) \quad (2-8)$$

$$\tau = A \frac{P}{4\pi r_c^2} \text{Exp}(-Ax/2r_c) \quad (2-9)$$

The stress distribution for $A=0.01$ is approximately uniform, while for $A>0.01$ it is exponential, see Fig. 2-16. Philips [68] formulated a hypothesis of a linear relationship between E_a/E_r and $1/A$ and confirmed the basic parameter of Hawkes and Evans [33].

The distribution of the bond stress along a cylindrical anchor root has been studied numerically in the elastic range by Coates and Yu [69]. They investigated anchors with a strictly elastic behavior modeled by the axisymmetric finite element method in a set of two materials with two different moduli of elasticity. However, they demonstrated a uniform stress distribution in the soft rock and an exponential form in the medium hard rock and hard rock environment. Soft rocks were defined as those with uniaxial compressive stress less than 7 MPa where the E_a/E_r ratio was greater than 10 (see Fig. 2-17).

The behavior of anchors grouted in rock was modelled in a set of three materials (steel bar, grout and rock) by Hollingshead [70]. Based on published results [69], the anchors with an elasto-plastic behavior were simulated by an axisymmetric finite element method. With the Tresca criteria, Hollingshead [70] explained that yielding begins to develop at the loaded end of the pull-out specimen and progresses inward with a consequent stress transfer to the bar as the load increases. The shear bond stress distribution in the elastic range showed an exponential form of distribution along the embedded length. The maximum shearing stress moves deeper with the increase of load, upon which the upper part of the bar is progressively debonded.

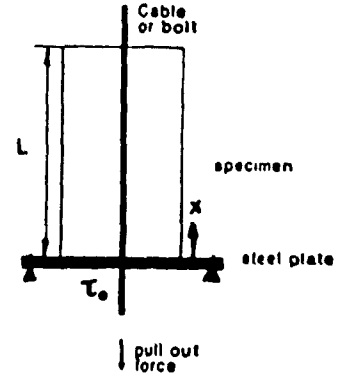
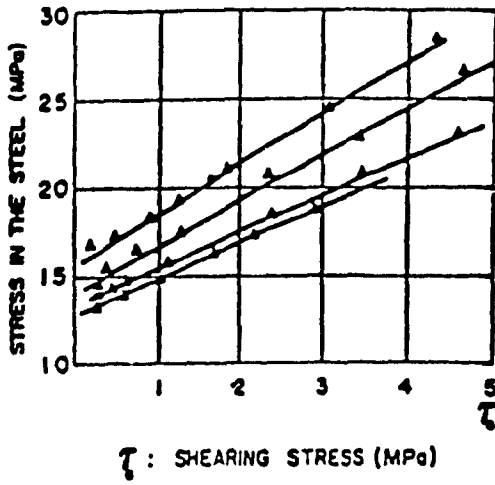


Fig. 2-15 Steel stress versus shear bond stress [33]

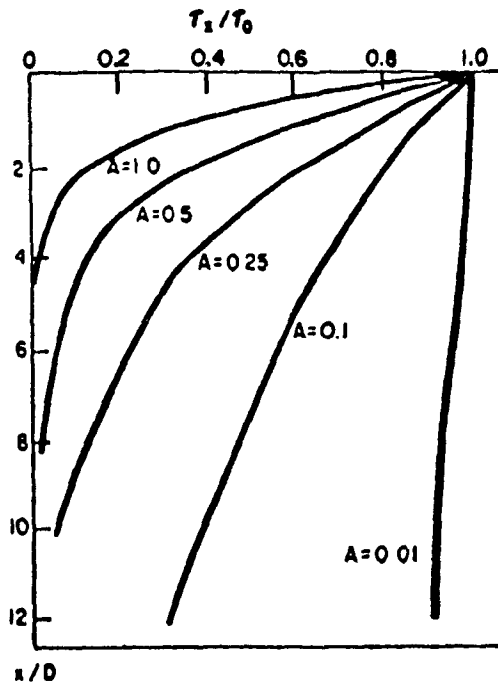


Fig. 2-16 Stress distribution along the embedded length [68]

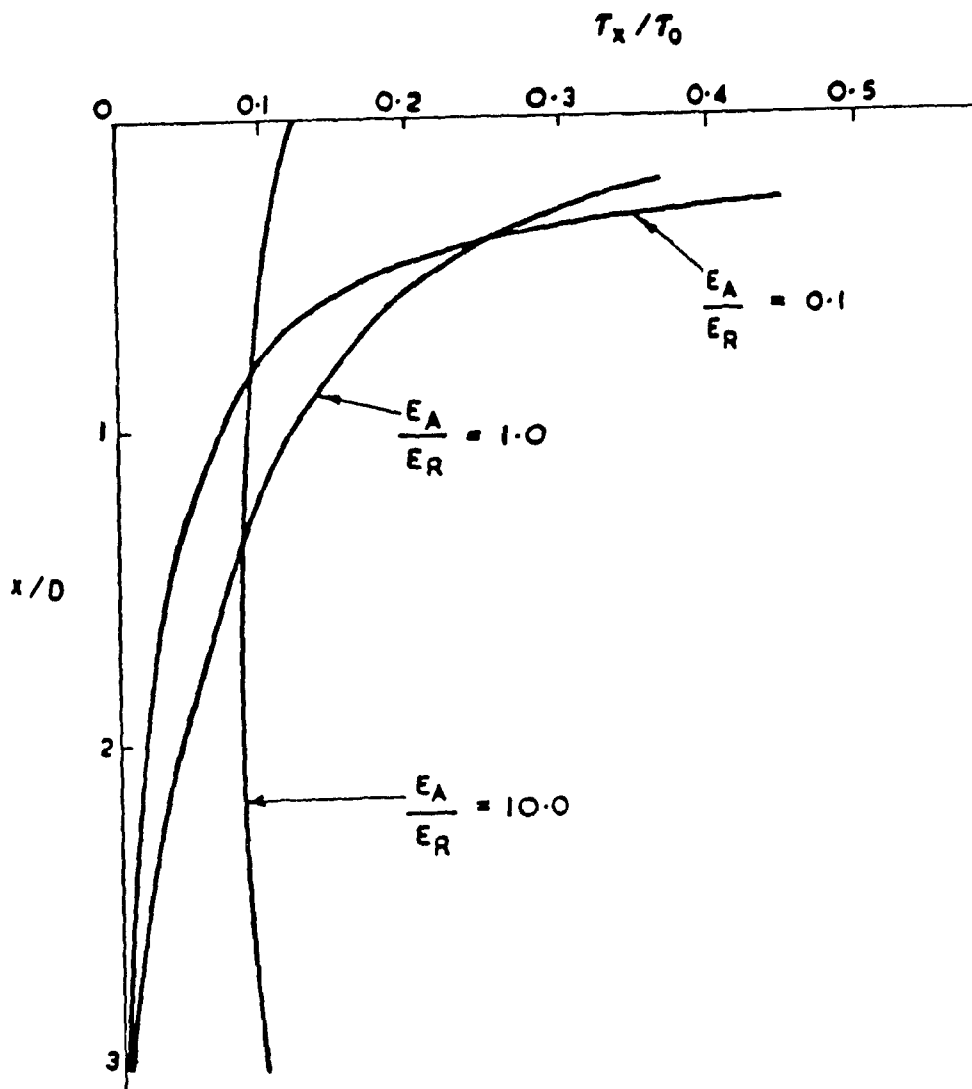


Fig. 2-17 Distribution of load along the embedded length [69]

Farmer [71] developed an analytical approach which investigated the behavior of the bar and grout assuming that the rock was rigid. He supported his outline with experimental results and proved that if the boundary conditions were satisfied, then the distribution of bond stress is non-linear for hard rock prior to the bar yielding as follows:

$$\tau_0 = \alpha \frac{P}{2\pi r_c} \exp(-\alpha x) \quad (2-10)$$

where

$$\alpha^2 = \frac{E_g}{E_c r_c (r_g - r_c)}$$

Properties of resin simplified the eq. 2-10 as follow:

$$\tau_0 = 0.1 \sigma_0 \text{Exp}(-0.2(x/r_c)) \quad (2-11)$$

where σ_c is the tension stress at load end face, r_c is the radius of cable and r_g radius of borehole.

Based on the Farmer [71] approach, the distribution of bond stress was studied experimentally by Dunham [72, 73]. He explained that the trend of the bond stress distribution remains sensibly exponential due to small movements. The experimental results showed that at low normal loads the initial stress distribution was close to the theoretical. At higher loads debonding of the anchor occurred over at least half of the anchor length and the stress was distributed according to the amount of the relative movement. Hence the degree of frictional shear strength was mobilized. The load on the anchor was dissipated over a transfer length equivalent to the optimum design length for any prescribed anchor.

In small scale models, pull-out tests were carried out by Ballivy and Dupuis [32]. They showed that the distribution of stress in brittle rock is exponential along the length of the anchor. The value of the "A" parameter of Philips [68] was verified to be $A=0.29$.

The experimental and theoretical studies concerning the breaking phenomenon of the deformed bar which was sealed with the grout in brittle rock were performed by Ballivy [74]. He explained that once the elastic limit of the seal is attained, then a progressive failure of the seal is produced at the bar-grout contact. This failure is characterized by shearing of the grout at the steel-grout contact, which is a progressive failure due to the propagation of a deep concentration of stresses. Locally, the phenomenon is similar to the shearing failure of grout, or to a compressive failure of the grout links at 45° . The maximum value of the shear stress for the steel-grout shearing stress is given by:

$$\tau_{\max} = \tau_0 = \frac{\sigma_c}{2} \tan(45 - \phi/2) \quad (2-12)$$

Ballivy [74] explained the anchor failure by the elastic behavior of steel. In order for the grout to be formed by a system of links at 45° which work in uniaxial compression, it is necessary for the bar to have radial contraction. If the bar is only slightly distorted, then the links of the grout are subjected to a triaxial system of stress. In theory, then, it is possible to obtain a cohesive stress τ_{\max} , the value of which is greater than $\sigma_c/2$, if a bar with a very high elastic limit is used and if the breaking of the first link is prevented, thus confining the following link. The loss of linearity in

the load versus distortion curve corresponds to the elastic limit of the steel and the breaking load corresponds to the grout break.

Yap [75] investigated the Finite Element Method, based on the Von Mises failure criterion, and showed similar results as Hollingshead [70]. In fact, the field conditions including the surface characteristics of both models, did not consider the quality of the contacts between cable, grout and rock-grout interface. Mechanical parameters were not considered in either models. Such values are to be determined by tension or compression tests on specimens of the grouted rock. It has also been shown by Ballivy [76] that the mechanical characteristics of the sealing products tested in laboratory conditions do not display valid results with respect to the pull-out force.

2.12 CONCLUSION

In general two different support concepts, passive and active, have been employed for rock reinforcement. It is apparent that pretensioning of the cable bolts is not required in the majority of underground cable bolting situations except where the horizontal stresses are low.

Untensioned fully grouted cable bolts are employed in rock masses before relaxation arises from rock deformation. After stoping then the relative displacement between the rock and the steel strands produces the tension in the cable bolts. Relatively few failures of cable bolts take place due to breaking of the steel strands. Often large blocks slip off the cables and the strands tend to be left with a curled and twisted shape and totally stripped off the grout. This mode of failure is due to the weakness of the shear bond strength between the

cable and the surrounding matrix.

Some efforts have been made to modify the shear bond strength as follows:

- Modification of profile, attaching extra pieces on the exposed surface, changing of configuration, increasing the friction of the exposed surface and using epoxy resin are some improvements that can be made to the shear bond strength of cable bolts.
- Since grout is the bonding element in cable bolting, its properties can be controlled by modification of the water-cement ratio, curing time, diameter of the borehole and compressive strength of the grout. Little published data on the effect of aggregate on the shear bond strength of cable bolting is available.
- The load carrying capacity of the cable bolt depends on the distribution of load and shear bond strength along the embedded length of cable. The properties of the grout, rock mass and slip between the cable and the surrounding matrix are important factors that can affect such strength distribution.

CHAPTER 3

SCOPE AND OBJECTIVES

3.1 INTRODUCTION

Cable bolting is a method of underground support which offers an internal reinforcement of rock structures and the stabilization of large rock mass volumes. The support consists of cement grout pumped into pre-drilled holes that have one or more cables installed in them. This method was developed in parallel to the other major technological changes in underground mining methods, in order to take advantage of large mechanized equipment. The advantages of the cable bolt support system are as follows [77]:

- Easily combined with other support systems;
- Added space: more flexibility due to increased work area;
- Versatility: application to any shape of excavation;
- Ease of mechanization: installation can be totally mechanized;
- Economical: in terms of the stability improvement offered.

Neither pre-tensioned nor untensioned cable bolts provide adequate reinforcement in highly fractured, soft, or wet ground where proper anchorage is difficult or excessive corrosion may occur. The pre-tensioned cable bolts subject to loss of tension if installed in areas close to blasting operations.

When a tensile force is applied to the cable bolt, then this will be transferred to the cement grout and rock mass through the shear bond stresses at the steel-grout and grout-rock interfaces (see Fig. 3-1). This causes differential bolt extension and shear along the interfaces. Therefore, the efficiency of the fully grouted untensioned cable bolt depends upon the bonding preparation between the bolt and the borehole's wall. Its behavior depends on the properties of grout, rock mass and cable bolt in addition to the initial stresses.

3.2 PROBLEM DEFINITION

According to Fuller and Cox [6], the bond stress between cable and surrounding matrix fails with minimal slip. Further resistance relates to the mechanical interlocking between grout and surrounding matrix. In conventional cable bolting the poor performance of shear bond strength is demonstrated by the lack of broken cables. Essentially the improvement of the load carrying capacity of the cable bolt is provided by utilization of the potentially large residual strength between cable and borehole's wall. The behavior of the shear bond stress depends on the properties of the cable, rock mass, and grout.

Steel cable is manufactured under carefully controlled conditions; its properties are determined in the laboratory and described in a manufacturer's certificate. Therefore, the designer only needs to specify the cable as accepted within the relative standard. A number of modifications have been used to expand the range of cable bolting systems available to design engineers, e.g. adding an internal anchor (button), changing the configuration of conventional cable bolts (bird caging cable) and using epoxy resin cable bolts (see Fig. 3-2).

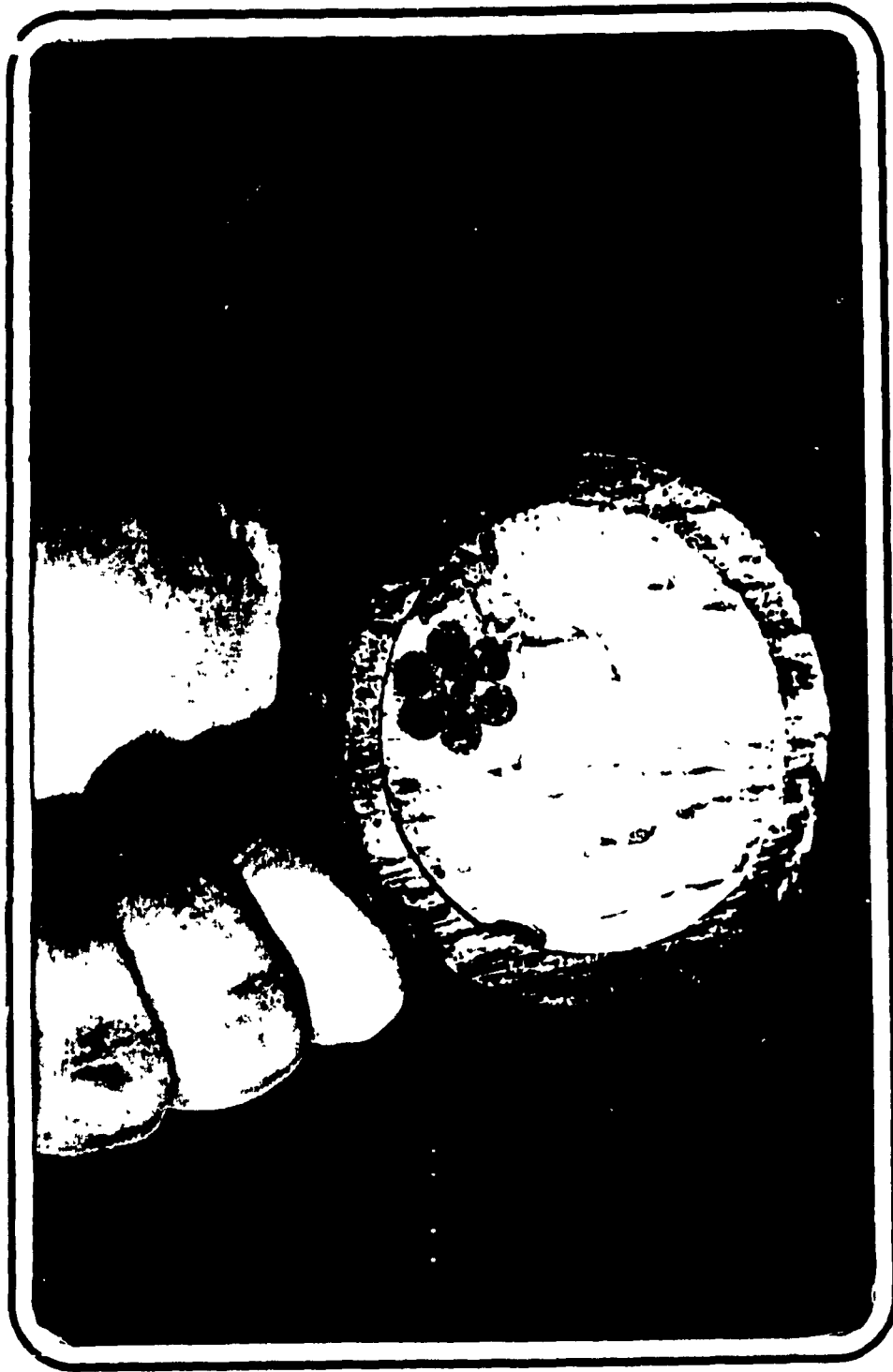


Fig. 3-1 Force in the cable is transmitted to the surrounding matrix through the bond element (grout)

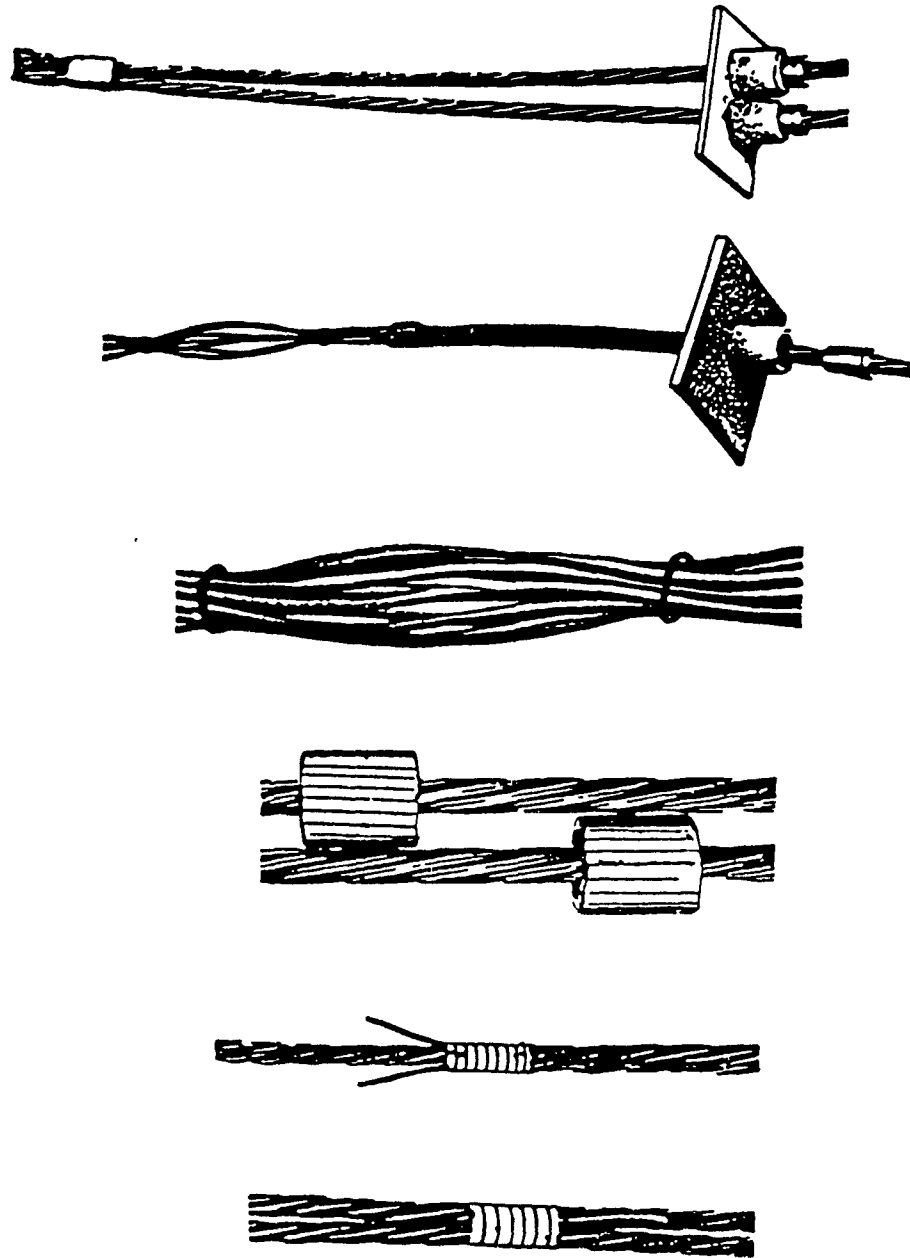


Fig. 3-2 Modification of exposed surface of a cable

Since the behavior of the fractured rock immediately surrounding the excavation surface is not sufficiently well known; it is difficult to determine the corresponding support requirements. Basically the supports must ensure the integrity of the fractured rock surrounding the opening as far as possible. To do this it must restrain the relative displacements between individual blocks or fragments while accommodating the inevitable bulk movement of the fractured mass. However, the requirements of the support elements are that they should:

- a) be stiff so that they can act as soon as possible, but
- b) retain the ability to yield through applicable displacement at load values less than critical.

Although the qualities of cement are guaranteed by the manufacture, as in the case of steel, the properties of the grout are more dependent on the production process than the actual placing of grout and cable bolt. However, due to practical restrictions on the modification of the steel strands, the improvement of the grout material is key to contributing to any significant increase of the load carrying capacity of cable bolts.

In comparison with other support systems, such as rock bolts and steel sets, sufficient research has not been conducted in industry on the support mechanisms or improvement of cable bolt design.

The author considers that adding aggregates larger than sand grains would be beneficial since it has been demonstrated that aggregate size increases resistance to slippage along planes formed when the grout cracks. In this approach the bond element could be modified rather than the chemical composition or improvement of the cable element. The investigation technique conventionally employs cable bolt with a diameter of 15.2 mm.

The main variations with this technique relate to the grout material and installation technique.

In order to increase the interlocking properties between cable and the surrounding borehole's wall, aggregate with an appropriate size distribution can be introduced into the conventional grout material consisting of proper water-cement ratio. The aggregate size distribution together with the cement to water ratio has a major influence on the mechanical properties of the support element.

3.3 OBJECTIVES AND METHODOLOGY

The following are the objectives of this study.

- 1- To evaluate by appropriate field trials and testing
 - a- The concept and feasibility of using a grout-aggregate mix (aggregate+cement+water) instead of normal grout (water+cement) as an alternative bonding material in cable bolting
 - b- The pumpability of this mixture.
 - c- The practicality of the installation technique as well as the installed cable bolt support capability.

- 2- To develop an appropriate grout-aggregate mix which would give the optimum bonding resistance between the cable bolt surface and the surrounding matrix. This objective is to be met by a laboratory based testing program of pull-out tests using cylindrical segments of concrete with a central hole that hosts the cable and the grout-aggregate mix. The laboratory

investigation is to cover a number of important design parameters such as the specimen size, its length and the mix properties, such as water-cement ratio, aggregate-cement ratio.

3- To develop an analytical model that is capable of calculating the shear bond stress distribution along the cable bolt surface. The variational method is to be employed in the formulation of the analytical model. The model is to be verified using the test results from the laboratory. A parametric study will then undertaken for a better understanding of the support strength characteristic of cable bolts in the different mix properties.

4- To develop a numerical model based on the finite element method which would have the capability of simulating cable bolts in underground excavations in rock. The finite element computer model called MSAP2D (Microcomputer Static Analysis Package for 2-Dimensions problems) which has been developed at McGill for the design/analysis of underground openings in a rock mass is to be adopted to include the simulation of cable bolts. A special cable bolt "element" is to be developed and incorporated into the MSAP2D.

5- It is planned to undertake a comparison between the experimental results, variational model and finite element method. To examine the effect of cable bolts on the stability of the mine stope, a simulation will be carried out using the above mentioned numerical model to demonstrate a practical example.

CHAPTER 4 IN SITU INVESTIGATION

4.1 INTRODUCTION

In order to evaluate the workability and concept of the grout-aggregate mix for fixing cable bolts in underground mining environments, an in situ investigation was conducted at the Dome Mine, Ontario, Canada. In this preliminary in situ trial the following parameters were evaluated.

- Bond strength;
- Effect of bond length;
- Effect of the grout mix on strength;
- The feasibility of the application of the grout-aggregate mix as a grout material.

4.2 MATERIAL SPECIFICATIONS

a) Cable bolt:

The steel cable generally used in practice was chosen for this investigation. Its specifications is given in Table 4-1.

b) Grout aggregate:

The mix proportions of the grout-aggregate is given in table 4-2. However, there were no admixtures incorporated into the mix. The concrete sand was from a natural gravel source

which was crushed; the crushed stone is from a quarry and would be 100 percent crushed to minus 3/8 in. The grading limits of combined aggregate is given in Table 4-3.

Parameters	Metric
Standard diameter	15.2 mm
Number of wires	7
Breaking load	270 kN
Weight per meter	1.1 kg/m
Metallic section area	138.7 mm ²
Modulus of elasticity	194 ± 6 GPa

Table 4-1 Cable bolt specifications

Mix proportions	Weight %
Portland Cement Type 10	22
Concrete sand	59
Crushed stone 3/8 in	19
Total	100

Table 4-2 Mix proportion of grout-aggregate

Sieve	Retained %	Passing %	ACI Spec.[78]
3/8	6.4	93.6	90 ~ 100
# 4	17.4	76.2	70 ~ 85
# 8	7.7	68.5	50 ~ 70
# 16	12.3	56.2	35 ~ 55
# 30	17.5	38.7	20 ~ 35
# 50	19.0	19.7	8 ~ 20
# 100	13.0	6.5	2 ~ 10
# 200	5.5	1.2	-
pan	1.2	-	-

Table 4-3 Grading limits for combined aggregate

4.3 TESTING EQUIPMENT

An Enerpac hydraulic pump and jack with a capacity of 600 kN was applied for the pull-out test. Two plates with dimensions of 25 x 25 cm and 13 x 13 cm were used at the back and front of the jack. The cables were fitted with small gripping devices for the pull-out test operation. A potentiometer was used for displacement measurements (see Fig. 4-1). Due to the longevity of each test, the hydraulic pump was subsequently replaced with a pneumatic pump. The pneumatic pump applies a constant

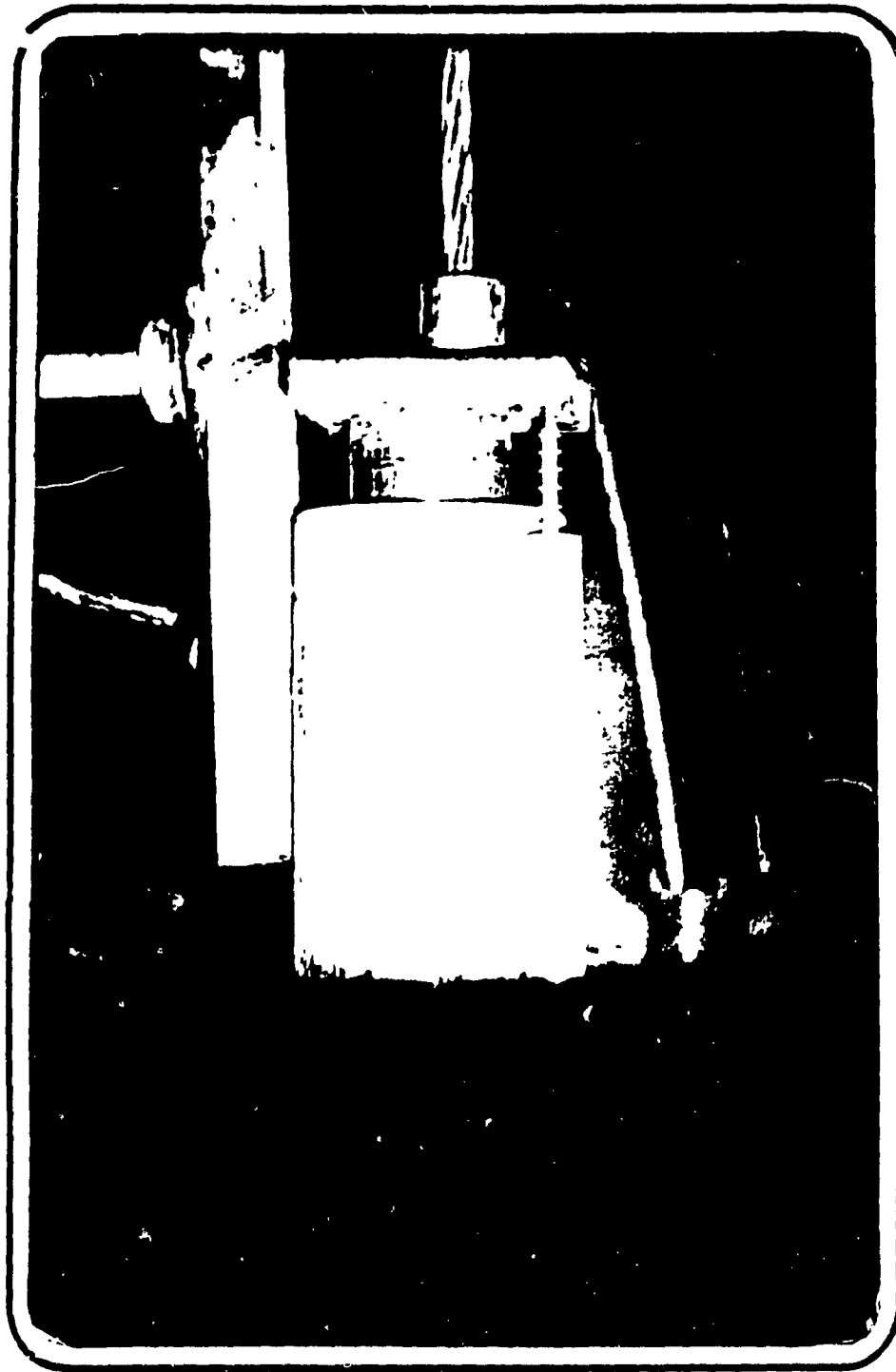


Fig. 4-1 View of the jack and potentiometer

and regular pressure with comfortable operation. This method was successfully applied for the majority of the pull-out tests.

4.4 TESTING SITE

The testing was conducted at the Dome Mine in South Porcupine, Ontario. A total number of 64 holes of different length were drilled in one of the development areas at a depth of 1100 m. All the holes were drilled horizontally and for a longer length than the cable to obviate end effects between the cable and the hole. The location of holes are shown in Fig 4.2 and size, length of the holes and cable are given in Table 4-4.

No. of holes	Length of the cable		Diameter of hole		Hole length	
	m	ft	m	in	m	ft
16	3.35	11	50	2	4.27	14
16	2.74	9	50	2	3.35	11
16	1.82	6	50	2	2.44	8
16	0.91	3	50	2	1.52	5

Table 4-4 Dimensions of the cable and borehole parameters

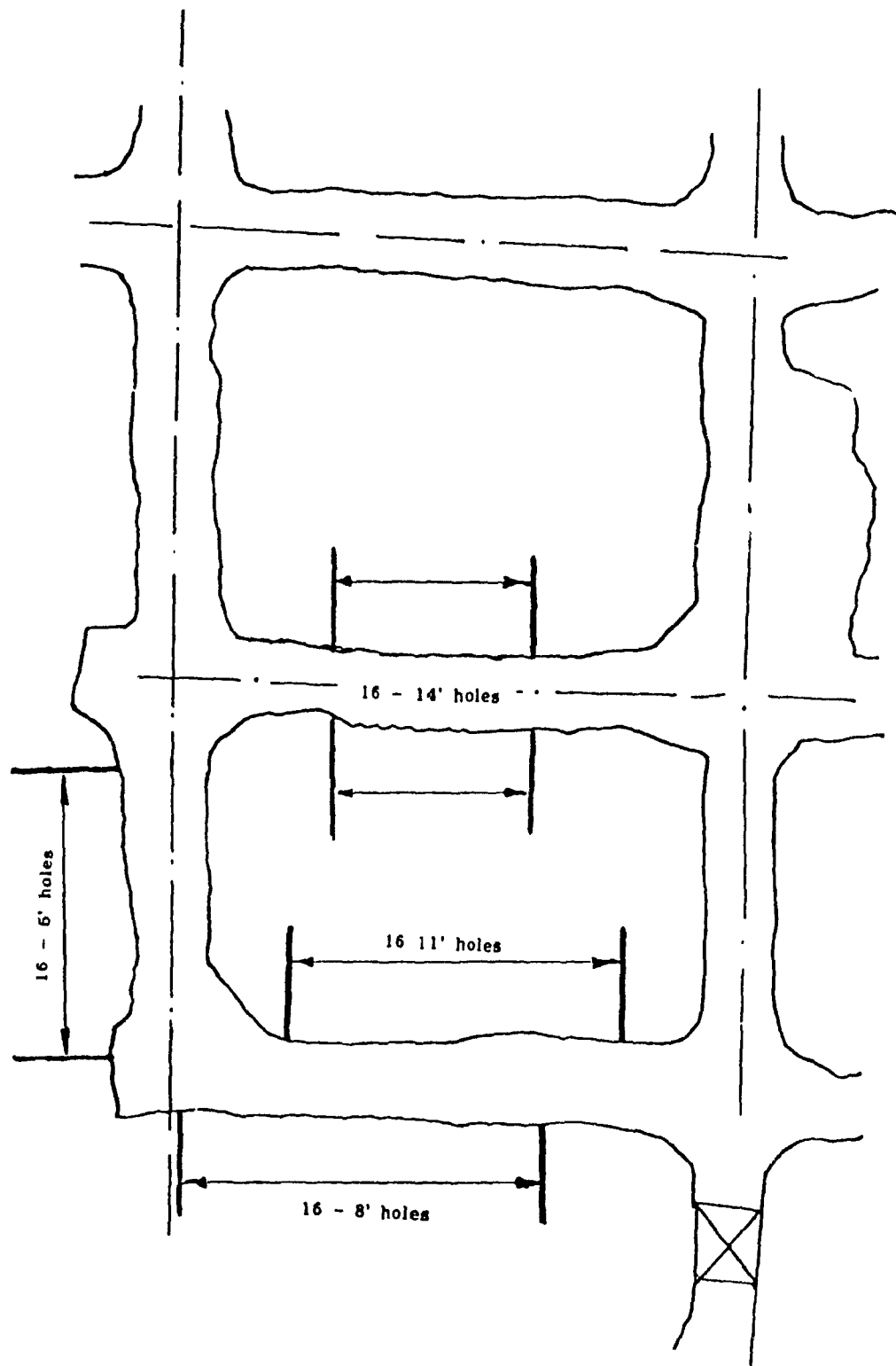


Fig. 4-2 Layout of the in situ test area, Dome Mine

In order to conduct an accurate pull-out test, the rock faces must be in close and intimate contact with the jack and its associated plate. Hence, flat faces were created with quick setting grout and/or shotcrete for any uneven rock surfaces prior to pull-out tests. Substantial amounts of material and time were necessary for this careful collar preparation (see Fig. 4-3).

4.5 FIELD PERFORMANCE OF THE GROUT PUMP

A unit applicable to shotcrete pumping which was capable of delivering the grout-aggregate mix under pressure 60 ft into the borehole was employed in this investigation. The shotcrete pump, which was mounted on a two wheel frame weighs 75 kg and is of manageable size for underground use. Although the test site was far from ideal from the point of accessibility and ventilation, the pump was easily transported by pulling it along the roadway and lowering it down a raise into the test stope. This operation required two men.

The setting up period for the pump was only around 30 minutes, provided that compressed air and water line were available. The operation of the pump is simple. However, it is important that the operators are trained on the surface for a few days in order to familiarize themselves with the operation and learn the technique to maintain the desired consistency of the final grout product, (see Fig. 4-4).

During the grouting operation of the 64 holes, the pump did not malfunction and the only problem encountered was the clogging up of the dry mix in the hopper and in the feed hose, which caused minor delays. This was most often overcome by



Fig. 4-3 Cable bolt together with rock surface



Fig. 4-4 View of the in situ grouting operation

knocking the hopper base, or disconnecting the delivery hose, pulling it up a nearby raise, and shaking it out. This occurred on 6 occasions during the grouting of the 64 holes and caused delays of approximately 15 minutes on each occasion.

Two factors were felt to contribute to the clogging-inconsistent aggregate size distribution, and low mine air pressure.

4.6 INSTALLATION TECHNIQUE

The boreholes were pre drilled and the cable was fed manually to the bottom of the hole. The new grout hose was also fed to the bottom of the hole. The grout material, which consisted of grout and aggregate (grout-aggregate) was injected at high pressure by the pump. As the grout was being injected, then the grout tube was withdrawn gradually from the toe to the collar of the hole, see Fig. 4-5. The synchronization of pumping and pulling of the cement hose could be adjusted to ensure the consistency and accurate placement of the grout.

The installation of the cable and the placement of the grout was much more rapid than in the conventional technique. Neither a breather tube nor a plug for the cable of the borehole was required. Under controlled conditions a 10 meter hole could effectively be grouted in two minutes. The consistency of the grout in the borehole depended on the rate of withdrawal of the grout tube from the hole. The operator with limited experience can vary the speed accurately to achieve good consistency. The mechanization of this operation would insure that each borehole is effectively grouted. The withdrawal rate of the grout tube from hole of 12 sec/m gave a good grout

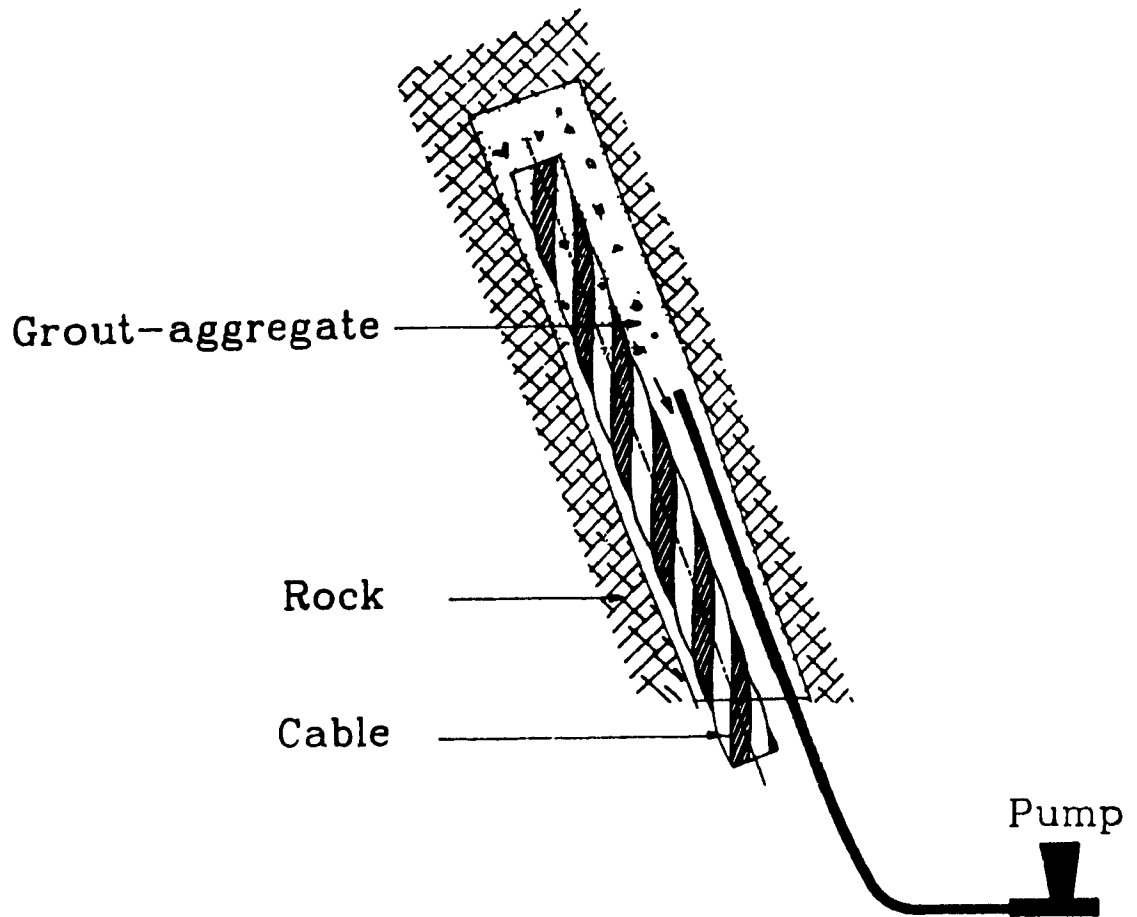


Fig. 4-5 Installation technique

consistency and placement in the borehole. The successful in situ trial showed that there is no major or practical problem with the systematic use of such a technique.

4.7 EFFICIENCY OF THE GROUT

In order to assess the efficiency of the grout pump in a controlled environment, six 9 m (30 foot) long and 5 cm (2 inch) diameter clear plexi-glass tubes were assembled from 1.8 m (6 foot) sections. The tubing was chosen in order to provide for a better visual inspection of the grouted hole during and after the grouting operation. This proved to be very useful.

The tubes were laid out horizontally on the ground and each was marked and coded for identification purposes. The pump was connected to compressed air (with a line pressure of 100 psi.) and water was provided for the tube. Injection of grout in each 9m (30 foot) length of plexi-glass tubing then proceeded as follows.

12 m (40 foot) of 1.9 cm (3/4 inch) diameter flexible PVC tubing was connected to the feed nozzle where the dry sand and cement mixed under pressure, joined the water line. The operator then manually adjusted the water flow, while inspecting the consistency of the final mixed grout by placing a test patch on the ground (see Fig. 4-6). The feed was then shut off, the long applicator tube was introduced into plexi-glass pipes, and the filling operation begun.

The placement technique was initiated by inserting the flexible PVC applicator tube to within 60 cm (2 foot) of the bottom of each of the plexi-glass columns and turning on the feed. As grouting continued, then the applicator tube was withdrawn as the plexi-glass tube filled.

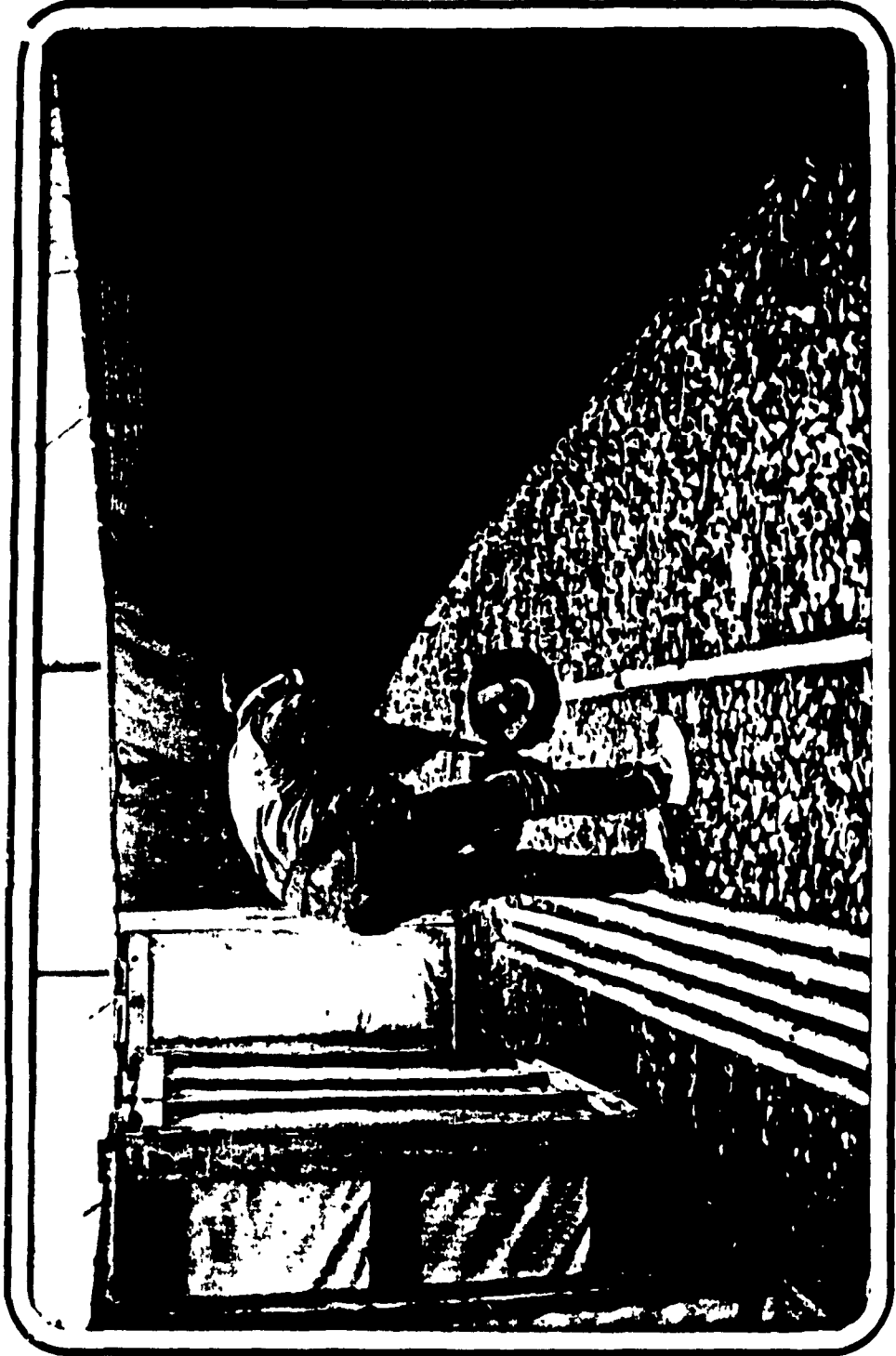


Fig. 4-6 View of 9 m plexi-glass tube

Injection times for each of the six 9 m (30 foot) long tubes is shown in table 4-5.

After a week, the six fully grouted plexi-glass tubes were cut by a masonry circular saw to 1.8 m (6 foot) lengths and then marked for the laboratory tests. In the lab all six grouted tubes belonging to each of the 9 m (30 foot) assembly tubes were accurately weighed. Then, each of the 1.8 m (6 foot) tubes were cut to 90 cm (3 foot) and weighed. Finally, each of the three feet sections were cut to 30 cm (1 foot) sections and weighed.

The data obtained from this experiment has been plotted in order to show the consistency of the grout placement in the cable bolt holes. The results are presented in Fig. 4-7 to Fig. 4-9 which show the variation in weight along the length of each 9 m (30 foot) plexi-glass tube.

tube No.	time (sec)	operation
1	143	continuous without any delays.
2	129	feed tube became clogged after having filled 2/3 of the tube. (78 sec time.)
3	134	continuous without any delay
4	94	continuous without any delay
5	103	ran out of feed after having filled 2/3 of the tube. (68 sec time)
6	97	continuous without any delay.

Table 4-5 Durations of the grout-aggregate filling of 9 m tubes

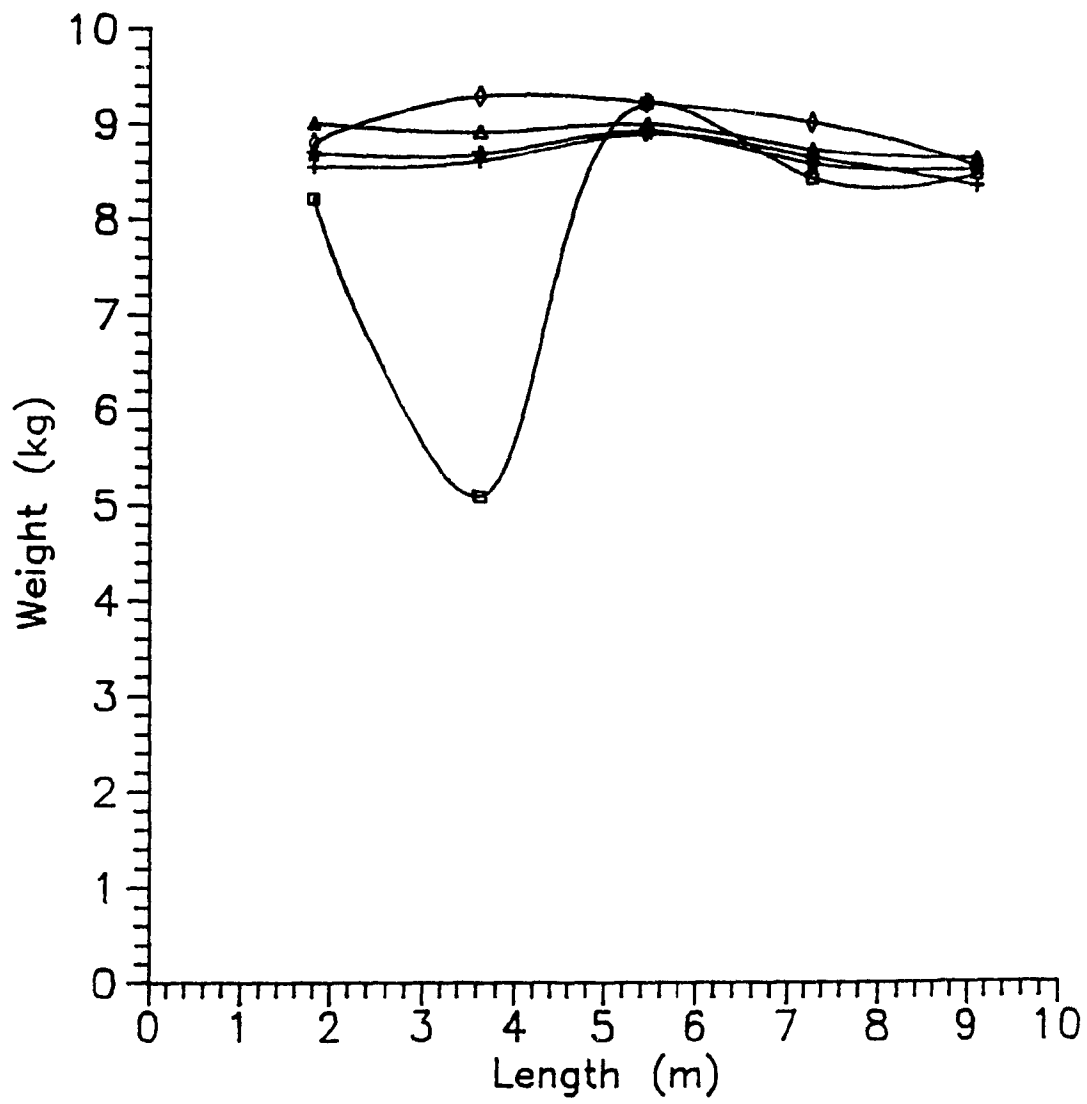


Fig. 4-7 Weight versus length for 180 cm length

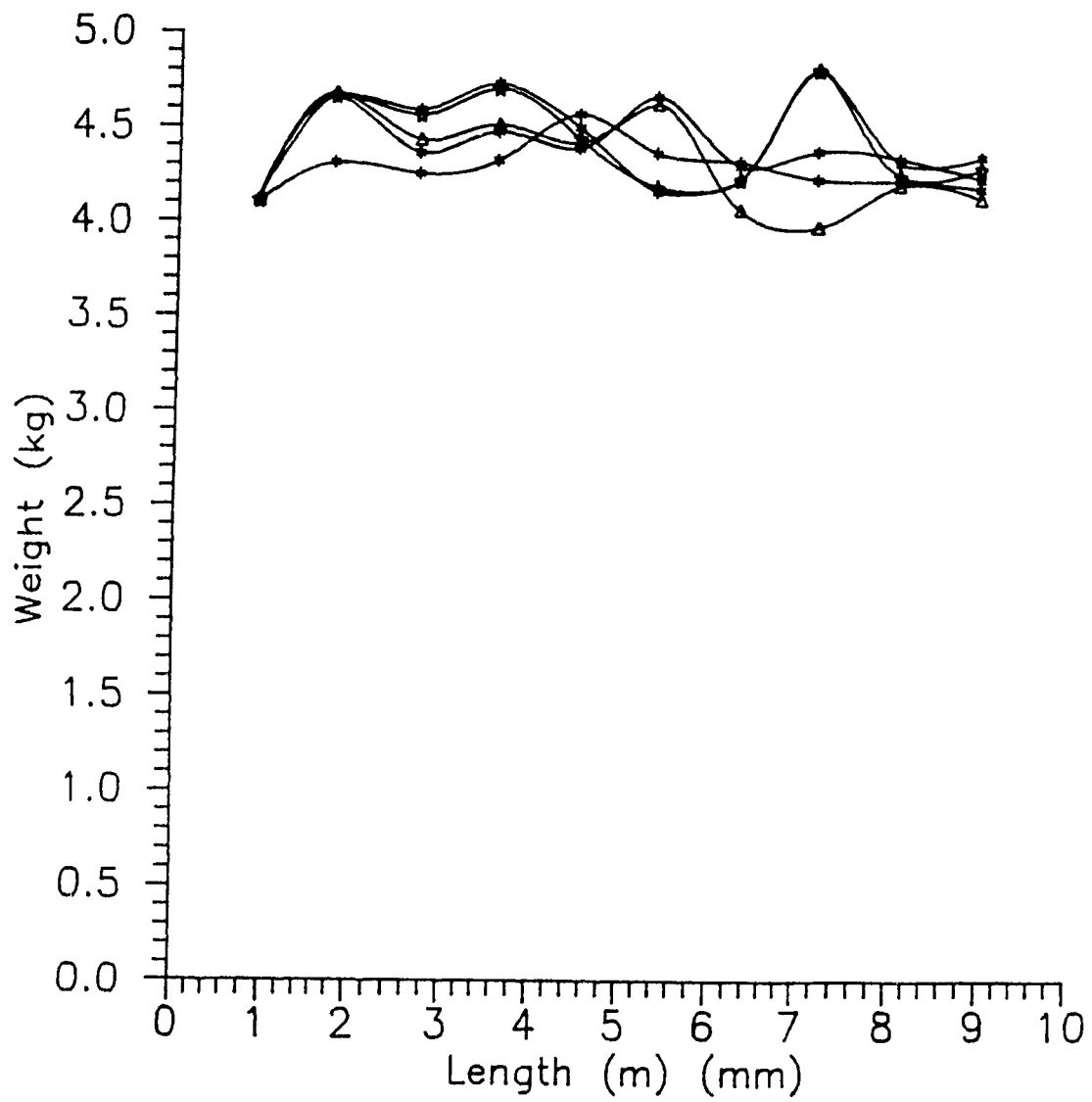


Fig. 4-8 Weight versus length for 90 cm length

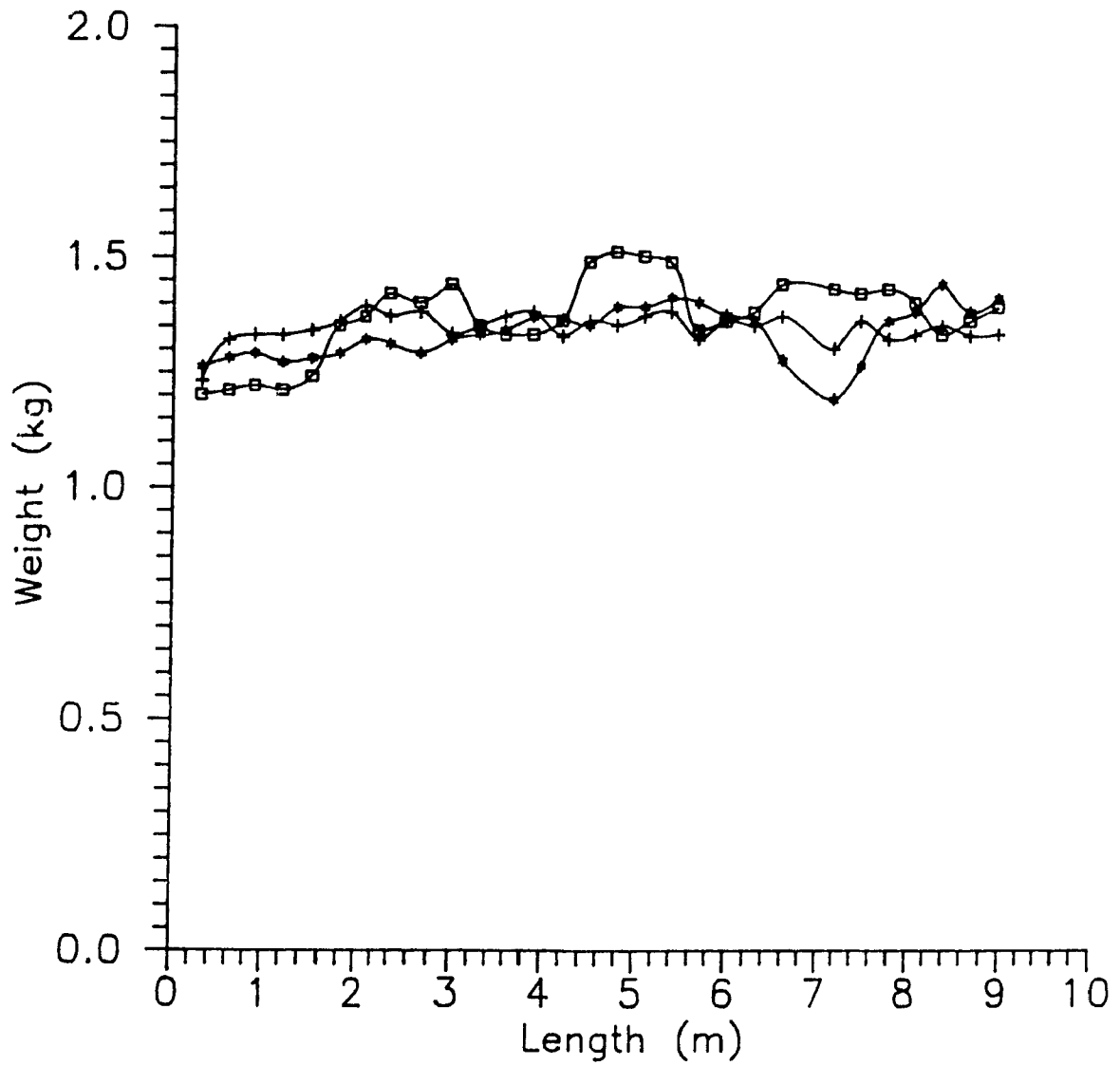


Fig. 4-9 Weight versus length for 30 cm length

4.8 STRENGTH EVALUATION OF THE GROUT

Over 30 uniaxial compressive tests were conducted on the grout specimens obtained from the laboratory grout placement study. The specimens were chosen randomly from the 30 cm (1 foot) plexi-glass grouted sections. The specimens, with a diameter of 5 cm (2 in) and length of 10 cm (4 in) were cut and released from the plexi-glass tubing. Their ends were then ground planar and perpendicular in order to ensure a uniform stress distribution during testing. All of the specimens were cured for 28 days. The uniaxial strength test was conducted on a servo-controlled, stiff testing machine according to I.S.R.M. [79] suggested techniques. The average uniaxial compressive strength value of the placed grout was 13.3 MPa.

The uniaxial compressive strength was less than expected, especially when compared with standard shotcrete material used for civil engineering purposes, where a typical average uniaxial compressive strength would be 25 to 30 MPa [54]. The strength of grout is greatly dependent on its constituents. It is very important to investigate and optimize the strength of grout since this exerts significant control over the overall performance of the cable bolting system.

4.9 IN SITU RESULTS

Typical in situ pull-out test results showing the relationship of the load carrying capacity and associated displacement of a 3.35 m cable bolt at different curing times of the grout-aggregate material are given in Fig. 4-10. It is clear that the curing of the bonding material has a significant effect on the peak load carrying capacity as well as the

I
stiffness (indicated by initial slope of the curve) of the support system. The increase in curing time subsequently increases both the load carrying capacity as well as the stiffness of the support element. It is important to notice that, independent of the curing time, the residual strength or load carrying capacity of the bolt remains very high and approximately equal to that of the peak load carrying capacity. This is very similar to the behavior of yielding support elements. The effect of cable length on the load bearing capacity of the cable is demonstrated in Fig. 4-11. It is shown that with an increase in cable length and curing time the load bearing capacity increases. The ductile behavior of this support system is not dependent on the length of the cable (or bond length). The high strength is comparable to peak bond strength due to the especially high frictional properties of the grout-aggregate mix.

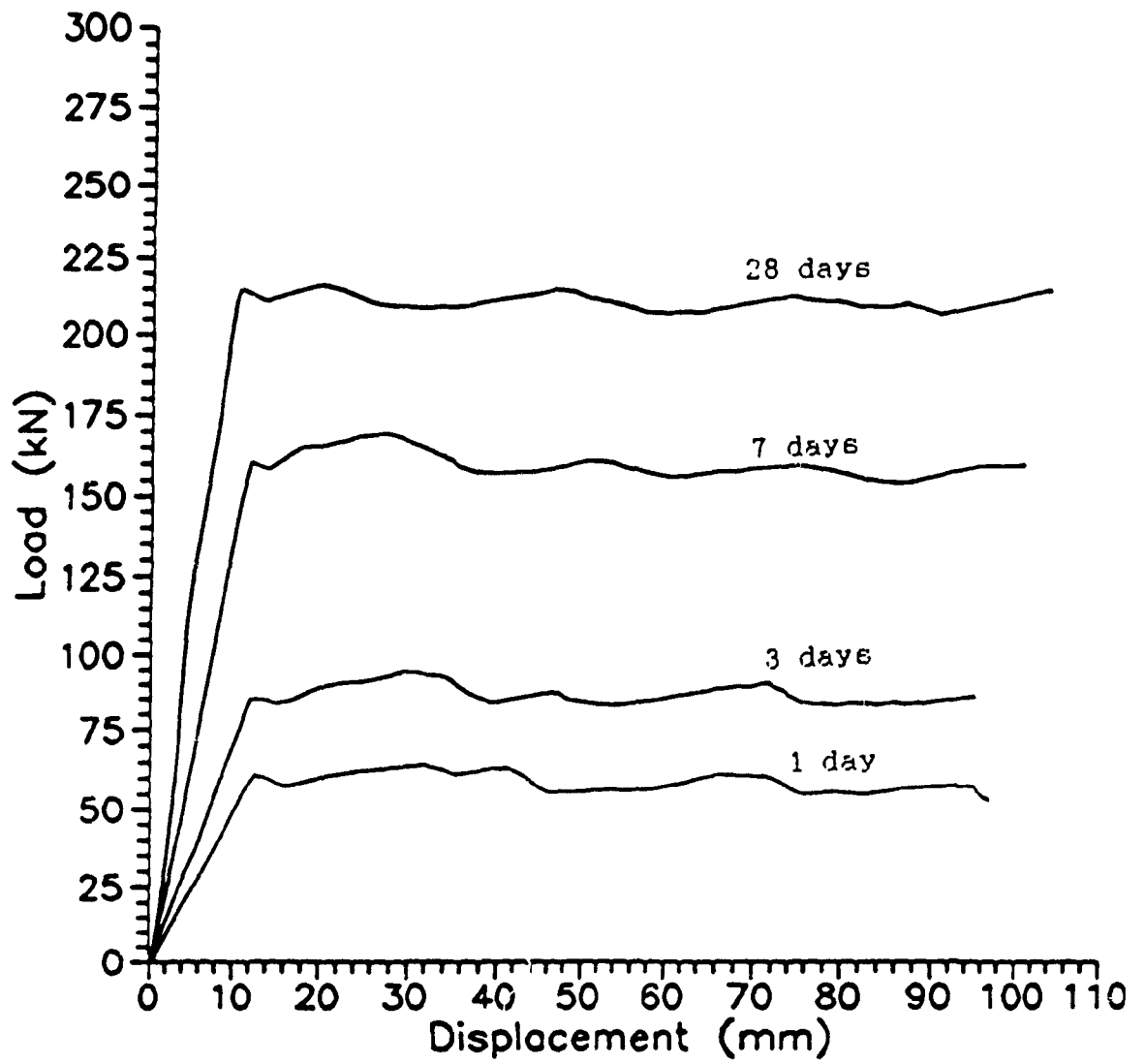


Fig. 4-10 Effect of curing time on the behavior of cable bolt

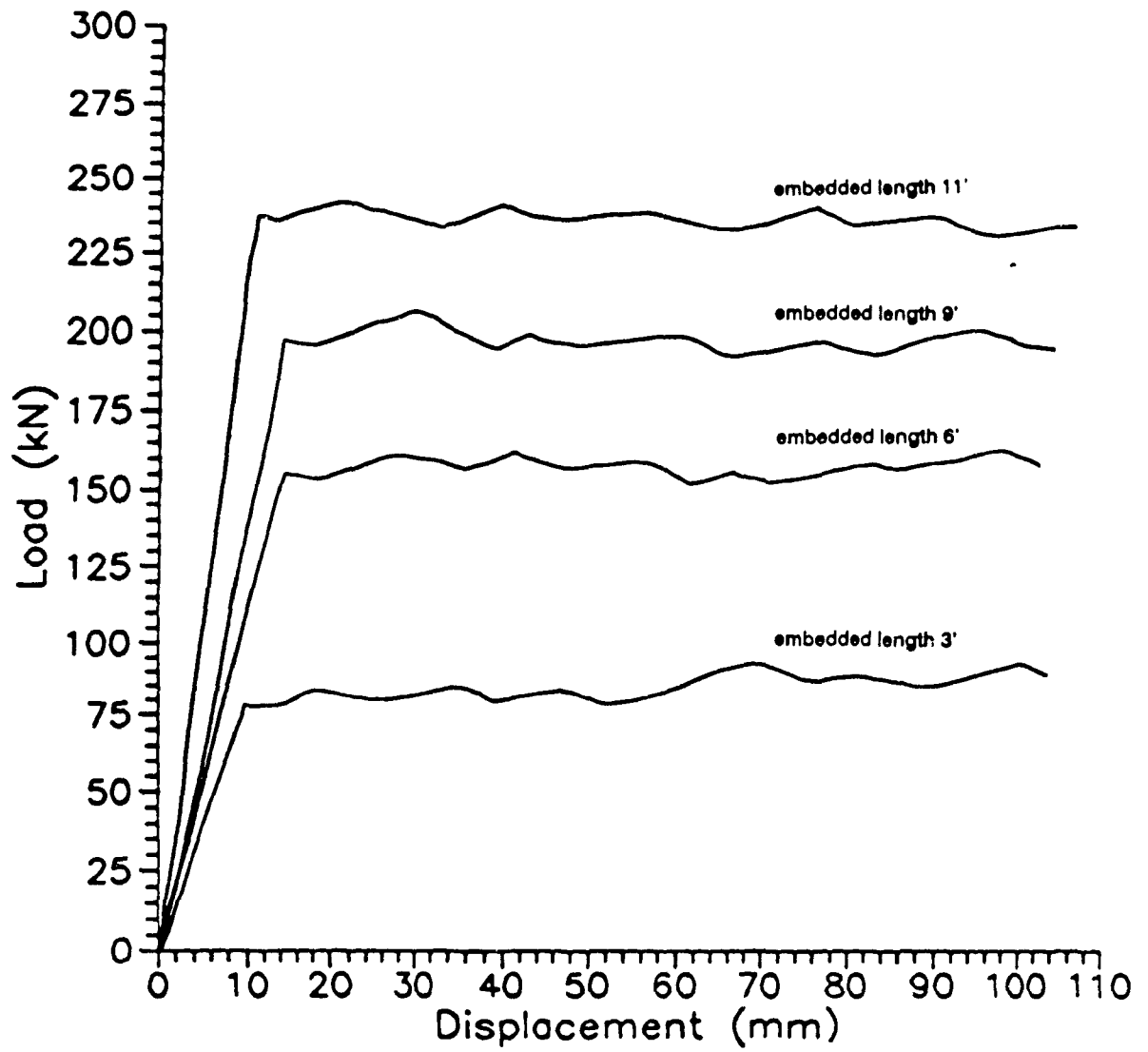


Fig. 4-11 Effect of embedded length on the behavior of cable bolt

4-10 CONCLUSION

- Installation of cable bolts are quite feasible and practicable in the field by employment of an appropriate grout-aggregate pump.
- The installation time is potentially much more rapid than conventional cable bolting.
- Residual strength of the cable bolt is high and remains relatively constant even after long displacement.
- Both length and curing time have a considerable effect on the final load carrying capacity of the support element.
- None of the actual cables ruptured and failed during the field study. The ultimate strength of this type of cable is approximately 270 kN, however, the maximum obtained from the cable bolts was 220 kN. As was discussed earlier, the ultimate strength of this support system could not be evaluated at this stage, because the grouting material used had a significant effect on the overall strength. The optimization of the grout material is very important in the overall strength of this support element. Therefore, subsequent investigation were considered under controlled conditions in the laboratory, and are reviewed in the next Chapter.

CHAPTER 5 EXPERIMENTAL PROGRAM

5.1 INTRODUCTION

Upon successful completion of the in situ trials, a testing program for various possible mixes of the grout material to maximize the support capability of the cable bolt with the grout-aggregate mixture was necessary. The experimental results obtained would not only provide information for an improvement of cable bolt support elements but also help in the development of analytical models as well as in the verification of their adequacy.

The approach was undertaken in order to study the influence of different design parameters on the behavior of cable bolting; complete details of the study are given in this chapter. 295 pull-out tests were performed in order to provide an understanding of the characteristic behavior of the cable bolt element using conventional grout and the grout-aggregate. Experimentation with conventional grout was found necessary in order to establish a standard pull-out test, to determine guidelines for the workability of the grout-aggregate and to compare the characteristic behavior of conventional grout and the grout-aggregate mix.

5.2 TESTING ARRANGEMENT

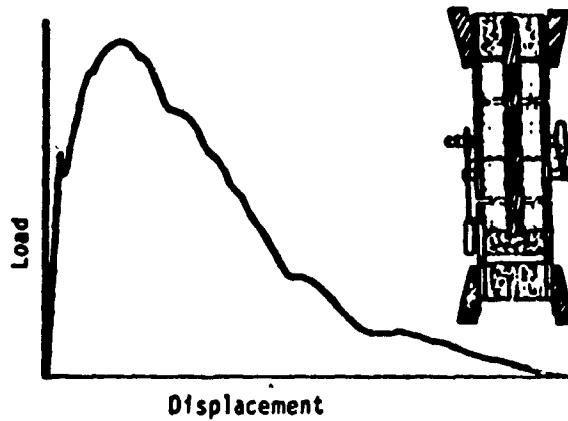
For the purpose of simplicity it would be desirable to establish a "standard method of bond testing ". However, this has not been an easy task in view of the many various physical stresses manifested as bond failure. An evaluation of the requirements for the bond test, formulated by members of ACI committee 408 [37, 38], led to the following conclusion:

- The bond test specimen must simulate as closely as possible the actual manner of loading in the structure.
- The bond test specimen must have a reasonable cover.
- The bond test specimen must avoid the confinement effect of the loading system and reaction which influences the bond.

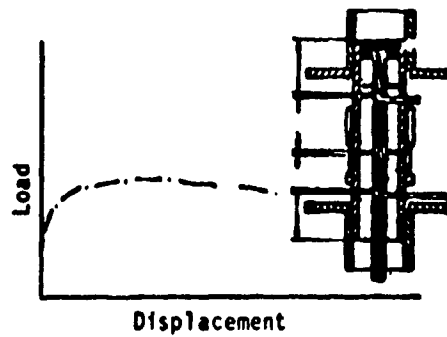
Based on these recommendations different testing methods have been applied by several investigators [4, 6, 48, 50].

Fuller [4] investigated the behavior of a single wire and cable bolt by means of pull-out tests. Two grout columns having different lengths were formed within two steel tubes. This arrangement forced the eventual shear bond failure to the smaller embedded length of the grout cable section and prevented the rotation of the cable with respect to the grout. A typical result of load displacement and testing arrangement is shown in Fig. 5-1a.

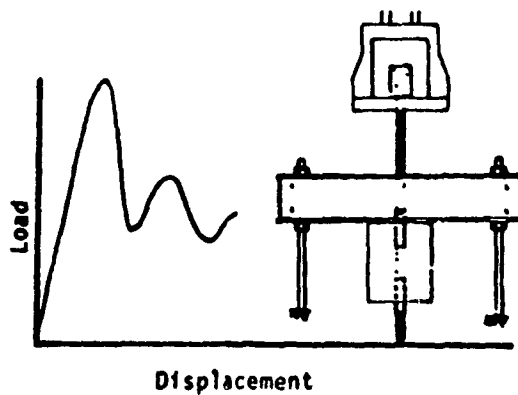
Goris [48] demonstrated the characteristics of the different configurations of cable bolts by the testing arrangement which is shown in Fig. 5-1b. In order to prevent slippage of the end cable, a steel washer was welded to the one end face of steel strands. The displacement of the cable was monitored by two potentiometers attached to the pull-out test sample.



a) Technique used by Fuller



b) Technique used by Goris



c) Technique used by Stillborg

Fig. 5-1 Different testing arrangements [4,6,48]

Stillborg [4] studied the behavior of cable bolts in detail by means of the pull-out test. The cables were fixed into the cylindrical concrete and after the appropriate curing time were pulled out. The testing system and typical results are shown in Fig 5-1c. As can be seen, the residual strength of the cable in comparison with the maximum shear bond strength is low.

In the absence of a standard testing technique, the results obtained from the above testing techniques have generally been accepted. Comparison of the load-displacement characteristic curves shown in Fig. 5-1 for different arrangements reveal that, employing a steel tube to simulate the rock mass material could result in high confinement and consequently high shear bond strength between the cable and the grout material. With this in mind a testing technique similar to that of Stillborg [4] was employed for this study.

Furthermore, the following parameters were considered to be of prime importance in affecting the behavior of the cable bolt and it was intended that their effects should be investigated in this research:

- Diameter of sample
- Diameter of borehole
- Mix design of grout-aggregate
- Embedment length of sample.

The parameters were varied within their practical range by assuming at least three values. Testing parameters at three levels was considered a minimum to detect the influence of each parameter. This approach led to a basic experimental matrix within 28 series of tests with conventional grout and 31 series of tests with grout-aggregate mixture. Since the fine aggregates were the major portion of solid material in

the grout-aggregate mixture then one series of tests with only fine aggregates were conducted.

The samples was marked with GAC (Grout-Aggregate-Cement ratio) and a number representing the portion of aggregate with respect to cement. There was an exception for the grout-aggregate where only fine aggregate was used as solid material and specified as GACF2. The experimental test program is summarized in Table 5-4. To prevent the possibility of unpredictable factors affecting the results, every test was repeated five times. The reliability of the results was controlled by the statistical procedure on standard deviation for load carrying capacity of the cable bolt.

All test specimens and their specific parametric values are described in the following subsections. To maximize the performance of the grout-aggregate with respect to the shear bond strength the following tests were involved:

- Compressive strength;
- Triaxial test;
- Grading and size distribution of aggregates.

5.3 SAMPLE PREPARATION

The preparation of samples, as shown in Fig. 5-2, was as follows:

- a) The exposed surface of cable was cleaned and cut to the desired length.
- b) In order to have a reliable simulation of field conditions at the laboratory scale, the cable should be placed in rock. However, due to the number and size of

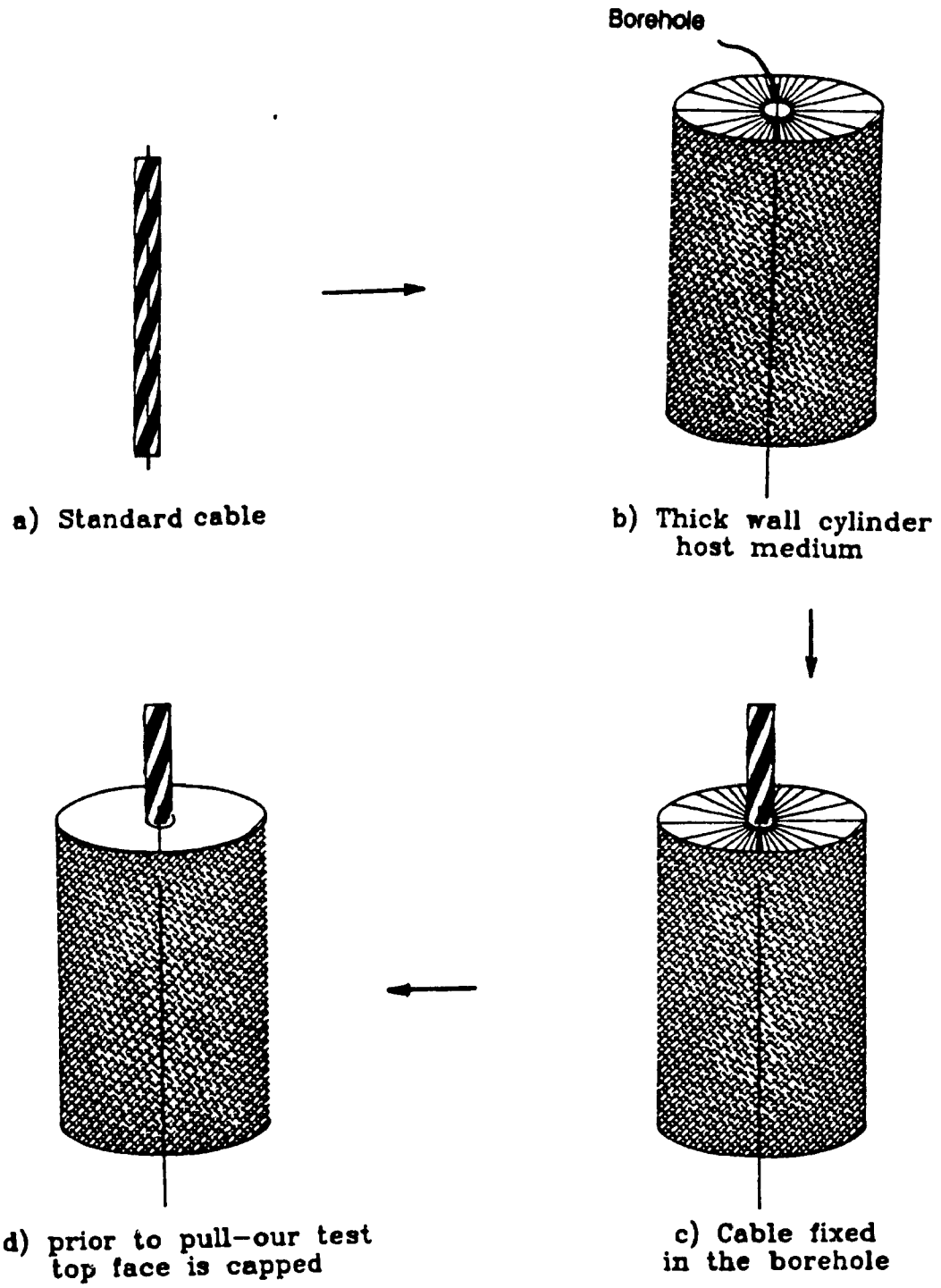


Fig. 5-2

Preparation of a test specimen for a pull-out test

setting elements this was not possible. Consequently, in order to have a sound control on properties and geometry of samples, the host rock was simulated with thick wall concrete cylinder whose center hole represented a borehole.

- c) The cable was placed at the center of borehole in the concrete cylinder. In the short length specimen, cable was extended approximately 20 cm from both end faces.
- d) The specimens were stored in the curing room at a temperature range of $20 \pm 3^{\circ}\text{C}$; being kept highly moist during the curing period (28 days).
- e) The load end face of specimens were capped with sulphur in order to prevent premature failure due to eccentricity or bending moments. This precaution was necessary especially for short length specimens when cable bolts were subjected to axial load.

5.4 MATERIAL PROPERTIES

The following is a summary of the materials which were used in this study.

5.4.1 ORDINARY PORTLAND CEMENT

Type 10 Portland cement was obtained from a supplier in Quebec. This cement was selected because of its wide availability and common use in practice. The properties of this cement conformed to ASTM 150 standards.

5.4.2 CABLE BOLT

A number of different types of cable have been introduced to the industry. In general, any type of wire and lying technique for cable bolting is acceptable, but it should be insured that the surfaces are free of grease. Cable with seven wires, which is most commonly used in practice, was employed in this study. The specifications are given in Table 5-1.

Total number of wires	7
Wire diameter	5.05 mm
Nominal cable diameter (measured)	15.2 mm
Calculated diameter of cable [60]	15.15 mm
Calculated perimeter [60]	63.34 mm
Cross section area	138.7 mm ²
Modulus of elasticity	194 ± 6 GPa
Poisson's ratio (estimated)	0.30

Table 5.1 Specifications of cable bolt.

5.4.3 AGGREGATE

Aggregate employed in grout-aggregate mixtures usually occupies more than 50 percent of the total volume of the matrix. Therefore, its properties have a definite influence on the behavior of the cable bolt. Experience has shown that application of very coarse or very fine aggregate in concrete or shotcrete produces an unsuitable mix [80]. For the mixtures

with the same amount of aggregate, more coarse aggregate results in harshness, bleeding and segregation while fine aggregate requires a comparatively large amount of water to produce the necessary fluidity; it also tends to cause segregation.

In conventional cable bolting it has been proven that the shear bond strength between cable and surrounding matrix can be modified by increasing the compressive strength of the grout material [54]. Therefore, in this investigation the aggregate is graded in order to provide maximum compressive strength while it produces reasonable workability in the grout-aggregate mix.

The capability of pump, available space between the cable surface and borehole wall as well as workability of the grout-aggregate mix give limitation for the maximum size of coarse aggregate in the mixture. Based on Table 4-3, in laboratory work the maximum size of coarse aggregate for grout-aggregate mix was formulated to 9.5 mm. The grading limit of aggregates were selected based on the requirement of the CSA specification [81].

Natural sand as a fine aggregate and crushed stone as a coarse aggregate were employed in this research. In Fig. 5-3 sieve analysis of the fine and coarse aggregates with dash lines are shown. In order to decrease the amount of water in the mixture, then more coarse aggregate and a combination of one weight coarse aggregate with two weights of fine aggregate was tried in the mixture and gave a satisfactory response. The results are presented in Table 5-2.

Sieve No.	Sieve size	percent of passing		Mixture	CSA [81]
		Fine (F)	Coarse (C)		2F+1C
U.S.	(mm)				passing %
3/8	9.50	100	100	100	100
4	4.75	100	40	80	95 ~ 100
8	2.36	98	2	66	80 ~ 90
16	1.00	79	0	52.7	50 ~ 85
30	0.60	48	0	32	25 ~ 60
50	0.30	32	0	21.3	10 ~ 30
100	0.15	8	0	5.3	2 ~ 10

Table 5-2 Sieve analysis and CSA specification grading requirement [81]

5.4.4 WATER

Regular tap water was used in grout-aggregate mix preparations.

5.5 TESTING SYSTEM

The test system employed for this investigation was a RDP-Howden electrohydraulic servo-controlled testing system, comprising:

- a) straining frame;
- b) SL 2000 analogue control consul;
- c) hydraulic power pack;
- d) Apple II Micro-computer system.

The testing frame comprises of four steel columns fitted with variable daylight crosshead which is automatically clamped (hydraulically) to the columns. The crosshead is positioned by twin electrically driven screws. A double acting, servo-controlled, equal area actuator lies on the top crosshead. The

testing frame is designed to apply maximum compressive and tensile loads of 1000 kN over a total working stroke of 100 mm with an overall machine stiffness of greater than 2500 kN/mm. The SL 2000 analogue control console provides all the necessary feedback control system to perform closed-loop servo-control testing. An Apple II micro-computer was interfaced with the control console to provide the extra facilities of test ramp generation and data logging. Software programs were written to provide these facilities.

5.5.1 TESTING TECHNIQUE

A photograph of the pull-out test apparatus is shown in (Fig. 5-4). A special frame had to be designed and manufactured in order to perform the pull-out tests with the available servo-hydraulic universal testing machine in the McGill Rock Mechanics Laboratory. Two sets of stiff plates were used to provide end faces of the frame. At the center of the top plate a hole with a diameter of 50 mm was made through which to pass the cable. The corners of these plates were connected by bolts to allow for different embedded lengths and diameters in pull-out tests. A special grip device was made which permitted adjustments to the machine and frame.

The specimen rested in the frame whereas the cable was passed through the hole in the top plate. The cable was fixed with a small grip which was fitted into the gripping device. The testing machine was employed to supply the tension load to the cable bolt while the top end face of thick wall cylindrical concrete was supported by the frame.

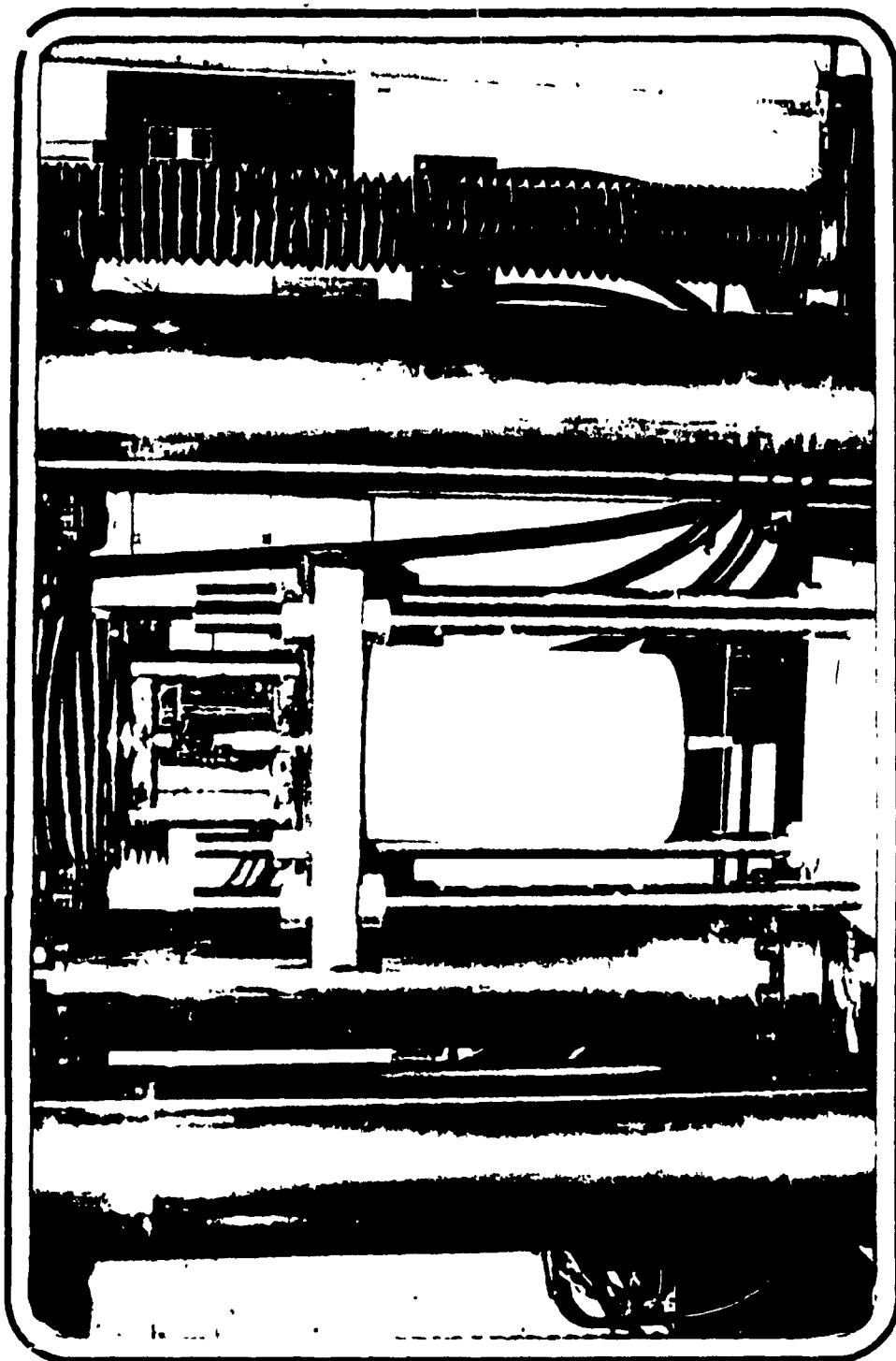


Fig. 5-4 Testing arrangement

Actual loading conditions of cable bolts in the field should correspond as closely as possible to the ideal loading conditions in the laboratory. Displacement or load control are two methods for applying load on the sample in the lab. In principal, from the material point of view, the behavior of steel cable with respect to the surrounding matrix leads to the same results, although the types of curve are different. A load of approximately 2 kN was applied before testing to settle in the specimen and obtain initial readings. The tests were conducted under constant displacement by using the testing machine under displacement control mode. The magnitude of the displacement increments was selected to be small enough (i.e. 1 mm/min) to reflect the nonlinearity of the response for bond stress between cable and surrounding matrix. The number of increments were sufficiently large to provide 100 mm displacement in each test. Attempts were made to record data past the point of peak load as well as residual load.

The load and displacement were measured directly by load and displacement transducers respectively, enabling the monitoring of the slip between the cable and surrounding matrix at the load end face of sample. A chart recorder was used to plot load against displacement during test.

5.6 PREPARATION OF GROUT-AGGREGATE MIX

The procedure was as follows:

- a) The mixture of two portions of fine and one portion of coarse aggregate was provided.
- b) To control the components of the mixture the specific gravities and absorption values were determined for coarse (ASTM C 127) and fine aggregate (ASTM C 128).

- c) According to the Abrams [80] the amount of water in a mixture is a function of the grading and shape of aggregate. To provide fluidity for the mixture of the grout-aggregate close to the conventional grout, slump tests [54] were conducted to simulate similar workability to those obtained by conventional grout with water to cement ratio indicated in Table 5-3.
- d) For each batch of grout-aggregate, five samples for testing the modulus of elasticity as well as five more cylindrical samples (d=50.8 mm, h=101.6 mm) to identify the angle of friction and cohesion of the mixture were prepared and kept in the curing room over the curing period.

Workability of grout-aggregate	Water-Cement ratio of conventional grout
Type I	0.3
Type II	0.35
Type III	0.45

Table 5-3 Workability simulation of conventional grout with grout-aggregate mix

The mixing of grout-aggregate was done according to ACI 544 Committee (1978) recommendations. Mixing was accomplished by using a 2.5 cubic foot capacity rotary tilt drum mixer. The following routine was preferred because it produced more uniform mixes:

- The calculated cement, fine and coarse aggregate fractions were blended in the mixer for two minutes.

- Water was added and mixing continued for 1 minute.
- All mixtures were shoveled and then mixed for an extra minute.

The water-cement ratio for each mixture of grout-aggregate was verified, based on the analogy of its workability with conventional grout. Fig. 5-5 shows the result of variation of workability versus water-cement ratio for the grout-aggregate and conventional grout. The following explains how the water-cement ratio for the grout-aggregate mixture was obtained:

The value of the water-cement ratio for the conventional grout (point a) was interpolated to determine the corresponding workability (point b) as shown in Fig. 5-5. A horizontal line was then drawn through point b to cut the grout-aggregate curves mixtures at point d, e and f. Then a vertical line was plotted downwards to the water-cement ratio axis to obtain the desired water for each grout-aggregate mixture.

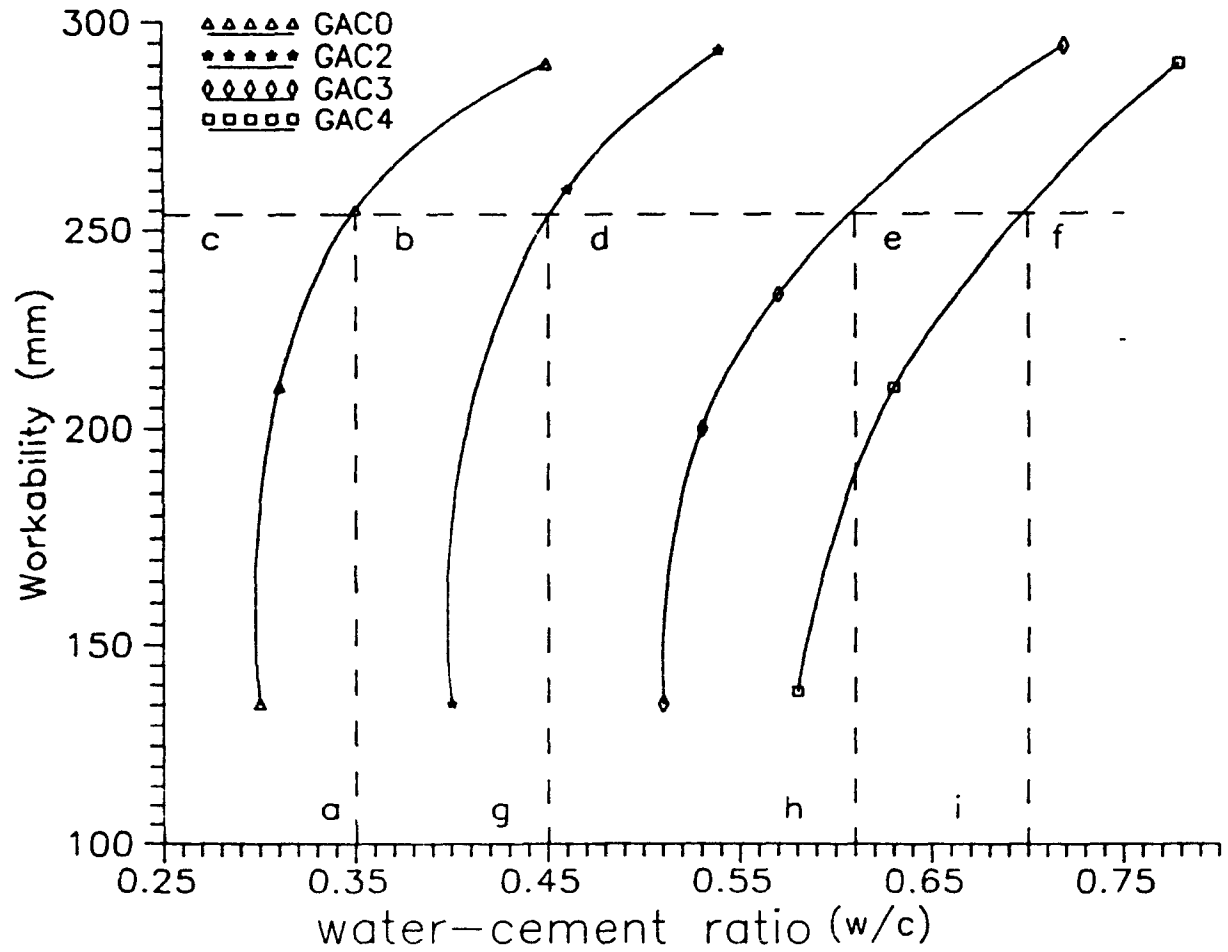


Fig. 5-5 Workability in terms of water-cement ratio for different grout-aggregate mixes

Specimen Type	Workability [Type]	External diameter [Cm]	Length of specimen [Cm]	hole [cm]
GAC0	I	10, 15, 20, 25, 30	20	5.1
GAC0	I	25	20	2,4,6
GAC0	I	25	15, 20, 30, 40, 50, 60, 70	5.1
GAC0	II	25	15, 20, 30, 40, 50, 60, 70	5.1
GAC0	III	25	15, 20, 30, 40, 50, 60, 75	5.1
GAC2	I	25	15, 20, 30, 40, 50, 60, 75	5.1
GAC3	I	25	15, 20, 30, 40, 50, 60, 75	5.1
GAC4	I	25	15, 20, 30, 40, 50, 60, 75	5.1
GAC2	II	25	20	5.1
GAC2	III	25	20	5.1
GAC3	II	25	20	5.1
GAC3	III	25	20	5.1
GAC4	II	25	20	5.1
GAC4	III	25	20	5.1
GACF2	I	25	10, 20, 30, 40	5.1

Table 5-4 Experimental Test-Program

5.7 TEST RESULTS

The measurements of load and displacement taken during pull-out tests were used to examine the cable's behavior from two different perspectives:

- 1- Load-slip Behavior;
- 2- Shear bond strength.

5.7.1 EFFECT OF SAMPLE DIAMETER

Before investigating the behavior of untensioned grouted cable bolt, it was necessary to establish a standard for the external diameter of the concrete cylinders. Therefore, a series of pull-out tests were conducted using constant embedded lengths (200 mm) and different concrete cylinder diameters (100, 150, 200, 250 and 300 mm). The cables were fixed in place into the simulated borehole (51 mm diameter) by the conventional grout with type I workability. The relevant properties of the materials are summarized in Table 5-5.

Prior to applying any load to the cable, it was assumed that the exposed surface of cable was bonded to the surrounding matrix along its embedded length and that deterioration in the bond was dependent on the amount of pull-out force applied to the cable bolt.

At the end load face of 100 mm diameter cylinder considerable cracks were observed. The first splitting tension crack on the load end face and longitudinal crack on the side of the block emerged simultaneously at a pulling force of about 8 kN. As loading increased, then more splitting cracks were formed and longitudinal cracks extended further toward the unloaded face of sample. At a force level of about 10 kN splitting and longitudinal cracks began to connect. In a cylinders with 150 mm diameter the splitting cracks at the load end face of the

sample were radially distributed to the side wall of the specimen. There were fewer radial cracks than in the test samples with 100 mm diameter. In specimens with diameters of 250 mm no cracks were observed on the side wall of the specimen. Due to the slip of the cable at the load end face of the sample, splitting cracks formed a cone shape fracture zone which began at the cable grout interface. As the load was further increased the formation of a cone was more evident. At a load about 40 kN the cone was completely fractured from the rest of block. The diameter of the cone was between 50 mm to 53 mm , while its angle with respect to the axis of the cable was between 40 to 60 degree. Fig. 5-6. shows the development of radial cracks in the sample.

The results are summarized in Table 5-6 and shows that the load carrying capacity of the cable increases as the cylinder diameter is increased. This tendency is more pronounced for small diameters of the thick wall concrete cylinder. As can be seen in Fig. 5-7, increasing the diameter of cylinder more than 200 mm, the load carrying capacity of cable bolts does not significantly increased. This is mainly due to the stress distribution in the cylinder which consequently affects the confining pressure on the grout and cable grout interface. In order to avoid this effect on the subsequent tests for this investigation, all the pull-out test cylinder diameters were standardized to 250 mm.

Material	Workability	q		Cohesion	ϕ	E
	(type)	(MPa)	std.	(MPa)	(deg)	(GPa)
concrete	-	35.3	2.8	8.6	34.3	19
GAC0	I	42.3	1.9	11.2	30.1	21.2
GAC0	II	39	1.7	10.7	29.4	19.5
GAC0	III	35	1.8	9.8	28.3	18.1
GAC2	I	36	2	8	35.5	19.1
GAC2	II	32.3	1.8	7.6	34.5	18.6
GAC2	III	25	2.25	7.3	33.3	17.3
GAC3	I	33	1.3	7.6	34.7	16.8
GAC3	II	27	1.6	7.2	33.8	16.3
GAC3	III	21	1.6	7.1	33	14.8
GAC4	I	28	1.3	6.8	33.9	16.4
GAC4	II	22	1.5	6.4	33.1	15.1
GAC4	III	16.3	1.7	6.1	32.3	14.2
GACF2	I	31.2	1.4	9.3	32	17.2

Table 5.5 Compressive strength, cohesion and friction angle of grout and grout-aggregate.

q = compressive strength

ϕ = friction angle

std = standard deviation

E = modulus of elasticity

specific gravity of coarse aggregate = 2.57 g/cm³

specific gravity of fine aggregate = 2.66 g/cm³



Fig. 5-6 Development of radial cracks in the sample

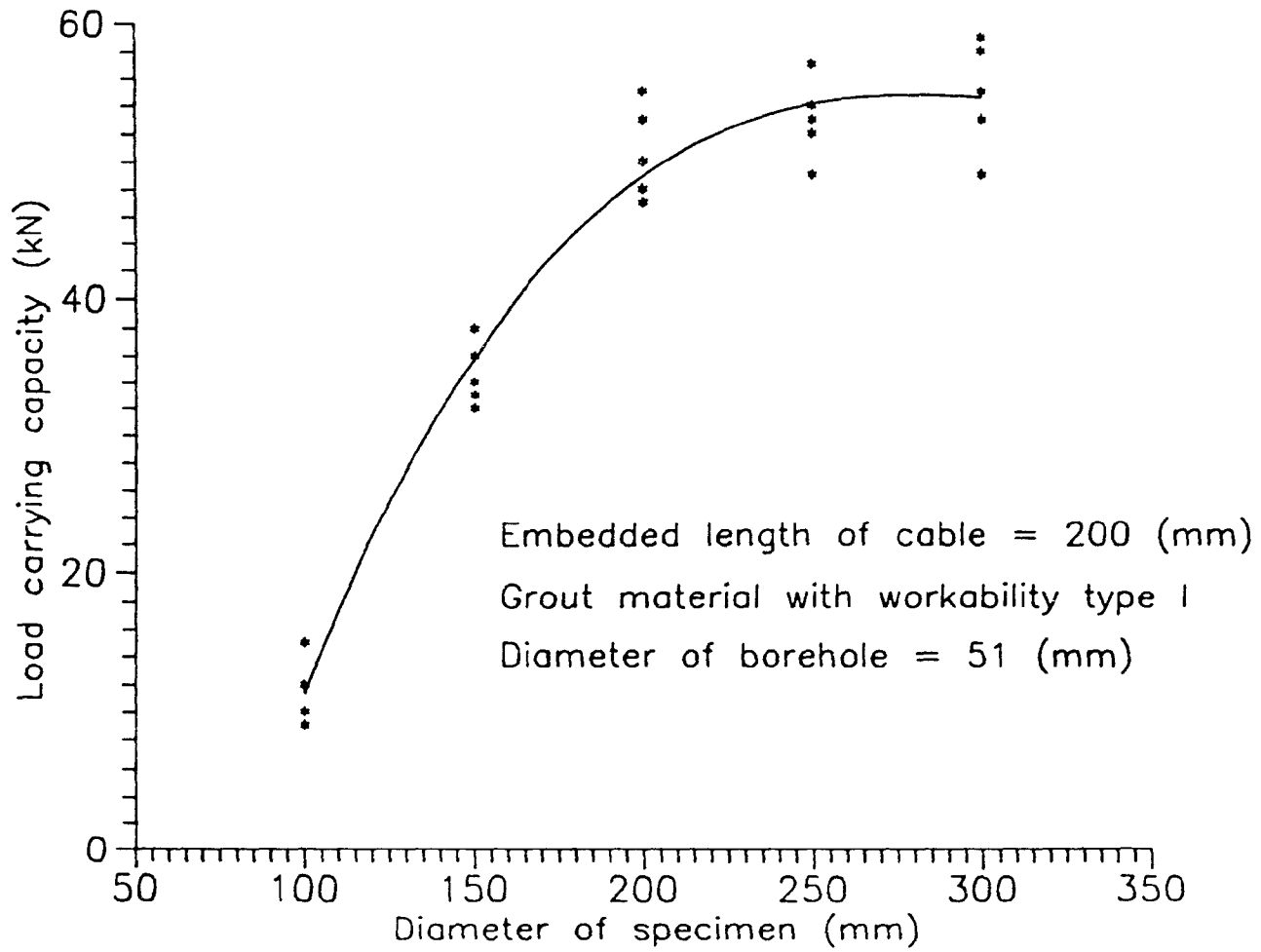


Fig. 5-7 Load carrying capacity for different external diameter of sample

External diameter (mm)	Load carrying capacity (kN)					
	Test number					Mean
	1	2	3	4	5	
100	15	10	12	9	12	11.6 ± 2.3
150	33	32	36	34	38	34.6 ± 2.4
200	48	53	47	50	55	50.6 ± 3.4
250	54	52	57	53	49	53 ± 2.9
300	55	58	53	49	59	54.8 ± 4

Table 5-6 Load carrying capacity of cable for different external diameters of thick wall concrete cylinder and 200 mm embedded length with conventional grout

diameter of borehole (mm)	Load carrying capacity (kN)					
	Test number					Mean
	1	2	3	4	5	
20	57	55	59	54	49	54.8 ± 3.8
40	59	58	50	53	57	55.4 ± 3.8
60	59	56	58	52	53	55.6 ± 3

Table 5-7 Load carrying capacity of cable for different borehole diameters and 200 mm embedded length with conventional grout

5.7.2 DIAMETER OF BOREHOLE

In order to consider the effect of diameter of borehole, series of pull-out tests were examined with constant embedded length (200 mm). The cables were placed in the samples with different borehole diameters (i.e. 20, 40 and 60 mm) and fixed by the conventional grout with workability type I. With reference to Table 5-7 and Fig. 5-8 can be expressed that the load-slip behavior are in all respects very similar. Apparently, the borehole size in practical range has no effect on the characteristic of the pull-out test.

5.7.3 EFFECT OF WATER-CEMENT AND AGGREGATE-CEMENT RATIO

Most of the research on grout for cable bolting in the mining industry has been limited to the properties of the cement and water. A commonly used water-cement ratio of grout for rock reinforcement is between 0.3 to 0.5. Therefore, in order to compare the characteristic of grout-aggregate mix with grout material it was decided to investigate further the behavior of grout mixes with water cement ratios of 0.3, 0.35, 0.45. Typical load-displacement behavior is shown in Fig. 5-9. It can be seen that the lower water-cement ratios resulted in higher shear bond strength. Increasing the water-cement ratio contributes to a decrease in the compressive strength of grout or grout-aggregate mixture as shown in table 5-5.

The average load-displacement relationships for the pull-out tests with grout-aggregate mixtures of aggregate-cement ratio of 2, 3 and 4 are given in Fig. 5-10, Fig. 5-11 and Fig. 5-12 respectively. In each of the graphs, three load-displacement curves are given representing the effect of

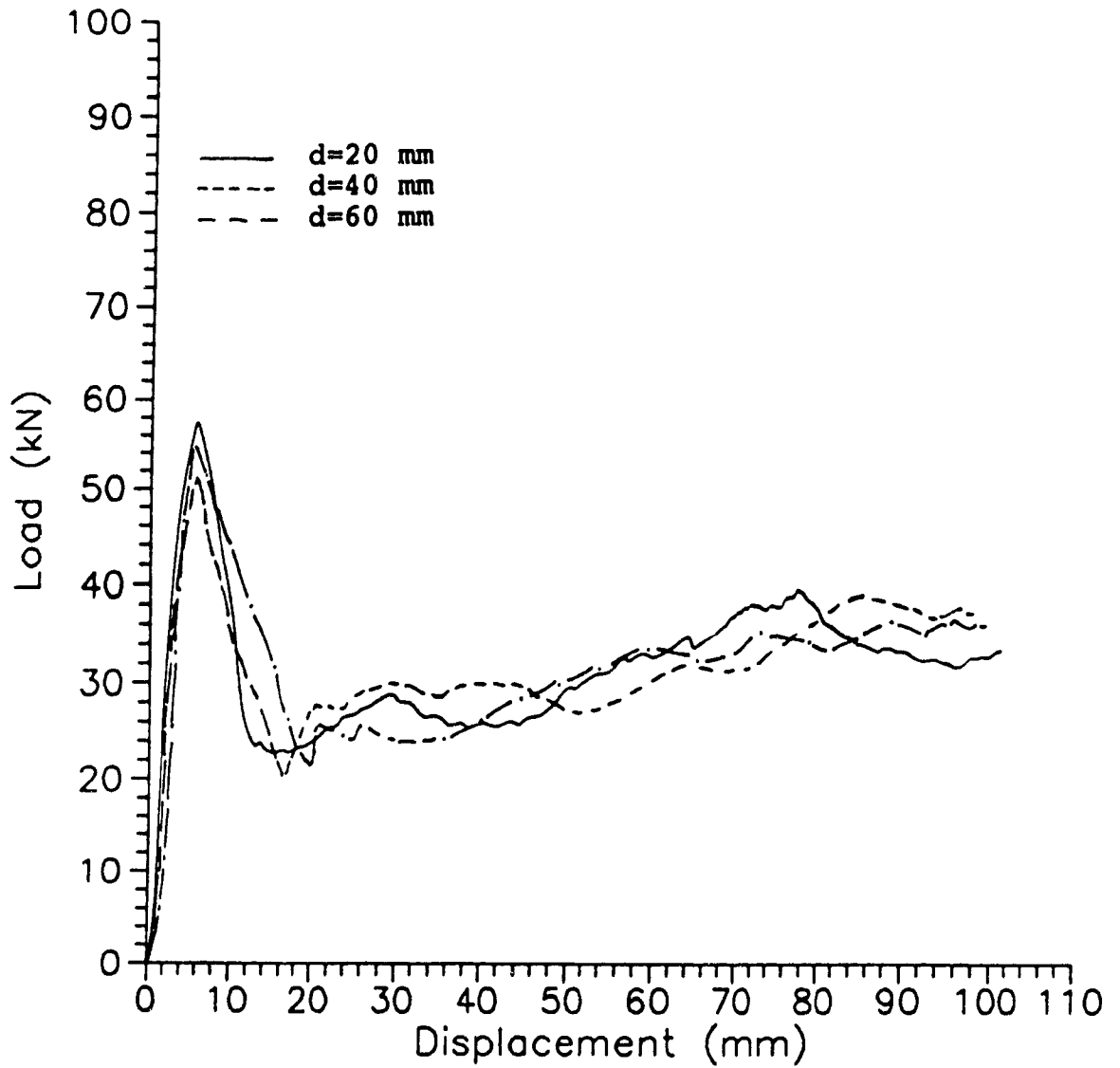


Fig. 5-8 Load-displacement behavior of cable with conventional grout for different diameter of borehole

Embedded length of cable for all the tests = 200 (mm)
GAC0

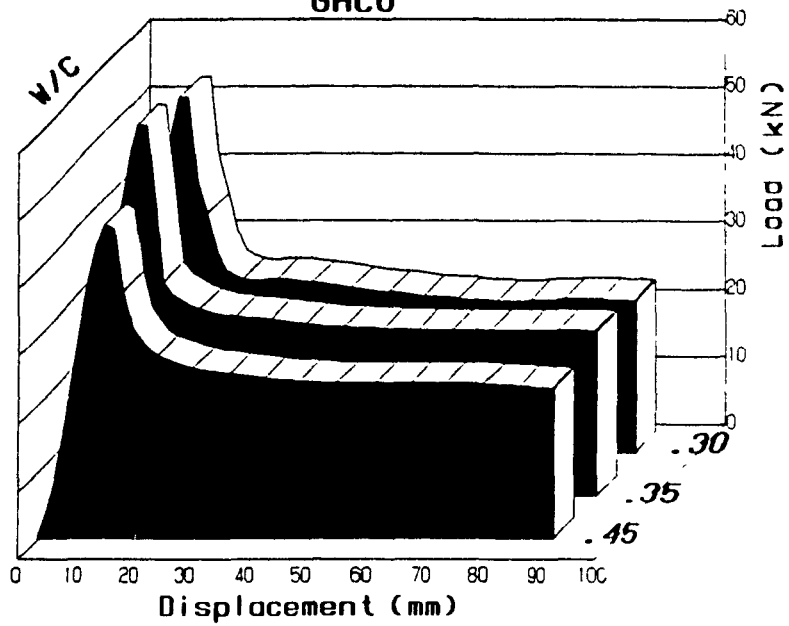


Fig. 5-9 Load versus displacement (mix GAC0)

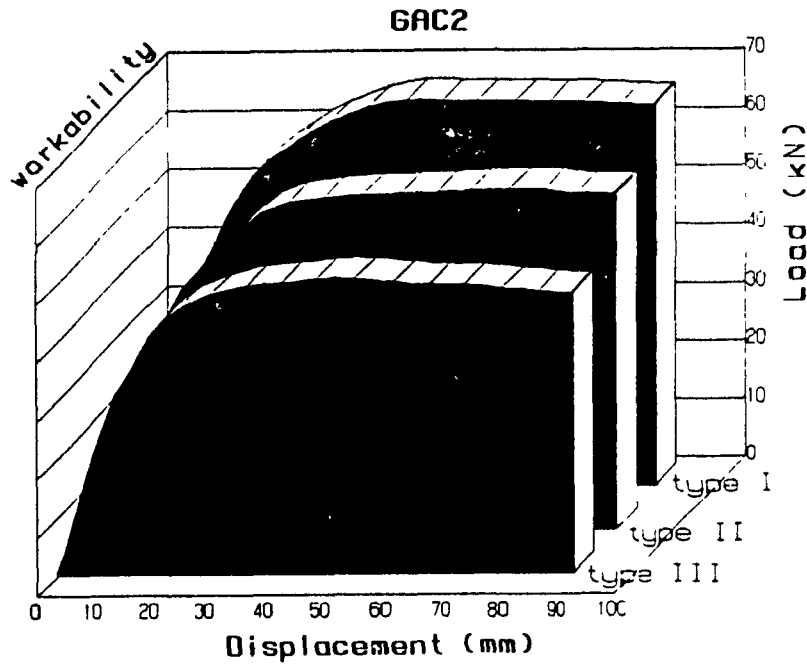


Fig. 5-10 Load versus displacement (mix GAC2)

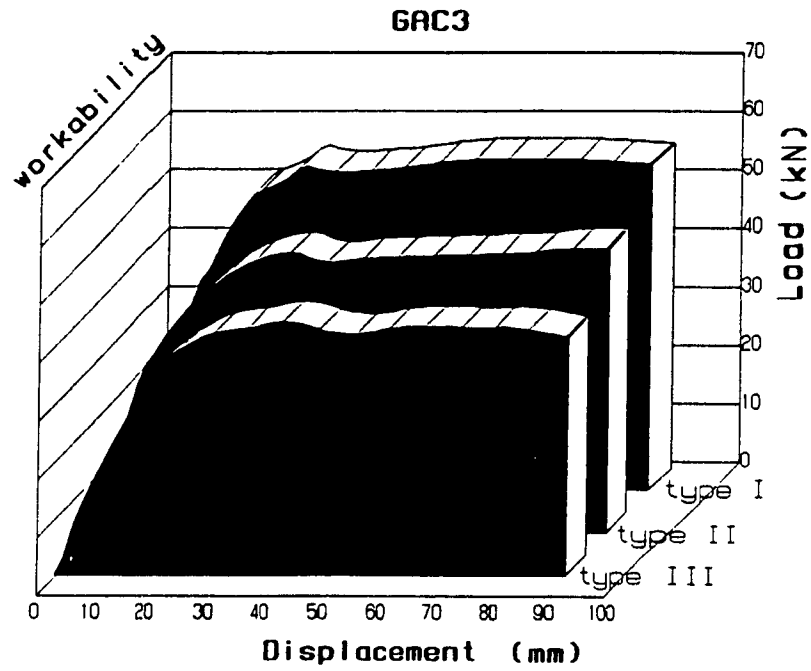


Fig. 5-11 Load versus displacement (mix GAC3)

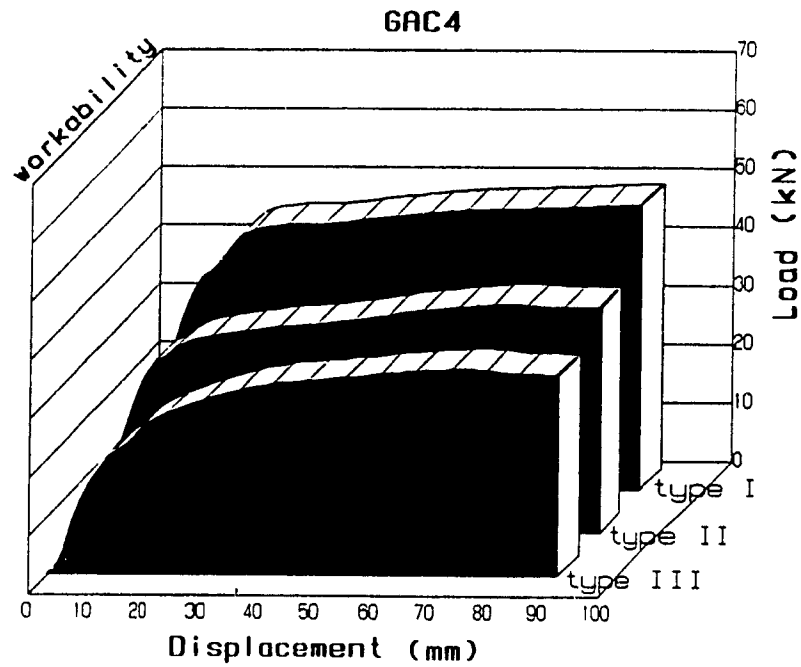


Fig. 5-12 Load versus displacement (mix GAC4)

different water-cement ratio or workability of the grout-aggregate material. As mentioned before, these grout-aggregate mixtures (marked I, II and III) correspond to the workability of the conventional grout with 0.3, 0.35 and 0.45 water-cement ratio respectively.

It is important to notice that employing a grout-aggregate mix as a bonding material results development of higher in residual bond strengths. This behavior of this bond is dependent on both the aggregate-cement ratio and the water-cement ratio. The workability has a significant effect on the load carrying capacity of the cable bolts. Lower water-cement ratios in both conventional grout and grout-aggregate mixes with the same workability improve the shear bond strength. Increasing the amount of aggregate in the grout-aggregate mix leads to the decrease of initial bond stiffness (initial slope of the load displacement curve) as well as a decrease in overall load carrying capacity of the cable bolt. The optimum bond strength was obtained with the aggregate-cement ratio of 2 with workability type I, which gave a 25 percent higher residual strength than conventional grout with similar workability.

After the pull-out tests a number of samples were sawed to examine the crack pattern in the matrix. Due to the friction force between the cable and the surrounding matrix numerous fine cracks were developed. Examination of the wider cracks showed that the coarse aggregates bridged the bond cracks as presented in the Fig. 5-13 allowing shear bond stresses to bridge the cracks. In some samples the failure of the aggregate interlocking mechanism was attributed to the cut-off peaks of aggregates and the protrusion of cement paste particles across the interface of cracks. The crack propagation for different samples was seen to be sensitive to the water-cement ratio and aggregate-cement ratio.

In order to highlight the superiority of the performance of the grout-aggregate mix over the conventional grout, the results of load-displacement for pull-out tests for the grout or grout-aggregate mixes providing the greatest support performance are given in Fig 5-14.

The ductile behavior of this cable bolt system using the grout-aggregate is well demonstrated. This is evident when compared with results of the tests on the cable bolt using only cement and water as the grout mix. The length (200 mm), curing time (28 days), grout workability and test procedure for all these samples were standardized. It is important to bear in mind that by variation of the grout-aggregate mix, variation in bond strength can be obtained but also a higher shear bond strength than with conventional grout mix can be achieved. Depending on the peak and residual strength values and support stiffness required by the engineer for any particular excavation, the grout-aggregate mix can be altered according to meet that support requirement without any change or modification to the steel strand. The unique strength and ductility of this support system is due to the adhesion, friction and especially the mechanical interlocking capability of the grout-aggregate material.

It should be noted that each of the curves in the load-displacement behavior represents an average of five samples, and no data points symbols appear. The maximum shear bond strength for each of the samples tested was determined and mean and standard deviation calculated. The results are summarized in Table 5-8.

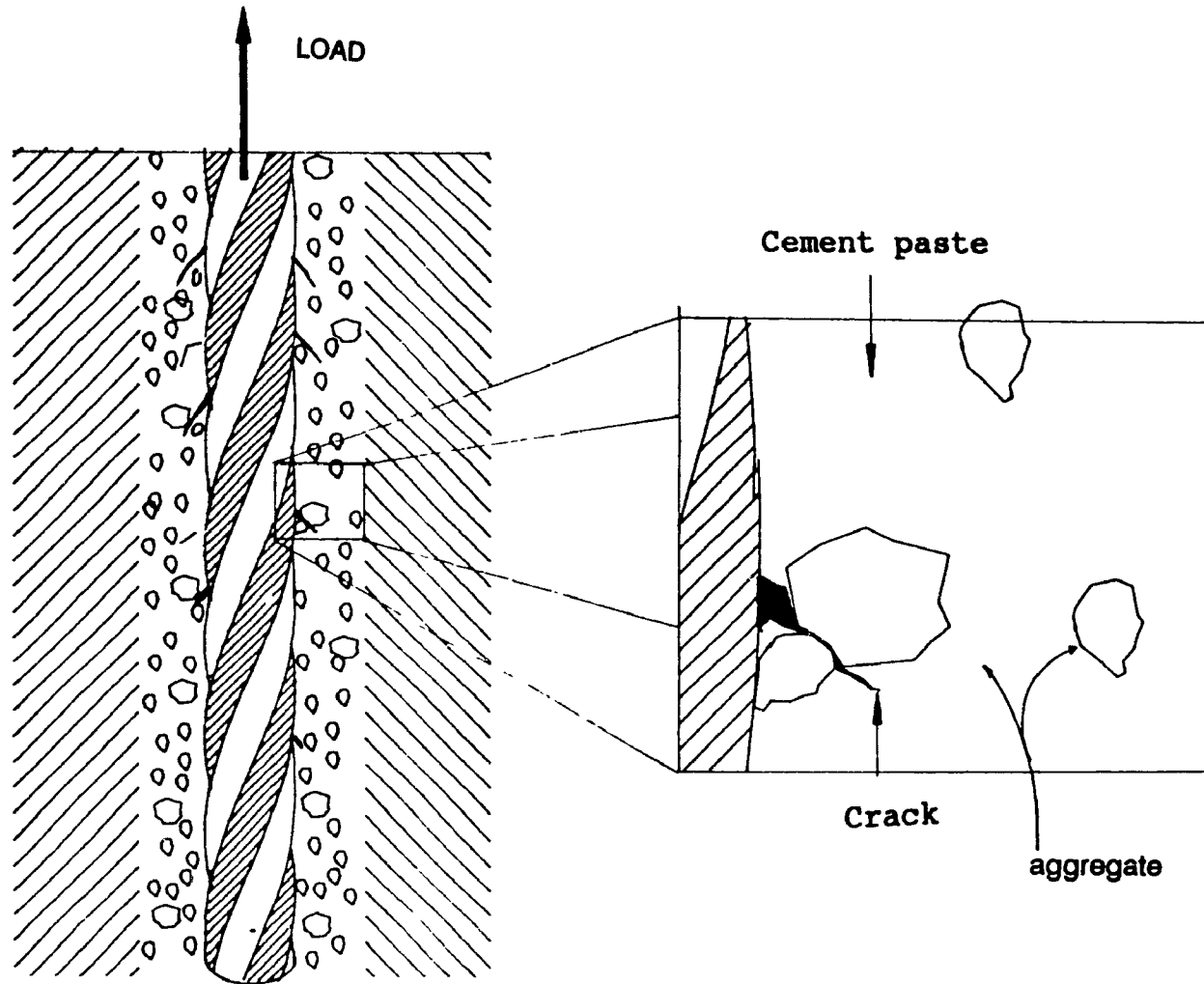


Fig. 5-13 Propagation of cracks observed in the grout-aggregate

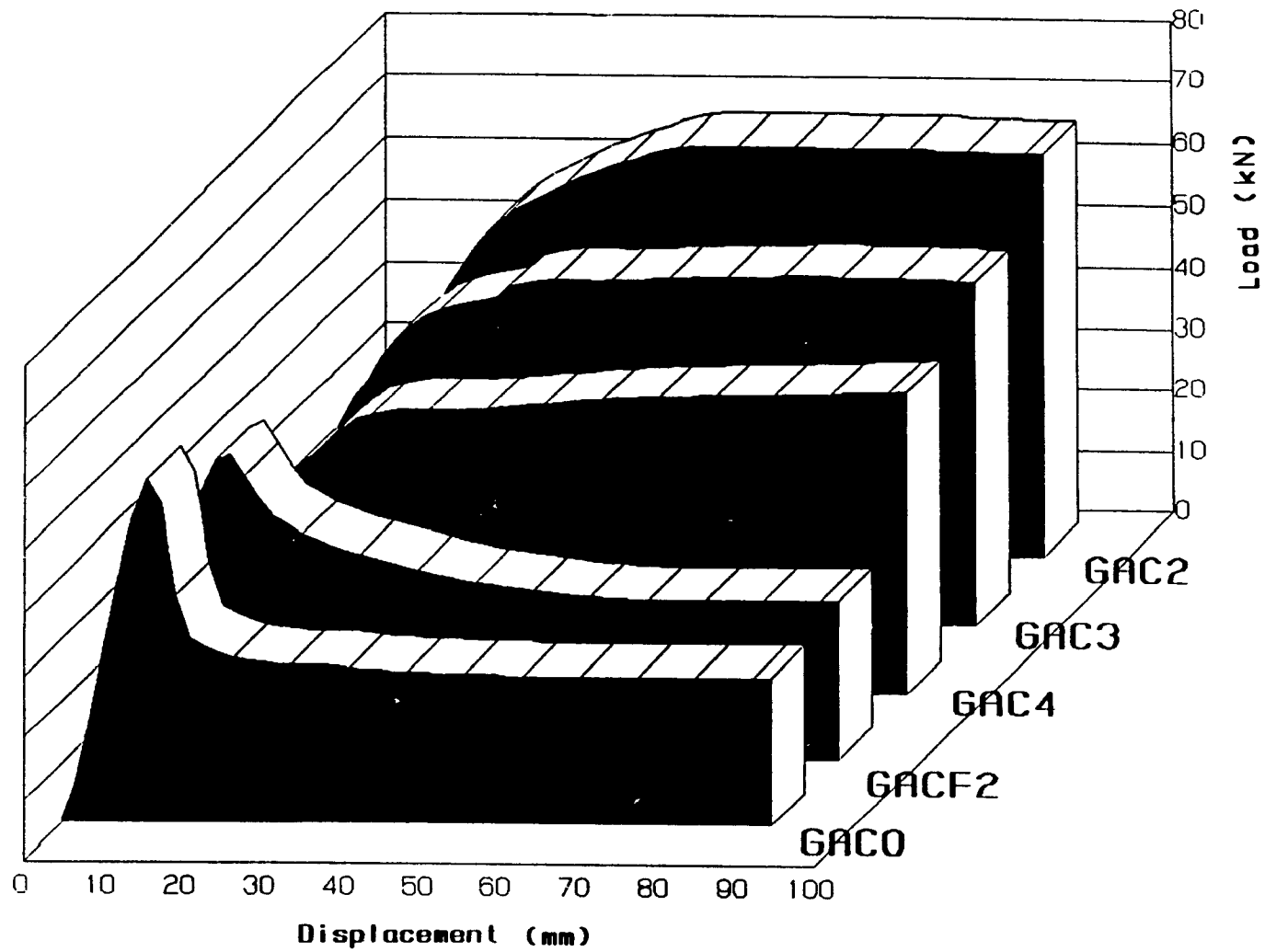


Fig. 5-14 Load versus displacement for different mixes

Material	Workability	test number					Mean (MPa)
	(type)	1	2	3	4	5	
GAC0	I	4.4	4	4.6	4.5	4.7	4.44 ± 0.27
	II	3.8	3.5	4.3	4	4.2	3.96 ± 0.32
	III	3.2	3	3.5	3.3	3.1	3.22 ± 0.20
GAC2	I	5.6	5.8	6.0	5.3	6.2	5.78 ± 0.35
	II	5.0	4.6	4.9	4.8	5.2	4.90 ± 0.22
	III	4.2	4.4	3.9	3.8	4.6	4.18 ± 0.33
GAC3	I	4.4	4.2	4.7	4.1	4.8	4.44 ± 0.31
	II	3.7	3.4	4.2	3.2	4.0	3.70 ± 0.41
	III	3.1	3.4	2.8	2.9	3.5	3.14 ± 0.30
GAC4	I	3.8	3.6	4.2	3.5	3.9	3.8 ± 0.27
	II	3.0	2.8	3.4	3.5	2.7	3.08 ± 0.36
	III	2.6	2.2	2.8	2.7	2.4	2.54 ± 0.24
GACF2	I	3.9	3.6	3.3	3.7	3.8	3.66 ± 0.23

Table 5-8 Shear bond strength of cable for different grout and grout-aggregate material with 200 mm embedded length

5.7.4 EFFECT OF EMBEDDED LENGTH OF CABLE

The critical bond length of a cable bolt is defined as that length of the cable which develops a total shear bond strength just greater than the tensile strength of the cable bolt (270 kN). To determine the critical bond length, series of pull-out tests were conducted using the different embedded length of the cable (15, 20, 30, 40, 50, 60 and 75/70 cm). The cables were fixed in the borehole with either grout or grout-aggregate and different types of workability (I, II and III). During the test rotation of the cable was prevented by the friction between socket and the supporting plate. This restriction was effected on the configuration of the steel strands. Fig. 5-15 and 5-16 show the rotation of the strands due to axial force of cable and shear bond stress at cable grout interface. As clearly can be seen the new position of strands provide more confinement on the exposed surface of cable and eventually could increase the residual strength of the cable bolt. A typical average load-displacement curve for 28 days curing time and different embedded length is shown in Fig. 5-17.

Mean and the standard deviation of the load carrying capacity of the cable were determined and the results for different grout mixes are summarized in Tables 5-9 and 5-10. The maximum load carrying capacity versus the embedment are shown in Fig. 5-18 and Fig. 5-19. A linear relationship between load and embedded length of the cable satisfies the experimental results. It can clearly be seen that the water-cement ratio has a significant effect on the results.



Fig. 5-15 Configuration of cable in the sample after pull-out test

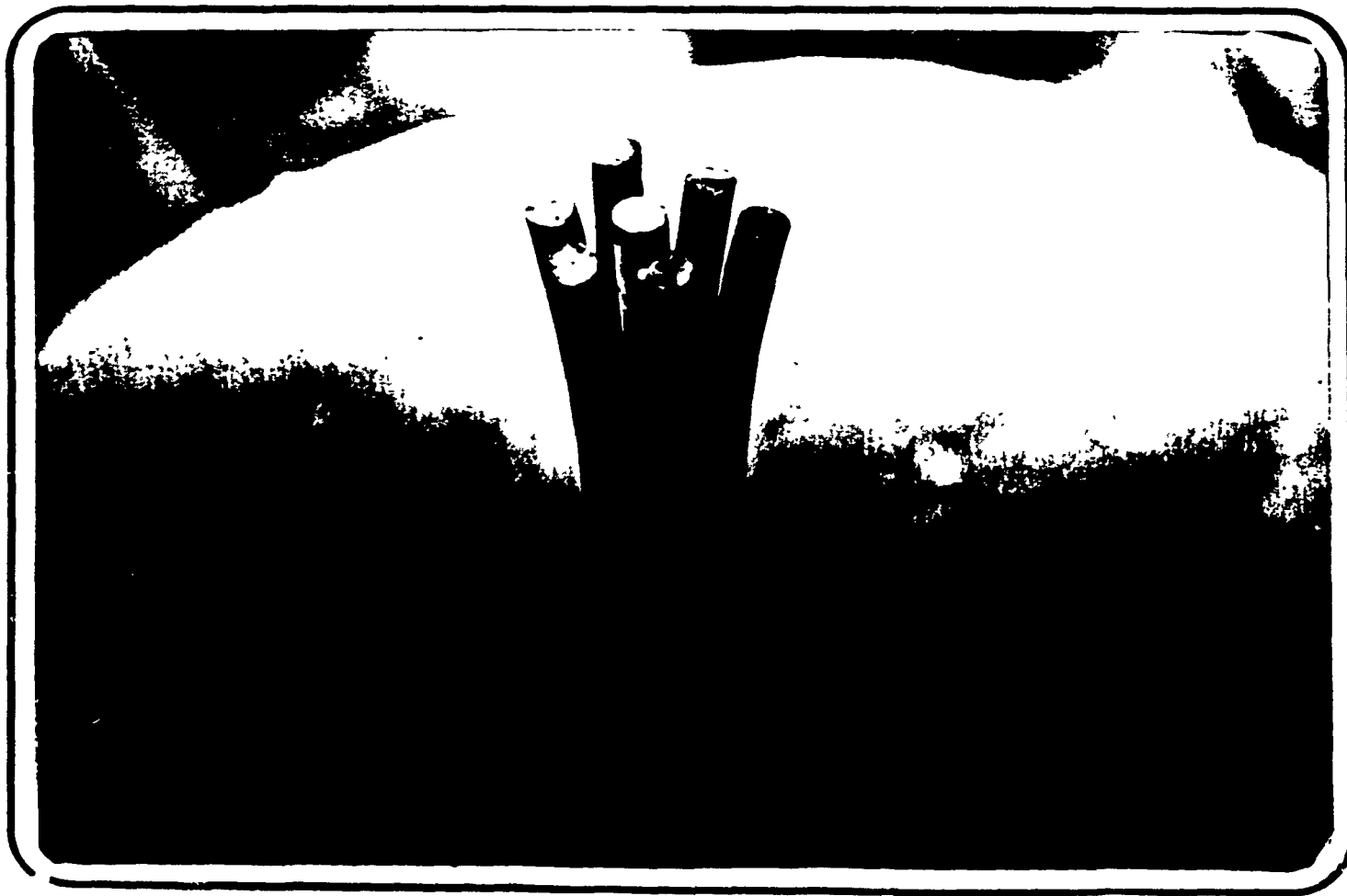


Fig. 5-16 Configuration of cable at the unloaded face of sample after pull-out test

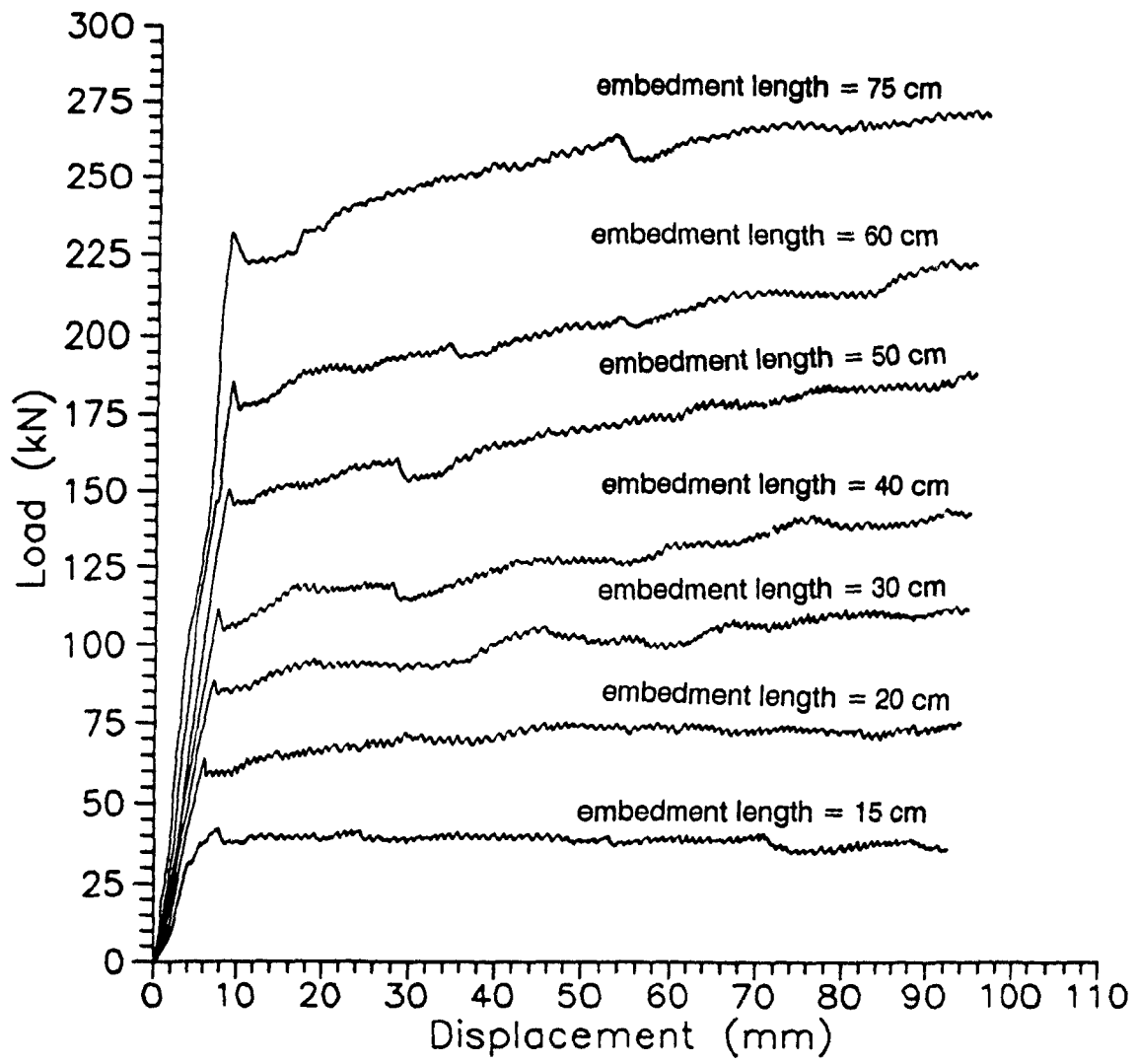


Fig. 5-17 Load-displacement behavior for different embedded length of cable with grout-aggregate mix type I

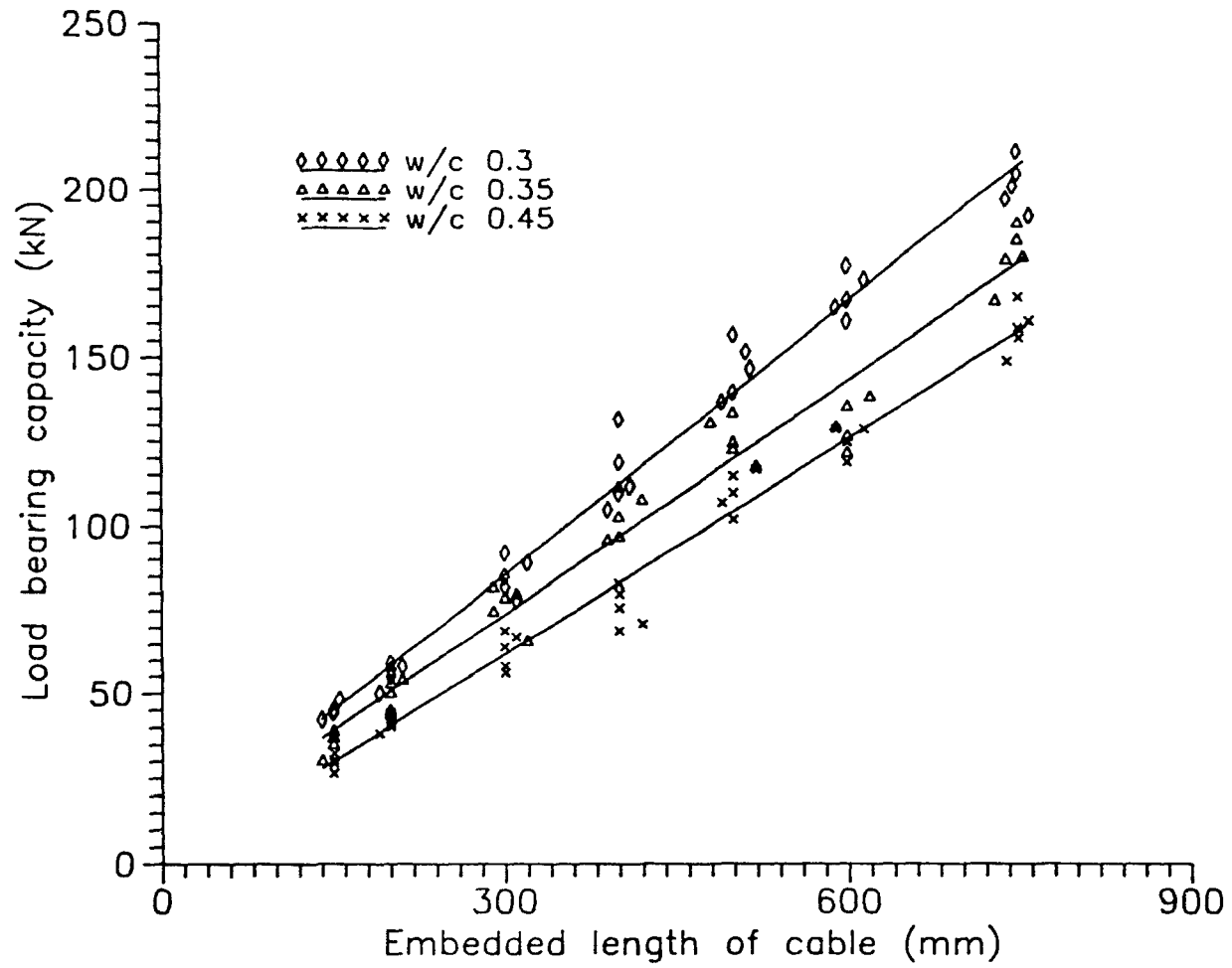


Fig. 5-18 Load carrying capacity versus embedded length for conventional grout

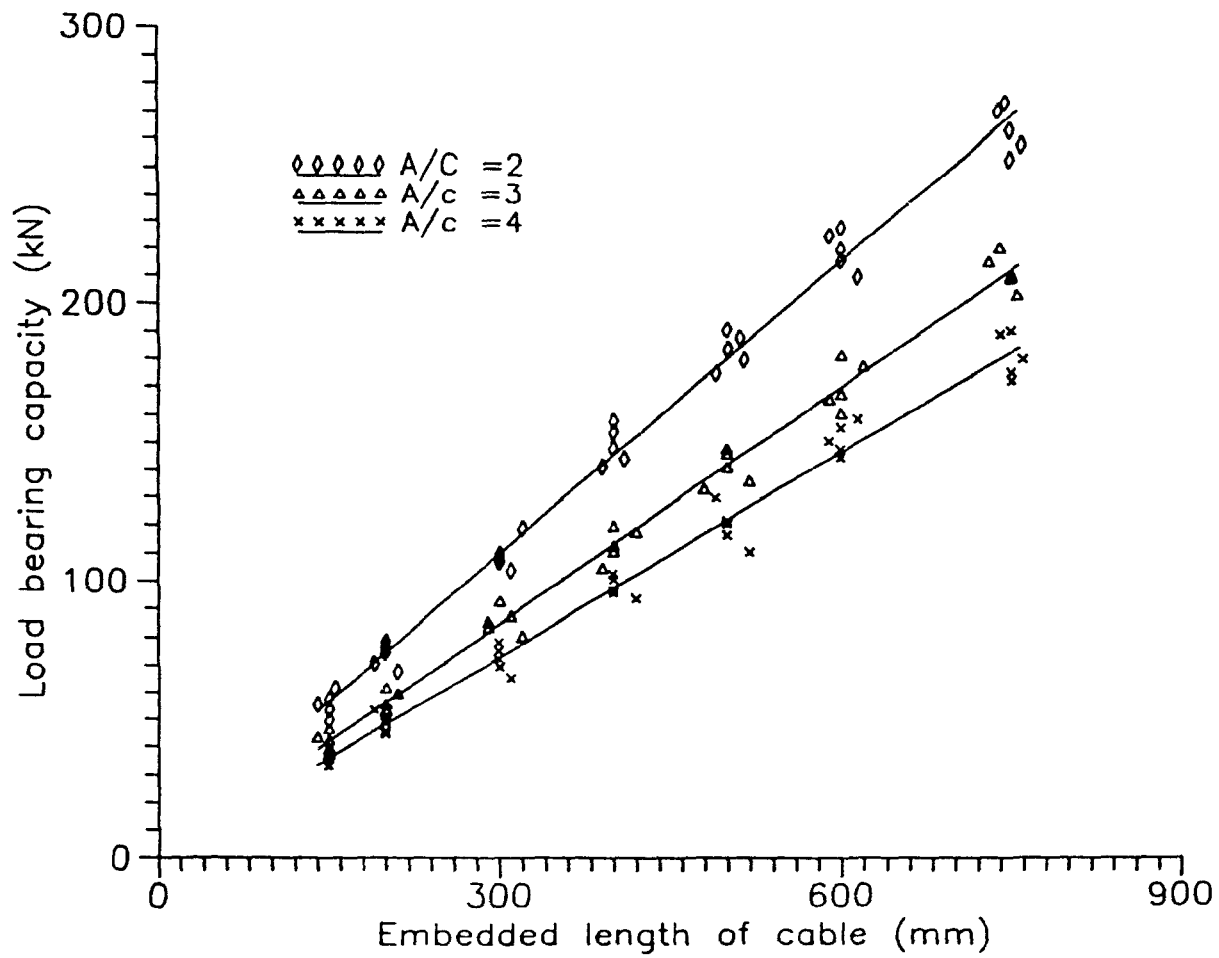


Fig. 5-19 Load carrying capacity versus embedded length for grout-aggregate mix (type I)

Workability (type)	Length (cm)	test number					Mean (kN)
		1	2	3	4	5	
I	15	42	44	48	45	38	43.4 ± 3.7
	20	55	50	58	57	59	55.8 ± 3.6
	30	85	89	92	82	78	85.2 ± 5.5
	40	112	119	105	132	110	115.6 ± 10.4
	50	140	152	147	157	137	145.6 ± 9.8
	60	167	173	177	165	161	168.6 ± 6.4
	70	197	183	181	185	180	187.2 ± 6.8
II	15	35	37	39	30	42	36.6 ± 4.5
	20	48	44	54	50	53	49.8 ± 4.0
	30	75	66	72	79	82	74.8 ± 6.2
	40	97	108	112	96	99	102.4 ± 7.2
	50	125	131	123	118	134	126.2 ± 6.4
	60	136	135	127	130	122	130.0 ± 5.8
	70	160	154	143	159	148	153.8 ± 7.0
III	15	30	37	26	29	32	30.8 ± 4.1
	20	42	40	38	44	41	41.0 ± 2.2
	30	64	58	67	56	69	62.8 ± 5.6
	40	76	80	71	69	83	75.8 ± 5.9
	50	107	110	102	117	115	110.2 ± 6.0
	60	125	130	119	132	127	126.6 ± 5.0
	75	156	168	149	159	161	158.6 ± 6.9

Table 5-9 Load carrying capacity with normal grout for different embedded length of cable by means of pull-out test

A/C	Length	test number					Mean
ratio	(cm)	1	2	3	4	5	(kN)
2	15	55	57	61	49	53	55.0 ± 4.5
	20	70	74	76	67	78	73.0 ± 4.4
	30	109	118	106	107	103	108.6 ± 5.7
	40	147	153	140	157	143	148.0 ± 7.0
	50	183	187	179	190	174	182.6 ± 6.3
	60	219	224	215	209	227	218.8 ± 7.1
	75	263	270	253	273	258	263.4 ± 8.2
3	15	42	43	39	46	37	41.4 ± 3.50
	20	55	53	59	52	61	56.0 ± 3.9
	30	85	80	87	92	83	85.4 ± 4.5
	40	112	117	110	104	119	112.4 ± 5.9
	50	140	135	145	132	147	139.8 ± 6.4
	60	167	165	160	177	181	170.0 ± 8.7
	75	210	215	220	203	209	211.4 ± 6.4
4	15	35	33	37	39	36	36 ± 2.2
	20	48	45	53	44	49	47.8 ± 3.6
	30	72	75	65	69	78	71.8 ± 5.1
	40	96	100	93	102	95	97.2 ± 3.7
	50	120	110	116	121	129	119.2 ± 6.9
	60	144	150	147	158	155	150.8 ± 5.7
	75	180	175	189	190	172	181.2 ± 8.1

Table 5-10 Load carrying capacity with the grout-aggregate material and workability type I for different embedded length of the cable by means of pull-out test

5.8 EXPERIMENTAL CONCLUSIONS

The following conclusions can be drawn from the test results presented in this chapter:

1- The pull-out tests on cables embedded in thick wall concrete cylinders with different borehole diameters had similar results. Apparently the practical range of borehole diameters has only a minor effect on the load carrying capacity of cable bolts because failure is initiated at the cable/grout interface.

2- The workability has a significant effect on the load carrying capacity of cable bolts. Lower water-cement ratio in conventional grout and grout-aggregate mixture with the same workability improves the capacity of the cable bolt.

3- The presence of aggregate in the mixture does not have a significant effect on the chemical adhesion of the steel-grout interface.

4- Increasing the amount of aggregate in the mixture of grout led to the decrease of the initial slope of the load-slip behavior.

5- Comparison of the results in load-slip behavior shows that the area between the curves and the slip axis for grout-aggregate is more than conventional grout. It thus indicates that cable bolting with grout-aggregate is more ductile with respect to conventional grout.

6- Due to the friction properties between the grout-aggregate and the cable bolt, the residual strength between the cable and surrounding matrix is higher than the conventional grout.

7- A linear relationship could be correlated for the experimental load carrying capacity of the cable bolt versus the different embedded length up to 75 cm.

8- Variation of the diameter of the concrete cylinders above 200 mm did not have a significant effect on the results.

9- The distribution of the internal cracks in the surrounding matrix of cable bolt make an angle with the cable's axis between 40 to 60 degrees.

10- The presence of only fine aggregates decreases the load carrying capacity of the cable bolt, but increases the residual strength.

CHAPTER 6

DISTRIBUTION OF SHEAR BOND STRESS

6.1 INTRODUCTION

The stress field around a cable bolt embedded in rock and fixed with grout, when subjected to uniaxial load, is a complicated three-dimensional problem. It is difficult to model mathematically and equally difficult to verify the results experimentally. The laboratory tests show that even with low axial loads in pull-out tests high stresses still develop at the load end face of the specimen. This causes a local cohesion bond breakdown around the cable and crushing of the matrix at the root of the leading lugs. This in turn shifts the bond stress curve along the cable bolt axis bringing into action additional lugs which sustain the load by bearing. Thus, neither the height, the shape nor the position of the bond stress curve is known quantitatively at any loading stage.

An equally difficult problem is encountered when attempting to model the stresses around a typical cable lug. Depending on the configuration of the cable bolt, normal compressive stresses can develop radially into the surrounding matrix [42]. Even when neglecting all cohesion bonding along the length of the cable in areas of low bond stress, it is difficult to determine how many lugs are actually loaded and what percentage of the load is taken by each lug.

Due to the interlocking behavior of bond elements between the cable and the surrounding rock, large amounts of slip occur at the cable-matrix interface. In order to predict the load bearing capacity of a cable bolt, it is necessary to consider

the slip phenomenon in the solution method.

The literature review in Chapter 2 shows that several researchers have worked on this subject [32, 69, 75, 76], though most of the works were related to rock bolts. The purpose of this chapter is to present an analytical model which can be used to determine the distribution of shear bond stress along the embedded length of a cable bolt in an intact rock environment. The model developed simulates the interaction between the cable surface and borehole wall in rock through a continuous spring system which utilizes the Winkler hypothesis. Linear elastic behavior of both the rock and the cable materials are assumed whereas a trilinear model is employed for the Winkler springs. The total potential energy is formulated and the variational principle is then applied to minimize the functional of the total potential energy and hence arrive at the governing differential equation.

6.2 ANALYTICAL MODEL

The underlying philosophy of the analytical model is that the grout material between the cable and the surrounding rock, (Fig. 6-1a) can be idealized by a set of continuous springs parallel to the cable axis (Fig. 6-1b). The objective is then to select the characteristic of shear bond-slip model for those springs so as to conform to the load-slip relationship observed in uniaxial pull-out tests, such as described in Chapter 5.

The relationship between the shear bond stress and normal (bursting or radial) stress depends upon the orientation of the resultant stress which act on the surface of the cable bolt. At the root of the lug, very high compressive stresses

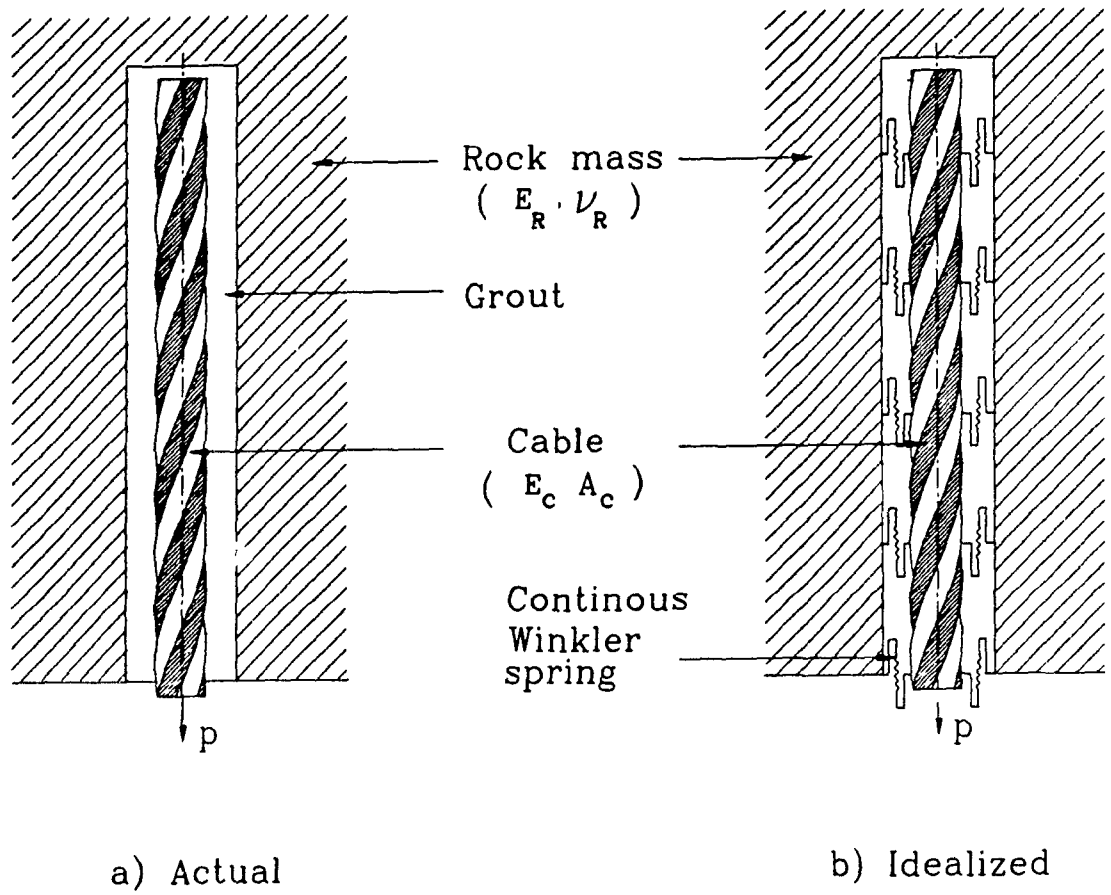


Fig. 6-1 Simulation of grout and interfaces

develop which may cause local crushing of the surrounding matrix and lead to readjustment of the direction of the resultant force. Thus, there is no direct way of determining the relationship between the shear bond stress and the radial normal stress. Tapfer [82], for example, adapted the analogy of this situation with the well known bursting problem of a pipe under internal pressure to calculate the normal stresses in the radial direction. In this study, it will be assumed that the radial normal stress is linearly proportional to the shear bond stress on the cable surface at any loading stage. The proportionality coefficient is called the rib factor.

Referring to Fig. 6-2, the radial normal, σ_n , stress acting on the cable surface is given by:

$$\sigma_n = k \cdot \tau_c \quad (6-1)$$

where

τ_c = shear bond stress

k = rib factor

The analytical model is developed with the assumption of linear elastic behavior for both rock and cable bolt materials. The effect of the installation of the cable bolt is left out at this stage, in other words it is assumed that rock mass characteristics are not affected by the installation procedure.

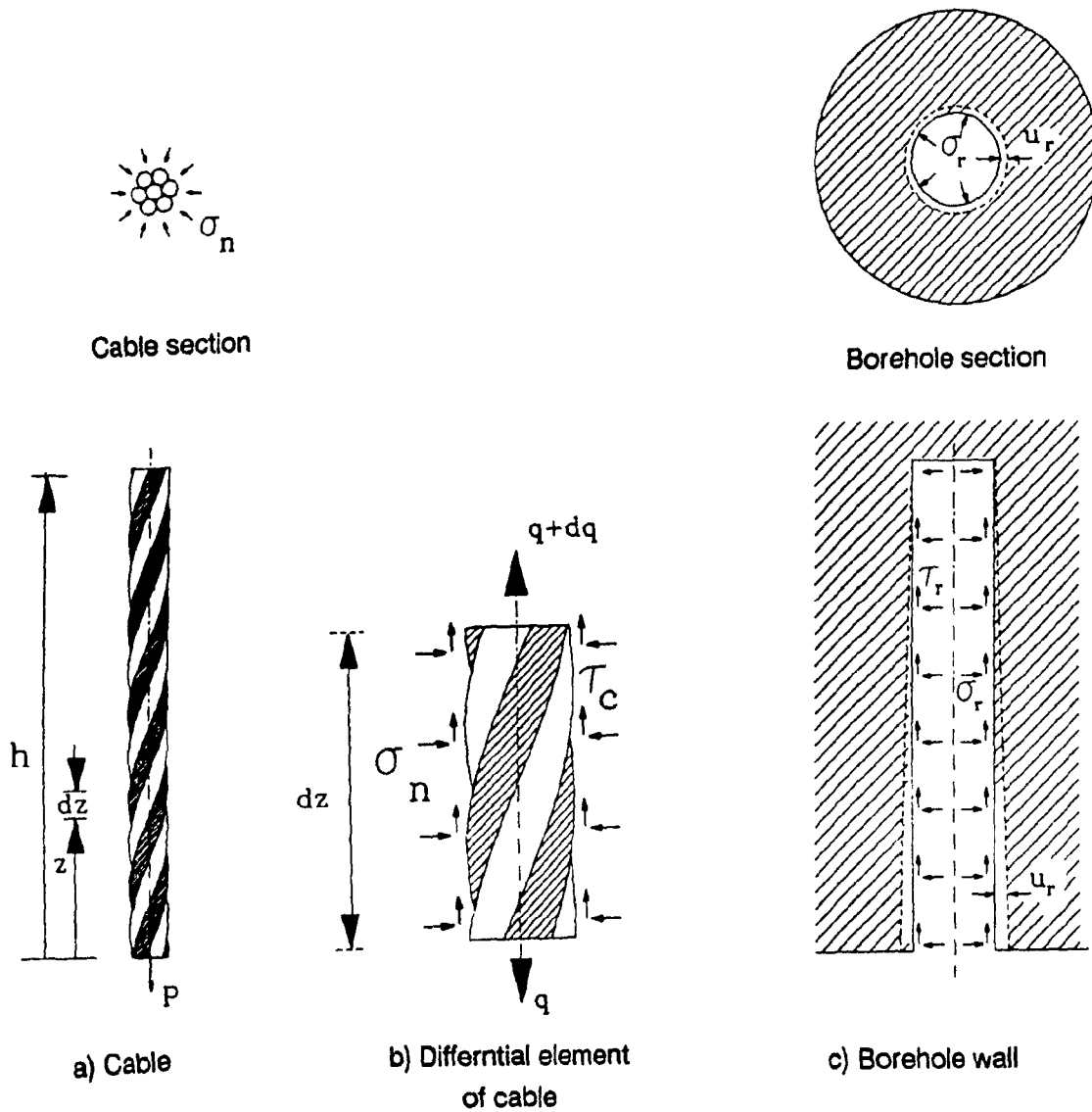


Fig. 6-2 Definition of stress and deformation components

6.3 VARIATIONAL APPROACH

The variational approach relying on calculus of variation involves optimizing a functional. In solid mechanics the functional could be the potential energy, the complementary energy or some derivative of it [83].

Using calculus of variation, a differential equation is found equivalent to a variational principle. This is relatively easy compared with the reverse process of arriving at a variational or functions form starting from a differential equation.

Let us consider a functional expressed as [84]:

$$I = \int_{z_1}^{z_2} F(z, q, q') dz \quad (1)$$

where $q = q(z)$ $q' = dq/dz$

The equation is defined in the range of domain (z_1, z_2) and $q(z_1) = q_1$ and $q(z_2) = q_2$. Assume that function $\phi(z)$ makes the functional I stationary, then for a small variation ϵ of $\phi(z)$ we have

$$\left(\frac{dI}{d\epsilon} \right) = 0$$

where $\epsilon \Rightarrow 0$

Let us assume that an approximating function to $\phi(z)$ is $q(z)$

where $q(z) = \phi(z) + \epsilon \eta(z)$

$\eta(z) =$ arbitrary sufficiently differentiable function

$\epsilon =$ small quantity

By allowing ϵ to tend to zero, the approximate curve $q(z)$ approaches $\phi(z)$ (see Fig. 6-3). Furthermore, according to the boundary conditions: $\eta(z_1) = \eta(z_2) = 0$. Thus for a given $\eta(z)$, I is a function of ϵ and we require $I(\epsilon)$ to attain a stationary value of $\epsilon = 0$ i.e. $\left(\frac{dI}{d\epsilon}\right)_{\epsilon \rightarrow 0} = 0$

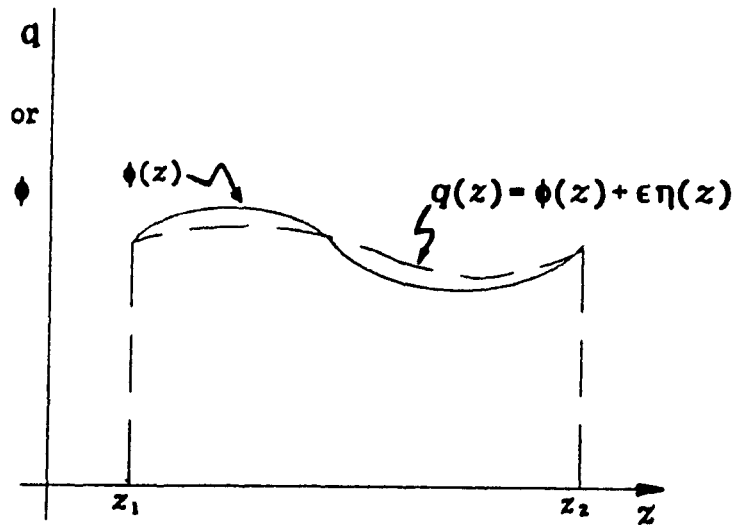


Fig. 6-3 True and varied curves in a variation problem

Therefore, equation (i) becomes

$$I = \int_{z_1}^{z_2} F(z, \phi + \epsilon\eta, \phi' + \epsilon\eta') dz \quad (ii)$$

Expanding as a Taylor series about x, ϕ, ϕ' and differentiating with respect to (ϵ) gives:

$$\left(\frac{dI}{d\epsilon}\right)_\epsilon = 0 = \int_{z_1}^{z_2} \left[\eta \frac{\partial F}{\partial \phi} + \eta' \frac{\partial F}{\partial \phi'} \right] dz = 0 \quad (iii)$$

Integration eq. (iii) part by part yields:

$$\int_{z_1}^{z_2} \eta \left[\frac{\partial F}{\partial \phi} - \frac{d}{dz} \left(\frac{\partial F}{\partial \phi'} \right) \right] dz = 0 \quad (iv)$$

As $\eta(z)$ is an arbitrary quantity then equation (iv) can only be satisfied if the integral and other terms vanish. Thus the necessary conditions are:

$$\frac{d}{dz} \left(\frac{\partial F}{\partial \phi'} \right) - \frac{\partial F}{\partial \phi} = 0 \quad (v)$$

$$\left. \frac{\partial F}{\partial \phi'} \right|_{z_1}^{z_2} = 0 \quad (vi)$$

$$\eta(z_1) = \eta(z_2) = 0 \quad (vii)$$

Equation (v) is the Euler-Lagrange equation. It is possible to show that for a functional that has one independent variable and three higher order derivatives of the form:

$$I = \int_{z_1}^{z_2} F(z, q, q', q'', q''') dz \quad (6-2)$$

The corresponding Euler-Lagrange equation is

$$\frac{d^3}{dz^3} \left(\frac{\partial^3 F}{\partial q'''} \right) - \frac{d^2}{dz^2} \left(\frac{\partial^3 F}{\partial q''} \right) + \frac{d}{dz} \left(\frac{\partial F}{\partial q'} \right) - \frac{\partial F}{\partial q} = 0 \quad (6-3)$$

where

$$q' = \frac{dq}{dz} \quad q'' = \frac{d^2q}{dz^2} \quad q''' = \frac{d^3q}{dz^3}$$

This is used in verifying the variational principle equivalent to the governing differential equation for distributions of the shear bond stress and the load along the embedded length of cable bolt. The conditions expressed by equations (vi and vii) are called natural and geometric (or kinematic) boundary conditions, respectively [84].

6.4 TOTAL POTENTIAL ENERGY

The approach of the present analysis is based on the minimization of the total potential energy for a cable-grout assembly using calculus of variation. Thus, the first variation of total potential energy of the system must be found and set to zero, i.e. [83].

$$\delta^{(1)}(U + V) = 0 \quad (6-4)$$

where U strain energy
 V potential energy of loads.

In general, the strain energy can be calculated from:

$$U = \int_{vol} \left[\int \sigma d\epsilon \right] dv \quad (6-5)$$

The components of strain energy, for different components of the system are described in the following subsections.

6.4.1 Strain energy in the cable bolt (U_c)

The lateral strain effect due to the radial bursting stress acting on the surface of the cable bolt is assumed negligible. From Fig. 6-2 the axial strain and stress in the cable can be calculated by [82]:

$$\epsilon_c = -\frac{dv_c}{dz} = \frac{q}{E_c A_c} \quad (6-6)$$

$$\sigma_c = \frac{q}{A_c} \quad (6-7)$$

Substitution of eq. (6-6) and eq. (6-7) into eq. (6-5) gives

$$U_c = \int_0^h \frac{q^2}{2E_c \cdot A_c} dz \quad (6-8)$$

where q = load of cable;
 h = embedded length of cable;
 E_c = modulus of elasticity of cable;
 A_c = cross sectional area of cable.

6.4.2 Strain energy stored in the grout or Winkler springs (U_p)

A free body diagram of the parallel spring system representing the grout is shown in Fig 6-4b. In accordance with the results of pull-out tests (Chapter 5), the springs are modelled as elastic-softening-plastic material. This trilinear model is described by the relation:

$$\tau_c = ms + n \quad (6-9)$$

where τ_c = shear bond stress at exposed surface of cable;
 s = slip between cable and borehole wall.

The coefficients m and n for the three stages of shear force-displacement of the cable are given in given in Fig. 6-5.

Based on the assumption that the shear bond stress for a short length of cable is uniform, equilibrium conditions in the longitudinal direction of the cable furnish the following equation (see Fig. 6-2b):

$$\tau_c = - \frac{dq}{dz \cdot \Sigma_0} \quad (6-10)$$

where Σ_0 is the perimeter of the cable bolt.

The strain energy for a segment of parallel springs dU_p along a differential length dz of the cable is given by:

$$dU_p = \int dq \cdot ds \quad (6-11)$$

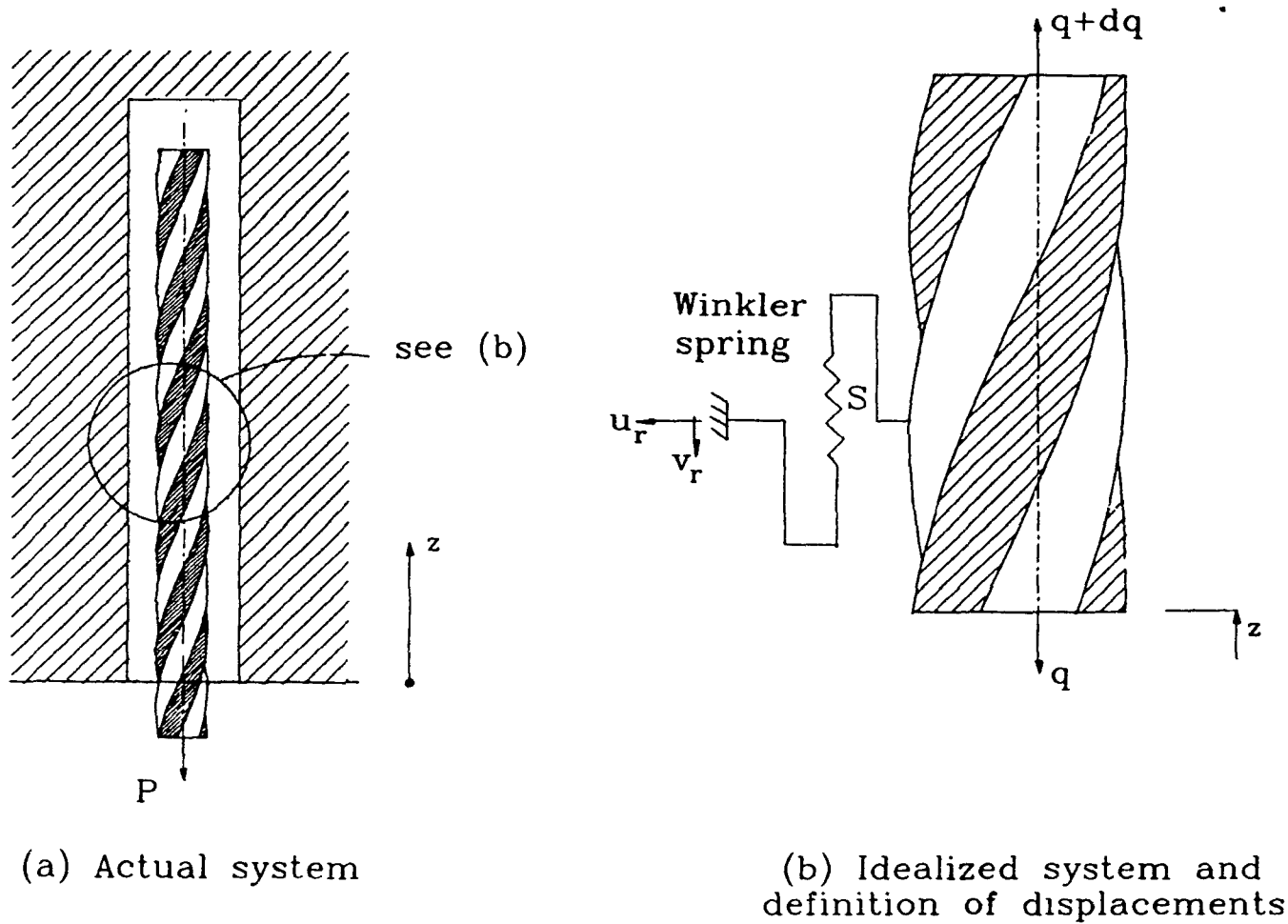
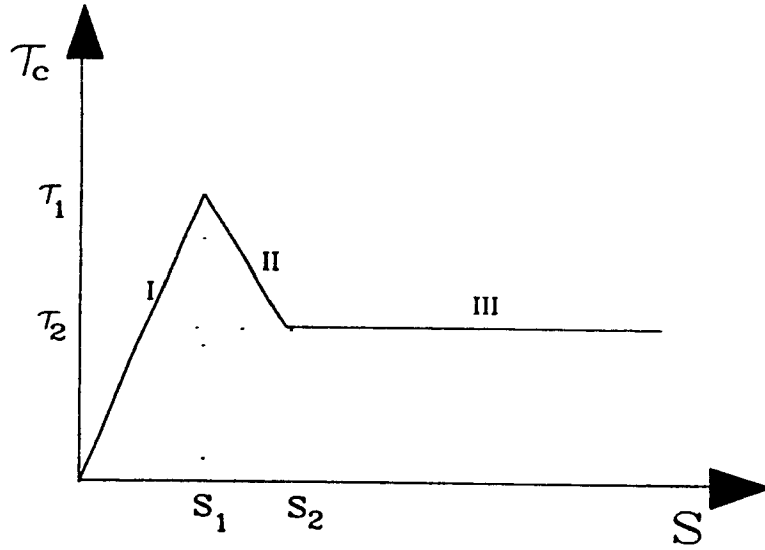


Fig. 6-4 Simulation of actual and idealized systems



$$\tau_c = ms + n$$

	m	n
I	$\frac{\tau_1}{S_1}$	0
II	$\frac{\tau_1 - \tau_2}{S_1 - S_2}$	$\frac{-\tau_1 + \tau_2}{S_1 - S_2} S_1 + \tau_1$
III	0	τ_2

Fig. 6-5 Slip characteristics of the Winkler spring

Substitution of eq. (6-9) into eq. (6-11) and then using eq.6-10 leads to:

$$U_p = \int_0^h \left[\frac{\Sigma_0}{2m} \cdot \left(\frac{dq}{dz \cdot \Sigma_0} + n \right)^2 - \frac{n\Sigma_0}{m} \cdot \left(\frac{dq}{dz \cdot \Sigma_0} + n \right) \right] dz \quad (6-12)$$

6.4.3 Strain energy stored in host rock

i- Shear strain energy in the longitudinal direction (U_s)

The deformation of the rock around the cable is shown in Fig. 6-5. Equilibrium conditions in the longitudinal direction of the cable axis for an element of rock in a cylindrical coordinate system are given by Goodman [85]:

$$-\frac{\partial(\tau r)}{\partial r} - \frac{\partial \sigma}{\partial z} \cdot r = 0 \quad (6-13)$$

where τ = shear stress in rock at radius r
 σ = normal stress in rock at radius r
 z = distance from load end face of cable

Ignoring the variation of σ with respect to z and then substituting the boundary conditions (at $r=r_g$ shear is $\tau=\tau_g$) in the radial direction in the eq. (6-13) results in:

$$\tau = \frac{\tau_g r_g}{r} = \frac{\tau_c \cdot \Sigma_0}{2\pi r} \quad (6-14)$$

where τ_g = shear bond stress at grout-rock interface
 r_g = radius of borehole

In practice the distribution of shear stress (τ) in a radial direction around the cable shaft in the rock decreases more rapidly than with increasing the radius r , given in eq. (6-14). Unfortunately, the monitoring of the distribution of shear stress due to the cable load is very difficult and there is no data in the available literature. However, the settlement profile for the case of a pile having a length equal to forty times its radius has been reported. At a distance equal to 52 times the radius of the pile into the surrounding matrix the magnitude of settlement of the soil tends to zero [86]. However, monitoring shows that this distance can be increased to 93 times the radius of the pile when the Poisson's ratio of the soil decreases (approaching zero). In cable bolting the effect of the radius of the surrounding rock mass depends on the properties of the rock mass, length of the cable bolt, structural geology and geometry of the underground excavation. However, in the case of a hard rock environment, based on the available design pattern [5], the effective radius of the rock is less than fifty times the radius of the borehole. To present the relative formulation more simply it is assumed that an average value equal to 54 times the radius of the borehole applies.

The shear strain in the rock is expressed by Timoshenko [87] as:

$$\gamma = \frac{\tau}{G} = \frac{\partial u_r}{\partial z} + \frac{\partial v_r}{\partial r} \quad (6-15)$$

where u_r = radial deformation of rock
 v_r = vertical deformation of rock
 G = shear modulus of rock

The shear strain energy in the rock is thus given by

$$U_s = \int \left[\int \tau d\gamma \right] dv \quad (6-16)$$

where $dv = 2\pi r \cdot dr \cdot dz$

Substituting eq. (6-15) into eq. (6-16), then using eq. (6-14) and assuming that the effective radius of the cable is 54 times the radius of borehole then:

$$U_s = \int_0^h \left[\frac{(dq/dz)^2}{\pi \cdot G_r} \right] dz \quad (6-17)$$

where G_r is the shear modulus of the rock

ii- Strain energy in the host rock due to bursting pressure

The strain energy in the borehole wall as a result of bursting pressure due to the radial and hoop stresses in the rock is:

$$U_b = \int_0^h (\sigma_r d\epsilon_r + \sigma_\theta d\epsilon_\theta) dv \quad (6-18)$$

The bursting stress p_b due to the bond action at the grout-cable interface may be regarded as a hydraulic pressure which acts on a thick wall rock cylinder (see (Fig. 6-2)). The plane strain solution for the homogeneous thick-wall cylinder subject to internal and external pressures has been derived by Timoshenko [87]. If the external radius with respect to the internal radius is assumed to be large enough and the effect of external pressure is neglected then the following simplified equations are obtained:

$$u_r = \frac{p_b}{2G_r} \cdot \frac{r_g^2}{r} \quad (6-19)$$

$$\sigma_r = -\sigma_\theta = -\frac{p_b \cdot r_g^2}{r^2} \quad (6-20)$$

Radial and hoop strains are given as:

$$\epsilon_\theta = \frac{u_r}{r} \quad \epsilon_r = \frac{du_r}{dr} \quad (6-21)$$

where p_b = bursting pressure
 r_g = radius of borehole
 G_r = shear modulus of the rock
 u_r = radial deformation of the rock
 σ_r = radial stress in the rock
 σ_θ = hoop stress in the rock

Due to the slip of the cable and processing of the interlocking behavior of the bond element, it is assumed that the grout material has been crushed radially. Therefore, concerning the equilibrium conditions in a radial direction, the bursting stress on the borehole's wall (σ_b) has the following relationship with the normal stress on the cable:

$$\sigma_b = \frac{k \cdot \tau_c \cdot \Sigma_0}{2\pi r_g} \quad (6-22)$$

Substituting eq. (6-20) and eq. (6-21) into eq. (6-18) and using eq. (6-22) yields:

$$U_b = \int_0^h \left[\frac{k^2 \cdot (dq/dz)^2}{8\pi G_r} \right] dz \quad (6-23)$$

6.4.4 Potential of the external load (V_p)

The potential of the external load is given by:

$$V_p = -P\Delta \quad (6-24)$$

Where the tip displacement Δ shown in Fig. 6-6 consists of the following components:

$$\Delta = s + v_c + v_r \quad (6-25)$$

where s = slip of cable with respect to the borehole's wall,
 v_c = vertical deformation of the rock,
 v_r = vertical deformation of the cable.

Substituting eq. (6-22) into eq. (6-19) and using eq. (6-14) gives:

$$u_r = -\frac{k \cdot r_g \cdot (dq/dz)}{4\pi r G_r} \quad (6-26)$$

Substituting eq. (6-26) into eq. (6-15) and using eq. (6-10) gives the vertical deformation of the rock at the borehole wall v_c .

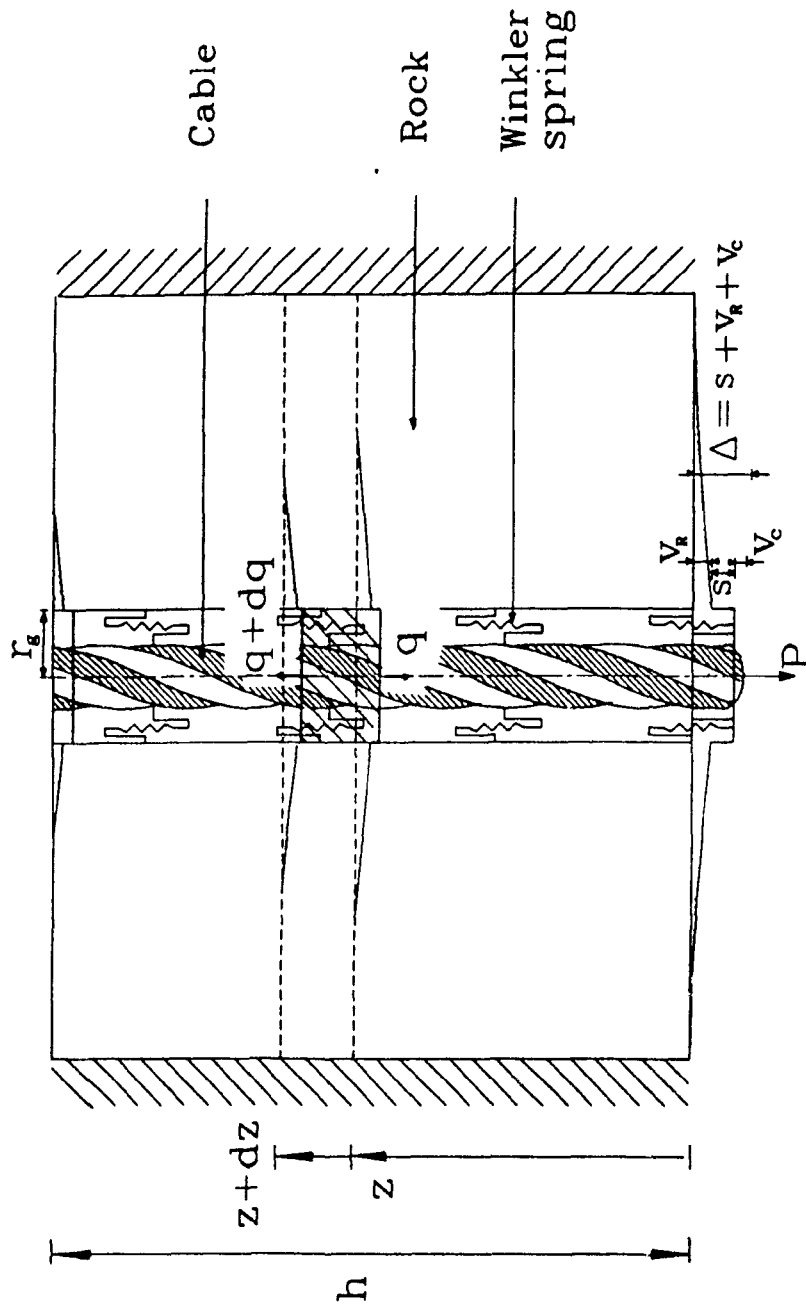


Fig. 6-6 Definition of displacement components at loaded end of cable

$$v_r = \frac{1}{\pi G_r} \left[kr_g \left(\frac{d^2 q}{dz^2} \right) - 2 \left(\frac{dq}{dz} \right) \right] \quad (6-27)$$

To provide the total potential energy in a functional form it is necessary to rewrite eq. (6-25) in the following form:

$$\Delta = \int \left[\frac{ds}{dz} + \frac{dv_c}{dz} + \frac{dv_r}{dz} \right] dz \quad (6-28)$$

Using eq. (6-6), eq. (6-9) and eq. (6-27) the following equations can be derived:

$$\frac{dv_r}{dz} = \frac{1}{\pi G_r} \left[kr_g \cdot \frac{d^3 q}{dz^3} - 2 \frac{d^2 q}{dz^2} \right] \quad (6-29)$$

$$\frac{dv_c}{dz} = - \frac{q}{E_c A_c} \quad (6-30)$$

$$\frac{ds}{dz} = - \frac{1}{m \Sigma_0} \cdot \frac{d^2 q}{dz^2} \quad (6-31)$$

Substituting eq. (6-28) into eq. (6-24) and using eq. (6-29, 6-30, 6-31) and eq. (6-9) the load potential is obtained as follows:

$$V_p = \int_0^h P \left[\frac{q}{A_c E_c} + \left(\frac{2}{\pi G_r} + \frac{1}{m \Sigma_0} \right) \frac{d^2 q}{dz^2} - \frac{kr_g}{\pi G_r} \cdot \frac{d^3 q}{dz^3} \right] dz \quad (6-32)$$

6.5 MINIMIZATION OF TOTAL POTENTIAL ENERGY

Summation of eq. (6-8), eq. (6-12), eq. (6-17), eq. (6-23) and eq. (6-32) provides total potential energy:

$$\begin{aligned} \Pi = \int_0^h \left\{ \frac{q^2}{2E_c A_c} + \frac{Pq}{E_c A_c} + \left(\frac{dq}{dz} \right)^2 \cdot \left(\frac{1}{2m\Sigma_0} + \frac{1}{\pi G_r} + \frac{k^2}{8\pi G_r} \right) \right. \\ \left. + \frac{d^2q}{dz^2} \cdot \left(\frac{P}{m\Sigma_0} + \frac{2P}{\pi G_r} \right) - \frac{d^3q}{dz^3} \cdot \frac{Pkr_g}{\pi G_r} + \frac{3\Sigma_0 n^2}{2m} \right\} dz \quad (6-33) \end{aligned}$$

Employing the eq. (6-33) in the Euler-Lagrange equation (eq. 6-3) yields:

$$\frac{d^2q}{dz^2} - \beta^2 q = \alpha \quad (6-34)$$

where

$$\beta^2 = \frac{1}{E_c A_c \left[\frac{1}{m\Sigma_0} + \frac{k^2+8}{4\pi G} \right]} \quad (6-34a)$$

$$\alpha = P\beta^2 \quad (6-34b)$$

The general solution of eq. (6-34) depends upon the shear bond-slip characteristics of the cable bolt. It should be pointed out that β^2 may be numerically positive, negative or equal zero. This will depend on the magnitude of the parameter m in eq. (6-34a) since the other parameters in that equation are positive. Thus, three possibilities exist, discussed below.

CASE I

When β^2 is numerically positive, the characteristic of the Winkler spring is such that it is in the elastic region ($m > 0$). The general solution of eq. (6-34) is then:

$$q = C_1 \cdot \text{Exp}[\beta z] + C_2 \cdot \text{Exp}[-\beta z] - \frac{\alpha}{\beta^2} \quad (6-35)$$

$$\tau_c = -\frac{\beta}{\Sigma_c} [C_1 \cdot \text{Exp}(\beta z) - C_2 \cdot \text{Exp}(-\beta z)] \quad (6-36)$$

The coefficients C_1 and C_2 depend upon the boundary conditions. For the boundary conditions shown in Fig. 6-7:

$$\begin{array}{lll} \text{at} & z = 0 & q = P \\ \text{at} & z = h & q = 0 \end{array}$$

Employing these boundary conditions in eq. (6-35) and eq. (6-36) results in:

$$q = \frac{\text{Exp}(\beta h)}{1 - \text{Exp}(2\beta h)} \left[\left(P + \frac{\alpha}{\beta^2} \right) \cdot \frac{1 - \text{Exp}[2\beta(h-z)]}{\text{Exp}[\beta(h-z)]} + \frac{\alpha}{\beta^2} \cdot \frac{1 - \text{Exp}(2\beta z)}{\text{Exp}(\beta z)} \right] - \frac{\alpha}{\beta^2} \quad (6-37)$$

However, the shear bond stress can be calculated from eq. (6-10).

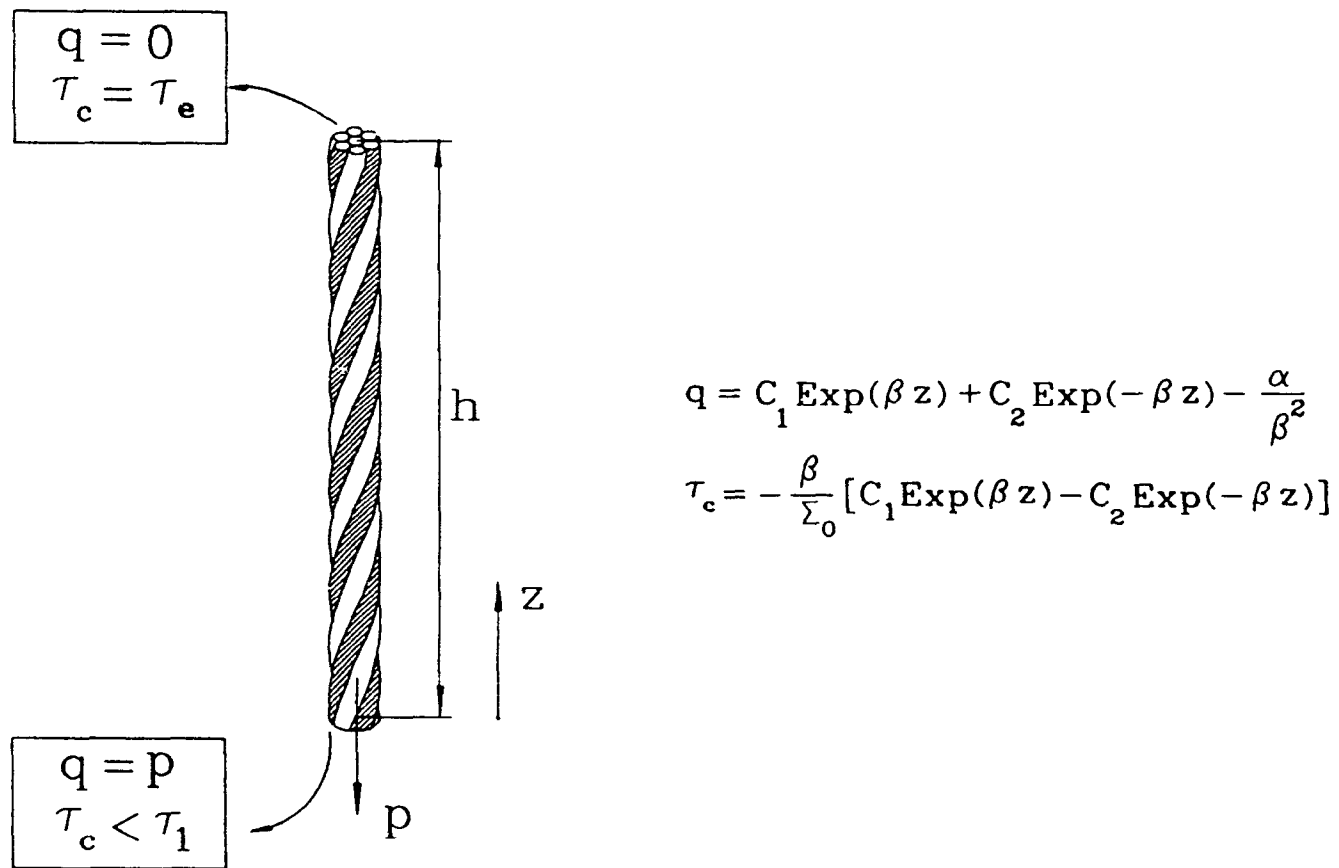


Fig. 6-7 Boundary and compatibility conditions for CASE I ($\beta^2 > Q$)

CASE II

When β^2 is numerically negative, the behavior of the Winkler spring is in the softening region. For simplicity assume $\xi^2 = -\beta^2$; i.e. ξ^2 is positive, thus the general solution of eq. (6-34) is:

$$q = C_3 \cdot \cos(\xi z) + C_4 \cdot \sin(\xi z) + \frac{\alpha}{\xi^2} \quad (6-38)$$

$$\tau_c = \frac{\xi}{\Sigma_0} [C_3 \cdot \sin(\xi z) - C_4 \cdot \cos(\xi z)] \quad (6-39)$$

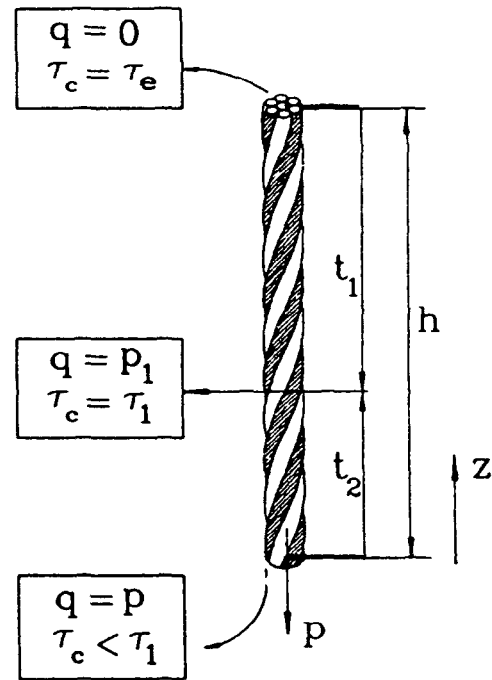
The coefficients C_3, C_4 can be obtained by selecting appropriate boundary conditions.

Considering the boundary conditions shown in Fig. 6-8, the Winkler springs in part of the embedded length of the cable are in the elastic region and the rest are in the softening area. Therefore, at the elastic-softening interface which has a distance t_2 from the load end face of cable the ultimate bond strength (τ_1) should be imposed. Employing these boundary conditions in eq. (6-38) and eq. (6-39) the coefficients C_3, C_4 can be formed in terms of t_2 .

$$C_3 = \left(P_1 - \frac{\alpha}{\xi^2} \cos(\xi t_2) + \frac{\tau_1 \Sigma_c}{\xi} \sin(\xi t_2) \right) \quad (6-40)$$

$$C_4 = \left(P_1 - \frac{\alpha}{\xi^2} \sin(\xi t_2) - \frac{\tau_1 \Sigma_c}{\xi} \cos(\xi t_2) \right) \quad (6-41)$$

where P_1 = load at the cable in elastic-softening interface.



$$q = C_1 \text{Exp}(\beta z) + C_2 \text{Exp}(-\beta z) - \frac{\alpha}{\beta^2}$$

$$\tau_c = -\frac{\beta}{\Sigma_0} [C_1 \text{Exp}(\beta z) - C_2 \text{Exp}(-\beta z)]$$

$$q = C_3 \cos(\xi z) + C_4 \sin(\xi z) + \frac{\alpha}{\xi}$$

$$\tau_c = -\frac{\xi}{\Sigma_0} [C_3 \sin(\xi z) - C_4 \cos(\xi z)]$$

Fig. 6-8 Boundary and compatibility conditions for CASE II ($\beta^2 < Q$)

Making use of boundary conditions at the elastic-softening interface, one can find the unknowns t_2 and P_1 . The computer program developed to handle this part of the problem will be discussed later.

CASE III

When β^2 is numerically zero, then the residual strength is the only part which contributes to the load carrying capacity of the cable bolt. The general solution of eq. (6-34) is:

$$q = C_5 z^2 + C_6 z + C_7 \quad (6-42)$$

Employing eq. (6-10) then:

$$\tau_c = -\frac{1}{\Sigma_0} (2C_1 z + C_2) \quad (6-43)$$

The coefficients C_5 , C_6 , C_7 can be identified if the boundary conditions of the problem are satisfied. To verify the coefficients, let us consider a cable bolt for which the behavior of the Winkler spring in part of the embedded length is in the elastic range (t_1), part of that in the softening region (t_2) and the rest in the residual shear (t_3).

The boundary conditions at the elastic-softening and softening-plastic interfaces are shown in (Fig. 6-9). The boundary conditions at the load end face of cable are:

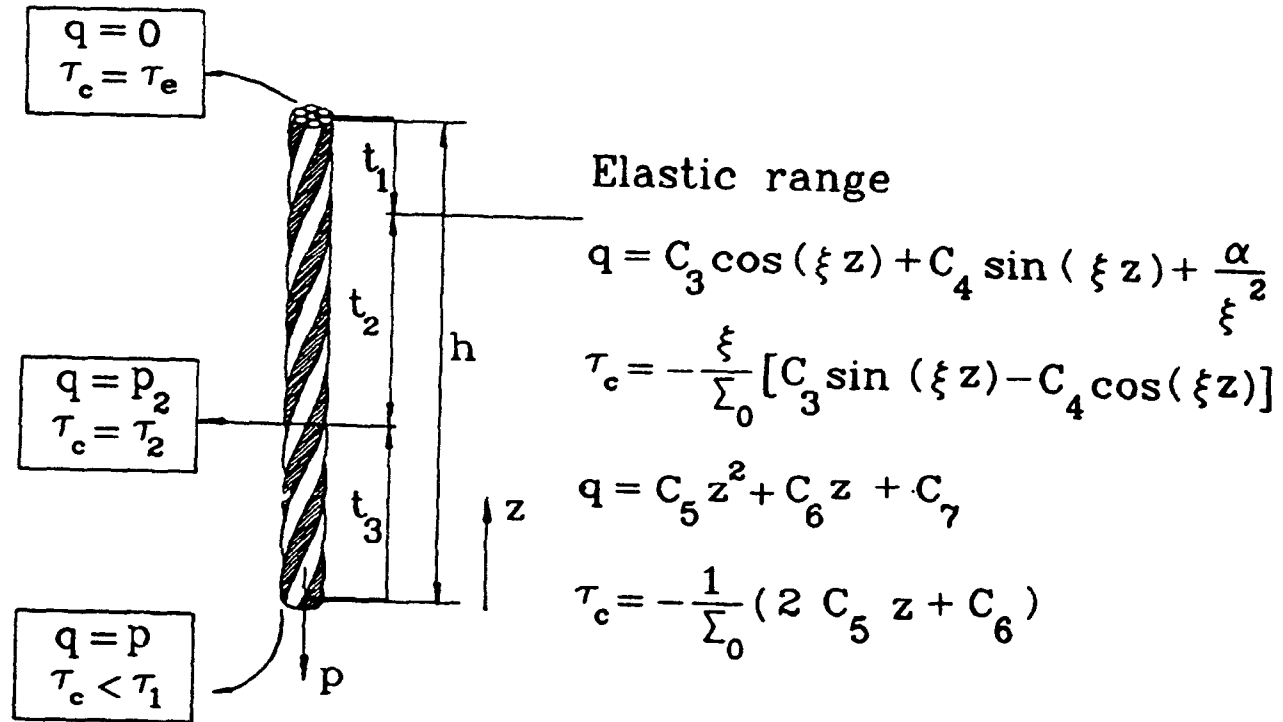


Fig. 6-9 Boundary and compatibility conditions of the Winkler springs in the elastic-softening-plastic range

$$\begin{array}{ll} z = 0 & \tau = \tau_2 \\ z = 0 & q = P \end{array}$$

Applying the boundary conditions to eq. (6-42) yields the following relationships for load and shear bond stress in the plastic range.

$$q = P - \tau_2 \sum_0 z \quad (6-44)$$

$$\tau_c = \tau_2 \quad (6-45)$$

To verify the distribution load and shear bond stress in the elastic and softening regions the compatibility conditions for shear bond and load can be applied at elastic-softening and softening-plastic interfaces. Therefore, t_1 , t_2 and load for each section can be formed.

Due to the number of problems which are involved, a complicated equation is formed by imposing compatibility conditions. To simplify the calculations, a computer program was written to handle the load and shear bond stress distributions for different boundary conditions.

The computer program is composed of six subroutines represented as rectangular boxes in the flowchart (Fig. 6-10).

- Subroutine C1C2 calculates the used C_1 and C_2 for the elastic range of behavior of the Winkler springs.
- Subroutine t1t2 is concerned to satisfy the compatibility conditions at the elastic softening interface of the bond element along the embedded length of the cable bolt.
- Subroutine t2t3 is considered to satisfy compatibility conditions at the softening and plastic interface along the embedded length of cable.

- Subroutines qt1, qt2, qt3 were written in order to calculate the distribution of load and shear bond stress along the embedded length of each region.

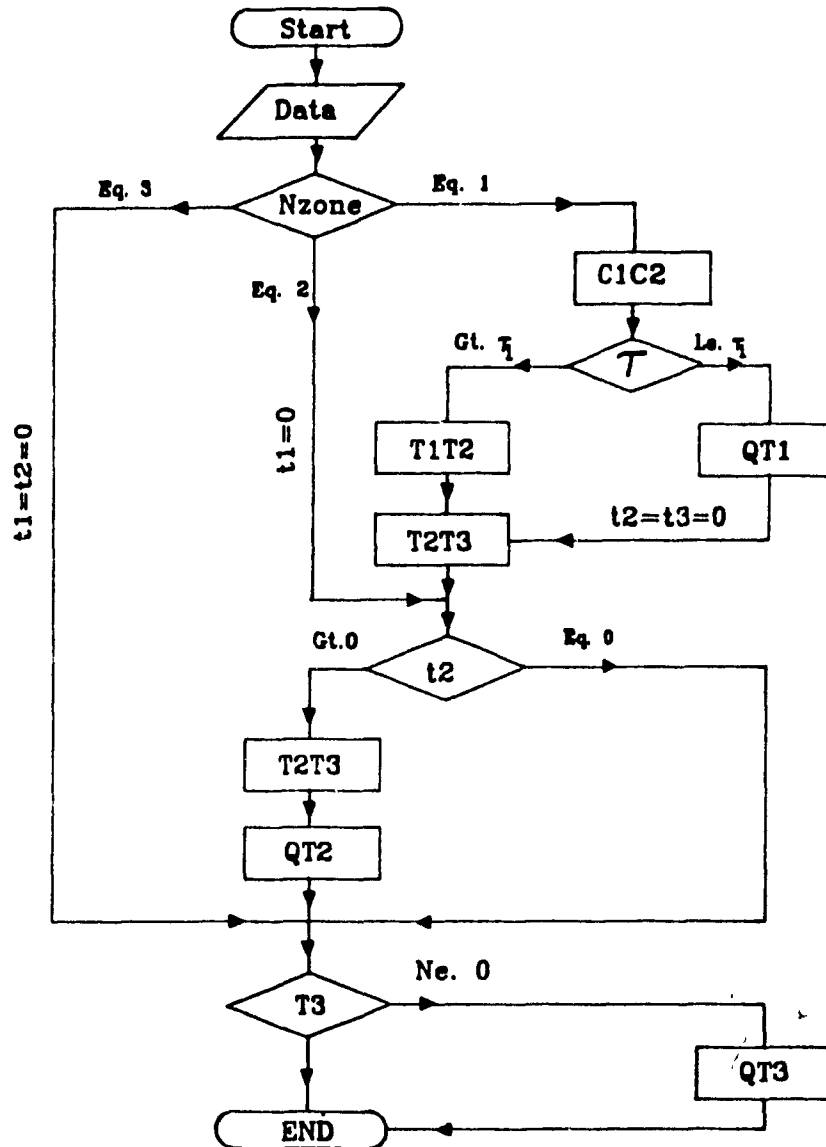


Fig. 6-10 Flow chart of program distribution of shear bond stress

6.6 PARAMETRIC STUDIES

To evaluate the analytical model, the pull-out test for the conventional grout with $w/c=0.35$ for which the experimental results have been presented in Chapter 5 is examined.

Fig. 6-11 shows the effect of a change in the embedded length of a cable bolt versus the ultimate load bearing capacity. Superimposed on the same graph is the result of the analytical method. As can be seen, the analytical model underestimates the load carrying capacity of the cable for short embedded cable bolt lengths (less than 65 cm). However, the trend is very close to the observed experimental results. The difference between the experimental and analytical approach is expected, due to the effect of boundary conditions during the pull-out tests and the assumption of elastic behavior of the material made in the analytical approach.

In order to evaluate the sensitivity of the model with respect to the input parameters, parametric studies have been performed. The bench mark for the comparison has been taken as a guillotine test, where a 15.2 mm diameter cable is embedded in the cement grout in a hole 50 mm in diameter. Relevant parameters for this study are taken from chapter 5.

The effect of embedded length of cable on distribution of the shear bond stress is shown in Fig. 6-12. All the curves are plotted based on the assumption of equal slip at the unloaded face of the different embedded lengths. Clearly, it can be seen that distribution of the shear bond stress is almost uniform for the short embedded length of the cable bolt. The difference of shear bond stress at both ends of the cable for a sample with twenty centimeters embedded length is less than 10 percent. By increasing the embedded length, the dif-

ference in bond stresses at the both end faces of the sample is increased. This confirms that the load slip characteristic of the Winkler spring has good accuracy for samples of up to 20 cm embedded length.

Distribution of shear bond stress for different slips at the unloaded face of the cable is presented in Fig. 6-13. The curves show the elastic, softening and plastic zones in the cables.

Fig 6-14 shows change of load distribution along the embedded length of cable. It can be seen that the variation of the load in the elastic range has an exponential form, while a linear response is shown in the plastic range.

Figure 6-15 investigates the effect of changes in the perimeter of the cable bolt on distribution of the load. The influence of the cross sectional area of the cable is plotted in Fig 6-16. It can be seen that the perimeter of the cable bolt has a significant effect on the load bearing capacity of the cable bolt. This outcome explains the effectiveness of the birdcage technique in cable bolting.

The influence of the yield bond strength on slip is demonstrated in Fig. 6-17 and Fig. 6-17. It can be seen that increasing the bond strength has a significant effect on load bearing capacity. Decreasing the amount of slip at the peak point of the load slip characteristic also increased the load carrying capacity of the cable. Due to the requirements of rock support interaction discussed in Chapter 2, restriction of slip between the cable and the surrounding matrix is not desirable. Finally in Fig. 6-19 the effect of residual strength is studied. Increasing the mechanical interlocking between the cable and the surrounding matrix can significantly improve the behavior of the cable bolt in the plastic range.

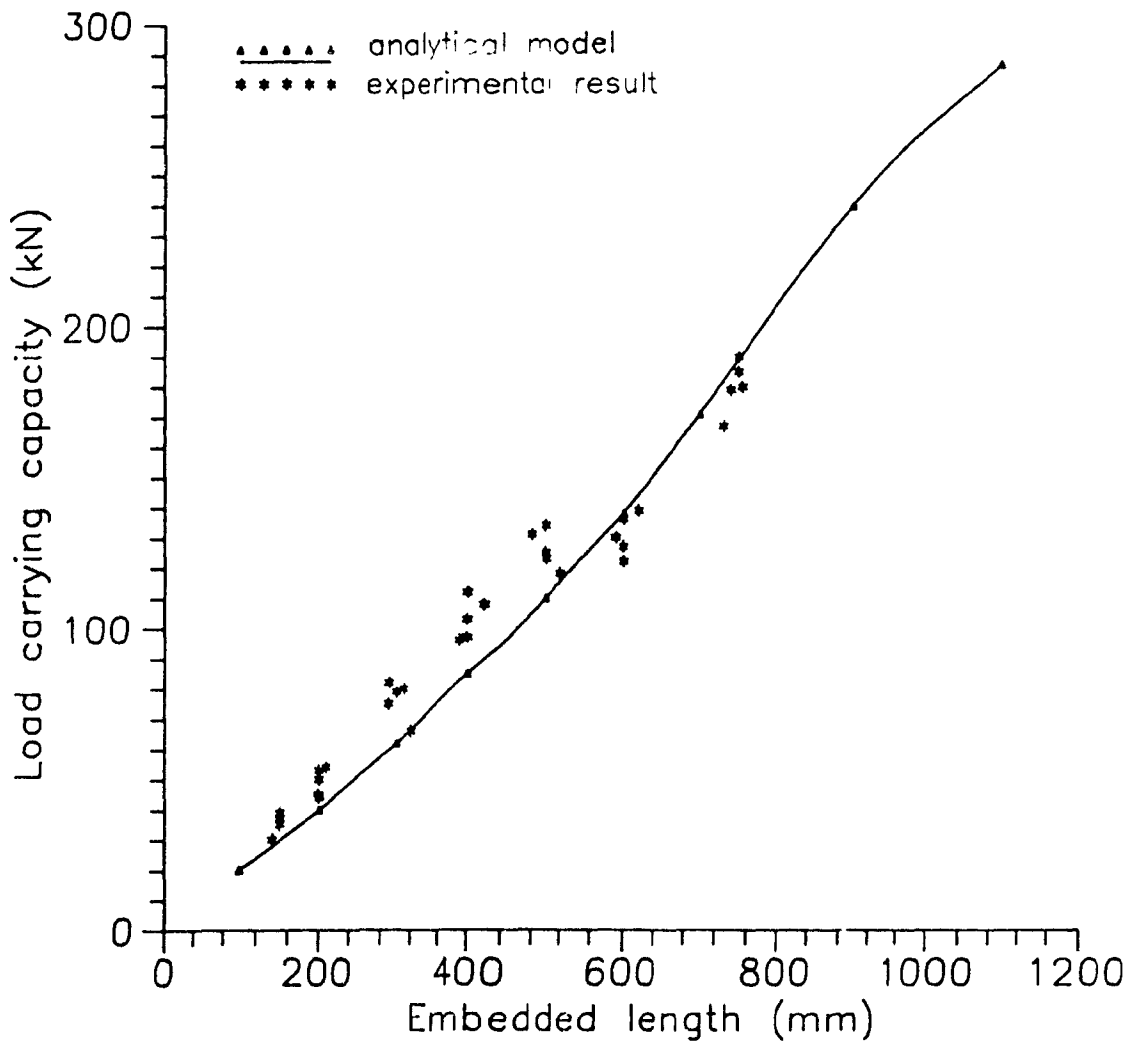


Fig. 6-11 Load carrying capacity versus embedded length of cable

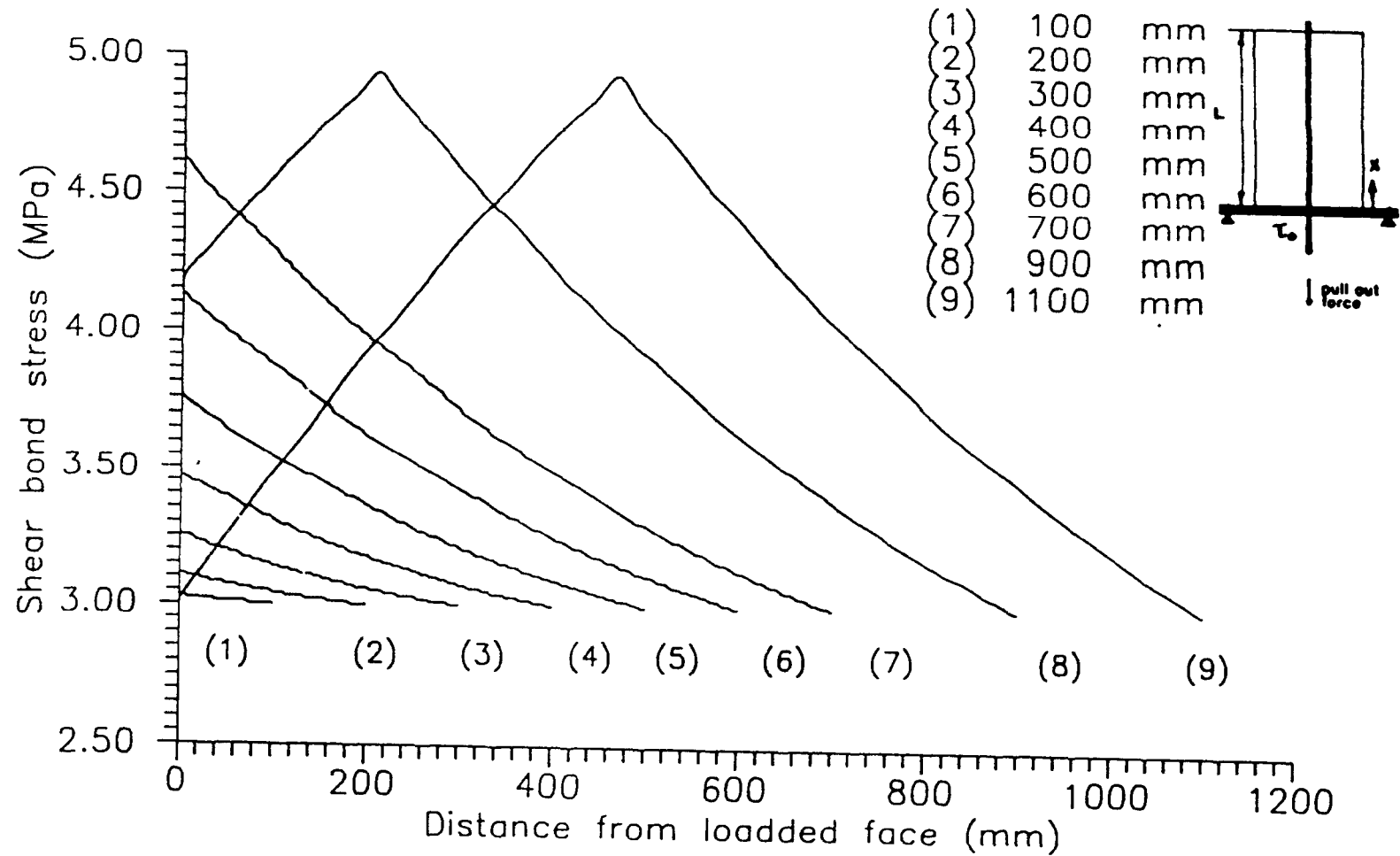


Fig. 6-12 Distribution of shear bond stress along the cable for different embedded lengths

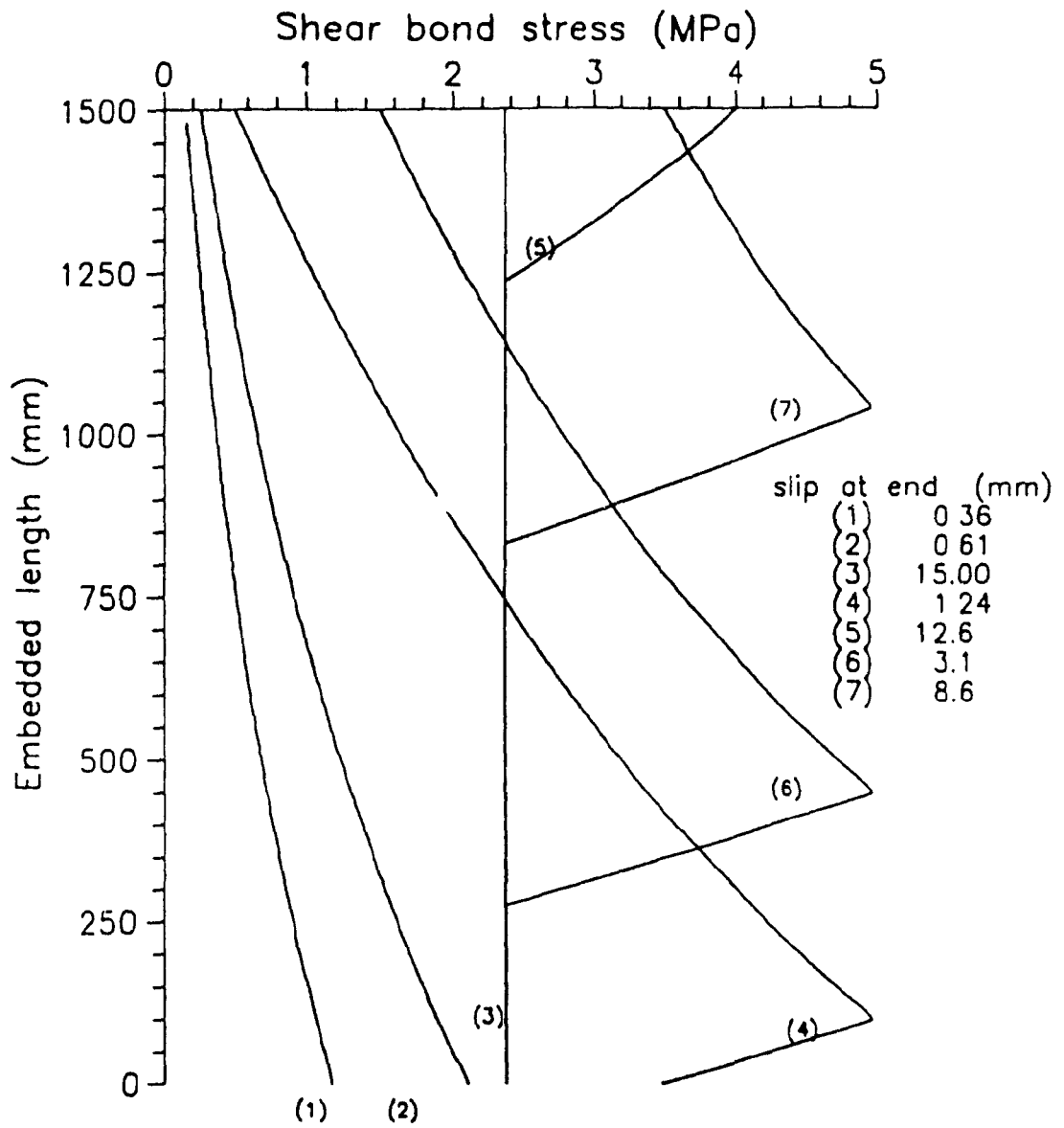


Fig. 6-13 Comparison of distribution of shear bond stress along the length of cable

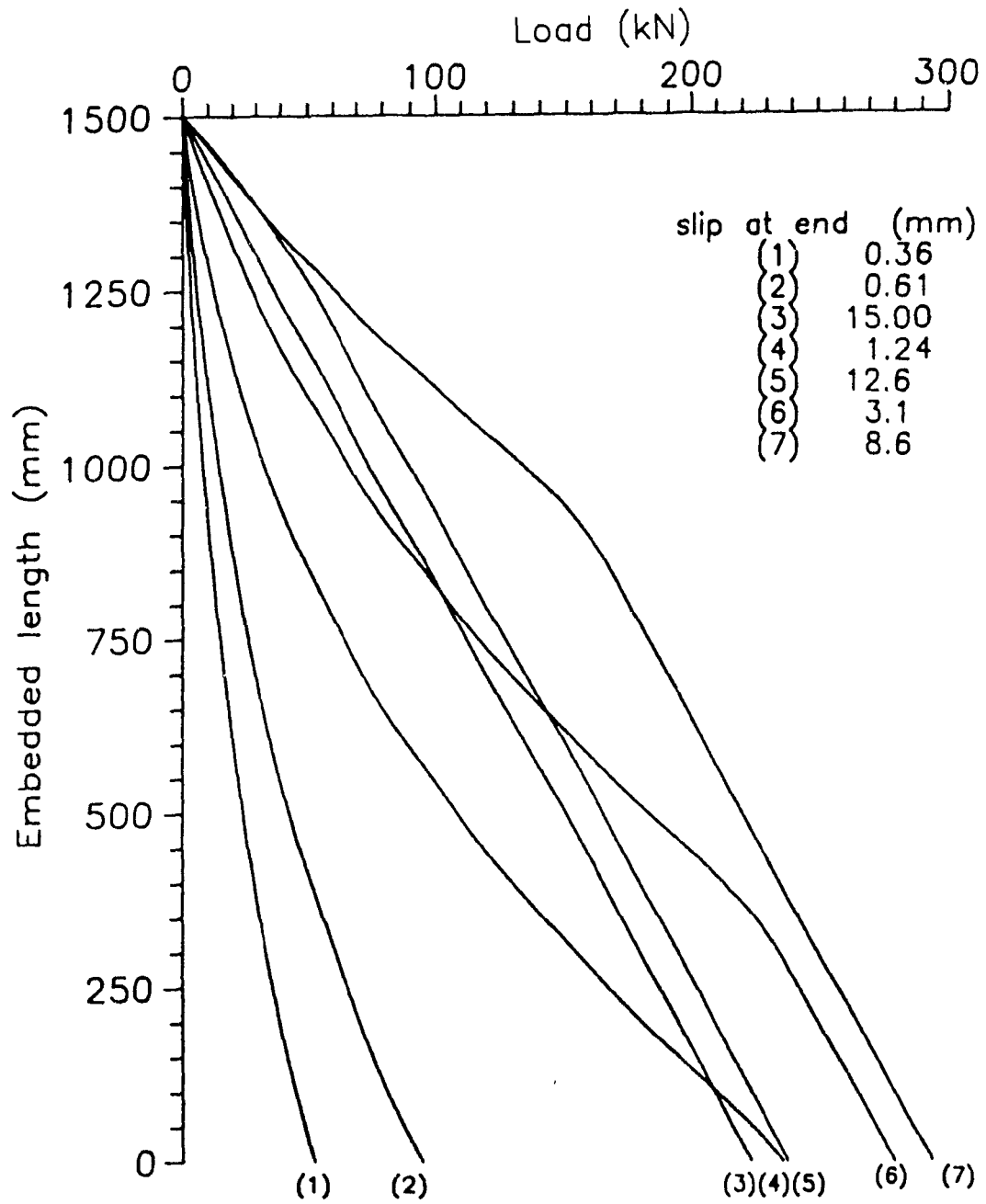


Fig. 6-14 Comparison of distribution of load for different slips

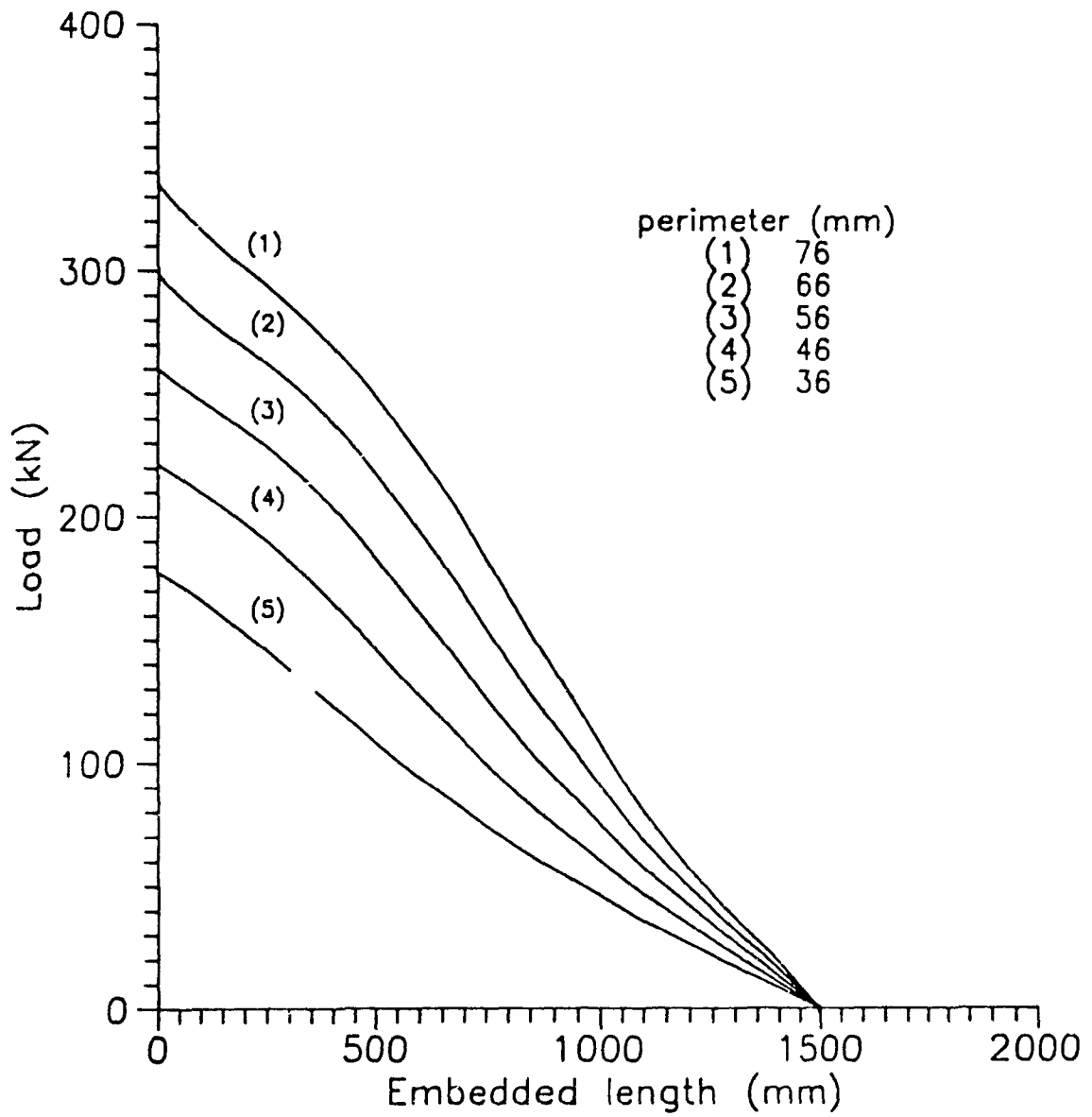


Fig. 6-15 Effect of perimeter of cable on the load distribution

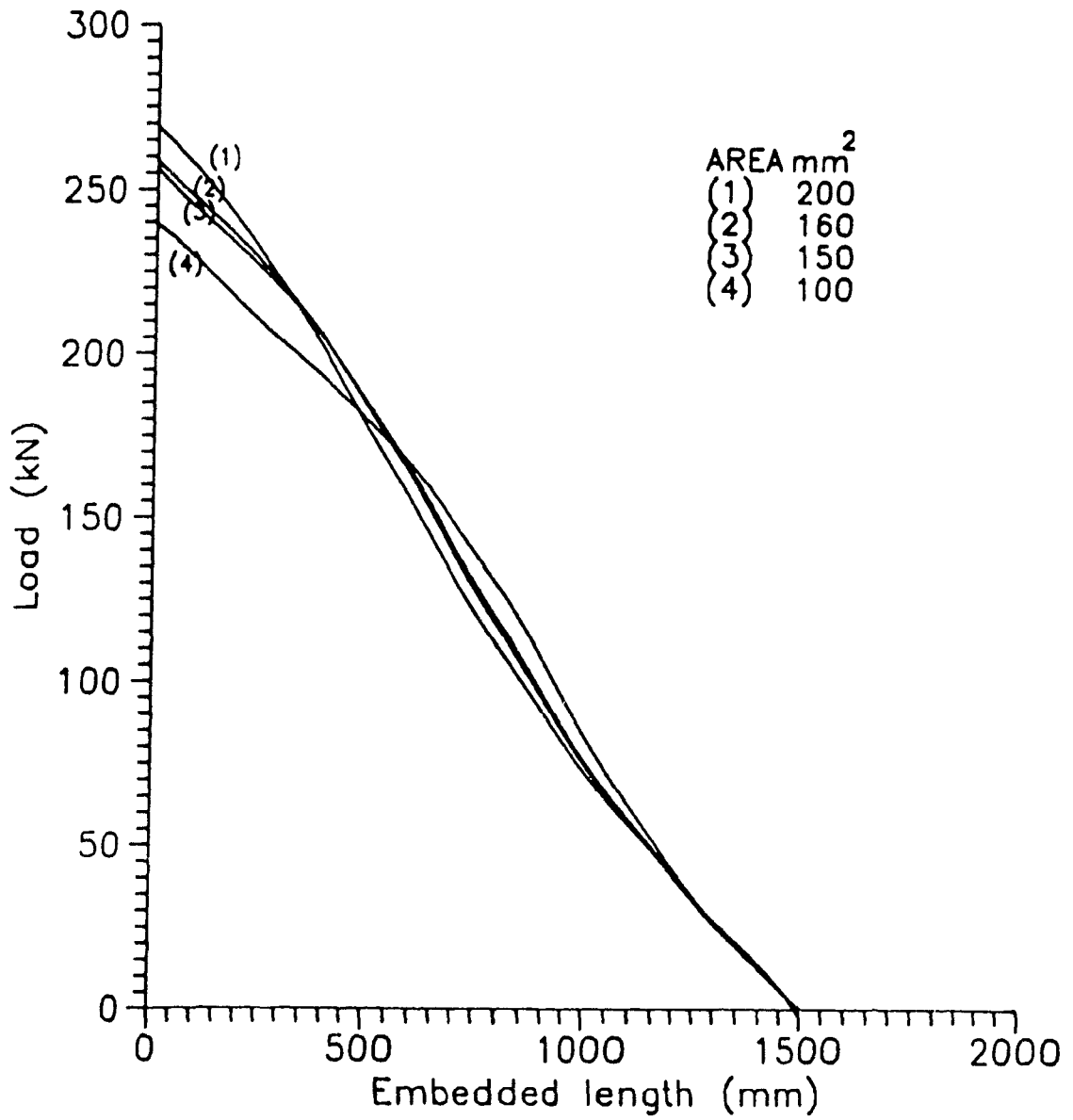


Fig. 6-16 Effect of cross sectional area of cable on the load distribution

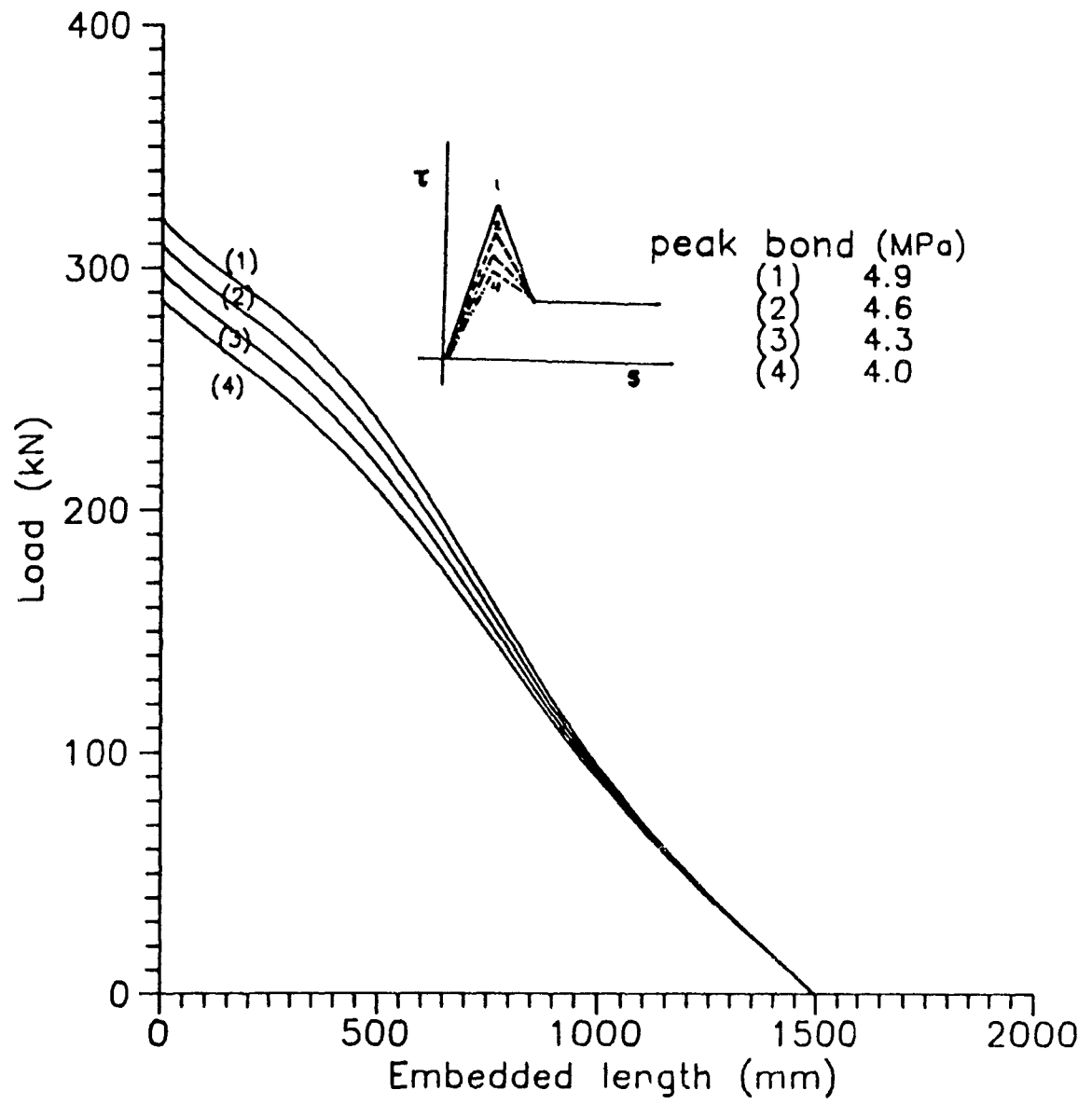


Fig. 6-17 Effect of peak bond stress on the load distribution

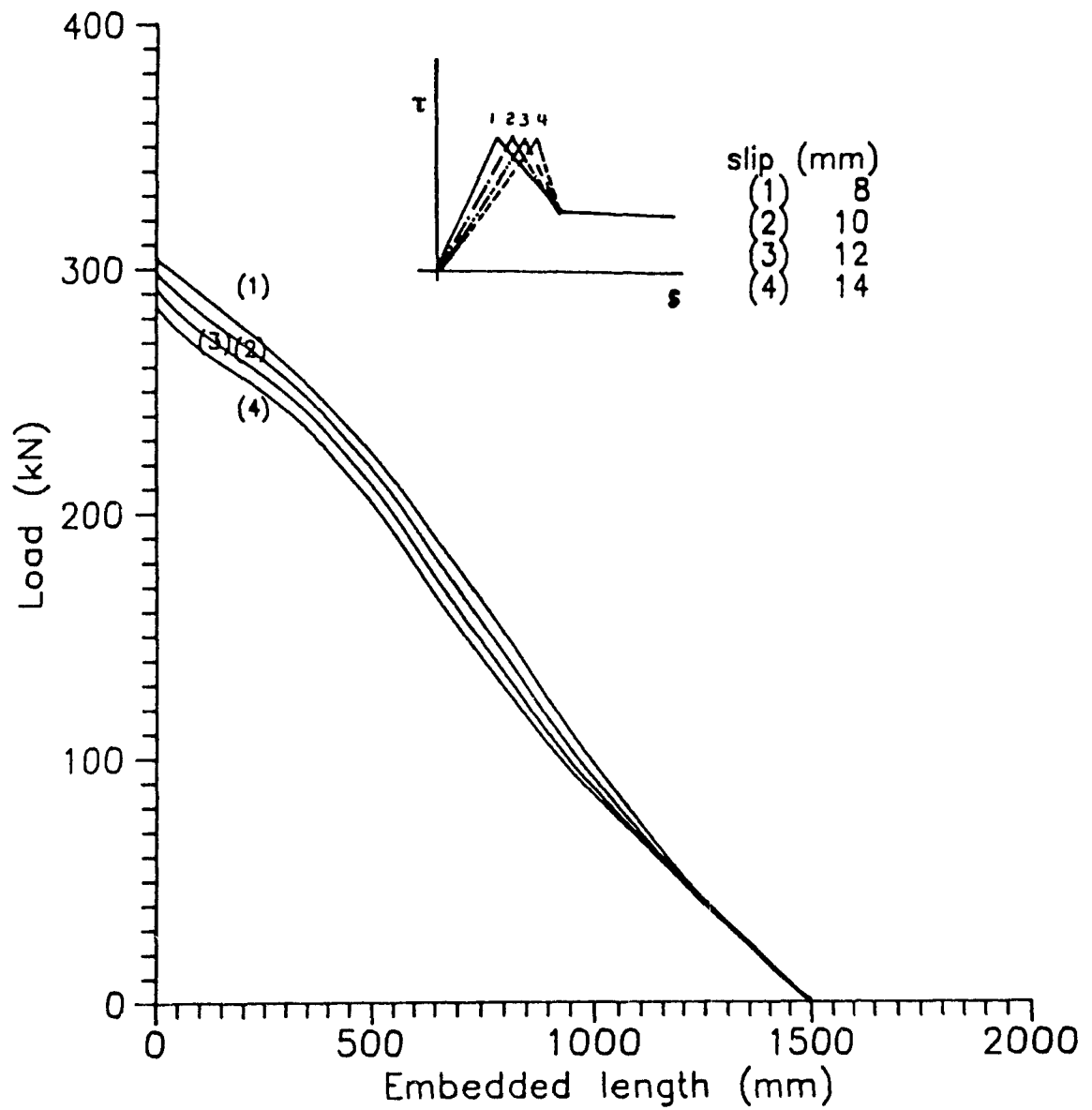


Fig. 6-18 Effect of slip at peak bond stress on the load distribution

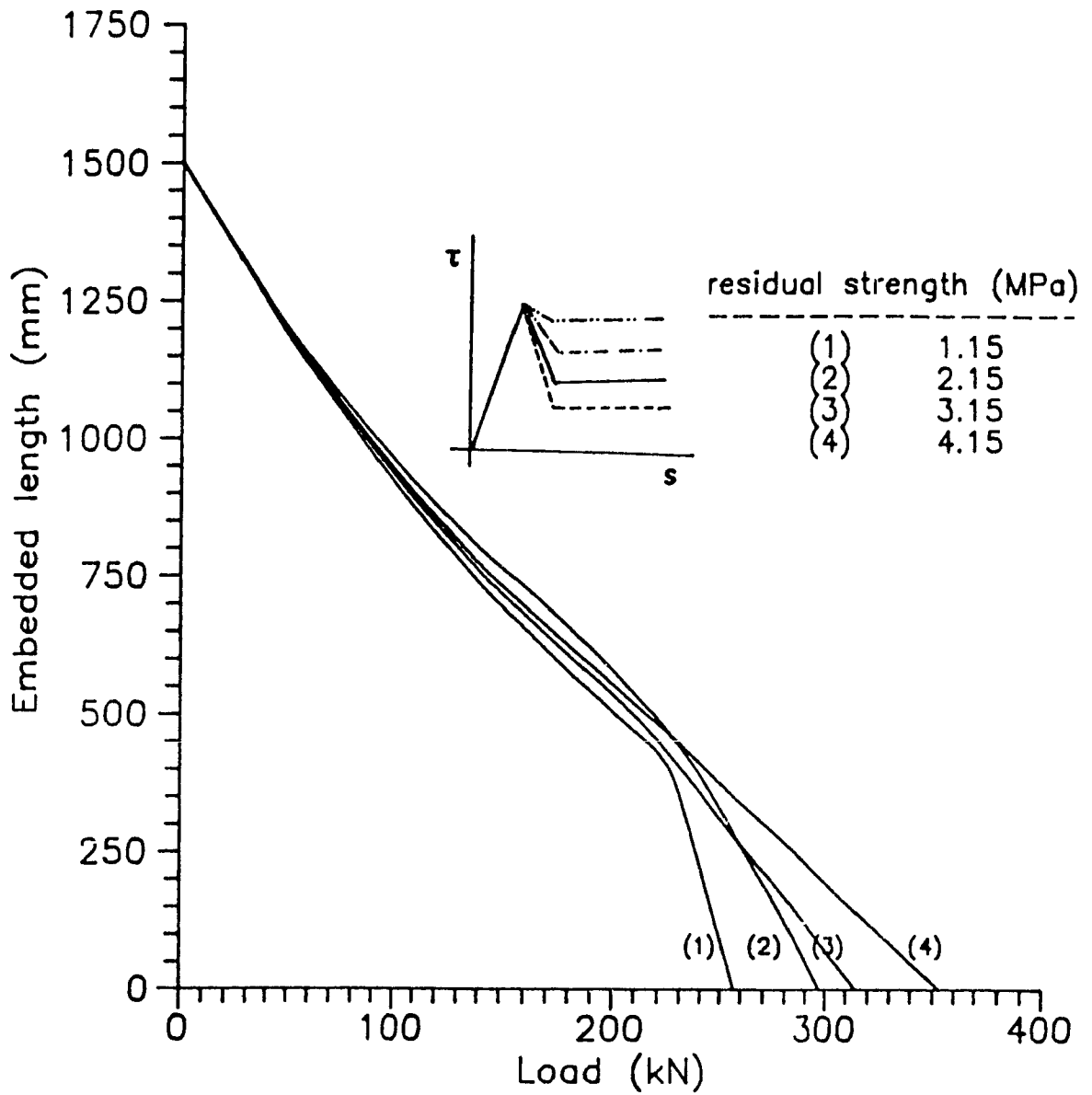


Fig. 6-19 Effect of residual strength on the load distribution

6.7 CONCLUSION

An analytical approach based on the variational method has been developed in order to provide the distribution of shear bond stress and axial load along the embedded length of a fully grouted cable bolt. The model takes into account the behavior of the cable with respect to the borehole wall and the mechanical properties of the rock mass.

The prediction of the load carrying capacity of the cable bolt with the analytical model was compared with the experimental results of Chapter 5. In general, the approach shows good correlation with the shear force measured in the laboratory.

A sensitivity analysis was performed to demonstrate the relative effect of the input parameters on the model. In particular, the perimeter of the cable has been shown to have a significant effect on the load bearing capacity of the cable. The peak shear strength of the Winkler spring influences the load carrying capacity of the anchor.

The distribution of the shear bond stress in the axial direction of the sample for short embedded cable bolt lengths is almost uniform. This result can be employed in the proper definition of the Winkler spring characteristic. The distribution of the shear bond stress depends on the amount of slip at the unloaded face of cable. It has an exponential form when the slip lies in the range of the elastic behavior of the Winkler spring. The load bearing capacity of the cable can be derived for a particular amount of slip at the loaded face of cable bolt.

CHAPTER 7

FINITE ELEMENT MODEL

7.1 INTRODUCTION

The general concept underlying the finite element method is the division of the whole problem domain into a number of elements, calculation of the load vector and stiffness matrix for each element and then assembly of these into a global stiffness matrix and a global load vector. A system of simultaneous equations results and is solved for the unknown nodal displacements. Stresses and strains can then be obtained using interpolating shape functions and the constitutive stress-strain relations of the material.

A stress analysis of a rock excavation with a cable bolt support system requires the consideration of the inherent slip behavior between the cable and the surrounding matrix. In this chapter, a special interface element is formulated and augmented to an existing finite element model, MSAP2D (Micro computer Static Analysis for Program 2-Dimensional problems) [88] in order to allow the simulation of cable bolts in underground excavations. The new element formulation is based on the assumption that the grout material and slip occurring between the cable surface and the surrounding matrix can be simulated by a continuous tangential spring. The approach provides a cable element that should be able to reasonably predict the response of the loaded cables due to the deformation of a surrounding rock mass.

7.2 BASIC MODELLING TECHNIQUE

The well-known four node, 8-degrees of freedom, (DOF), quadrilateral isoparametric element [89] is used in MSAP2D to simulate the rock mass. The element nodes as well as the sides are numbered counterclockwise, as shown in Fig. 7-1.

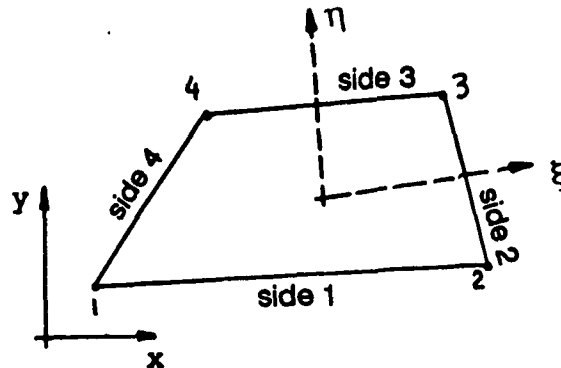


Fig 7-1 Quadrilateral isoparametric element

The element stiffness matrix is obtained by numerical integration using a four point (2 x 2) Gauss quadrature scheme [89]. The load vector $\{P\}$ for each element may be composed of several load vectors as follows.

$$\{P\} = \{F^n\} + \{F^b\} + \{F^s\} - \{F_{o_0}\} \quad (7-1)$$

- where $\{F^n\}$ = Load vector due to concentrated loads;
 $\{F^b\}$ = Load vector due to body forces; e.g. gravity load;
 $\{F^s\}$ = Load vector due to boundary interactions, i.e. pressures and shear stresses acting along the element sides;
 $\{F_{o_0}\}$ = Load vector due to initial stresses.

The thickness of the grout between the cable and the surrounding rock mass in comparison with the dimensions of the rock mass is quite small. Consequently, this condition makes it reasonable to assume that the nodal points of the rock mass elements before loading of the cable bolt will have the same coordinates as the nodal points of the cable element at the interface. As discussed in Chapter 5, when the cable is loaded, relative displacement or slip between the cable and the borehole wall occurs. This slip behavior is simulated by a mechanical model consisting of continuous springs connecting the surface of the cable to the borehole wall and has its stiffness acting in the axial direction of the cable, (see Fig. 7-2).

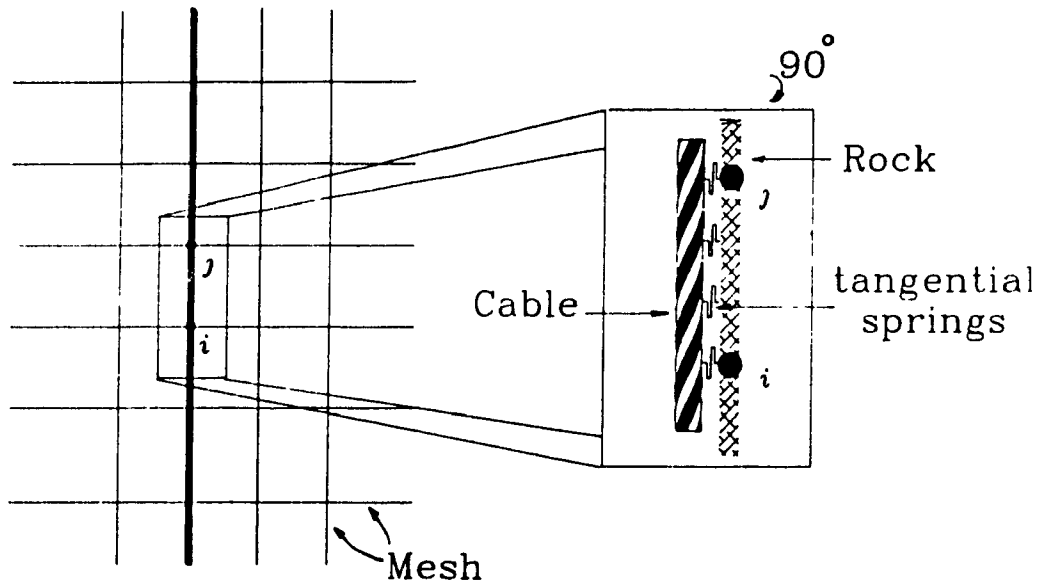


Fig. 7-2 Simulation of the grout and slip for a cable bolt

This section will focus on the formulation of the "cable element". Fig. 7-3 depicts the degrees of freedom and the dimensions of the cable element. The numbers with the bar sign i.e. $\bar{1}, \bar{2}, \bar{3}, \bar{4}, \bar{5}, \bar{6}$ represent global degrees of freedom, and those without bar sign i.e. 1, 2, 3, 4 indicate the local degrees of freedom.

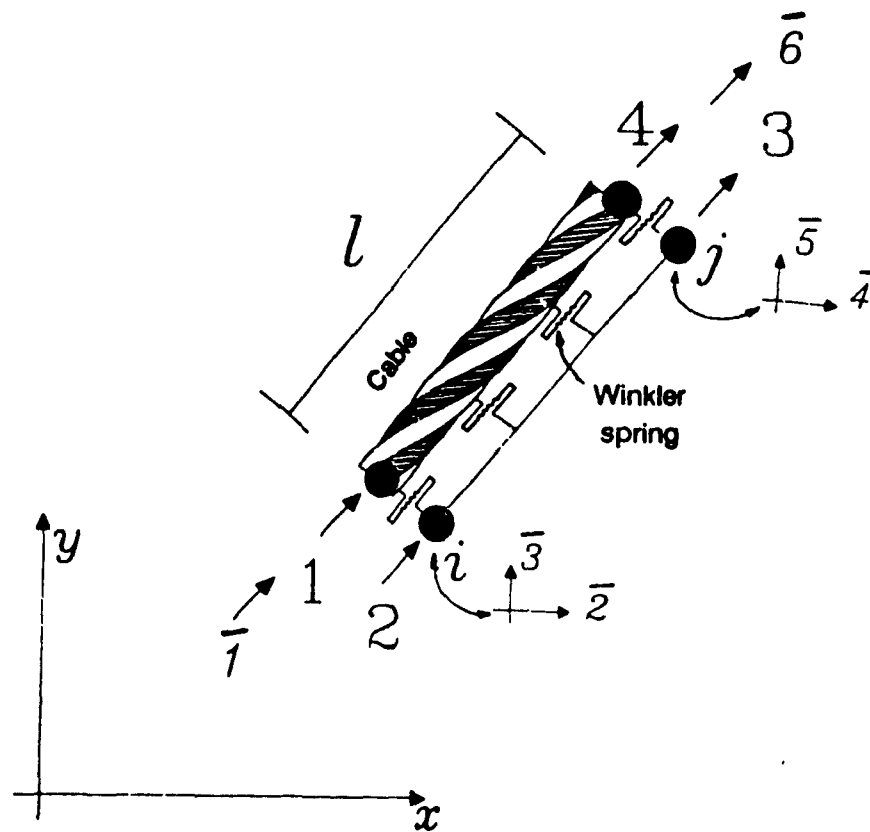


Fig. 7-3 Geometry and degrees of freedom of a cable element

The slip, u_s , and spring stiffness, k_s , at any point (x, y) along the cable element can be calculated using the element shape functions. Thus:

$$u_s = (u_1 - u_2)N_i + (u_4 - u_3)N_j \quad (7-2)$$

$$k_s = k_i N_i + k_j N_j \quad (7-3)$$

$$u_s = [N] \{u^e\} \quad (7-4)$$

$$\{u^e\}^T = \{u_1 \quad u_2 \quad u_3 \quad u_4\} \quad (7-5)$$

$$[N] = [N_i \quad -N_i \quad -N_j \quad N_j] \quad (7-6)$$

where k_i and k_j = stiffness of continuous spring at nodes i and j respectively

u_1, u_2, u_3 and u_4 displacements of nodes 1, 2, 3, 4

N_i and N_j = element shape functions

furthermore N_i and N_j = are given by:

$$N_i = 1 - \xi \quad N_j = \xi \quad \xi = x/l \quad (7-7)$$

7.3 FORMULATION OF CABLE ELEMENT

The strain energy (dU) for an element consisting of tangential continuous springs with a stiffness per unit length, k , length, dl , and displacement, u_s , is given by:

$$dU = \int_0^u k_s \cdot u_s \cdot du_s = \frac{1}{2} k_s \cdot u_s^2 \quad (7-8)$$

Integration of eq. (7-8) over the length of the element (l) gives the strain energy of the continuous springs along the length of the cable element as follows:

$$U = \frac{1}{2} \int_0^l k_s \cdot u_s^2 \cdot dl \quad (7-9)$$

Substitution of eq. (7-4) into eq. (7-9) gives:

$$U = \frac{1}{2} \int_0^l \{u^e\}^T \cdot [N]^T \cdot k_s \cdot [N] \cdot \{u^e\} \cdot dl \quad (7-10)$$

The strain energy U for any finite element can be written as:

$$U = \frac{1}{2} \{u^e\}^T \cdot [K^e] \cdot \{u^e\} \cdot dl \quad (7-11)$$

where $[K^e]$ is the element stiffness matrix.

Comparing of eq. (7-10) with eq. (7-11) shows that the stiffness matrix of the spring element is:

$$[K^e] = \int_0^l [N]^T \cdot [k_s] \cdot [N] \cdot dl \quad (7-12)$$

Substituting eq. (7-3) into the above, and noting that $ds = l \cdot d\xi$ gives:

$$[k^e] = l \cdot \int_0^1 [N]^T \cdot ((1-\xi)k_i + \xi k_j) \cdot [N] \cdot d\xi \quad (7-13)$$

It can be shown that after integration of eq. (7-13) the resulting spring element stiffness matrix is:

$$[k^e] = \frac{l}{12} \times \begin{bmatrix} 3k_i + k_j & -3k_i - k_j & -k_i - k_j & k_i + k_j \\ & 3k_i + k_j & k_i + k_j & -k_i - k_j \\ & & k_i + 3k_j & -k_i - 3k_j \\ \text{symmetric} & & & k_i + 3k_j \end{bmatrix} \quad (7-14)$$

The total stiffness matrix of a cable element, k^c , is obtained from the algebraic addition of its two components: the spring element stiffness matrix (i.e. eq. 7-14) and the truss element stiffness matrix. Thus:

$$[k^c] = \frac{l}{12} \times \begin{bmatrix} 3k_i + k_j + \frac{12E_c A_c}{l^2} & -3k_i - k_j & -k_i - k_j & k_i + k_j - \frac{12E_c A_c}{l^2} \\ & 3k_i + k_j & k_i + k_j & -k_i - k_j \\ & & k_i + 3k_j & -k_i - 3k_j \\ \text{symmetric} & & & k_i + 3k_j + \frac{12E_c A_c}{l^2} \end{bmatrix} \quad (7-15)$$

where $l =$ length of cable element
 $E_c =$ modulus of elasticity of cable bolt
 $A_c =$ cross section area of cable bolt

In order to compute the stiffness matrix of a cable element the values of k_i and k_j must first be determined. This information may be derived from the load-slip curves obtained by means of the pull-out tests reported in Chapter 5.

The above equation represents the local stiffness of the cable element. It is a straightforward procedure to transform this to the global X-Y coordinates i.e.

$$[k_g^c]_{[6 \times 6]} = [T]_{[6 \times 4]}^T \cdot [k^c]_{[4 \times 4]} \cdot [T]_{[4 \times 6]} \quad (7-16)$$

where

$$[T] = \begin{bmatrix} 1 & 0 & 0 & 0 & 0 & 0 \\ 0 & c & s & 0 & 0 & 0 \\ 0 & 0 & 0 & c & s & 0 \\ 0 & 0 & 0 & 0 & 0 & 1 \end{bmatrix}$$

$$c = \frac{x_j - x_i}{l}$$

and

$$s = \frac{y_j - y_i}{l}$$

7.4 EQUATION OF EQUILIBRIUM

The assembly of a global stiffness matrix and load vector leads to a system of simultaneous linear algebraic equations of the form:

$$[K_G]_{[n \times n]} \cdot \{\Delta_G\}_{[n \times 1]} = \{P_G\}_{[n \times 1]} \quad (7-17)$$

Where n is the total number of degrees of freedom in the structure, $\{\Delta_G\}$ is the vector of unknown nodal displacements, $\{P_G\}$ is the load vector and K_G is the global stiffness matrix. The global matrix is symmetric, positive definite, sparse and banded. The symmetry condition allows storage of only the elements in the upper or lower part of the matrix including the diagonal coefficients. The bandwidth of the stiffness matrix depends on the method of numbering of the nodal points. Although the mesh generation program (described in section 7.5) produces a uniform bandwidth, sometimes the bandwidth can vary substantially in size from one row to another in the matrix for large and complex problems. The presence of nodal points on the "cable element" may increase the bandwidth of the stiffness matrix.

7.5 EQUATION SOLVER

Several solution methods are available to reduce not only the solution time, but also the amount of computer storage for solving the equilibrium equations which are presented in eq. (7-17). The popular Gauss elimination method [90] is employed in MSAP2D; nevertheless, in the CABLE program the Skyline solution method was preferred for solving the simultaneous

equilibrium equations [91].

In the Skyline solution method the upper triangle of the symmetric and sparse global stiffness matrix is stored. Then the active portion of each column is banded by the diagonal and farthest non-zero element. In the subroutine of the equation solver the number of equations in each block need not be equal to the band width. This means it is possible to solve sets of equations with very large band widths. The block length is automatically set by the computer program. It is made as large as possible in order to be consistent with the band width and the number of central core storage locations available, and also with the fact that two blocks must be stored in the central core storage at any time. For example, if there are 6000 central core storage locations available in the computer, a set of equations with a half band width of 60 will be assigned a block length of 50. Assigning block length in this way results in efficient utilization of the available central core storage. For example, if the half band width was 1000 there would be only three equations per block. The solution time would be very large for this case. The minimum amount of central storage is that required to store two equations simultaneously, with only one equation per block. The smaller the number of equations per block, the greater the required number of transfers from core storage to auxiliary files, and the more costly the solution procedure.

7.6 CABLE BOLT ANALYSIS SYSTEM

The CABle bolt analysis system (CAB) is a numerical model which was developed to facilitate stress analysis using the finite element program CABLE. All the sub-units in CAB are written in ASCII Fortran 77 and are compiled with Microsoft

Fortran 3.3. The plotting routines are written using IBM Graphics Development Toolkit version 1.0. The program runs on IBM personal computers and compatibles which are equipped with mathematical co-processors and hard disks.

CAB is composed of five basic modules which are highlighted as rectangles in the system's flowchart represented in Fig. 7-4. The first three modules, LAYCAB, PRECAB and MESH CAB are pre-processors which generate a data file and display the geometry as well as mesh grading. The fourth module, program CABLE, is the core processor of the system. The next component is the post processor POSTCAB which displays displacements and safety levels as well as principal stresses.

LAYCAB

LAYCAB is a graphic program for checking the input data file for program PRECAB. Material type, position of the cable, node number of rock-mass, zone number and boundary conditions of the structure can all be graphically displayed and checked. Originally this program was developed for SAP2D by Chau [92] and has been modified for the cable system.

The input data required for execution of LAYCAB are:

- 1) Coordinates and boundary conditions of the nodal points of each zone element.
- 2) The type of material and nodal points associated with each zone element.
- 3) The material properties.
- 4) Initial stresses of the problem.
- 5) Number of starting nodal point and end point of each cable as well as its cross section area and perimeter.
- 6) Spring stiffness of the cable.

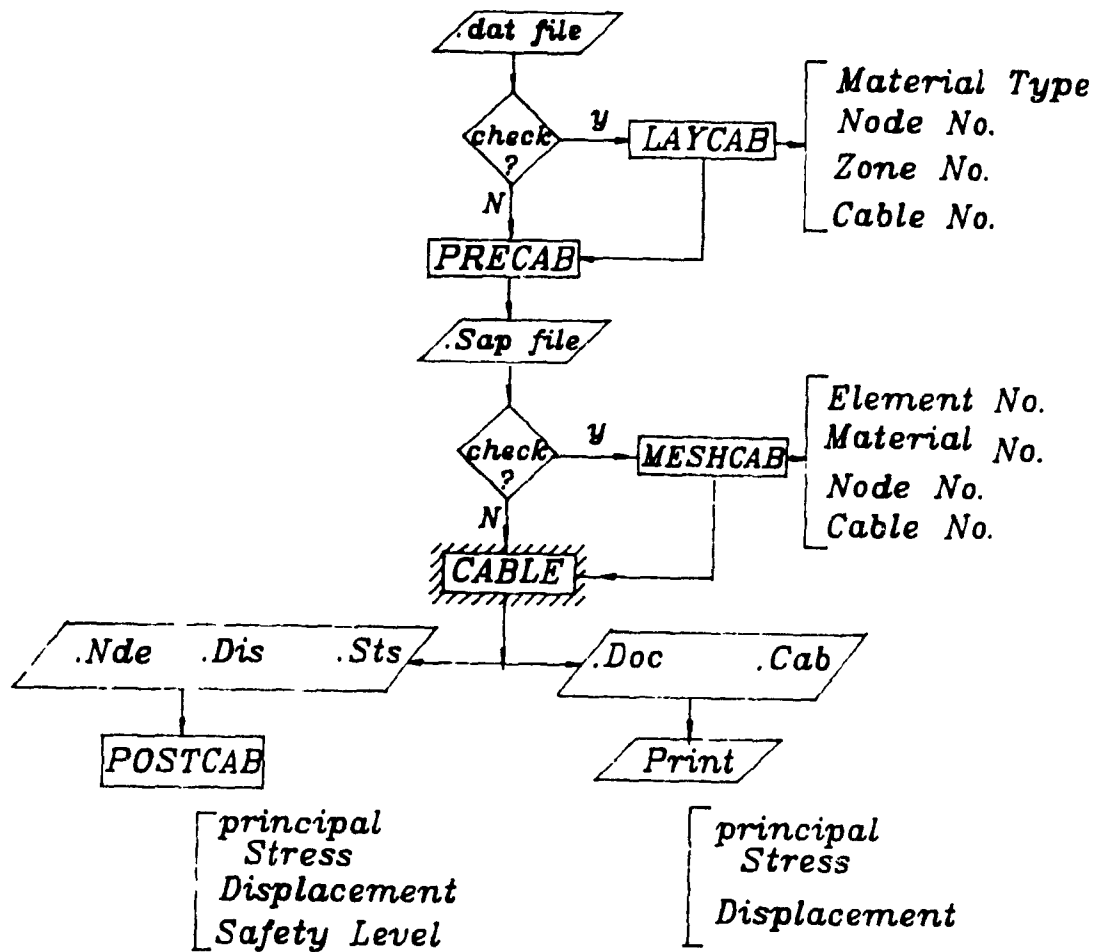


Fig. 7-4 Flow chart of CAB analysis system

PRECAB

Proper grading of the mesh in the finite element analysis method plays an important role in terms of computational time as well as the accuracy of the results. Only a very simple mesh can be prepared by hand and even then, a thorough check is necessary. PRECAB is a mesh generator for the main program CABLE. The data file, which is checked by the LAYCAB program, is read by PRECAB and then the mesh is generated based on the feed data. The program produces three files: the first one with the extension (.msh) for Meshcab, the second one with the extension (.cab) for program CABLE, and the third one with the extension (.dat) for checking the input data file. The concept of the program PRECAB is based on the model zone (key zone) in a local curve linear coordinate system which is explained by Ziekiewicz [93] and the Mesh2d program manual [92]. Fig. 7-5 describes the model zone where each zone is defined by eight nodes. Nodal points are numbered counterclockwise with numbers 1 to 4 assigned for corners and 5 to 8 for the intermediate nodal points to control the curvature of the sides as well as the grading of mesh. If the grading parameter for one or more of the side nodes (5 to 8) is zero it means that this side has no curvature and mesh grading along the side length is of equal distance.

The program can generate a mesh for the cables if they pass either between nodes 2 and 3 or between nodes 3 and 4 in each zone (see Fig. 7-5). The zone model also checks for corners having an angle greater than 180° , in which case it aborts to prevent improper mesh generation.

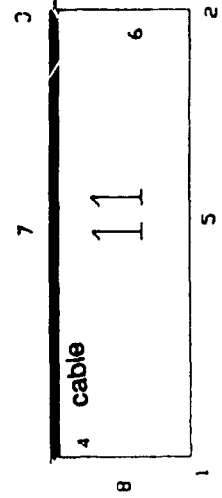
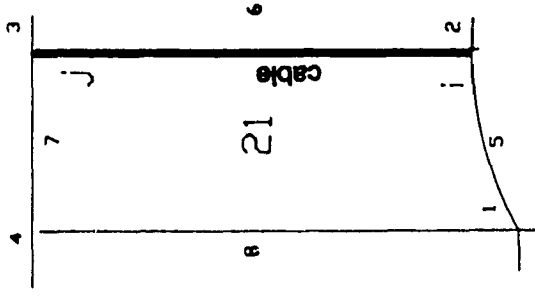
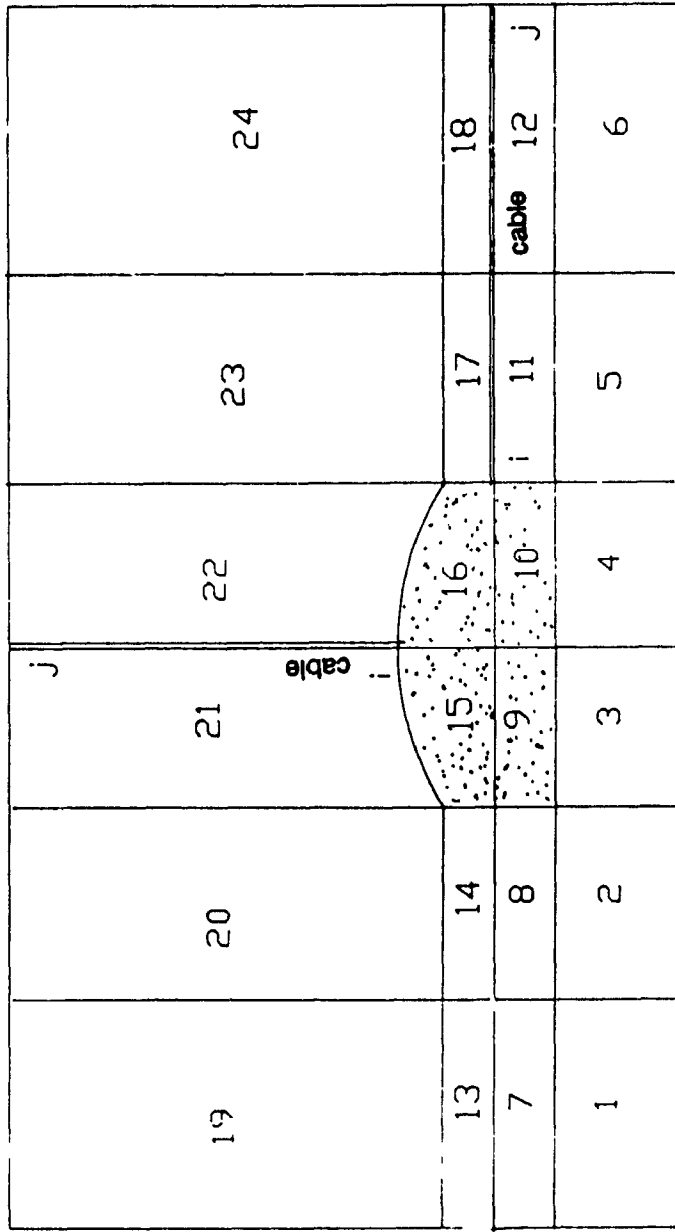


Fig. 7-5 Description of model zone

MESH CAB

MESH CAB is a graphic program for checking the input data of the CABLE program. In general, the MESH CAB program can be applied to control the grading of mesh, boundary conditions, mining sequence and the position of the cable bolts all of which graphically can be displayed for checking.

CABLE

CABLE is the core program of the CAB system. It has the same specifications as MSAP2D [92] which is based on the well known program SAP IV [94]. The program has been written for static, linear elastic finite elements to analyze two dimensional (plain or axisymmetric) cable bolting problems.

All core storage of the computer is allocated at the time of execution; if desired, the storage can be adjusted to provide the minimum storage required for the problem under analysis. In order to increase or decrease the capacity of the program it is necessary to alter two FORTRAN statements at the start of the program. They are: COMMON A(n) and MTOTAL=n where "n" controls the capacity of the program. The maximum value of "n" depends on the computer being used. For a personal computer with 1 mega byte of RAM, the maximum value of n is about 25000.

Initial stresses, simulation of excavation sequences, arbitrarily distributed loading, gravity loading and concentrated face loading and tensioned and untensioned cable bolts can be handled by the CABLE program.

The conventional sign for compression of a rock mass is negative while tension is positive. The direction of principal stresses is considered positive and counterclockwise from the horizontal (x) axis. The "cable element" can be employed in tension while bond stress and load for nodal points of the

"cable element" are considered in the direction of the cable axis.

Movements at each nodal point can be constrained in the X or Y direction or both. If a nodal point is constrained in the X and Y directions, no equation is assigned for that nodal point. If a nodal point is constrained in the X direction only or in the Y direction only, just one equation is assigned for that nodal point. Consequently, the number of equations to be solved is minimized.

The output of the program consists of the global displacement at the nodes, principal stresses of the rock mass elements as well as the bond stresses and load in the "cable element". The direction of load and shear stress at the nodal points of the cable is in the direction of the cable axis. The stresses in the rock mass elements can be located at the center each element, as well as along the four sides of each element.

POSTCAB

PRECAB is a graphic program which can display principal stresses of rock mass elements. The safety level of the materials can also be displayed. When the stresses exceed the strength of material the element colored red on the screen, indicating material failure. Whenever the stress of the element is close to the allowable strength of the material the element will appear yellow on the screen. Otherwise the element will be appear green. In all graphics programs (LAYCAB, MESH CAB and POSTCAB) it is possible to get a hard copy of the screen image on a printer or a plotter.

The most common failure criteria employed in rock mechanics today are those attributable to Hoek and Brown [15], Mohr-Coulomb [95] and Drucker Prager [96], which are listed in

Table 7-1. These are employed in the POSTCAB module. The shear strength τ_{max} along the failure plane is calculated and then is compared with the shear stress τ of the element. The calculation of the safety index for failure criterion is shown in Table 7-2.

FAILURE CRITERIA	REQUIRED PARAMETERS		
	Mohr-Coulomb	C	ϕ
Drucker-Prager	C	ϕ	-
Hoek & Brown	m	s	σ_c

Table 7-1 Failure criteria and required parameters

Where

C = cohesion

ϕ = angle of friction

m & s = parameters related the type of rock mass

σ_c = uniaxial compressive strength of rock mass

Criterion	index(IX)
Mohr-Coulomb	τ_{max}/τ
Drucker Prager	K'/K
Hoek & Brown	σ_{max}/σ

Table 7-2 Means of Assessing Material Safety Level [92]

7.7 SOLUTION PROCEDURE

The solution procedure of the CAB system is given as follows:

- 1) Prepare a data file for the program PRECAB with the extension (.dat), based on the description which is given in user manual [97]
- 2) Using this data file, run the program PRECAB. This generates data files with the extensions (.msh) for the MESH CAB program and (.cab) for the core program CABLE respectively. There is also an option for output of input data to a file, the screen or printer for checking.
- 3) The user has the option to verify his input data file through the visual check available with LAYCAB.
- 4) To check the grading mesh and mining sequence on screen, the data in the (.msh) file may be viewed by running the MESH CAB program.
- 5) Run CABLE using the data file with extension (.cab) to produce the four output files with extensions (.nde), (.sts), (.dis) and (.doc). These documentary output files can be used as the input files for the graphical postprocessor.
- 6) Finally the POSTCAB program enables checking of the stresses, displacements and failed material. The safety level of the material may be checked by the Mohr-Coulumb, the Drucker Prager or the Hoek and Brown failure criteria.

CHAPTER 8

MODEL VERIFICATION

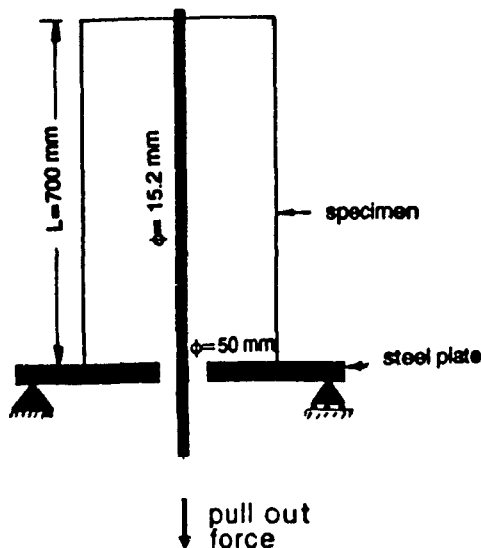
8.1 INTRODUCTION

In this Chapter two studies are made; the first is a comparison between the variational approach described in chapter 6, the finite element model and laboratory results of pull out tests. This comparison serves as a method of verifying the accuracy of numerical and analytical models developed. The second studies in this Chapter demonstrates the effect of the cable bolting patterns on the stability of the hanging wall of a hypothetical open stope. Two commonly used cable patterns were selected, and the results compared.

8.2 MODEL VERIFICATION

Before comparing the numerical model predictions with the analytical solution or experimental values, the effect of the number of elements, the analysis method and the nodal spring stiffness of the "cable element" must be ascertained.

This section illustrates the distribution of load and shear bond stress along the embedded length of the cable bolt for a pull-out test. The cable is axially loaded from the lower end, which is prevented from downward movement by rollers. The geometry of the problem is shown in Fig. 8-1. The materials properties were chosen as for a conventional grout with workability type II, as explained in Chapter 5 (see Table 5-5). The stiffness of the Winkler springs linking the nodal points of the cable to the nodal points of the borehole wall was calculated from the load-displacement characteristic of the cable bolt.



$E_{\text{cable}} = 194 \text{ GPa}$
 $E_{\text{grout}} = 19.5 \text{ GPa}$
 $E_{\text{rock}} = 19.0 \text{ GPa}$
 Length = 700 mm
 Diameter = 250 mm
 Borehole = 50 mm
 $W/c = 0.35$
 $K_i = K_j = 26 \text{ MPa}$

Fig. 8-1 Geometry of pull-out test

Because of cylindrical shape of the sample an axisymmetric finite element an axisymmetric condition can be assumed. One of the important aspects of finite element simulation relates to the proper selection of the number of elements for each model. This has an impact on both the computing time and the accuracy of the analysis. In order to achieve this, a sensitivity analysis was performed.

Three finite element meshes were generated; these are shown in Fig. 8-2. They were used to check the effectiveness of the number of elements on the distribution of load and shear bond stress along the embedded length of the cable bolt. The distribution of both the load and the shear bond stress along the embedded length of cable are plotted in Fig. 8-3 and Fig. 8-4. The results of the variational analysis approach are also shown. It can be seen that increasing the number of elements in the finite element method caused the load distribution to converge to that of the variational model. Since the slope of different curves of load distribution for different mesh is close to each other, consequently the distribution of shear bond strength for different meshes are not sensitive (see Fig. 8-4).

Ideally, the best way of checking the accuracy of a numerical or analytical method is by a comparison with an exact solution of a certain problem. However, in the absence of an exact solution the experimental results that were presented in Chapter 5 are used in this study. The load and displacement at the loaded end of cable for the finite element model, variational approach and experimental results of pull-out tests are given in Table 8-1. Comparison of the results shows good agreement.

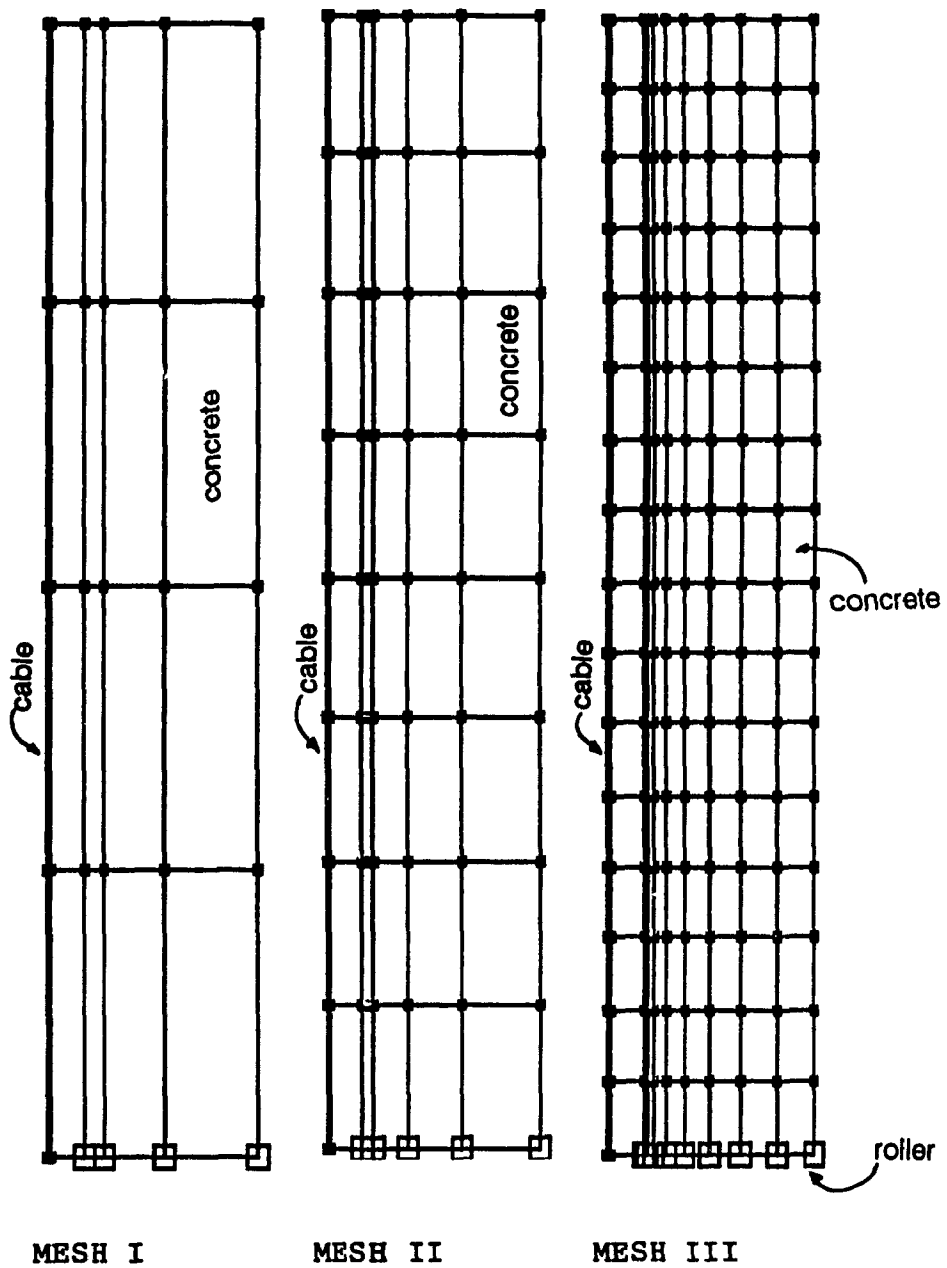


Fig 8-2 Finite element meshes

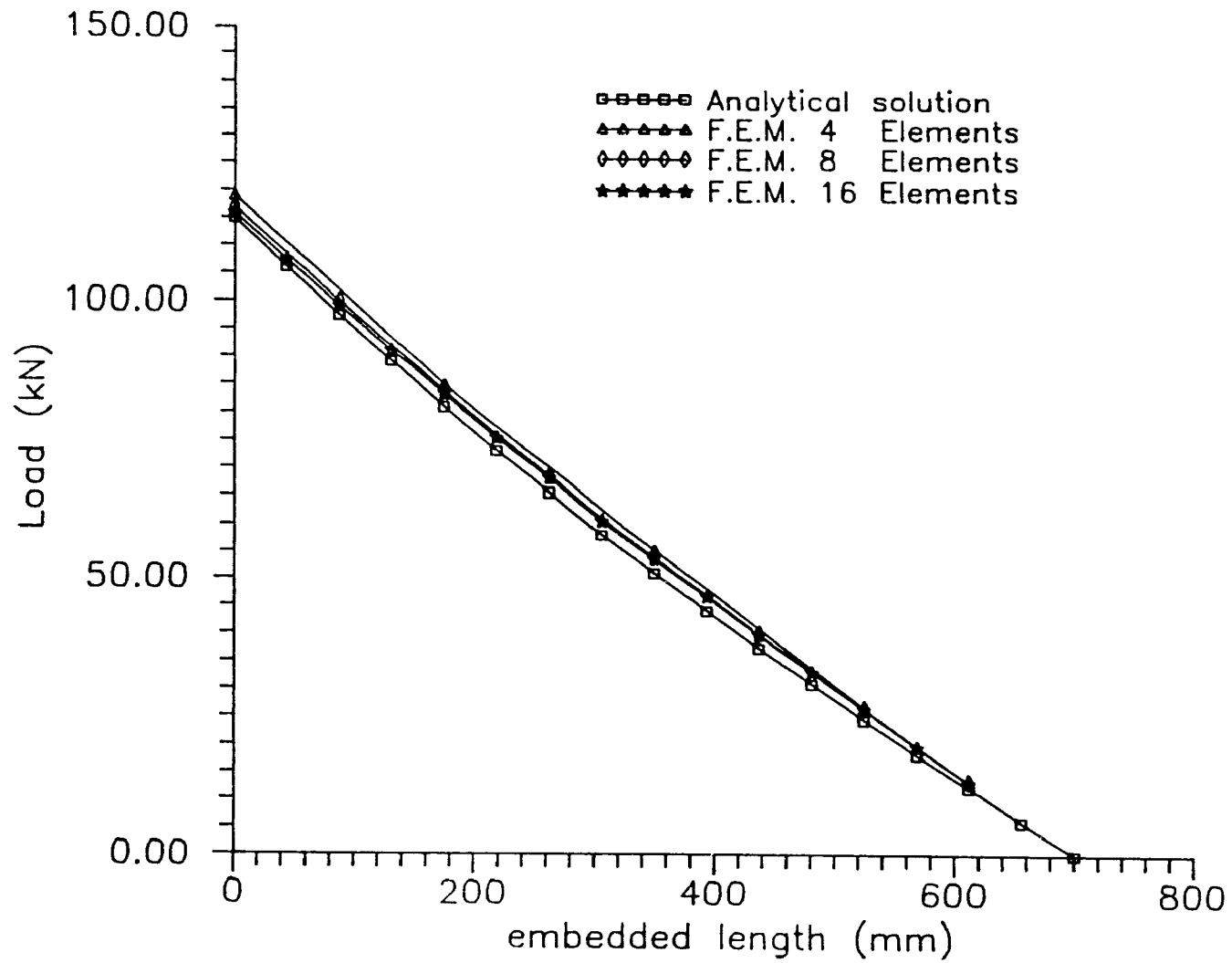


Fig. 8-3 Comparison of load distributions

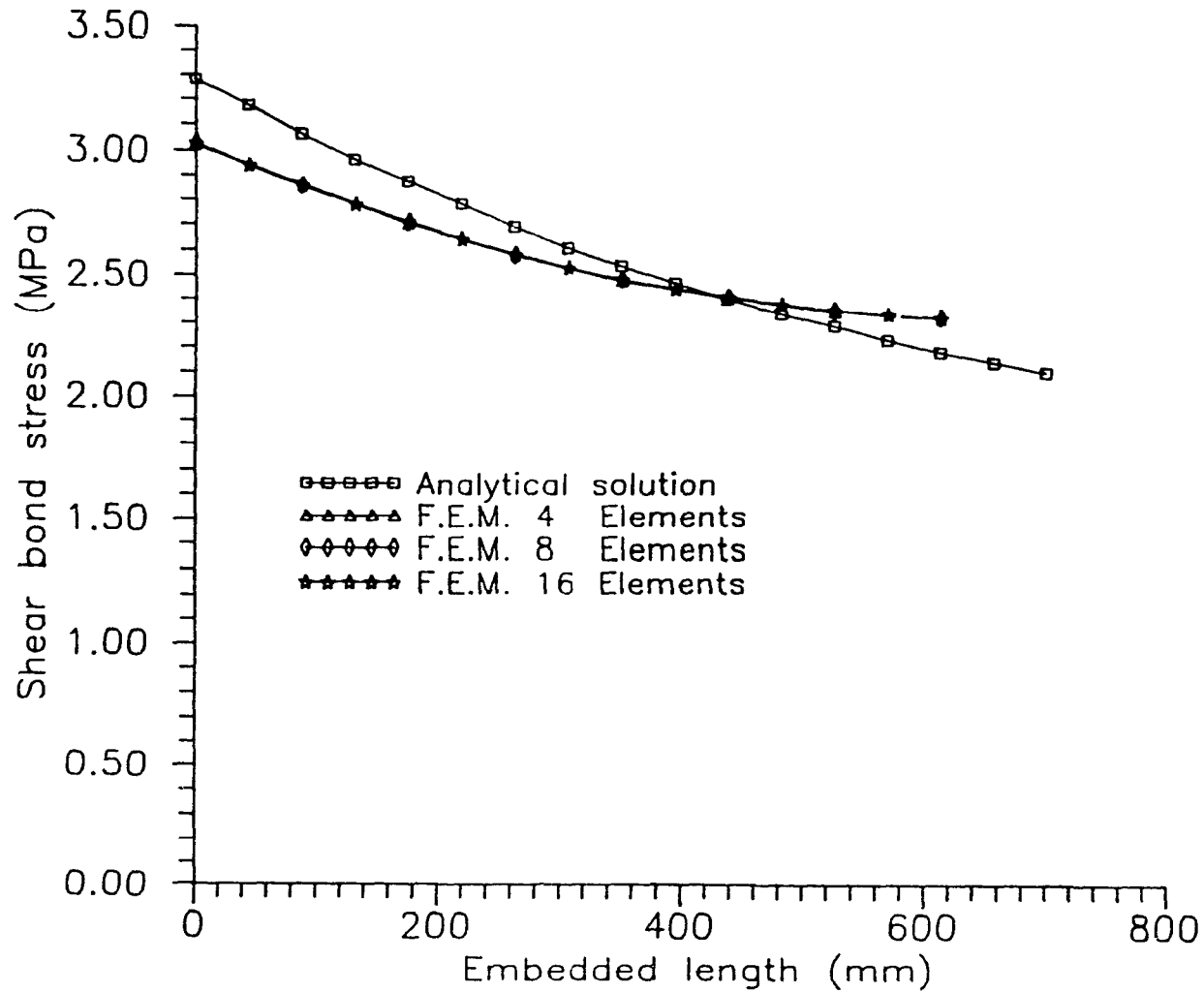


Fig. 8-4 Comparison of shear bond stress distributions

Model	No. of Element		Applied load (kN)	End displacement (mm)
	Rock	Cable		
Mesh I	16	4	114.4	6.506
Mesh II	40	8	114.4	6.520
Mesh III	128	16	114.4	6.524
Variational	-	-	114.7	5.86
Experimental	-	-	112	5.6

Table 8-1 Comparison of end displacements for different models and the experimental results.

8.3 PRACTICAL EXAMPLE

To demonstrate the capability of the CAB system, a stress analysis of a practical example similar to the sulphide deposit at Winston lake in Noranda Mines [99] is considered. The depth of the underground open stope is assumed 600 meters below ground surface. The problem is modelled with three different materials: 5 m wide (horizontal) sulphide ore dipping at 50°, gabbro that forms the hanging and foot walls and a weak chert zone between the hanging wall and ore body with a thickness of 7m. The stope has an average vertical height of 18 m while the ore development headings are 4 m high and 8 m wide. The geometry of the openings and the rock mass properties for different zones are summarized in Fig. 8-5 and Table 8-2 respectively [99].

Material	I	II	III
Rock type	Gabbro	Sulphide Ore	Chert
Unit weight (MN/m ³)	0.028	0.024	0.023
Modulus of elasticity of rock mass (GPa)	40	10	10
Poisson's ratio	0.2	0.25	0.21
Cohesive strength (MPa)	2.3	4.2	3.6
Friction angle (deg)	42	40	36

Table 8-2 Types and properties of material [99]

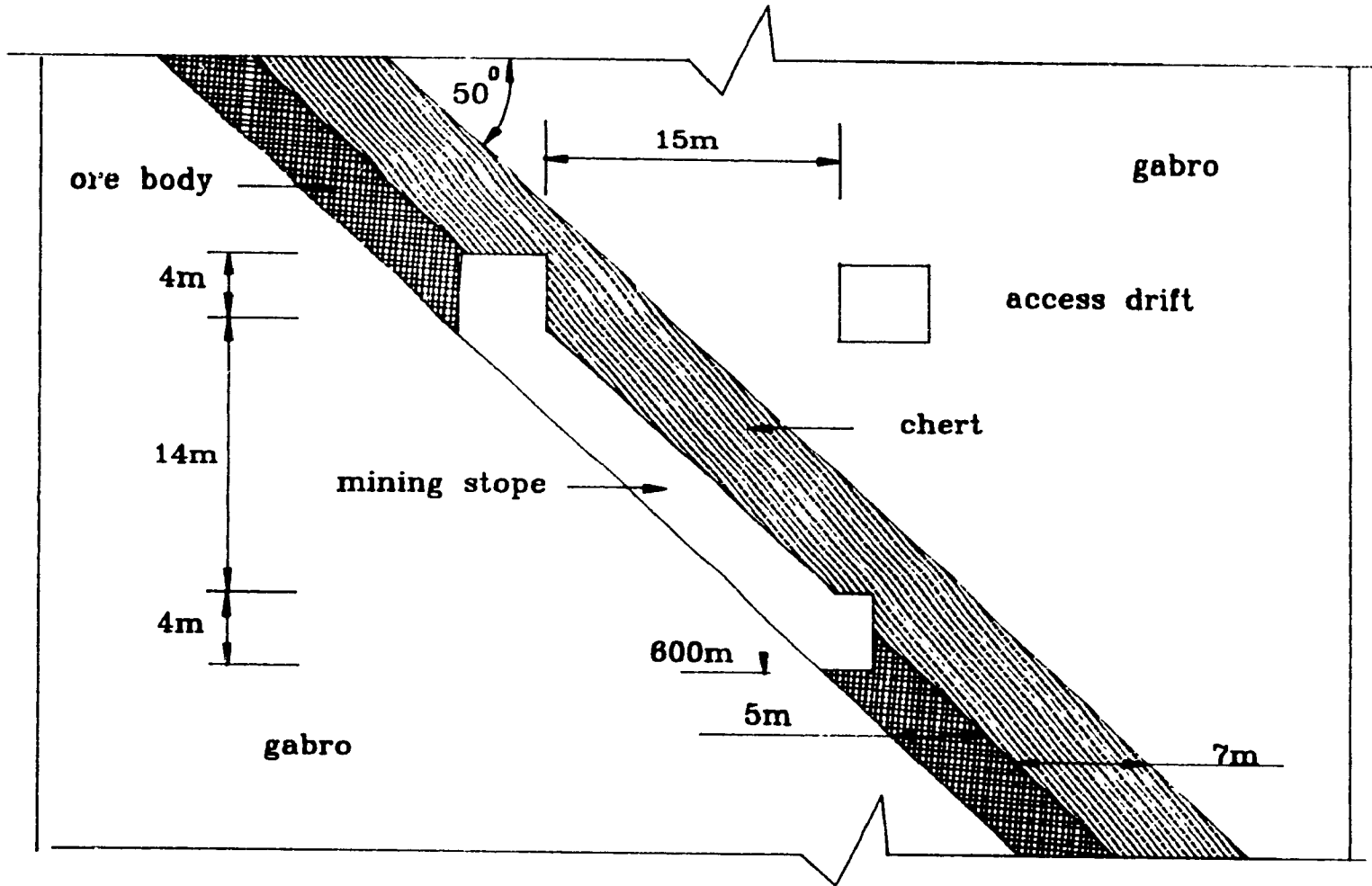


Fig. 8-5 Geometry and material properties

To compare the effectiveness of the different patterns of cable bolting the analysis was carried out using three different models. The first model does not considered cable bolt support and its finite element mesh is shown in Fig. 8-6. The second includes a pattern of localized cable bolting with two meter spacing of reinforcement elements at the surface of the opening. For the third model, a fan form pattern of the cable bolts installed from a drift was selected. The cable bolts are assumed to be constructed from 15.2 mm diameter standard steel cable with 270 kN ultimate tensile strength. The properties of the cable used in the model given in Table 5-1. According to the results of Chapter 5 the stiffness of the Winkler springs is assumed uniform for all the elements and equal to 337 Mpa. The distance between reinforcement elements in the direction perpendicular to the section is assumed to be one meter with a length sufficient to provide at least 3 m anchorage in the gabbro. The corresponding finite element meshes around the opening are given in Fig. 8-7 and Fig. 8-8 respectively.

The gravitational stress at a given depth is due to the weight of the overlying strata; it is a stress due to body forces and its vertical component is, given by:

$$\sigma_v = \gamma gh \quad (8-1)$$

where

σ_v = vertical stress

γ = density

g = acceleration due to gravity

h = depth

1

According to Obert and Duvall [98], most stress determinations made by stress-relief and hydraulic fracturing techniques indicate that for engineering purposes eq. (8-1) is reasonably valid although significantly higher and lower values have been reported in the vicinity of large geological anomalies, such as faults and shear zones.

The lateral component of in situ stress depends upon the stress-strain behavior of the rock as well as upon the restriction of lateral expansion, this being associated with vertical pressure during formation of the rock mass.

Hoek and Brown [15] indicate the range of horizontal to vertical stress ratios with depth. Measured mainly in hard rock, these are shown in Fig. 8-9 and Fig. 8-10. Referring to the depth of excavation and using Fig. 8-9 and Fig. 8-10 the vertical and horizontal stresses are estimated 16.35 MPa and 26.45 MPa respectively.

8.3.1 RESULTS

The analysis results of the CAB system are illustrated in Fig. 8-11 to 8-15. In Fig 8-11, distribution of displacement around the opening for model 3 is shown. The relatively large displacements at the hanging wall side are attributed to the presence of weaker material and the high value of initial field stress. The maximum calculated displacement is 27 mm at the excavation surface in hanging wall when no support is employed. Application of cable elements restricts the maximum displacement to 19 mm for drift bolting and 23mm for localized cable bolting.

Fig 8-12 shows the distribution of the principal stresses around the opening in the drift cable bolting (model 3). As can be seen at locations which are far from the surface of opening, the stress remains almost unchanged. Higher variation of stresses appears at the wall sides because of the excavation.

The tensile stress at the hanging wall may lead to the failure of that hanging wall. The Mohr-Coulomb failure criterion is employed in this analysis. The failure zone at the intersection between the hanging wall cross-cut access and the drilling drifts is shown in Fig. 8-13 to 8-15. As can be seen, the failure progresses through the hanging wall and disturbs the chert rock mass for further failure when no cables were employed. Apparently, application of the high density localized cable bolting did not properly improve the safety level of rock mass (see Fig. 8-14). Fig. 8-15 shows that the installation of cable bolts from a parallel bolting drift is more effective for stability of the hanging wall.

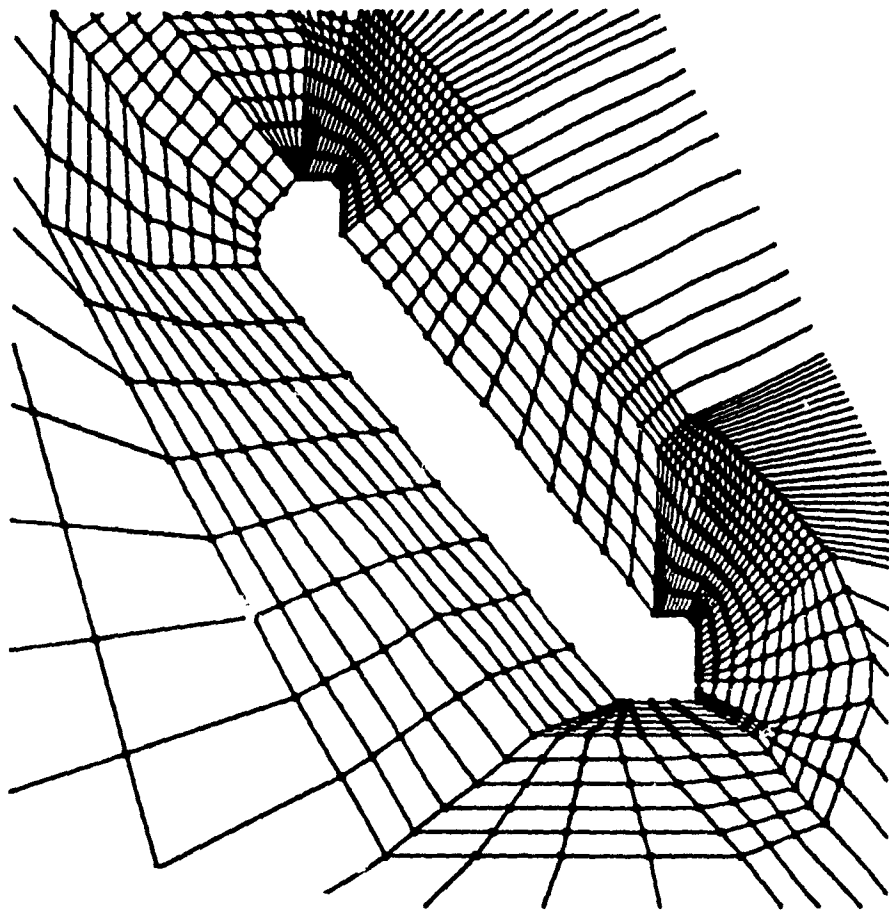


Fig. 8-6 Finite element mesh when slope is not supported

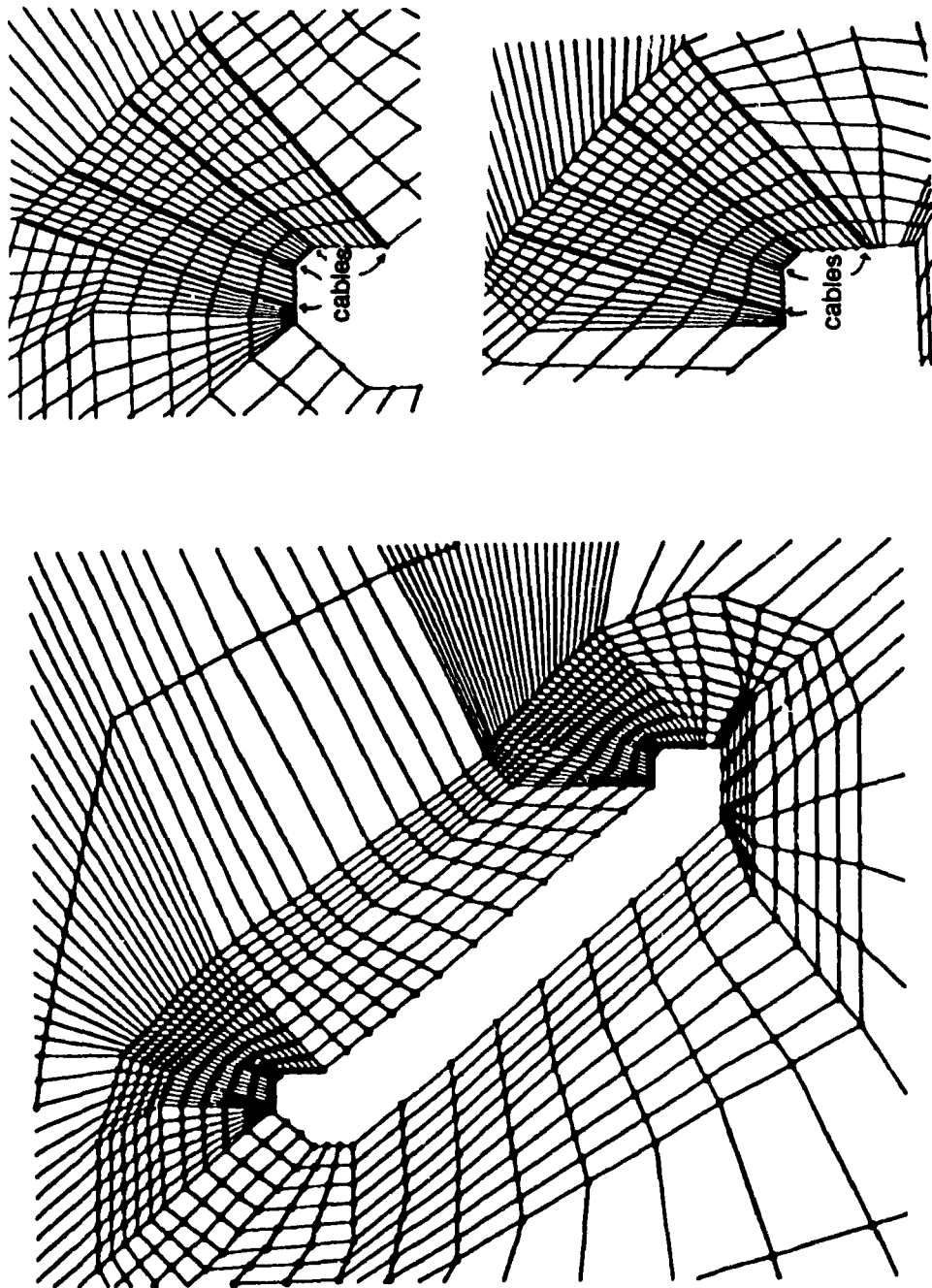


Fig. 8-7 Finite element mesh for localized cable bolt support

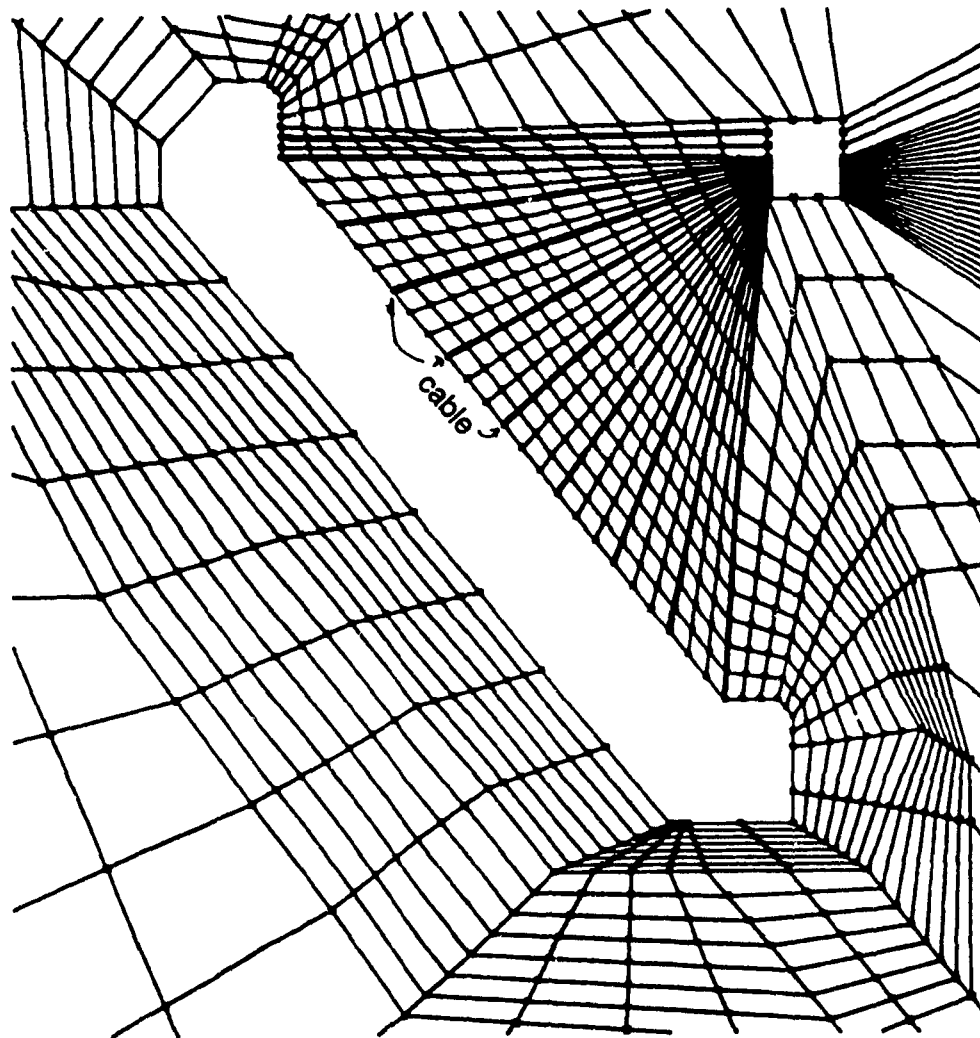


Fig. 8-8 Finite element mesh when cables are installed from top access drift

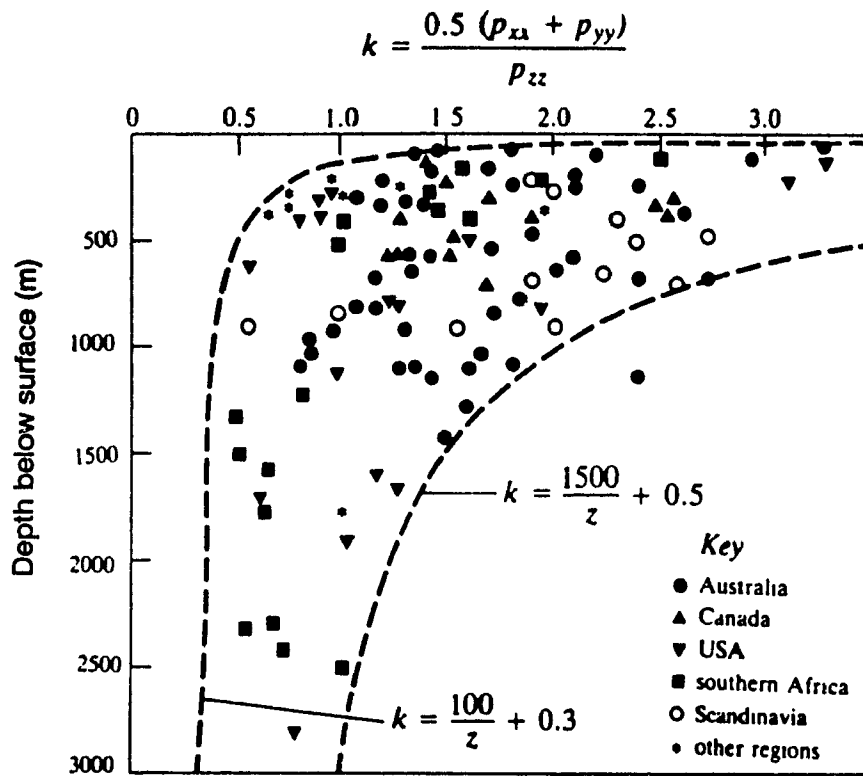


Fig. 8-9 Variation of ratio of average horizontal stress to vertical stress with depth below surface [15]

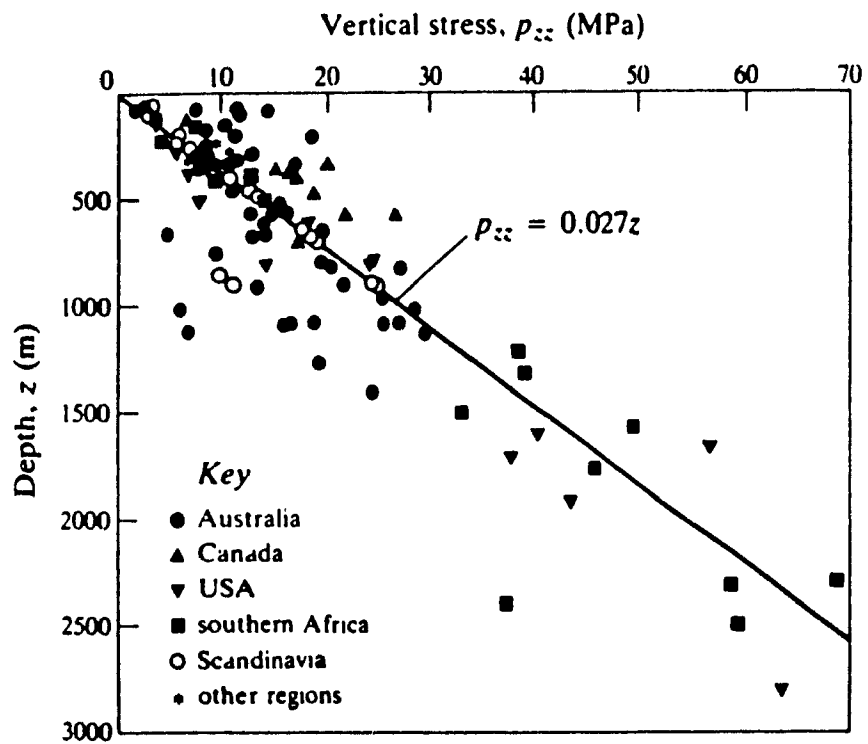


Fig. 8-10 Plot of vertical stress against depth below surface [15]

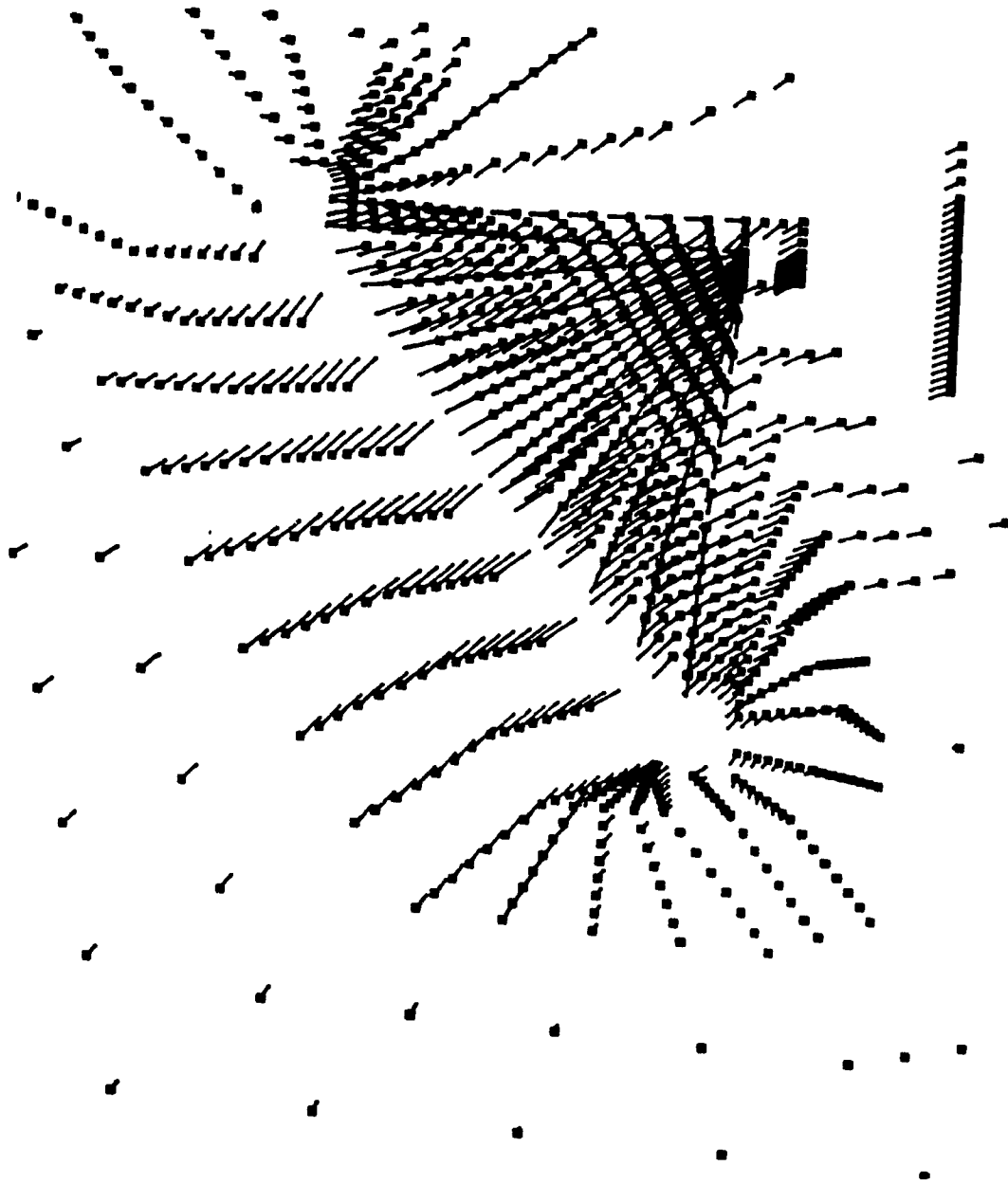


Fig. 8-11 Typical distribution of displacement around the opening

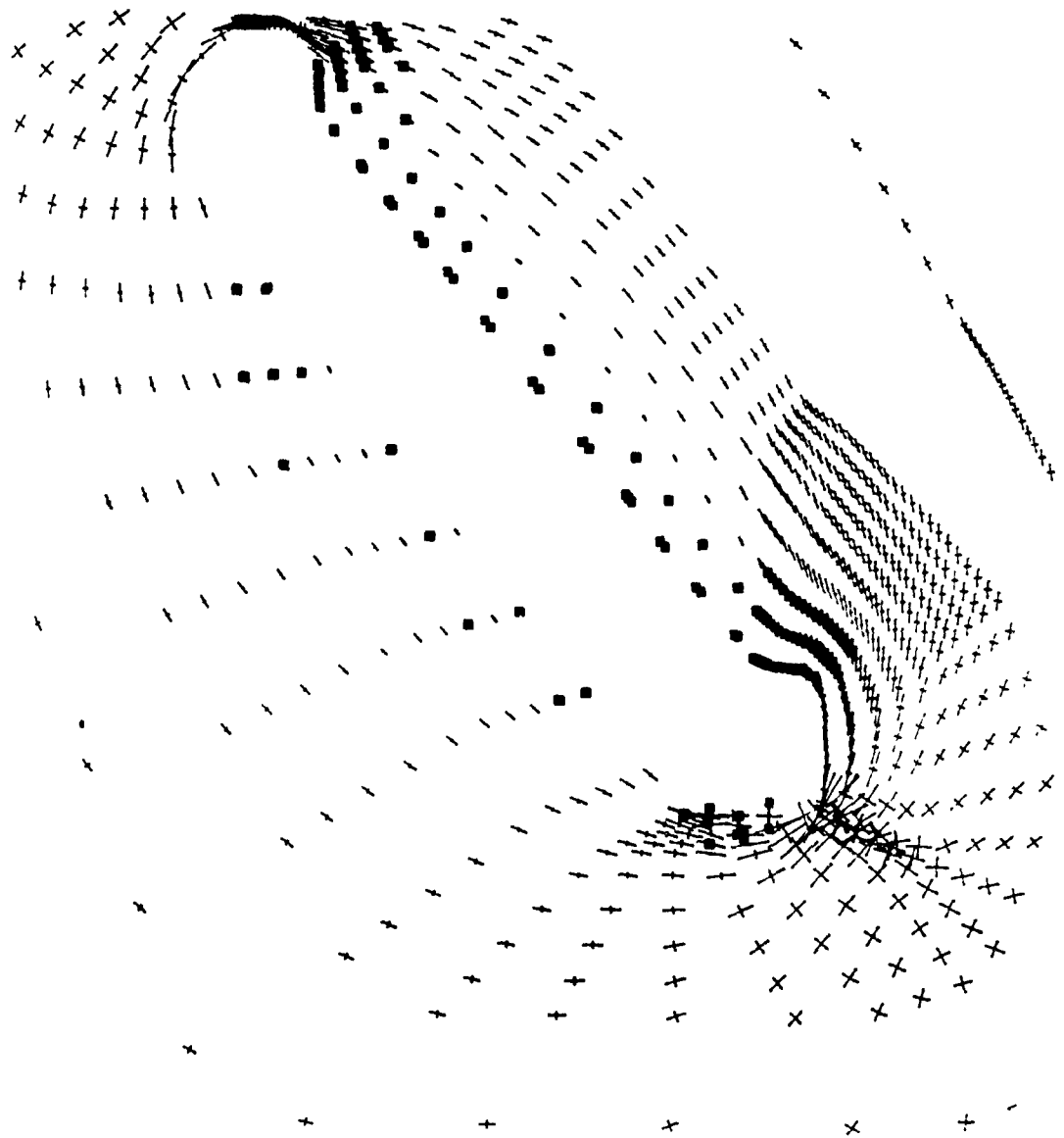
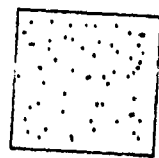
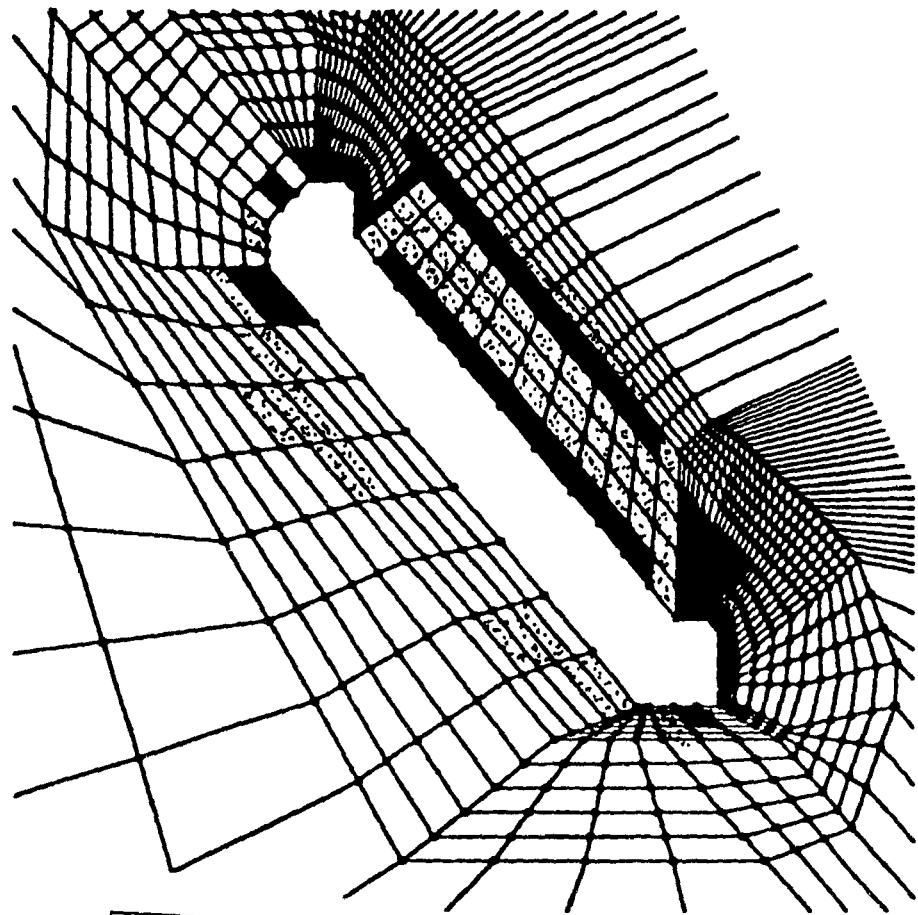


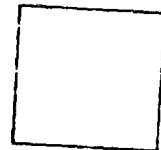
Fig. 8-12 Typical distribution of principal stresses around the opening



critical

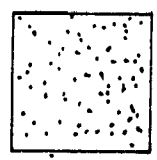
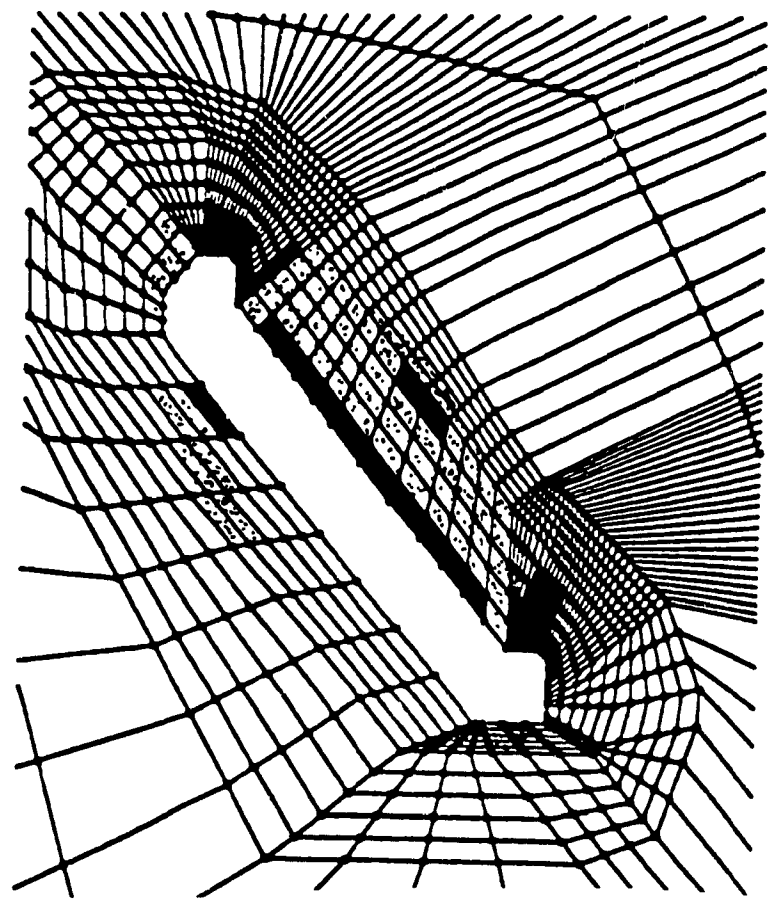


failed

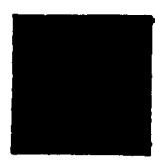


safe

Fig. 8-13 Safety level when stope is not supported



critical

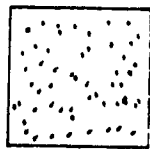
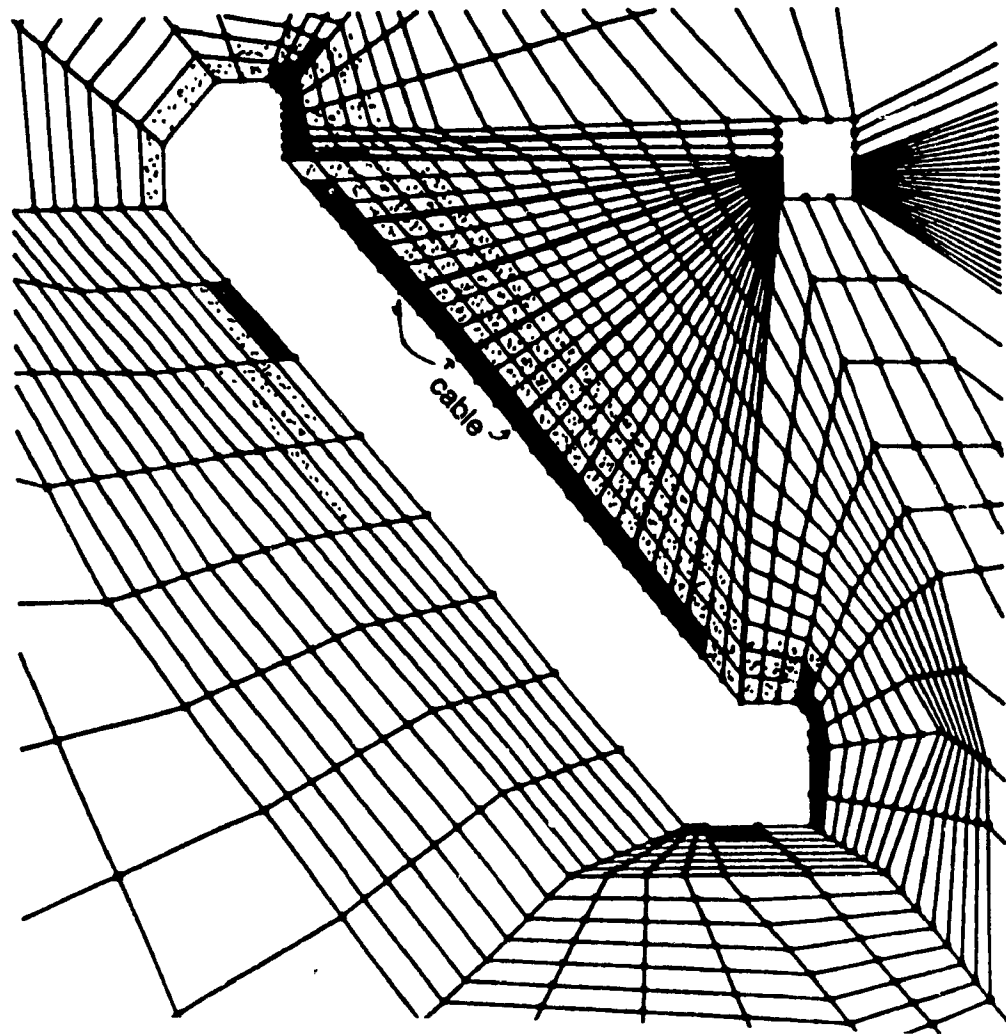


failed



safe

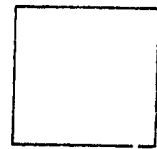
Fig. 8-14 Safety level when stope is supported by the localized cable bolting



critical



failed



safe

Fig. 8-15 Safety level when slope is supported by the cable bolting from the top access drift

8.4 CONCLUSION

The two dimensional finite element program (CAB) was developed and used to verify by the experimental results from Chapter 5, as well as simulate two different patterns of cable bolting. The analysis leads the following concluding remarks:

- There is a good correlation between the finite element program and the variational model for the load distribution along the embedded length of cable.
- The distribution of the shear bond stress for the variational model is smoother, while in numerical model the slope is steeper. This is due to calculation of the shear bond stress in the finite element program, which assumes that the shear bond stress is uniform along the length of each element of cable.
- Comparison of displacement at the end of the cable confirms the accuracy of the variational and finite element method with respect to the experimental data.
- The investigation of different patterns of cable bolting showed that the cable bolting installed from the parallel bolting drift was more effective than the localized dense cable bolting.

CHAPTER 9 CONCLUSION AND FURTHER RESEARCH

9.1 CONCLUSION

Experimental and analytical investigations carried out in this research program have led to the following conclusions:

1) Results obtained from use of the installation technique in the field indicate that the concept of cable bolting with grout-aggregate material is practicable. It was demonstrated that the installation and grouting time was more rapid in comparison with conventional techniques. Furthermore the installation technique was easy, requiring only two operators men and neither a breather tube nor a plug.

2) The laboratory investigation indicated that the behavior of grouted untensioned cable bolts was related primarily to the diameter of the cylinder. Other factors which also controlled the behavior of the cable bolt and its contribution to the shear bond strength include:

- Workability of the mix
- Size distribution of the aggregate
- Embedded length of cable.
- Compressive strength of the grout
- Aggregate-cement ratio
- Diameter of the borehole

The effect of workability and size distribution of the aggregate in the grout-aggregate mix were the key critical controlling factors in providing the optimum shear bond strength between cable and borehole wall.

The variation of the embedded length did not show a direct relationship to the shear bond strength. A linear relationship between load carrying capacity of the cable bolt and embedded length was appropriate up to a 75 cm embedded length of cable bolt. It was observed that increasing the compressive strength of the grout increases the bond shear strength.

Cement comprises 45% of the grout-aggregate mix is in a conventional grout. It is observed that in conventional cable bolting, some of the grout may enter joints or fractures in the rock mass and jeopardize the shear bond strength of the cable bolt. Application of the grout-aggregate mixture could reduce the risk of losing the grout into the rock mass. The other advantage of the presence of the aggregate is the improvement of the friction properties between cable and borehole wall. Therefore, grout-aggregate mix provides more ductile behavior for the cable bolt with respect to the conventional grout.

The diameter of the borehole in a practical range was shown to have no effect on the load carrying capacity of the cable bolt. Therefore, the practical size of borehole is acceptable when there is no restriction on shear bond strength at the grout-rock interface.

3) An analytical model based on the variational method, capable of calculating the distribution of load and shear bond stress along the embedded length of a cable bolt was developed. This model was able to predict the experimental pull-out testing results obtained in this research work. The degree of the

correlation between experiment and variational model was very good.

Sensitivity analysis identified that the exposed surface area of the cable bolt has a significant effect on the contribution of the load carrying capacity of the cable bolt. The interaction between the cable and the borehole wall was seen to depend on the properties of the rock and the grout material. However, the parametric study showed that the higher yield bond strength behavior of cable in pull-out tests, the higher the load carrying capacity of the cable bolt.

4) A numerical model based on the finite element method was developed to simulate the cable bolt in underground excavations. The model results were compared with pull out testing program results. A case study was then used to demonstrate the capability of the CAB program and the efficiency of different patterns of cable bolt installed.

9.2 SUGGESTIONS FOR FURTHER RESEARCH

- A number of modification has been used to expand the range of cable bolting systems available to design engineers. With reference to the cost and simplicity, application of twin cable bolting with conventional grout is gained popularity in the mining industrial. Presence of two cables in a borehole could require a more workable grout or grout-aggregate mix. Therefore, the behavior of twin cable should be investigated in a testing program.
- Blasting can jaoprize the stability of the support element [5]. Therefore, ductile behavior of cables with grout-aggregate mixes close to blsting should be

investigated. This program could be involved to monitoring the behavior of cable bolt for different embedded lengths with conventional grout and grout-aggregate mixes.

- Most of the failure of cable due to shear bond strength has occurred due to poor performance of installation. One of the major factors is the pressure of grouting. According to Litteljohn [23]. The load carrying capacity of the cable with respect to the grouting pressure is not clear.
- Recently popularity of composite materials in industry has increased. Therefore, provided costs and installation methods appear to be favorable, composite materials for cable bolting could be introduced to the mining industry. Practical installation and load carrying capacity could be investigated.

REFERENCES

1. Fuller, P.G., "Pre-reinforcement of cut and fill stopes", Proc. Application of Rock Mechanics to Cut and Fill Mining, Uni. of Lulea, Sweden, Published by Institution of Mining and Metallurgy, London, pp. 55-63, 1981.
2. Littlejohn, G.S. and Bruce, D. A., "Rock anchors-design and quality control", Sixteen Symposium on Rock Mechanics, Published by American Society of Civil Engineers, pp. 77-88, 1977.
3. Potvin, Y., Hudyma, M. and Miller, H.D.S., "Design guidelines for open stope support", Presented at the 90th CIM AGM, Edminton, Alberta, Canada, 1988.
4. Stillborg, B., "Experimental investigation of steel cables for rock reinforcement in hard rock", Doctoral Thesis Lulea University, Sweden, 1984.
5. Fuller, P.G., "Cable bolt in mining", International Symposium on Rock Bolting, Abisko, Lapland, Sweden, Vol. 2, September 1983.
6. Fuller, P.G. and Cox, R.H.T., "Mechanics of load transfer from steel tendons to cement based grout", Fifth Australians Conf. on the Mechanics of Structures and Materials, Melbourne, pp. 189-203, 1975.
7. Jeremic, M.L., "Ground mechanics in hard rock mining", A.A. Balkema Co. Ltd., Rotterdam, pp. 415-503, 1987.

8. Cassidy K., "The implementation of a cable bolting program at the Con Mine", CIM sp. Vol. 22, Canadian Inst. of Mining and Metallurgy, pp. 67-71, 1980.
9. Bieniawski, Z.T., "Rock mass classification in rock engineering", Proc. of the Symposium on Exploration for Rock Engineering, Johannesburg, Vol. 1, 1976, PP. 97-106.
10. Deer, D.U., "Geological considerations. In Rock mechanics in engineering practice", K.G. Stagg and O.C. Zienkiewicz, London: Willey, pp. 1-20, 1968.
11. Rabcewicz, L.V., "The new Australian tunnelling method", Water pump, Vol. 1, pp. 453-457, Nov. 1964.
12. Daemen, J.K., "Problems in tunnel support mechanics", Underground space, Vol. 1, pp. 163-172, 1977.
13. Ladanyi, B., "Use of long-term strength concept in the determination of ground pressure on tunnel linings", Advances in Rock mechanics, Proc. third congr., Int. Soc. Rock Mech., Denver, Washington, DC: Nat. Acad. Sci., 2B, pp. 1150-1156 1974.
14. Jukes, S.G. and Hassani, F.P. and Whittaker, B.N., "Characteristics of steel arch support systems for mine roadways. Part 1, modelling, theory, instrumentation and preliminary results", Mining Science and Technology, pp. 43-48, 1983.
15. Hoek, E. and Brown, E.T., "Empirical strength criterion for rock masses", J. of the Geotechnical Engineering Division, ASCE, Vol. 106, No. GT 9, PP. 1013-1035, Sept. 1980.

16. Anon, G. "Equipment for shotcreting", Mining Magazine 147, pp. 547-557, 1982.
17. Lang, T.A. and Bischoff J.A., "Stabilization of rock excavations using rock reinforcement", In Issues in Rock mechanics, Proc. 23rd Sympo. Rock mech., R.E. Goodman and F.E. Heuze, New York: Am. Inst. Min. Metall. Petrolm Engrs., pp. 935-943, 1982.
18. Scott, J.S., "Friction rock stabilizer impact upon anchor design and ground control practice", International Symposium on Rock Bolting, Abisko, Lapland, Sweden, pp. 407-417, September 1983.
19. Hanna, T.H., "Foundation in tension-ground anchors", McGill Company, Canada, 1982.
20. Hobst, L. and Zajic, J., "Anchoring in rock and soil", Elsevier Scientific Publishing Company, 1983.
21. Hoek, E., "Practical rock mechanics developments over the past 25 years", Conference on rock engineering and excavation in an urban environment, Hong Kong, pp. A1-A6, February 1986.
22. Tamrock Canada, Inc., "Fully mechanized in cable bolting", Professional Development Seminar on Cable Bolting. Dept of Mining and Metallurgy Engineering, McGill University, Montreal Canada, March 1989.
23. Littelejohn, G.S., "Design estimation of the ultimate load-holding capacity of ground anchors", Ground Engineering, pp. 25-39, 1980.

24. Gramoli, L., "Tensioned cable rock anchorage at Geco Division of Noranda Mines Ltd.", CIM first Underground Operators Conference, Sudbury, February 1975.
25. Palmer, W.T., Bailey, S.G. and Fuller, P.G., "Experience with pre-placed supports in timber and cut and fill stopes", In: Influence of excavation design and ground support on underground mining efficiency and costs; Symp., Wollongong, pp. 45-71, 1976.
26. Parker, H., et al. "Strata reinforcement using the techniques of long hole resin dowelling", Min. Engr., no. 154, pp. 519-532, July 1973.
27. Mathews, S.M., Tilman, V.H. and Worotnicki G., "A modified cable bolt system for the support of underground openings", Proc. Aus. Inst. Min. Metall. Conference, Broken Hill, N.S.W., pp. 243-255, July 1983.
28. Bharti, S., Udd, J.E. and Cornett, D.J. "Ground support at Strathcona Mine", CIM Symposium on Underground Support Systems, Sudbury, Canada, 1983.
29. Pagel, C.W., "Cable bolting for ground support at no. 12 Mine of Brunswick Mining", CIM Symp. on Underground Support Systems, Sudbury, Canada, 1983.
30. Dight, P.M., "Improvement to the stability of rock walls in open pit mines", Doctoral thesis Monash University, Australia, 1982.
31. Cox, R.M., "Why some bolted mine roofs fail", AIME Transaction 256, pp. 234-241, 1974.

32. Ballivy, G. and Dupuis, M., "Laboratory and field evaluation of the bonding strength of grouted rock anchors", *Underground Rock Engineering*, 1980 pp. 97-102.
33. Hawkes, J.M. and Evans R.H., "Bond Stresses in reinforced concrete columns and beams", *Journal of the Institution of Structural Engineers*, Vol. XXIX, No. X, pp. 323-327, Dec. 1951.
34. Brian, O., "Practice at Falconbridge Ltd., operating, design and application", Professional Development Seminar on cable bolting. Dept of Mining and Metallurgy Engineering, McGill University, Montreal Canada, March 1989.
35. Choquet, P., "A method of estimating loose zone extent around a mine opening for support assessment", *CNCRM Symposium on Underground Support Systems*, paper No. 8, Sudbury, 1983
36. Mathews, K.E., Hoek, E., Wylie, D.C. and Stewart, S.B.V. "Prediction of stable excavation spans for mining at depth below 1000 m in hard rock", *CANMET Report 802-1571*, 1981.
37. ACI Committee 408, "A guide for determination of bond strength in beam specimens", *ACI Journal*, Vol. 61, No. 2, pp. 129-135, February 1964.
38. ACI Committee 408, "Bond stress, the state of the art", *ACI Journal*, Vol. 63, No.11, pp. 1161-1190, November 1966.

39. Mathey, R.G. and Watstein D., "Investigation of bond in beam and pull-out test specimens with high yield strength deformed bars", ACI Journal, Vol. 57, No. 3, pp. 1071-1090, March 1961.
40. Lutz, L. and Gergely P., "Mechanics of bond and slip of deformed bars in concrete", ACI Journal, Vol. 64, NO. 11, pp. 711-721, November 1967.
41. Brown, D.G., "Uplift Capacity of Ground Rock Anchors", Ontario hydro research quarterly, fourth quarter, pp. 18-24, 1970.
42. Goto, Y., "Cracks formed in concrete around deformed tension bars", ACI Journal, Vol. 68, No. 4, pp. 244-251, April 1971.
43. Houde, j., "Study of force displacement relationships for the finite element analysis of reinforced concrete", Ph.D. Thesis, McGill University, Montreal, December 1973.
44. Fuller, P.G. and Cox, R.H.T., "Rock reinforcement design based on control of joint displacement - a new concept", Third Australian Tunneling Conference, Sydney 1978 (Barton, A.C.T. Institution of Engineers Australia, pp. 28-35, 1978.
45. Kemp, E.L., Brezny, F.S. and Unterspan J.A., "Effect of Rust and Scale on the Bond Characteristics of Deformed Reinforcing Bars", ACI Journal, Proceedings, Vol. 65, No. 9, pp. 743-756 September 1968.
46. Clarck, A.P., "Bond of Concrete Reinforcing Bars", ACI Journal, Proceedings, Vol. 46, pp. 161-184, November 1949.

47. Wilhelm, W.J., Kemp, E.L. and Lee Y.T., "Influence of deformation height and spacing on the bond characteristics of steel reinforcing bars", Civil Engineering Studies Report No. 2013, Department of Civil Engineering, West Virginia University, 1971.
48. Goris, J.M. and Conway P., "Grouted fixable tendons and scaling investigation", World Mining Congress, Stockholm, Sweden, pp. 783-792, 1987
49. Thompson, A.G., Mathews, S.M., Windsor, C.R. and Bywater, S., "Innovation in rock reinforcement technology in the Australian mining industry", pp. 1275-1278, 1983.
50. Jeremic, M.L. and Delaire G.J.P., "Failure mechanics of cable bolt systems", CIM Bulletin 76, pp. 66-71, 1983.
51. Bernander, K.G., " An investigation of bond by means of strain measurements in high tensile bars embedded in long cylindrical pull-out specimens", Rilem Symposium on Bond And Crack Formation in Reinforced Concrete, Vol. I, pp. 203-214, Stockholm 1957.
52. Jonsson, P.Q., Osterman, J. and Wastlund, G., "Background of the swedish tentative standard specifications for limitation of crack widths in reinforced concrete structures", Rilem Symposium on Bond and Crack Formation in Reinforced Concrete, Vol. II, pp. 319-340, Stockholm 1957.
53. Ferguson, P.M. and Thompson, J.N., "Development length of high strength reinforcing bars in bond", ACI Journal, Proceedings, Vol. 59, No. 7, pp. 887-922, July 1962.

54. Nevil, A.M., "Properties of concrete", Pitman Publishing, (third edition), London. 1981.
55. Davis, R.E., Brown, E.H. and Kelly, J.W., "Some factors influencing the bond between concrete and reinforcing steel", Proceedings ASTM, Vol. 38-11, pp. 394-409, 1973.
56. Muline, N.M. and Astrova, T.I., "Etude de l'Influence de la composition du beton sur l'adherence acier-beton", Bulletin D'Information Du C.E.B. No. 48, April 1965.
57. Orchard, D.F., "Concrete technology", Vol. 3, Properties and testing of aggregates, Applied Science Publishers Ltd., London, 1976.
58. Murdock, L.J. and Brook, K.M. "Concrete materials and practice", 5th Ed., Edward Arnold, London, 1979.
59. Collis, L., and R.A. Fox, "Aggregates, sand, gravel and crushed rock aggregates for construction purposes", Publisher the Geological Society, 1985.
60. Stheeman, W.H., "A practical solution to cable bolting problems at the Tsumeb Mine", CIM Bulletin, pp. 65-77, February 1982.
61. Littlejohn, G.S. and Bruce, D.A., "Rock anchors, state of art", Ground Engineering, Vol. 8, No. 3, pp. 25-32, 1975.
62. Standards Association of Australia, "Prestressed Concrete code CA35", Section 5- Ground Anchorages pp. 50-53, 1973.
63. Mining Magazine, "Rock bolts", pp. 38-47, July 1983
64. Coates, D.F., "Rock mechanics principles ", In Mines Branch Monograph, pp. 7-15 to 7-25, 1970.

65. Menzel, C.A., "Effect of settlement of concrete on results of pull-out bond tests", Portland Cement Association, No. 41, November 1952.
66. Koh, Y., "Bond between concrete and reinforcement (with particular reference to cold weather concreting)", Rilem Symposium on Bond and Crack Formation in Reinforced Concrete, Vol. I, pp. 177-190, Stockholm 1957.
67. Plowman, J.M., "The Measurement of bond strength", Rilem Symposium on bond and Crack Formation in Reinforced Concrete, Vol. II, pp. 347-359, Stockholm 1957.
68. Phillips, S.H.E., "Factors affecting the design of anchorages in rock", Cementation research Ltd., report No. R48-70, December 1970.
69. Coates, D.F. and Yu, Y.S., "Three dimensional stress distributions around a cylindrical hole and anchor", Proc. of the 2nd International Conference on Rock Mechanics, Belgrade, pp. 175-182, 1970.
70. Hollingshead, G.W., "Stress distribution in rock anchors", Canadian Geotechnical Journal, vol. 8, No. 4, pp. 588-592, November 1971.
71. Farmer, I.W., "Stress distribution along a resin grouted rock anchor", International Journal of Rock Mechanics and Mining Sciences, vol. 12, pp. 347-351, 1975.
72. Dunham, R.K., "Anchorage tests on strain gaged resin bonded bolts", Tunnels and Tunneling, pp. 77-76, Sept. 1976.
73. Dunham, R.K., "Field testing of resin anchored rock bolts", Colliery Guardian, May, 1984.

74. Ballivy, G. and Martin, A., "The dimensioning of ground anchors", Proc. Int. Symp. on Rock bolting, Abisko, Lapland, Sweden, pp. 73-85 , Sept. 1983.
75. Yap, L.P. and Rodger, A.A., "A study of the behavior of vertical rock anchors using the finite element method", Int. J. of Rock Mech. and Min. Sci., Vol. 22, No. 2, pp. 47-61, 1984.
76. Ballivy et al., "Le role du scellement dans les ancrages actifs injectes dans le rocher", Can. Geotech. Jnl., Vol. 26, No 4, 1986.
77. Jonsson, G., Kareby, B., Lundgren, K. and Sylwan, B.A., "Mechnized scaling and roof support systems", World Mining Congress, Stockholm, Sweden, pp. 777-782, 1987.
78. "Standard specifications for concrete aggregates", (ASTM C33-74a), Philadelphia American Society for Testing and Materials, 1974.
79. Anis, F. and Aref K., "An Investigation of dynamic characteristics of cable bolts", 27th U.S. Symp. on Rock Mechanics, pp. 415-423, 1986.
80. Abrams, M.S., and Orals, D.L., "Concrete drying methods and their effect on fire resistance, research, Department Bulletin Rx 181, Portland Cement Association, 1965.
81. Canadian Standard Association, Specification CSA A23.1 1977, "Constituants du beton et methodes de construction en beton", Published 1977.

82. Tepfers, R., "Cracking of concrete cover along anchored deformed reinforcing bars", Magazine of Concrete Research: Vol 31, No. 106, March 1979.
83. Irving H. and Shames, H. "Solid Mechanics a variational approach", McGraw Hill, New York, 1973
84. Elsgolts, L., "Differential equation and the calculus of variations", Mir publishers, Moscow, 1980.
85. Goodman, R., "Introduction to rock mechanics", John Wiley, New York, 1980.
86. Randolph, M.F., and Peter W., "Analysis of deformation of vertically loaded piles" Journal of the Geo. Eng., pp. 1465-1487, 1978.
87. Timoshenko, S., "Strength of materials", Part II: Advanced theory and problems. Princeton, N.J., D. van Nostrand Company Inc. 1956.
88. Mitri, H. and Scoble, M.J., "A numerical procedure for stability analysis of hard rock mine structures", Int. Jnl. Mining Science and Technology, pp. 187-195, 1989.
89. Cook, R.D., "Concepts and applications of finite element analysis", second edition, John Wiley, New York, 1988.
90. Meyer, C. "Solution of linear equations, state of art", J. Struct. Div., ASCE, Vol. 99, 1973.
91. Fellipa, C.A., "Solution of linear equations with skyline-stored symmetric matrix", Computers and Structures, 5:13-29, 1975.

92. Chau, P., "A finite element model for stress analysis of underground openings", M.Eng. Thesis, Dep. of Mining and Metallurgical Engineering McGill university, Montreal, Canada, 1988.
93. Zienkiewicz, O.C. and Philios, D.V., "An automatic mesh generation scheme for plane and curved surfaces by isoparametric coordinates", Int. J. for Numerical Method in Eng., Vol 3, pp. 519-528, 1971.
94. Bathe, E.L. and Wilson, F. E., "SAP IV a structural analysis program for static and dynamic response of linear systems", 1973.
95. Craing, R.F., "Soil Mechanics", second edition, Van Nostrand Reinhold Company, New York, 1978.
96. Chen, W.F. and Saleeb, A., "Constitutive equations for engineering materials, elasticity and modelling", Vol. 2, John Wiley, New York, 1982.
97. Rajaie., H., Mitri, H. and Hassani, F.P., "User manual for CAB analysis system", Report to the Dept. of Mining and Metallurgy, McGill Uni., June 1990.
98. Obert, O. and Duvall, W.I., "Rock mechanics and the design of structures in rock", Jhon Wiley, New York, 1967.
99. Milne, D., personal communication, Noranda technology center, point claire, Quebec.